Development of *Helicobacter pylori* BabA minimal binding domain as a novel biomimetic moiety for gastric-targeted drug delivery

Aymen Mohammed

Thesis submitted to University Of Nottingham for the degree of

Doctor of Philosophy

August 2019

Dedication

This work is dedicated to the soul of my late mother, the origin of my life, for her endless support, powerful encouragement, unlimited love and tenderness.

I miss you so much, Mammy

"The only way to do great work is to love what you do. If you haven't found it yet, keep looking. Don't settle. As with all matters of the heart, you'll know when you find it."

Steve Jobs

Abstract

The need for efficient drug delivery systems / better treatment for human disorders remains a challenge in medicine. This demand could be addressed by developing a new strategy that assist the formulation to act specifically. Some drugs would benefit from targeting the gastric epithelium and retain the therapeutic in the stomach. However, drugs absorbed through the stomach or upper small intestine have a narrow absorption window. Developing a drug delivery system that can adhere to the surface of the gastric epithelial cells will significantly increase drug transit time and overcome this limitation.

The gastric bacterium *Helicobacter pylori* uses special proteins called adhesins to adhere to the gastric epithelium, providing a novel strategy for broadening the absorption window. Therefore, a novel drug delivery system was adapted from these adhesins to facilitate drug absorption.

The best studied adhesin is Blood group Antigen Binding Adhesin (BabA), which specifically mediates *H. pylori* adherence to ABO/Lewis b (Le^b) blood group antigens on the gastric epithelium. Recent co-crystal structure of the extracellular region of BabA with Le^b revealed a smaller binding domain which was termed the BabA-Crown. In the present study, BabA-Crown, as Le^b minimal binding domain, was studied towards usage as a gastric-targeting drug delivery system. By using this biomimetic strategy, a novel cytoadhesive drug system could be developed.

In the beginning, protocols for recombinant expression of BabA-Crown had to be established. We found that addition of Chloramphenicol to the growth medium had a major beneficial effect on the yield of BabA-Crown expressed in the periplasmic space of *Escherichia coli*. Then, BabA-Crown

protein resistance to acidity and peptic digestion were studied. It was revealed that BabA-Crown can partially resist peptic degradation. However, binding studies showed that BabA-Crown did not retain Le^b-binding affinity. To tackle this issue, further adjustments were made. These included structural modifications to increase the length of the protein, incorporation of a Lysine-tag to increase the expression as well as the creation of a new binding motif.

In conclusion, binding of BabA-Crown to Le^b was not achieved, however, BabA conjugated with microparticles still retained the binding ability to Le^b. The data generated in this study represents a good starting point for utilization of the minimal binding region for both biomimetic-drug platform and bacteriological studies.

Acknowledgements

All praise, glory and gratefulness go to Allāh (S.W.T) for the strength and blessing He gave to me to complete this thesis, Allhamdulliah.

Special and sincere thanks to my supervisor Dr. Franco H. Falcone, who saved no effort to guide me throughout this project. His continuous support, patient and advisability bring this work to reach such fruitfulness.

I am also thankful to my co-supervisor Dr Snjezana Stolnik-Trenkic (Snow), for her encouragement and the time she devoted to assist me.

I would like to extend my sincere gratitude to my colleagues all over the University Of Nottingham and especially to my friends in D35, D38 and D19. Special thanks to Geoffrey Holdgate at AstraZeneca, UK and Andrew Brennan at Centre for Biomolecular Sciences, University Of Nottingham for their kind help.

I am extremely grateful to my entire family, particularly my father, for the persistent support, encouragement and provisions. I am very thankful to my wife and children who gave me invaluable moments and went with me through all the bad and happy times. Honestly, without their constant cheers, kind appreciation and lovely help, my life would be meaningless. I wish them all the best.

Last but not least, this work would have not been possible without the kind and much appreciated funding from the Islamic Development Bank (IDB).

List of contents

Abstract ..... **III**
Acknowledgements ..... **V**
Table of Figures ..... **XI**
List of Tables ..... **XV**
List of abbreviations ..... **XVI**
1. Introduction **1**
1.1 The need for a novel gastric drug delivery system 1
1.2 Strategies for gastric retention 5
1.2.1 Floating strategy 8
1.2.2 Swelling strategy 9
1.2.3 Bioadhesion strategy 10
1.2.3.1 Mucoadhesion 10
1.2.3.2 Cytoadhesion 15
1.3 *Helicobacter pylori* 20
1.3.1 Mechanisms of persistence 22
1.3.1.1 Survival in high acidic environment 23
1.3.1.2 Survival in low acidic environment 24
1.3.2 *H. pylori* adhesins 25
1.3.3 BabA (Adhesin for cytoadhesion drug delivery) 29
1.3.4 BabA-Crown domain- the drug moiety? 39
1.4 Aim and objectives 41
2. Experimental methodology **43**
(General overview) **43**
2.1 Introduction 43
2.2 Recombinant expression 44
2.2.1 Recombinant protein expression in *E. coli* 47
2.2.2 The expression vector (pOPE101) 50

2.2.3 The expression host 52

2.3 Enzyme-linked immunosorbent assay 53

2.3.1 Direct enzyme-linked immunosorbent assay 54

2.3.2 Indirect enzyme-linked immunosorbent assay 55

2.3.3 Sandwich enzyme-linked immunosorbent assay 56

2.4 Circular Dichroism spectroscopy 57

2.5 Dynamic light scattering (DLS) 59

3. Cloning and expression of BabA J99 Crown region as the minimal Le^b-binding domain 61

3.1 General overview 61

3.2 Experimental procedures 66

3.2.1 Generation of BabA-Crown expression construct 66

3.2.1.1 BabA-Crown gene 66

3.2.1.2 Polymerase chain reaction amplification 67

3.2.1.3 Cloning 68

3.2.1.3.1 Digestion 68

3.2.1.3.2 Bacterial transformation 68

3.2.2 Protein expression (small-scale) 71

3.2.2.1 BabA protocol 71

3.2.2.2 Preparation of total cell protein fractions 71

3.2.2.3 Periplasmic extraction and spheroplast fraction preparation 72

3.2.3 Plasmid DNA purification and measurement 72

3.2.4 Subcellular fraction analysis 73

3.2.4.1 SDS-PAGE 73

3.2.4.2 Coomassie stain 73

3.2.4.3 Western blot analysis 73

3.3 Results 75

3.3.1 Construction of the BabA-Crown region 75

3.3.1.1 Crown region amplification 75

3.3.1.2 *E. coli* XL10-Gold Transformation 76

3.3.1.3 Confirmatory sequencing 77

3.3.2 Protein expression 79

3.3.2.1 BabA protocol 79

3.3.2.2 Addition of chloramphenicol 80

3.3.3 Chloramphenicol confines bacterial cell growth and increases the intracellular plasmid DNA concentration 84

3.4 Discussion 86

3.5 Conclusion 93

4. Testing BabA-Crown protein functional properties as a moiety for gastric drug delivery 94

4.1 General overview 94

4.2 Experimental procedures 99

4.2.1 Mutagenesis to introduce AviTag™ sequence 99

4.2.2 Protein expression 100

4.2.2.1 Large-scale protein expression 100

4.2.2.2 Protein purification 100

4.2.3 Tryptic peptide mapping 101

4.2.4 Characterization of peptic digestion 102

4.2.4.1 Pepsin cleavage sites modelling 102

4.2.4.1.2 Peptic digestion test 102

4.2.5 Sample analysis 103

4.2.5.1 Silver staining 103

4.2.6 BabA-Crown binding ability 103

4.2.7 Single-chain fragment variable recombinant antibody 104

4.3 Results 105

4.3.1 Introducing the AviTag™ sequence 105

4.3.2 Confirmatory sequencing 106

4.3.3 Protein purification 107

4.3.2 Tryptic peptide mapping 109

4.3.3 Pepsin digestion 110

4.3.4 Assessment of binding ability 116

4.3.4.1 Enzyme-linked immunosorbent assay 116

4.3.4.2 ELISA using Nickel nitrilotriacetic acid-Atto 488 for direct detection 117

4.3.5 Phage-displayed ScFv recombinant antibody 118

4.4 Discussion 119

4.5 Conclusion 127

5. Alternative strategies for BabA-Crown expression 128

5.1 General overview 128

5.2 Experimental procedures 132

5.2.1 Generation of truncated BabA expression constructs 132

5.2.1.1 Gene design - PCR amplification 134

5.2.2 Protein expression 136

5.2.3 Circular Dichroism Spectroscopy 136

5.2.4 Enzyme-linked immunosorbent assay 136

5.2.5 Peptic digestion 136

5.3 Results 137

5.3.1 Growth medium optimization 137

5.3.2 DNAJ domain 141

5.3.3 Circular Dichroism Spectroscopy 143

5.3.4 Expression of BabA-variants 146

5.3.5 Testing the capabilities of BabA truncates for the drug delivery moiety 151

5.4 Discussion 154

5.5 Conclusion 165

6. Proof-of-principle application: Development of biomimetic BabA–truncates microparticles 166

6.1 General overview 166

6.2 Experimental procedures 169

6.2.1 Protein expression and purification 169

6.2.2 Protein biotinylation 169

6.2.3 Conjugation of micro-particles to the proteins 170

6.2.4 Enzyme-linked immunosorbent assay (ELISA) 170

6.3 Results 171

6.3.1 Assessment of protein biotinylation 171

6.3.2 Functionality of protein-microparticles complexes and binding assessment 174

6.4 Discussion 181

6.5 Conclusion 187

7. General discussion 188

7.1 Study impact and importance 188

7.1.1 Improved periplasmic expression approach 190

7.1.2 Identification of the minimal binding mechanism 191

7.1.3 Creation of Crown-DnaJ-Crown 193

7.1.4 Discovery of partial BabA-Crown resistance to peptic digestion 197

7.1.5 Development of a novel glycan-binding drug using BabA-Crown 199

7.2 Future work 201

7.3 Conclusion 207

Table of Figures

Figure 1.1 Diagram of human stomach and the secretory cells..... 6
Figure 1.2 Schematic illustration of the strategies used for increased drug retention in the stomach 7
Figure 1.3 Schematic representation of effervescent system..... 8
Figure 1.4 Schematic representation of the gastric epithelial mucosal layer ..12
Figure 1.5 The two stages involved in mucus adhesion 14
Figure 1.6 Schematic representation of the interactions of different-sizes particles with the mucous membrane. 16
Figure 1.7 Helicobacter pylori persistence strategies used in the stomach 22
Figure 1.8 X-ray crystallography of BabA J99 (pdb:4ZH7) three-dimensional structure 31
Figure 1.9 Schematic representation of Helicobacter pylori adhesins.....32
Figure 1.10 Comparison of BabA J99 with BabB and BabC adhesins using Phyre2 33
Figure 1.11 Comparison of BabA J99 with SabA and LabA adhesins using Phyre2 34
Figure 1.12 Sequence alignments of BabA with multiples adhesins 35
Figure 1.13 Sequence alignment of BabAJ99 with BabA 17875 38
Figure 1.14 Schematic representation of the proposed biomimetic drug delivery system 41
Figure 2.1 Schematic representation of recombinant technology methodology 45
Figure 2.2 Schematic representation of recombinant protein fates after expression 49
Figure 2.3 Circular map of the plasmid pOPE101 51
Figure 2.4 Schematic representative of a direct ELISA 54
Figure 2.5 Schematic representative of indirect ELISA 55
Figure 2.6 Schematic representative of sandwich ELISA 56
Figure 2.7 Far-UV circular dichroism spectra associated with the various protein secondary structures.....58

Figure 2.8 Schematic representation of the principle of dynamic light scattering 60
Figure 3.1 crystal structure of BabA (pdb:4ZH7) showing the boundaries between the domains and the Hydrogen bonds. 62
Figure 3.2 Crystal structure of BabA-Crown molecular interactions with Le^b. 63
Figure 3.3 Detail of the BabA-Crown showing the Cysteine location 64
Figure 3.4 Interactions of N-acetylglucosamine in Le^b with BabA-Crown 65
Figure 3.5 Schematic representative of the expression cassette 66
Figure 3.6 Gel electrophoresis of BabA-Crown gene 75
Figure 3.7 PCR colony screening for an inserted BabA-Crown gene into pOPE 101 76
Figure 3.8 DNA sequencing analysis 78
Figure 3.9 Protein expression of BabA-Crown 79
Figure 3.10 Effect of addition of chloramphenicol to LB_{ATG} media 80
Figure 3.11 Expression in reducing and non-reducing conditions 81
Figure 3.12 Expression in different concentrations of inducer (IPTG) 82
Figure 3.13 Different IPTG concentrations in the presence and absence of Chloramphenicol 83
Figure 3.14 Bacterial growth and plasmid replication 85
Figure 4.1 Molecular determinant of BabA preferences to Le^b binding 95
Figure 4.2 Multiple alignment of Crown sequences 96
Figure 4.3 Structural organisation of the acid sensitivity system 98
Figure 4.4 Location of the AviTag in the expression cassette of the Crown construct 105
Figure 4.5 Representative PCR products of a mutagenised BabA-Crown construct 105
Figure 4.6 Representative DNA sequence of BabA-Crown construct 106
Figure 4.7 IMAC chromatogram of the purification of BabA-Crown 108
Figure 4.8 Schematic indicating tryptic potential sites 109
Figure 4.9 BabA-Crown protein predicted model 110
Figure 4.10 BabA-Crown after pepsin digestion at pH 4.5 112
Figure 4.11 Coomassie stain for BabA-Crown after pepsin digestion 113
Figure 4.12 BabA crystal structure showing pepsin cleavage sites 115
Figure 4.13 Prediction of BabA-Crown status on H. pylori surface 115
Figure 4.14 Binding of BabA-Crown using sandwish ELISA 116

Figure 4.15 ELISA using Ni-NTA-Atto-448 for direct detection of BabA-Crown binding 117
Figure 4.16 Immunoblotting of Bab-Crown with K22 118
Figure 5.1 Crown-Head-Partial-Length (CHPL) 129
Figure 5.2 structure of BabA-Crown and the Head 129
Figure 5.3 Crystal structure of J99-BabA protein 130
Figure 5.4 Cr.DnaJ-Cr 131
Figure 5.5 Schematic diagram representing the expression constructs built in pOPE101 vector 133
Figure 5.6 Comparison between different LB media 137
Figure 5.7 Effect of different IPTG concentrations 138
Figure 5.8 Comparison between the presence and absence of AviTag sequence after purification 139
Figure 5.9 Western blotting comparing purified BabA-Crown protein in with or without an AviTag 140
Figure 5.10 Screenshots of DnaJ sequence from National Center for Biotechnology Information (NCBI) website 141
Figure 5.11 Segment of BabA residues showing the DnaJ sequence 142
Figure 5.12 Secondary structure, thermal stability and absorbance of BabA-Crown 143
Figure 5.13: Secondary structure and absorbance of BabA-Crown 144
Figure 5.14 Secondary structure and absorbance of Cr-DnaJ-Cr 145
Figure 5.15 Expression of recombinant $BabA_{CHPL}$ protein in E. coli XL10-Gold 146
Figure 5.16 Immunodetection of recombinant BabA-CHPL protein in E. coli XL10-Gold 147
Figure 5.17 IMAC of recombinant $BabA_{CHPL}$ protein 148
Figure 5.18 Analysis of recombinant $BabA_{HCHF}$ protein 149
Figure 5.19 Expression of recombinant Cr-DnaJ-Cr protein 150
Figure 5.20 Coomassie staining for Crown-DnaJ-Crown after pepsin digestion at pH 4.5 151
Figure 5.21 ELISA binding assays for BabA and BabA truncates proteins 153
Figure 6.1 Schematic representation of the biotinylation 170
Figure 6.2 Biotinylation analysis of BabA-Crown proteins 171
Figure 6.3 Biotinylation analysis of Crown-DnaJ-Crown protein 172

Figure 6.4 Biotinylation analysis using ELISA 173
Figure 6.5 Optimisation of protein-microparticle complexation in Coomassie staining 175
Figure 6.6 Schematic diagram shows the possible ways for microparticles size increasing/aggregation 177
Figure 6.7 Evaluating homogeneity of protein solution 179
Figure 6.8 ELISA determination of binding of protein-microparticle complexes glycoconjugates 180
Figure 7.1 Multiple sequence alignment of BabA allelic variants..... 193

List of Tables

Table 1.1 Examples of Lectin-mediated drug delivery systems 18
Table 2.1 Representative of H. pylori Adhesins and their gastric cellular receptors.....28
Table 3.1 Primers for gene amplification 67
Table 3.2 Thermocycling conditions 67
Table 3.3 Primers for colony PCR screening and confirmatory DNA sequencing 69
Table 3.4 Thermocycling conditions for colony PCR.....69
Table 4.1 AviTagTM forward and reverse primers 99
Table 4.2 Thermocycling conditions for mutagenesis 99
Table 5.1 BabA truncated expression constructs 133
Table 5.2 BabA truncated expression constructs 135

List of abbreviations

Abbreviation	Full name
Arg	Arginine
Asn	Asparagine
Asp	Aspartic acid
ATP	Adenosine triphosphate
BabA	Blood group antigen-binding adhesion
BLAST	Basic local alignment search tool
bp	Base pairs
CagA	Cytotoxin-associated gene A
CAM	Chloramphenicol
CD	Circular Dichroism Spectroscopy
CEACAM	Carcinoembryonic Antigen-related Cell Adhesion Molecules
Con A	Concanavalin A
CV	Column Volumes
DLS	Dynamic light scattering
DNA	Deoxyribonucleic Acid
EDTA	Ethylenediamine tetraacetic acid
ELISA	Enzyme-linked immunosorbent assay
Fuc	Fucose
Gal	Galactose
Glc	Glucose
GlcNAc	N-acetylglucosamine
Gln	Glutamine
Glu	Glutamic acid
Gly	Glycine
GI	Gastrointestinal
His	Histidine
Hop	Helicobacter outer membrane porin
Hor	Helicobacter outer membrane relate-
HRP	Horseradish peroxidase
HSA	Human serum albumin

IMAC	Immobilised metal ion affinity chromatography
IPTG	Isopropyl β-D-1-thiogalactopyranoside
ITC	Isothermal titration calorimetry
Le	Lewis
LB	Lysogeny broth
LB_{amp}	Lysogeny broth supplemented with ampicillin
LB_{ATG}	Lysogeny broth supplemented with ampicillin, tetracycline and glucose
LB_{ATGC}	Lysogeny broth supplemented with ampicillin, tetracycline, glucose and chloramphenicol
LPS	Lipopolysaccharides
NCBI	National Centre for Biotechnology Information
NRSB	Non-reducing sample buffer
NCBI	National Centre for Biotechnology Information
Ni-NTA	Nickel nitrilotriacetic acid
NRSB	Non-reducing sample buffer
OD_{600}	Optical density at 600 nm
PBS	Phosphate buffered saline
PBS-T	Phosphate buffered saline supplemented with Tween-20
PCR	Polymerase chain reaction
PDI	Polydispersity index
pDNA	Plasmid DNA (deoxyribonucleic acid)
pelB	Pectate lyase B
SabA	Sialic-acid binding adhesin
SDS-PAGE	Sodium dodecyl sulphate-polyacrylamide gel electrophoresis
SEM	Standard error of the mean
Ser	Serine
SOC	Super optimal broth with catabolite repression
TBE	Tris/Borate/EDTA buffer
TCA	Trichloroacetic acid
TMB	Tetramethylbenzidine
VacA	Vacuolating cytotoxin A
WGA	Wheat Germ agglutinin

CHAPTER ONE

1. Introduction

1.1 The need for a novel gastric drug delivery system

Nano-medicine is the most recent application of nanoparticles in the medical field. This fast-growing application opened a new era for disease treatment, including cancers and fatal diseases (Hua *et al*., 2018, Patra *et al*., 2018). Nanoparticles are small particles, ranging from 1-100 nanometers in size (Shi *et al.,* 2017), which, for therapeutic purposes, are usually synthesised from safe-to-use polymers, e.g. polylactic acid. Natural/synthetic polymeric nanoparticles such as sugar-based compounds (glycopolymers) have been extensively used to mediate formulation delivery due to their biocompatibility and biodegradability (Zhang *et al.,* 2015). The polymer surface can be modified to perform specific functions, such as direct cell targeting, bio-adhesion, controlling cellular behaviour or involvement in sub-cellular interactions (Chen *et al.,* 2018b). These functionalised nanoparticles are formed after being loaded with a therapeutic formula, thus named drug carrier or drug delivery system. There are mainly two forms: nanocapsules, in which the formulation is encapsulated, and nanospheres, in which the formulation is distributed in the polymeric matrix (George *et al.,* 2019). Nanoparticles made from biodegradable substances are more efficient, for therapeutic purposes, than other conventional systems. They are characterised by high therapeutic effect, controlled release, deep tissue penetration and reactivity within localised site with reduced systemic side complications (Lai *et al.,* 2009, Hua *et al.,* 2015). However, the effectiveness of these nanomaterials depends on the therapeutic moiety being carried and their ability to sustain the association with the drug after administration (Choi and Frangioni, 2010).

There are two major routes for drug delivery, either parenterally through injection or orally through swallowing (Gupta *et al.,* 2009). The oral route is the most commonly used for drug administration because of its simplicity, lack of pain, ease of dosage administration and high patient compliance (Viswanathan *et al.,* 2017). However, it is not effective compared to the parenteral route, which directly exerts its therapeutic effects systemically, while drugs administrated orally need to be absorbed before passing through the liver to the blood circulation. Absorption of drugs in the gastrointestinal tract is affected by several factors including the drug (i.e. type, dosage and solubility), patient situation (i.e. disease, body physiology and fed/fasting condition), transit time (contact period between the drug and site of absorption) and gastric emptying rate. The latter is defined as the rate of emptying the solid and liquid from the stomach into the small intestine (Masaoka *et al*., 2006, Rouge *et al*., 1996, Goyal *et al*., 2019). For any absorbed drug to exert its systematic therapeutic action, a sufficient contact time with the site of absorption is an essential requirement (Wen *et al.,* 2015). Orally administrated drugs have a short time window for absorption, due to rapid passage through the stomach and the upper small intestine. The estimated transit time of the dosage formula in the stomach is 2 hours and depends on the feeding status, while in the small intestine it is ~3 hours and ~20 hours in the colon (Davis *et al.,* 1986, Davis, 2005). Obviously, the colon has a longer transit time and represents an optimal site for drug absorption. However, many features reduce drug absorption efficiency such as high viscosity, low mixing ability, high water absorption capacity and high content of diverse microflora which can metabolise many drugs (Philip and Philip, 2010). Accordingly, increasing drug bioavailability could be achieved by extending the therapeutics residence time in the upper gastrointestinal tract. Therefore, various gastroretentive drug delivery strategies have been attempted to significantly prolong drugs absorption in a controlled release and subsequently maximise the dosage bioavailability (Kumar and Kaushik, 2018).

Gastroretentive drug delivery systems as a promising strategy could provide many advantages such as broaden the narrow window, reduce the drug loss, increase drug solubility and promote drug local activity in both the stomach and duodenum (Lopes *et al.,* 2016). Many conditions affect drug retention time in the stomach related to the drug formulation, administration conditions and individual physiological factors. Formulation-related factors are drug density, size and shape

of the formulation. Administration conditions are stomach state (fed/fasted), type of diet and food caloric content, while the physiological factors are age, gender, body weight and disease status (Alomar, 2014, Martinez and Amidon, 2002).

Based on the pH-partition hypothesis, weakly acidic drugs (non-ionised at gastric acidic pH) would be absorbed through the stomach while basic drugs are absorbed through the intestine as they are protonated (Charifson and Walters, 2014). However, some weakly base drugs, such as the pain reliever antipyrine, are absorbed in the stomach (Masaoka *et al.,* 2006). Weakly acidic drugs such as furosemide and misoprostol can also benefit from prolonged gastric residency time. An example of a drug with high solubility in gastric acid but absorbed in the upper small intestine is Levodopa. Furosemide is a potent loop diuretic drug used for treating congestive heart failure (Oh and Han, 2015). It is unionized at gastric acidity (pKa=3.9) and can be easily absorbed across the stomach (Patel *et al.,* 2010). Misoprostol is a synthetic analogue of prostaglandin E1, acts as gastric acid anti-secretory drug and is used for treatment of peptic ulcers (Watkinson *et al.,* 1988). Levodopa, used for treatment of Parkinson's disease, is a large neutral non-proteinogenic amino acid absorbed mainly in the small intestine. It cannot cross the membrane without amino acid carrier proteins. Thus, slowing its passage in the stomach may add an advantage for its absorption (Nyholm and Lennernas, 2008). It is worth to note that prolonged residence time for some drugs, e.g. nonsteroidal anti-inflammatory drugs (NSAIDs), could lead to undesirable effects such as gastric lesions (Bjarnason *et al.,* 2018).

To achieve high therapeutic levels in the stomach, some hurdles must be overcome. Firstly, optimization of the dose/concentration that the nanoparticles need to carry for efficient transit time and controlled release pose a challenge. Therefore, site-specific interaction between the cellular receptor and coated nanoparticles is needed. Secondly, gastric acidity and enzymatic action of pepsin create a hostile environment, particularly for drugs of a proteinaceous nature. Thus, peptide/ protein stability in this condition is an additional challenge. However, directing the proteinaceous moiety of the gastroretentive drug system to the apical region of the gastric epithelial cells, where a neutral environment exists, would address the issue of peptic digestion, as pepsin is enzymatically inactive at neutral pH. Thirdly, gastric mucus' rapid trapping/shedding hinder drug penetration and subsequent absorption. To overcome these limitations, two recent

approaches to preserve the therapeutic and nanoparticle formulations are being developed. These are either encapsulation of the nanoparticle to dually shield the drug and control drug release or by nanoparticle surface modification to decrease the muco-adhesion ability while targeting specific cellular receptors (Ensign *et al.,* Kalita *et al.,* 2015). Despite these achievements, gastrointestinal absorption still depends on the ability of the therapeutic molecules to penetrate and cross the mucosal barrier (Kimura and Higaki, 2002). Thus, careful consideration of the nature of the nanoparticle and their interaction with the mucosal barrier must be taken into account (Laroui *et al.,* 2011).

Encapsulation of nanoparticles with molecules having specific interactions with gastric cellular receptor is a promising strategy for gastric drug delivery. If peptide-coated nanoparticles conjugated with a drug was developed to be administrated orally then cross the mucus layer to the plasma membrane, greater therapeutic effects could result. Coating the particles with a proteinaceous ligand to target a specific site, and hence, increasing the gastroretention time is the ultimate goal of the current project. From the aforementioned, possible relevant drugs can be candidates for developing the gastroretention system as categorised below:

1. Locally active drugs in the stomach:-
   These drugs are mainly used for either targeting the gastric epithelium cell such as misoprostol or for neutralising the gastric acidity e.g. antacids or targeting *Helicobacter pylori* e.g. amoxicillin (Kim *et al.,* 2015, Salmanroghani *et al.,* 2018) .
2. Drugs primarily absorbed in the stomach or have a narrow absorption window in the intestine:-
   These drugs use the gastric acidic environment to free the active compounds such furosemide or for drug that starts the action in the stomach such as riboflavin, member of vitamin B family, which is subsequently absorbed through carrier-mediated transport process after hydrolysed into flavin adenine dinucleotide (FAD) and flavin mononucleotide (FMN) (Darandale and Vavia, 2012, Szczuko *et al.,* 2019).

3. Degradable drugs in the intestine:-
   This category used to improve bioavailability of drugs that are susceptible to degradation by the microbiota present in the colon e.g. Ranitidine, H2 receptor antagonist used for peptic ulcer treatment (Swanson, 2015).
4. Low soluble drugs at high pH:-
   This category includes some lipophilic drugs that are poorly water soluble and highly soluble in acidic pH such as diazepam, antihypertensive (Sharma *et al.,* 2015).

1.2 Strategies for gastric retention

The stomach is a muscular organ located in the upper left part of the abdomen. It breaks down the food and the resulting chyme is released in a control way through the duodenum to the small intestine. Structurally, the human stomach (Figure 1.1) mainly consists of five anatomic parts: cardia (entrance), fundus, body (regions for undigested foods), antrum and pylorus (mixing and emptying pump). The pylorus presents in the proximal region of the stomach in contact with the intestinal upper part, the duodenum. It represents the major determinant of gastric residence time (Mandal *et al.,* 2016).

At the cellular level, the stomach has different types of secretory cells (Schubert and Peura, 2008).

1. The mucus cells (foveolar), which are subdivided into surface and neck cells. These cells secret mucus and bicarbonate to neutralise the gastric acidity.
2. Parietal cells, which gave the stomach the acidity by secreting the gastric acid, hydrochloric acid.
3. Chief cells, which produce the pepsinogen and lipase for protein and fat digestion, respectively.
4. G cells, which secrete gastrin hormone.

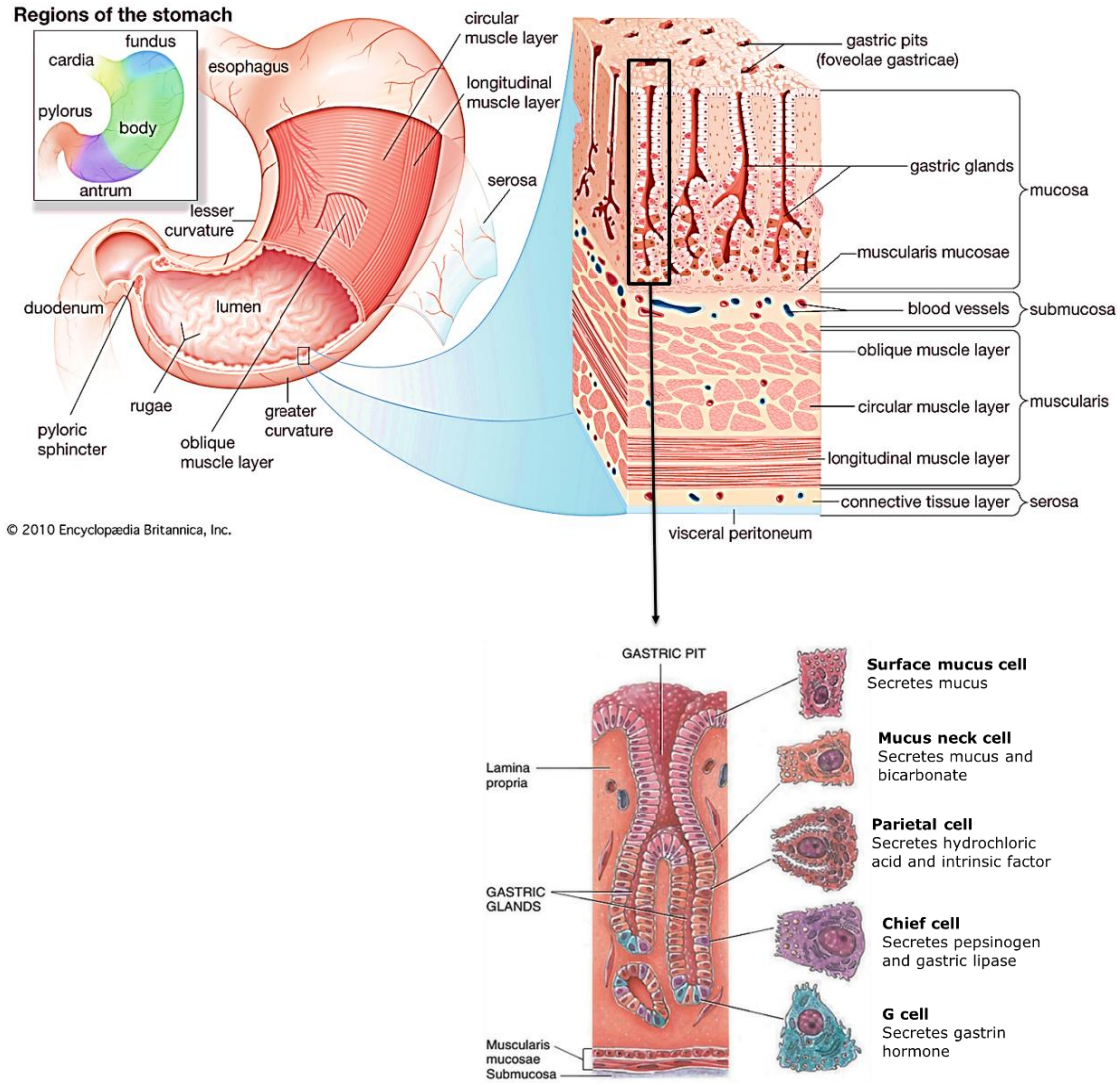


Figure 1.1 Diagram of human stomach and the secretory cells (Britannica, 2010, Proprofs, Schubert and Peura, 2008)

Many strategies have been tried to prolong the residence time of the therapeutic formula in the stomach. In spite of the difference in the concepts, all aimed to maximise the drug efficiency with minimum undesirable effects (Waterman, 2007). The main three gastric retention formulation approaches are floating systems, expanding or swelling systems, and bioadhesive systems (Figure 1.2)

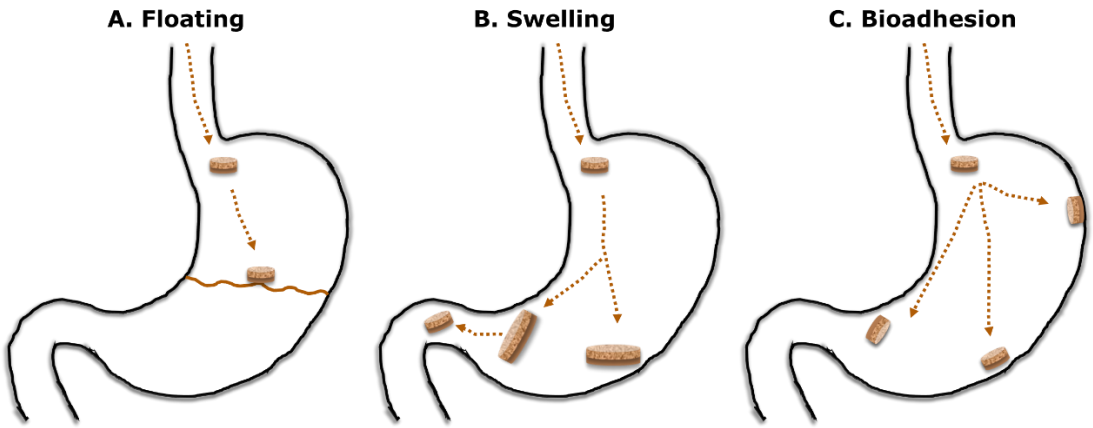


Figure 1.2 Schematic illustration of the strategies used for increased drug retention in the stomach (Fasinu *et al.,* 2011)

A: Low density (< 1 g.cm^3) drugs float on gastric fluid. B. High density (> 1 g.cm^3) drugs incorporated with heavy materials such as Barium sulfate or iron powder sink before swelling or expanding (super-swelling) in size due to water uptake and blocked within the pylorus. C. Bioadhesive delivery systems binding to the gastric wall (mucus layer or epithelium).

1.2.1 Floating strategy

In this low-density strategy, the therapeutic formulation, e.g. Levodopa or Madopar® HBS, remains at the top of the gastric fluid contents as buoyant without altering the gastric emptying rate. As the floating dosage is far from the pyloric sphincter, it will stay for a prolonged time in the stomach. Special criteria must be met such as forming a cohesive gel barrier, maintaining the lower gravity over the gastric fluid and dissolving slowly to preserve the drug (Pawar *et al.,* 2011). Floating systems are classified into two systems, effervescent and non-effervescent. In effervescent systems (Figure 1.3), floating is achieved by inert-gas formation, e.g. carbon dioxide, while in non-effervescent systems, floating results from foam-making polymers containing polypropylene (Streubel *et al.,* 2006a). However, successful application of this strategy is restricted to the patient in the fed state only, due to the need for gastric fluid in the stomach to be floated. It is also not suitable strategy for drug that have no stability/ are not soluble in the gastric fluid (Erni and Held, 1987, Pawar *et al.,* 2011).

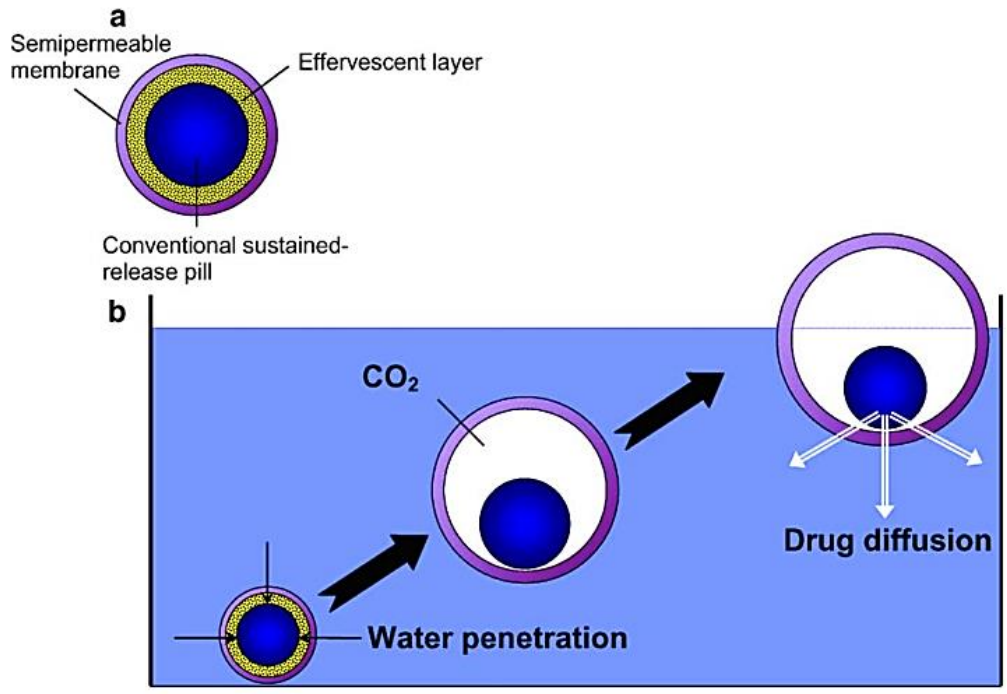


Figure 1.3 Schematic representation of effervescent system

a. Schematic diagram of the drug system.
b. Floating occurs when water penetrate the effervescent layer and generates CO_2 (Bardonnet *et al.,* 2006).

Floating strategy is mostly studied for the eradication of *H. pylori* using floating *in situ* gelling system containing amoxicillin (Rajinikanth *et al.,* 2007), floating alginate beads carrying metronidazole, or floating tablets for the delivery of the enclosed clarithromycin (Nama *et al.,* 2008).

1.2.2 Swelling strategy

Known also as a size-increased or expanding system, in which the normal-sized drug swell upon contact with the gastric fluid. This enlargement confines the drug, e.g. anti-type 2 diabetes mellitus (T2DM) metformin or Glutmetza®, in the stomach (Schwartz *et al.,* 2006, Jabbour and Ziring, 2011). It requires three configurations: 1. Small form for oral uptake, 2. Expandable gastroretentive form and 3. Small form, after dosage release, for stomach evacuation (Klausner *et al.,* 2003).

This strategy has an advantage over the floating because it is less dependent on the fed/fasted state as the size increase upon contact with the gastric juice (Tripathi *et al.,* 2019). However, it needs to display very controlled dosage-release properties to enable a constant absorption rate (Davis, 2005). This could be due to the slow increasing-rate of hydrogel materials and degradation after drug release (Chen *et al.,* 2000), in addition to the life-threatening hazard of long-lasting residence time or blockage in the stomach upon ingestion of multiple dosages (Streubel *et al.,* 2006a).

1.2.3 Bioadhesion strategy

In this strategy, attachment of synthetic/natural drug formulation to the stomach occurs through either specific interaction with the target cellular receptor or ligand (cytoadhesion) or non-specifically (mucoadhesion) with the gastric mucosal surface (Tripathi *et al.,* 2019) In contrast to the above-mentioned strategies, bioadhesive systems target the stomach wall for adherence via muco-adhesive polymers. Moreover, neither does it require the presence of gastric fluid nor does it depend on patient fed/fast states, as formulation absorption is achieved through passive diffusion (Zhao *et al.,* 2014). Immobilising the drug in close proximity to the mucus or the gastric epithelium generates a concentration gradient, which enhances absorption via passive diffusion (Woodley, 2001). In addition, the formulation could incorporate natural molecules for controlled release and extending contact time (Peppas *et al.,* 2009).

1.2.3.1 Mucoadhesion

Mucoadhesion refers to surface adhesion of formulation to the mucus gel layer above the gastric epithelial cells. This strategy has gained an increasing interest to deliver both small and large mucoadhesive particles/polymers (García-Díaz *et al.,* 2018).

The stomach internal surface is covered by gastric secretions which mainly are mucus, HCl, HCO_3^-, intrinsic factors and the digestive enzymes (pepsinogen and lipase) (Rangachari, 2007). Mucus forms a continuously renewed hydrogel layer lining the gastro-intestinal tract and acts as a dynamic milieu for nutrient exchange. In the stomach, the viscosity of the mucus gel layer maintains the retention of water and HCO_3^- near the gastric epithelium (Cone, 2009). It also protects the underlined epithelial cells from both exogenous and endogenous factors. Exogenous factors can be chemical agents or biological damaging agents, such as invading pathogens. Endogenous factors such as hydrochloric acid and proteolytic enzymes can lead the stomach to digest itself. Mucus mainly consists of water (~ 95%) and glycoproteins (~ 5%) called mucins (Bergstrom and Xia, 2013). Mucins are highly O-glycosylated proteins encoded by 20 genes which produce proteins composed of multiple tandem repeats of Serine and Threonine through which the oligosaccharides are O-linked (Bansil and Turner, 2018). Mucins

produced by mucosal epithelial cells can be subdivided into two types, membrane-bound (e.g. MUC1) and secreted (e.g. MUC6 and MUC5AC) mucins (Figure 1.4). MUC1 is highly expressed in foveolar cells as bound mucins and shed into the gastric juice, thus obstructing prolonged bacterial, e.g. *Helicobacter pylori*, adherence (Linden *et al.,* 2009). MUC1 also limits bacterial density through steric hindrance and by acting as a releasable decoy (Linden *et al.,* 2009). Secreted MUC5AC constitutively comprises the apical mucous layer of the gastric foveolar cells (Linden *et al.,* 2004), while MUC6, which originates from the mucous neck cells, lies deeper in the gastric glands (De Bolos *et al.,* 1995). In the stomach of healthy individuals, the glycan epitopes of gastric mucins are decorated by two types of ABO/Le blood group antigens. The difference between these types lies in the way the core N-acetyllactosamine (LacNAc) is linked to the ABO/Le blood group antigens. This core is anchored to the chains through Galβ1-3GlcNAc and Galβ1-4GlcNAc linkages in type 1 and type 2, respectively (Jin *et al.,* 2017). MUC5AC cells constitutively co-express type 1 Lewis a (Le^a) and Lewis b (Le^b) blood group antigens, whereas MUC6 a member of type 2, contains Lewis X (Le^x) and Lewis y (Le^y) antigens.

Even though mucins form a protective layer on the epithelial cells protecting these cells from the combined action of pepsin and low pH, it forms a preferred micro-environmental niche for *H. pylori* (Schreiber *et al.,* 2004). However, the gastric lumen is very acidic (pH median 1.4). This low pH is gradually neutralised until it reaches 7 at the epithelial cell surface (Schreiber *et al.,* 2004).

During food digestion, the luminal pH ranges between 5 – 7 as it buffered by the digested foods and bicarbonate secreted by the mucosal cells (Feldman, 1983), but during starvation the pH drops to about 2 as the stomach becomes an un-buffered environment (Scott *et al.,* 1998, Pflock *et al.,* 2004). During the meal-period pepsin (pepsinogen) is secreted by gastric chief cells for digestive processes. Simultaneously, the parietal cells secrete hydrochloric acid (HCl), which activates the pepsin (Gritti *et al.,* 2000). Thus, the acidic condition optimizes and regulates peptic activity. At low pH (1.5 -2.5) pepsin reaches the maximal peptic hydrolytic activity. This activity persists up to about 70% at pH 4.5 (Piper and Fenton, 1965). Further increase (pH 5 - 7.5) progressively inhibits enzymatic activity before it is irreversibly inactivated at pH 8 or above (Koufman and Johnston, 2012).

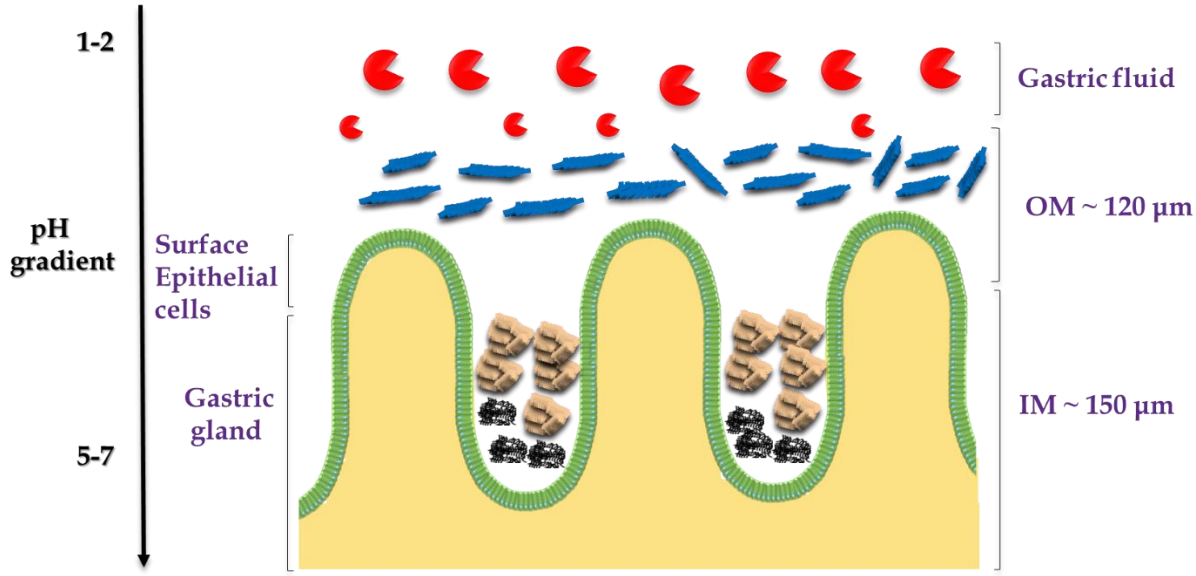


Figure 1.4 Schematic representation of the gastric epithelial mucosal layer

Gastric epithelial cells are covered by mucus layers. Inner mucus (IM) mostly consists of MUC6 and includes secreted MUC1, while MUC5AC comprises most of the outer mucus (OM) layer (Linden *et al.,* 2004, De Bolos *et al.,* 1995). Numbers indicate the thickness of the mucus gel layer. MUC1= , MUC5AC= , MUC6= , Pepsin= .

Research into mucoadhesive drug delivery strategies first began in 1984. Since then, various mucoadhesive polymers were tested *in vitro* and *ex vivo*. These polymers are divided into two broad subsets, cationic and anionic. Cationic polymers such as chitosan, adhere to mucins via electrostatic interactions such as ionic or through covalent disulfide bonds between thiolated polymers and the cysteine-rich glycoproteins in the mucus (Lai *et al.,* 2009). Anionic polymers, e.g. Polycarbophil, in which interaction occurs via single or a combination of interactions such as hydrogen bonding, van der Waal's or mucins-polymers entanglement (Laffleur *et al.,* 2017).

In general, the most studied polymers used as mucoadhesive formulations for drug delivery can be categorised into four classes:

1. Hydrophilic macromolecules, e.g. polyacrylic acid derivatives including carbomer or polycarbophil (Carlson *et al.,* 2018).

2. Semi-synthetic macromolecules, e.g. chitosan or acrylated chitosan, derived from chitin (Eliyahu *et al.,* 2018).

3. Modified by adsorption enhancers (thiolated polymer) such as thio-carbophil or chitosan-cysteine which forms a disulfide bond between the free thiols on the polymer and the cysteine residues on the mucin backbone. These materials have been classified as the first generation (Felt *et al.,* 1998, Lee *et al.,* 2000).

4. Plant mucoadhesive constituents such as gliadin, one constituent of gluten and derived from wheat and corn (Malekzad *et al.,* 2018).

Six hypotheses, reviewed in (Carvalho *et al.,* 2010, Carlson *et al.,* 2018), were invoked to explain the exact mechanisms of the sticky interaction between the polymers and the mucus layer. Due to the complexity of the interaction, the exact mechanism of adhesion is not fully elucidated. However, two stages for mucus adhesion have been identified, the contact and the consolidation stages (Figure 1.5). The first stage involves the formulation's initial contact with the mucus. The second stage is the consolidation stage, which entails many physicochemical interactions to tighten the adhesion (Smart, 2005).

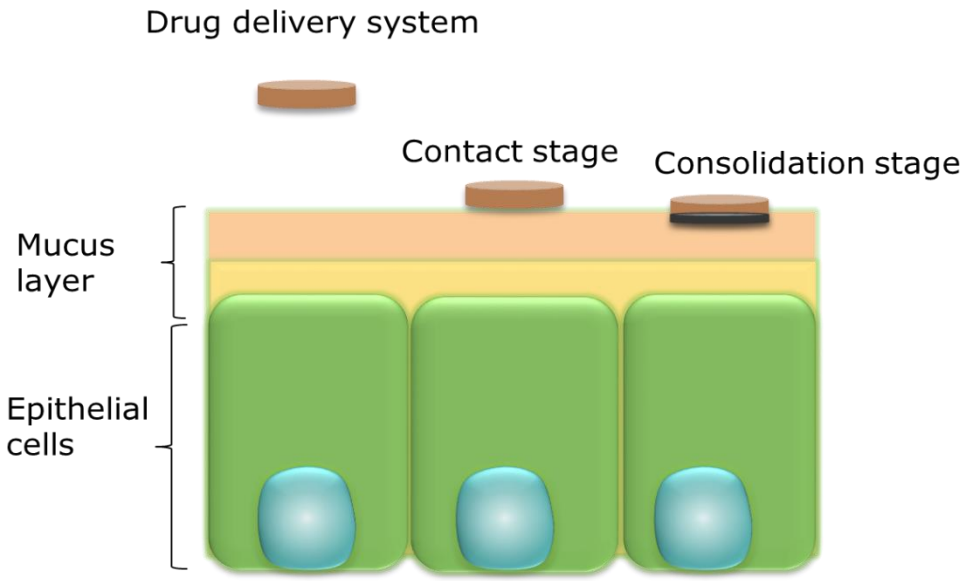


Figure 1.5 The two stages involved in mucus adhesion

Drug system reaches the mucus and comes close to the mucus. Then a consolidation step takes place to strength the interaction.

Although there is an increasing interest in mucoadhesion application and many polymers have been studied, *in vivo*, to mediate the attachment, two major obstacles exist. First, mucin is a thick and highly gelatinous layer and this affects formulation permeation/diffusion as it form an entangled network (García-Díaz *et al.,* 2018). Secondly, the frequent mucus secretion and turnover (Khanvilkar *et al.,* 2001) clears the mucoadhesive drug delivery systems (Streubel *et al.,* 2006b). Furthermore, due to non-specificity, some portion of the administrated drug may be subject to premature binding or spread over the mucus such as in case of polycarbophil, which forms sticky attachment (Ponchel and Irache, 1998, Khosla and Davis, 1987). This may also lead to difference in dosage concentrations or ulcer formation.

The main drawback for the mucoadhesive drug delivery system is its non-specificity. This is because mucins share common structures that are distributed throughout the gastrointestinal tract. This highlights the need for alternative strategies to develop better gastroretentive drug delivery systems.

1.2.3.2 Cytoadhesion

Cytoadhesion describes ligand-to-receptor interactions on the gastric epithelium, resulting in surface attachment. This is a very promising strategy towards achieving efficient gastric targeting strategy and longer retention time. In principle, the presence of various glycoproteins and glycolipids on the cell surface provides an arena for specific interactions. In addition, drug localisation will be less affected by the frequent mucus shedding and turn over. Gastric epithelial cells have a physiological turnover rate of 2 to 3 days (Kim *et al.,* 2010). Therefore, coating particles with a ligand, which would show high affinity to epithelial cell receptors, can significantly increase the duration of the adhesive interaction compared to non-specific mucoadhesion. To generate cytoadhesive drug delivery system, it is necessary to:

1. Identify the corresponding receptor-ligand pair to specify the target immobilised area (i.e. normal or diseased),

2. Using biomimetic ligand as a moiety for targeting the therapeutics with biodegradable and biocompatible particles.

From the aforementioned, it is better to have insights from Nature to learn about the ability of the formulations to reach the epithelial surface through the mucosal layer. A possible strategy was inferred from viruses that invade the underlying gastric epithelial cells (McGuckin *et al.,* 2011). It was proposed that diffusion of the formulation to reach the epithelium depends on the size (Figure 1.6). Human papillomavirus (~55 nm) and Norwalk virus (~38 nm) are two examples of natural nanoparticles that rapidly partition through the mucus, while viruses bigger than 100 nm (e.g. herpes simplex virus type 1 which is 180 nm) are slower mucus-penetrators (Olmsted *et al.,* 2001). Thus, small size (< 100 nm) is a characteristic which enable nanoparticles partition through the mucus avoiding the clearance mechanism. By mimicking these viral permeation mechanisms, it could be possible to increase drug bioavailability by employing rapid mucus penetrating carriers. Large polymeric nanoparticles (200 – 500 nm) coated with 2 kDa polyethylene glycol (PEG) also showed rapid diffusion ability (Lai *et al.,* 2007). It was thought that the hydrophilic nature of PEG results in a shield preventing the hydrophobic interactions between the particles and the mucins (Lai *et al.,* 2009). However,

decreasing the particles hydrodynamic diameter size to about 173 nm, resulted in rapid diffusion through fresh undiluted human cervicovaginal mucus (Tang *et al.,* 2009). Recently, mucus penetration nanoparticles coated with mucus-inert agent facilitated insulin delivery *in vitro* using HT29-MTX-E12 (E12) cell line and *in vivo* using diabetic rats (Shan *et al.,* 2015). Particles with a nanometer scale have a large surface area to volume ratio. This feature enables the nanoparticles to establish a longer period for mucus contact/ bonding than the larger-sized ones (> 1 mm). However, variable degrees of nanoparticles adsorption occurred. Large nanoparticle (~560 nm) may be, after initial contact, immobilised/ accumulated due to steric obstruction. This could lead to high drug concentration or uncontrollable release (das Neves *et al.,* 2011).

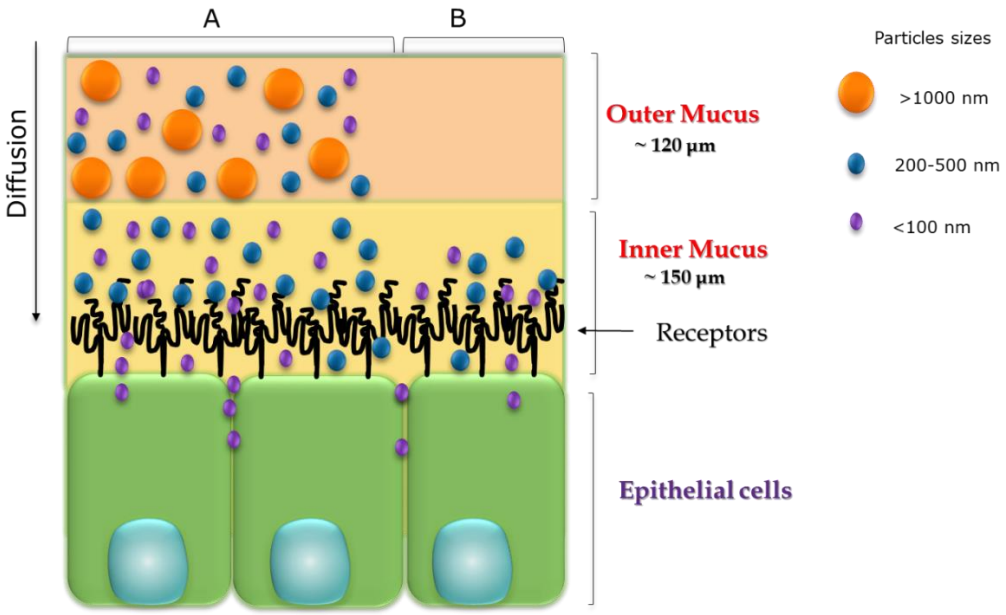


Figure 1.6 Schematic representation of the interactions of different-sizes particles with the mucous membrane.

(A) After administration to the mucus, particles with different sizes will interact and diffuse across the mucus based on their size and adhesive properties. Particles of micrometric size due to their steric hindrance will not pass through, but might form sticky adhesion, while moderate (200 nm) and smaller (less than 100) particles with adhesive properties can diffuse. Only smaller-size particles can reach the epithelial surfaces. (B) Upon mucus clearance, particles are eliminated from the luminal site, while smaller nanoparticles that already passed through will penetrate the cells (das Neves *et al.,* 2011).

In order to address the potential demand for specific receptor-mediated bioadhesive system, lectins were extensively studied. Lectins specifically bind the diverse glycans present on the surfaces of the gastric epithelial cells. This ability referred lectins as the "second-generation bioadhesives" (Lehr, 2000). Therefore, the concept of "Lectin-mediated drug delivery systems" has been an attractive objective for controlled delivery of the pharmaceuticals (Wirth *et al.,* 2002a).

"Lectin" comes from the Latin verb "*legere*" which in its oldest meaning can be translated as "to gather, or to choose" (hence the word 'selection') (Lam and Ng, 2011). It refers to a class of proteins, originally extracted from plants, which can agglutinate red blood cells. Later, the term was extended to describe a wide variety of carbohydrate-binding proteins from animals, plants, viruses and fungi (Brooks, 2017). Based on their sugar affinity, they are classified into five groups (1) glucose/mannose- (2) L-fucose- (3) sialic acid- (4) N-acetylglucosamine- (5) galactose- and N-acetyl-D-galactosamine- -specific lectins (Slifkin and Doyle, 1990). Recently, several types of lectins have been engineered to confer specific sugar-binding properties (Hirabayashi and Arai, 2019).

Lectins bear potential as formulation carriers due to their role as specific receptor-adhesin and their resistance to acidic and enzymatic degradation (Bies *et al.,* 2004), in addition to their ability to promote internalisation (Woodley, 2000). There are many studies which used several types of lectins for drug delivery (Table 1.1). However, neither all of the mucus-specific ligands are discovered nor their molecular interactions were elucidated as these studies are still restricted to *in vivo* studies (Corfield, 2015). Recent research uses lectins to study the changes in the glycosylation patterns found on the surface of gastric mucin glycans (Jin *et al.,* 2017), exploiting their specificity as a tool for early prognosis/diagnosis of gastric cancer (Li *et al.,* 2016b) or using its antagonistic activity for therapeutic purposes (Mazalovska and Kouokam, 2018, Lam and Ng, 2011). Lectins from *Urtica dioica* (UDA) displayed anti-proliferative and apoptotic effects on AGS cancer cell lines (Estrada-Martínez *et al.,* 2017). This anti-cancer therapeutic effect was confirmed using lectin from *Pseudomonas fluorescens* (Sato *et al.,* 2012). This study revealed that this mannose high binding lectin downregulates cell surface integrin/epidermal growth factor receptor and induces autophagy and programmed cell death in human gastric cancer cells *in vitro* and *in vivo* (Sato *et al.,* 2016).

Table 1.1 Examples of Lectin-mediated drug delivery systems

Lectin	Source	Receptor	Carrier nature	Targeting	Ref.
Lycopersicum esculentum (LEA/TL)	Tomato	N-acetyl-D-glucosamine	Polystyrene latex	The small intestine in the rat (*ex vivo*)	(Naisbett and Woodley, 1994)
				Pig enterocytes (*in vito*)	(Lehr *et al.,* 1992)
Triticum vulgaris agglutinin (WGA)	Wheat germ	N-acetyl-D-glucosamine/sialic acid	Polystyrene latex	M-cells Peyer's patches and enterocytes Uptaking by epithelial cells	(Haltner *et al.,* 1997) (Pusztai *et al.,* 1993)
Canavalia ensiformis Agglutinin (Con A)	Jack bean	α-D-Mannose/ Glucose	Microparticles	GIT Peyer's patches in mouse	(Foster *et al.,* 1998)
		α-D-mannose	Polystyrene nanoparticles	Human colon carcinoma cell line (Caco-2)	(Russell-Jones *et al.,* 1999)
Ulex europaeus lectin I (UEA I)	Gorse	α-L-fucose	vicilin (storage protein from Pisum sativum) nanoparticles)	*In vitro*	(Ezpeleta *et al.,* 1996)
			Carboxylated microspheres	Peyer's patches M-cells in mouse gut loop model	(Foster *et al.,* 1998)
Heat-labile toxin B subunit (LTB)	*E. coli*	Galactose	Polystyrene nanoparticles	glycolipids or glycoproteins on the luminal surface of the epithelial cells	(Russell-Jones *et al.,* 1999, Russell-Jones, 2001)

As reviewed from the above mentioned examples, lectin-mediated drug delivery systems have the potential for mucus targeting, however, the ability of lectins to diffuse through the mucus to target specific receptor was not fully studied. Most of the studies showed a variation in the specificity, toxicity and immunogenicity of the lectins used. More attention was devoted to developing strategies for particle conjugation, rather than to analyse their cyto-specific binding ability. Further research is required to improve the gastric cytoadhesive approach, as some promising results are increasingly obtained, but only for targeting the intestine, as exemplified below.

Oral colon-targeting controlled release delivery systems were developed using glycoprotein-resistant starch conjugated with concanavalin A and loaded with insulin, demonstrating a good release in Type II diabetic rats and prolonged adherence in the gut (Situ *et al.,* 2015). However, variable concentrations in the plasma glucose were observed, which may indicate variable bioadhesion property or different bioavailability of insulin delivered. In another study, after *in vitro* adjustment of the release property of concanavalin A-conjugated resistant-starch-acetate (RSA) bioadhesive film, a broad distribution of the microparticles and quick excretion from the body was observed in the mice used (Bie *et al.,* 2016). Lectins' nonspecific binding is a hindrance, preventing further clinical application (Montisci *et al.,* 2001). Lectin non-specificity results from the similarity of the carbohydrates/glycan pattern of the mucins throughout the gastrointestinal tract (Wirth *et al.,* 2002a). Other factors may restrict the clinical approval are lectins' activity as a growth factor, digestive enzyme inhibitor and modifier of the gut natural flora (Woodley, 2000). For these reasons, adopting bacterial lectin-binding ability offers a promising cytoadhesive strategy. Bacterial (*E. coli*) Type 1-fimbriae was investigated to produce receptor-specific drug, adhesive to intestinal K99-receptor. However, it was intended to prolong drug transit time in the gut (Gabor *et al.,* 1997, Bernkop-Schnürch *et al.,* 1995).

To our best knowledge, employing bacterial lectins for specific gastric cytoadhesion strategy has not been carried out. This study proposed for the first time the use of bacterial adhesins as novel way to simulate the gastric bacterium, *H. pylori*. This bacterium developed multiple adhesins for attachment to the stomach epithelial cells and survives in this hostile environment (Kim *et al.,* 2010).

1.3 *Helicobacter pylori*

In the last century, it was thought that human stomach is sterile, until Barry Marshall and Robin Warren's (Marshall and Warren, 1984) discovery of *Helicobacter pylori* (previously named *Campylobacter pyloridis*) in 1983. This finding radically changed our understanding of stomach ecology and bacterial survival. Intensive research was carried out to understand the nature of this spiral-shaped bacterium, to elucidate its survival strategies in this hostile environment, to understand its mechanism of attachment, and how the bacterium persists in the gastric mucosa. Recent research confirmed the coadaptation of this Gram-negative bacterium and ancient humans over several millennia (Atherton and Blaser, 2009). Human is the sole reservoir, so this bacterium could be used to track people's migration out of Africa (Megraud *et al.,* 2016). Interestingly, *H. pylori* is still present in the gastric mucosa of about half of the world's population (Yang *et al.,* 2013). Over 80% of *H. pylori* infected individuals are asymptomatic, and the disease is more prevalent in developing countries (up to 90% of the population) (Mishra and Verma, 2010) than in developed countries (40% or lower), where there are higher hygienic standards (Kusters *et al.,* 2006). Overall, epidemiology of disease is varied based on ethnicity, geographic regions and age (Bruce and Maaroos, 2008). Even though, *H. pylori* strains of European phylogeographic origin are more susceptible to lead to the development of gastric malignancies than the African strains (de Sablet *et al.,* 2011).

Prolonged bacterial adherence to the gastric epithelium progresses to cellular impairment, followed by a wide spectrum of pathologies, ranging from superficial gastritis, to chronic atrophic gastritis and peptic ulceration (Blaser and Berg, 2001). An accumulating body of evidence attributed the development of gastric cancer, gastric lymphoma, gastroduodenal ulcers and mucosa-associated lymphatic tissue (MALT) lymphoma to *H. pylori* (Yokota *let al.,* 2010, Algood and Cover, 2006). Among those diseases, gastric cancer is the most predominant form and comes second worldwide in terms of causes of cancer-related mortality (Moore *et al.,* 2011). In 1994 the World Health Organization's International Agency for Research on Cancer classified *H. pylori* as class 1 carcinogen (McClain *et al.,* 2009).

H. pylori has been suggested to play a protective role not only against asthma and allergic diseases (Zevit *et al.,* 2012), but also as a protective agent in tuberculosis reactivation (Perry *et al.,* 2010), diabetic patients (Chen and Blaser, 2012), oesophagal adenocarcinoma and Barrett's oesophagus (Rokkas *et al.,* 2007).

The mechanism of *H. pylori* transmission between individuals or from parents to their offspring is not exactly known, but potentially, this bacterium is transmitted through the oral-route from the mother or other family members during early childhood (Harris *et al.,* 2013). Furthermore, some studies stated the occurrence of the faecal-oral route from contaminated food (Vale and Vitor, 2010), milk (Dore *et al.,* 2001), drinking water (Hulten *et al.,* 1996) or coastal freshwater, estuary and marine waters (Twing *et al.,* 2011).

1.3.1 Mechanisms of persistence

H. pylori is a non-acidophilic bacterium but to overcome the gastric acidic conditions, it developed several survival mechanisms for persistence (Figure 1.7). These mechanisms (as discussed below) starts by using urease to neutralise the surrounding microenvironment, then use the flagella to move along the pH gradient. This is followed by utilising the outer membrane proteins (OMPs) or adhesins for adherence before releasing toxins to damage the gastric cells (Dunne, 2014). To colonize the mucosal layer of the gastric epithelia, *H. pylori* specifically interacts with host cellular ligands. Attachment to the gastric mucosa is a critical step in initiation of persistent infection. Binding helps the bacterium to obtain nutrients, resist peristalsis and gastric emptying forces as well as deliver its toxins (Odenbreit, 2005).

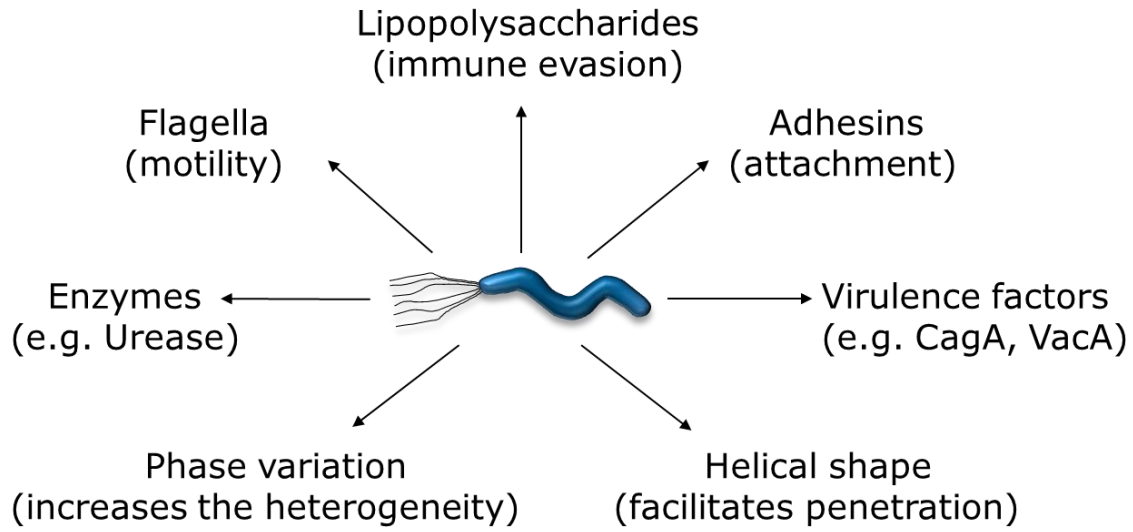


Figure 1.7 *Helicobacter pylori* persistence strategies used in the stomach

The luminal acidity decreases towards the epithelial surface, where a neutral environment is present. To remain in proximity to the gastric epithelial cells and overcome the luminal acidity, the bacterium developed two strategies, one in high acidic environment, pH ≤ 4 and the other in low acidity, pH≥ 4 (Harris *et al.,* 2013).

1.3.1.1 Survival in high acidic environment

For survival in acidic environment, e.g. pH below 4, *H. pylori* relies on urea chemotaxis and motility towards the neutral environment underneath the mucus layer (Croxen et al., 2006a). Urea and bicarbonate ions on the mucosal cell act as chemoattractants to the bacteria. The parietal cells secrete the bicarbonate into the gastric mucosa. Whereas, bacterial urease is produced intracellularly in the cytoplasm and found extracellularly from some lysed bacteria. It catalyses the hydrolysis of urea, releasing ammonia (NH_3) thereby forming a pH-neutral surface microenvironment. Bacterial uptake of urea is regulated by a proton-gated inner membrane channel, UreI, which is pH-dependent urea channel. Then urea is hydrolysed in the cytoplasm into NH_3 and CO_2 (carbon dioxide). NH_3 molecules combine with protons and enable the bacteria to neutralise its intracellular pH and microenvironment. CO_2 is converted into bicarbonate by periplasmic carbonic anhydrase (Yang *et al.,* 2013, Dunne, 2014, Lund *et al.,* 2014). This enables short-term bacterial survival at pH 2.5 in the gastric lumen. The two enzymes, urease and carbonic anhydrase, are regulated by ArsRS two-component signal transduction system through acid-responsive pathway (Pflock *et al.,* 2006).

H. pylori utilises chemotactic receptors as a means for sensing the chemical gradients and pass on the information to the flagella to escape from unfavourable environment. Two chemotactic receptors are well-studied, TlpA and TlpB. TlpA is used for movement toward the neutral niche (positive pH-taxis), where bicarbonate and arginine are concentrated. Arginine is used as a substrate in the urea cycle (Cerda *et al.,* 2011). TlpB is used to sense the pH and moves away (negative pH-taxis) from the strong acid in the lumen (Croxen et al., 2006b).

The exact mechanism of motility in the mucin is not fully understood. It has been proposed that motility and movement toward the epithelial surface is a consequence of urea-dependent pH elevation, which reduces the gastric mucin viscoelasticity from mucus gel to soft viscoelastic gel (Celli *et al.,* 2009). Another study proposed that force-driven actuation was used to propel the helicoidal-shape bacterium into the thick mucus layer lining the epithelial cells in a manner like a screw into a cork, then hide underneath the protective mucus gel (Montecucco and Rappuoli, 2001, Moore *et al.,* 2011). However, motility is rapidly lost in high acidic (pH range 2 - 4) lumen conditions by pepsin activity (Schreiber *et al.,* 2005, Amieva and El–Omar, 2008). The bacteria may also transform into a dormant, coccoid form (Reshetnyak and Reshetnyak, 2017).

1.3.1.2 Survival in low acidic environment

It was proposed that the bacteria upregulate several mechanisms above pH 4 (Moran *et al.,* 2002). One of these mechanisms states that the bacterium potentially establishes multiple binding sites particularly on the gastric mucins (Rossez *et al.,* 2012). A proportion (about 20 %) of *H. pylori* adhere to the gastric mucous cells by adhesive proteins called adhesins (Hessey *et al.,* 1990), while some bacterial cells invade the epithelial cells and can break down the mucus (Björkholm *et al.,* 2000). A growing body of evidence demonstrates that *H. pylori* can invade and proliferate inside epithelial cells (Chu *et al.,* 2010, Liu *et al.,* 2012, Huang *et al.,* 2016). This invasion elicits an immune response and leads to inflammation, which consequently determines the disease outcome (Lamb and Chen, 2013).

1.3.2 *H. pylori* adhesins

The first essential step in bacterial colonization is adherence to host cellular membranes or receptors. *H. pylori* devotes 4% of its genome to multiple *Helicobacter* outer membrane proteins (OMPs) (Bauwens *et al.,* 2018). OMPs are estimated to include about 64 proteins which can be divided into five families. The biggest family includes two subfamilies: Hop (*H. pylori* outer membrane proteins) with 21 members and Hor (Hop-related) with 12 proteins. The second and the third families are called Hom (*Helicobacter* outer membrane) and Hof (*Helicobacter* outer membrane protein family), consisting of 4 and 8 members, respectively. Iron-regulated proteins represent the fourth family, while efflux pumps are the fifth family (Alm *et al.,* 2000, Oleastro and Ménard, 2013).

It is currently thought that adhesins have evolved to mediate the *H. pylori* binding to the glycans or other ligands that are abundantly present on the stomach epithelium and mucus layer (Moore *et al.,* 2011). This adherence activates some signalling pathways and facilitates toxin or other molecule delivery into the gastric epithelial cells (Algood and Cover, 2006). It has been assumed that each of these adhesins has evolved to accomplish a specific function, e.g. to mediate the adherence at different stages, i.e. healthy or diseased tissue. However, many of the functions/ligands of the bacterial adhesins are still unknown. Persistent *H. pylori* infection leads to chronic inflammation, this in turn, changes the glycosylation pattern on the surface of the epithelial cells. Accordingly, the bacteria rapidly adapt to this alteration by switching to different adhesins to prolong the adhesion and evade the inflammatory response (Magalhaes and Reis, 2010).

The most studied Hops (Table 1.2) are blood group antigen-binding adhesin (BabA) and sialic acid binding adhesin (SabA), adherence-associated lipoprotein (AlpA, B), outer membrane inflammatory protein (OipA), duodenal ulcer promoting gene A (DupA) and neutrophil-activating protein (NAP)(Lu *et al.,* 2005, Yamaoka, 2008, Yamaoka, 2010, Namavar *et al.,* 1998). More recently, two novel adhesins were described: HopQ, which binds to human carcinoembryonic antigen-related cell adhesion molecule (CEACAM), and LacdiNAc-binding adhesin (LabA) which binds to MUC5AC mucins of the gastric mucosa (Javaheri *et al.,* 2016, Rossez *et al.,* 2014a). The broad array of specialised adhesins explains *H. pylori*

tropism to gastric tissue even after pathological changes. This could be exemplified by BabA, which is the dominant adhesin in the healthy gastric cells, followed by SabA which mediates bacterial binding to inflamed cells and HopQ, which facilities bacterial adherence to up-regulated receptors on gastric cancerous cells (Moonens *et al.,* 2018).

The *H. pylori* genome (~1.7 Mbp) has a bundle of genes for phase variation, a phenomenon which occurs through reversible DNA slippage at dinucleotides repeats (CT) and homopolymeric tracts. DNA slippage leads to translation shifts and thus reversible phenotypic variation, due to frequent "on/off" switches, in the corresponding gene product. This genetic heterogeneity occurs through frequent DNA recombination, switching and mutation to produce a diverse array of intra-strain nucleotide sequences in order to prolong the host colonisation (Ali *et al.,* 2015, Zhou *et al.,* 2014). Phase variation systems can be exemplified in BabA which has two paralogues (BabB/C), or in flagellar protein (FliP), Lipopoly-saccharides, and outer membrane phospholipase A (Salaun *et al.,* 2004, Kusters *et al.,* 2006, Josenhans *et al.,* 2000, McGowan *et al.,* 1998, Tannaes *et al.,* 2001).

It is well established that BabA facilitates *H. pylori* attachment to Human fucosylated glycans such as ABO H-type-1 and Lewis b (Le^b) blood group antigens (Boren *et al.,* 1993). In the mouth, BabA also mediates adherence through binding to salivary secreted mucin MUC5B (MG1) (Prakobphol *et al.,* 2005), salivary agglutinin such as glycoprotein-340 (gp-340) (Prakobphol *et al.,* 2000), and Deleted in malignant brain tumour 1 (DMBT1)(Issa *et al.,* 2010), as well as salivary proline-rich glycoprotein (PRG) (Walz *et al.,* 2009). In the stomach, BabA mediates attachment of the bacterium with high affinity to the gastric mucosa, promotes chronic inflammation (Moore *et al.,* 2011) and enhances the type IV secretion system (T4SS) for injection of CagA into host cells (Pachathundikandi *et al.,* 2013). In cancerous strains, BabA-Le^b adherence is a prerequisite for double-strand DNA breakage and triggers the host genome damage response (Toller *et al.,* 2011, Hanada *et al.,* 2014), which may occur due to bacterial induction of aberrant DNA methylation (Woo *et al.,* 2018). However, the critical question which remains unanswered, is how *H. pylori* manages to persist for such a long time in the stomach.

Many mechanisms have been proposed to explain how this bacterium can withstand the host immune system's attack while surviving in a hostile environment designed to kill bacteria and destroy proteins. Pride and Blaser (Pride and Blaser, 2002) suggest BabA homologous recombination to alter the outer membrane constantly. Other studies proposed phase variation during protein production in the 5' region to silence functional proteins (Yamaoka, 2008). This may lead to the existence of other Bab paralogues such as BabB and BabC (Hanada and Yamaoka, 2014), or hybrids of these genes. The functions and receptors of these paralogues have not been identified so far. Moreover, there are two chromosomal loci for *babA* gene, *babA*1 and *babA*2. The former lacks 10 bp in the signal peptide which result in silencing of the expression, while the latter is most commonly studied (Saberi *et al.,* 2016). However, *babA*1 gene recombination into homologous *babB* locus, results in regaining the binding ability to Le^b. This chimeric BabB/A adhesin is controlled by a cytosine-thymidine (CT) repeat mutation slippage (ON/OFF switching). Interestingly, protein expression of chimeric BabB/A is lower than the original BabA, reflecting the strength of the expression level as a strategy for colonisation (Bäckström *et al.,* 2004).

Table 2.1 Representative of *H. pylori* Adhesins and their gastric cellular receptors

Gene	Name	Abbreviation	Host ligand	Reference
HopS	Blood group antigen-binding adhesin	BabA	ABO/Lewis blood group antigens	(Ilver *et al.,* 1998, Boren *et al.,* 1993)
HopT		BabB	Unknown	
HopU		BabC	Unknown	
HopP	Sialic acid-binding adhesin	SabA	Sialylated glycans (Lea, sLex)	(Mahdavi *et al.,* 2002, Alm *et al.,* 2000)
HopO		SabB	Unknown	
HopD	LacdiNAc-binding ahdesin	LabA	*N*,*N*'-diacetyllactose-diamine	(Rossez *et al.,* 2014b)
HopH	outer membrane inflammatory protein	OipA	Unknown	(Yamaoka *et al.,* 2000)
HopC	Adherence-associated lipoprotein	AlpA	Laminin	(Odenbreit, 1999, Senkovich *et al.,* 2011)
HopB		AlpB		
HopQ	Helicobacter outer membrane protein Q	HopQ	Carcinoembryonic antigen-related cell adhesion molecule	(Javaheri *et al.,* 2016)
Hom	Helicobacter outer membrane	HomA	Unknown	(Alm *et al.,* 2000)
		HomB	Unknown	

Bacterial chronic colonisation of the stomach leads to alteration in the glycosylation pattern on the surface determinants of the mucosal cells from fucosylated to sialylated such as sialyl-Le^x and sialyl-Le^a (Mahdavi *et al.,* 2002). The bacteria adapt to this change by expressing SabA to mediate the adherence to the inflamed gastric mucosal cells. It functions also as sialic acid-dependent hemagglutinin by binding to gangliosides on human erythrocytes *in vitro*, activates neutrophils and contributes to *H. pylori* survival (Mahdavi *et al.,* 2002, Aspholm *et al.,* 2006). The SabA paralogue, SabB, has been mostly associated with duodenal ulcers but its cellular ligand has not yet been determined (de Jonge *et al.,* 2004). As part of consistent adhesion, *H. pylori* uses HopQ which is associated with the inflammatory response to enable bacterial intracellular delivery and phosphorylation of the CagA oncoprotein through disrupting the dimerization of CEACAM 1 (Moonens *et al.,* 2018). This disruption subsequently induces the cell to produce pro-inflammatory cytokines such as interleukin-8 (Javaheri *et al.,* 2016).

1.3.3 BabA (Adhesin for cytoadhesion drug delivery)

From the aforementioned, several challenges need to be addressed for developing a novel drug delivery moiety. These challenges are 1) recognising the exact mechanism of bacterial adhesion and cellular receptor, 2) studying the binding or dissociation constant and 3) exploring the ability of the adhesin to withstand gastric acidity/peptic digestion. The last point is not sufficiently covered in the literature and this study represents the first of its kind, since a purified adhesin was directly tested for pepsin digestion and coated with microparticles.

Crystallography has been used to elucidate the molecular interactions between the bacterial adhesins and their cellular ligands. SabA was the first adhesin to be crystallised, but only in the absence of its ligand (Pang *et al.,* 2014). Other adhesins were subsequently crystallised alone and in combination with its ligands, such as BabA and HopQ (Javaheri *et al.,* 2016, Hage *et al.,* 2015a). The crystallization and subsequent X-ray structure determination revealed that these adhesins, despite having different ligands and varying primary amino acid

sequences, share a similar overall structure. It is composed of a highly conserved (25 kDa) transmembrane β-barrel structure in the C-terminal and an equally conserved extracellular N-terminal region containing signal peptide sequence, but characterised by being highly variable in the middle region. The signal sequence is cleaved during periplasmic translocation (Nell *et al.,* 2014). *H. pylori* displays a unique transmembrane domain which is predicted to consist of seven β-strands at the C-terminal and one strand at the N-terminal (Coppens *et al.,* 2018).

The crystal structure of the extracellular domain of BabA J99 (Figure 1.8) revealed three domains, two in the C-terminal and one in the N-terminal domain. The two domains are predominantly α-helical, termed Handle and Head. The third domain, which was termed the Crown, or BabA adhesion domain (BabA-AD), mainly consists of four β-strands and is located on top of the two other domains (Hage *et al.,* 2015a, Moonens *et al.,* 2016). The boundaries between these domains were determined based on SabA superimposition and the corresponding matching sequences. The Crown (G179 to V255) contains the binding site for Le^b, and thus much attention was paid to its presence. The Crown region is shorter in HopQ, consisting of two instead of the 4 β-strands found in BabA (Javaheri *et al.,* 2016). However, the presence of such domain is not essential to determine the binding functionality in other adhesins such as SabA, which shows no Crown in its crystal structure. Phyre2 prediction can be used to devise an estimated picture of the overall structures (Figure 1.9). These predicted models and three existing crystal structures SabA (pdb: 4O5J), HopQ (pdb: 6AW2) and BabA 17875 (pdb: 5F7W) were superimposed with BabA J99 (pdb: 4ZH7) to get insight about the overall structures (Figures 1.10 and 1.11) and sequences were aligned, omitting BabA 17875 (Figure 1.12) to get a clear idea about the degree of sequence conservation between the different adhesins. A comparison between BabA J99 and BabA 17578 sequences will be discussed later.

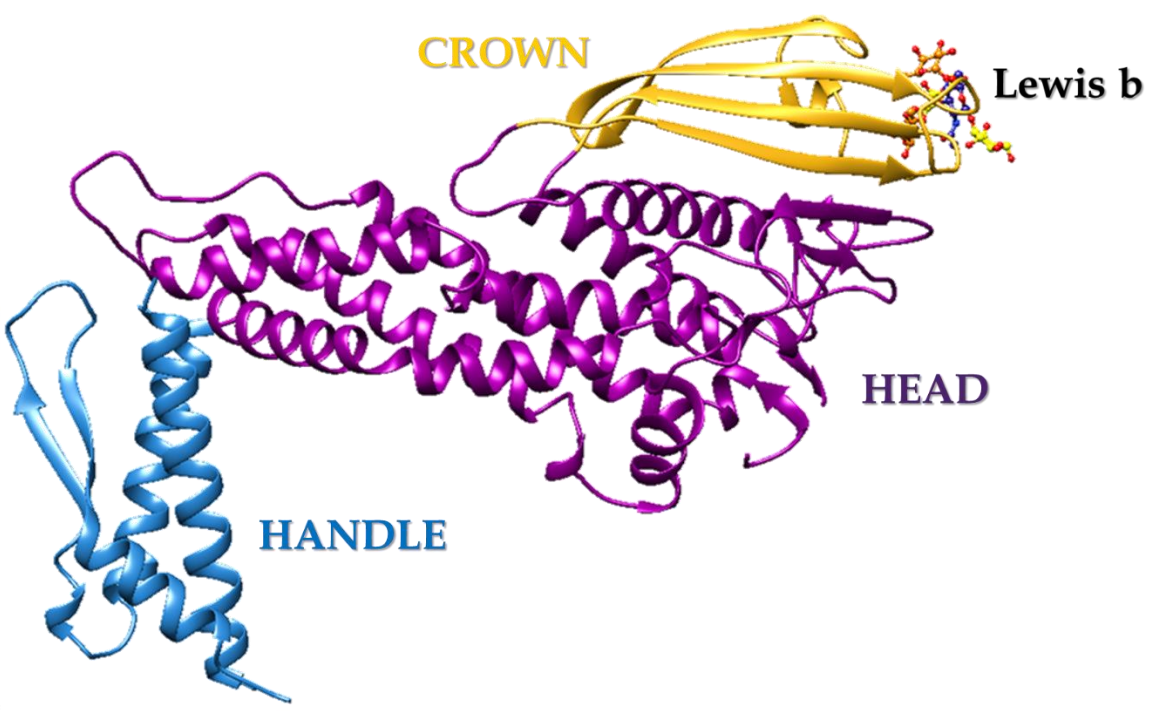


Figure 1.8 X-ray crystallography of BabA J99 (pdb:4ZH7) three-dimensional structure

BabA composes of three regions, Handle (blue), Head (violet) and the Crown (gold). Binding of *Helicobacter* BabA and gastric cellular receptor Le^b occurs in a shallow area on the tip part of the Crown.

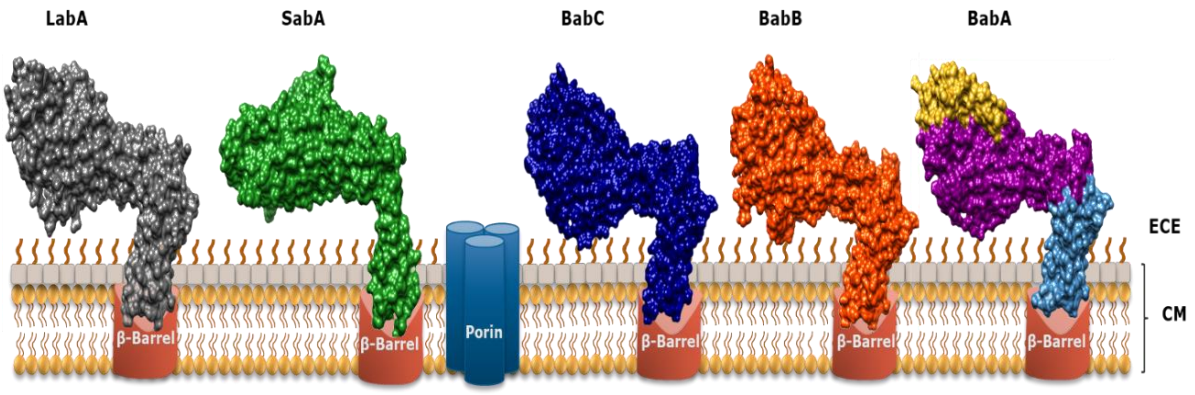


Figure 1.9 Schematic representation of *Helicobacter pylori* adhesins

The 3D-structures for *H. pylori* adhesins (BabB, BabC and LabA) were predicted by Phyre2 software. They share a similar structure in the membrane-embedded carboxylic (β-sheet) and the extracellular amino termini. The predicted conformations involve major similarities in the tips, although the Crown domain sequence is absent from some of them such as BabB and SabA. The Stalk domain at the N-terminal, obtained in BabA X-ray crystal structure predicted to form a part of the β-barrel that embedded in the outer membrane. CM = cell membrane, ECE = extracellular environment.

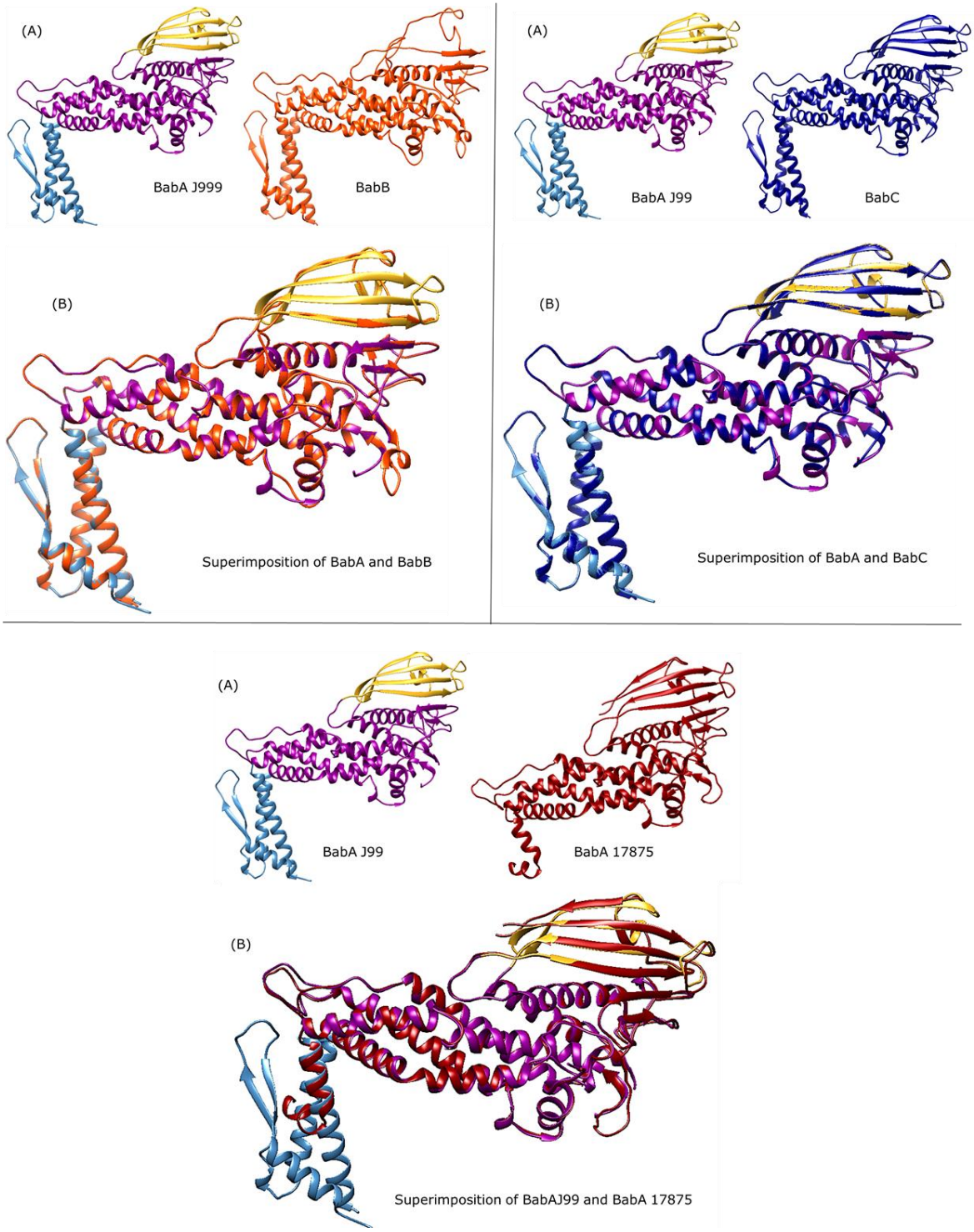


Figure 1.10 Comparison of BabA J99 with BabB and BabC adhesins using Phyre2

A) Ribbon representation of extracellular domain of the Bab paralogues

B) Superimposition of BabA and other Bab paralogue

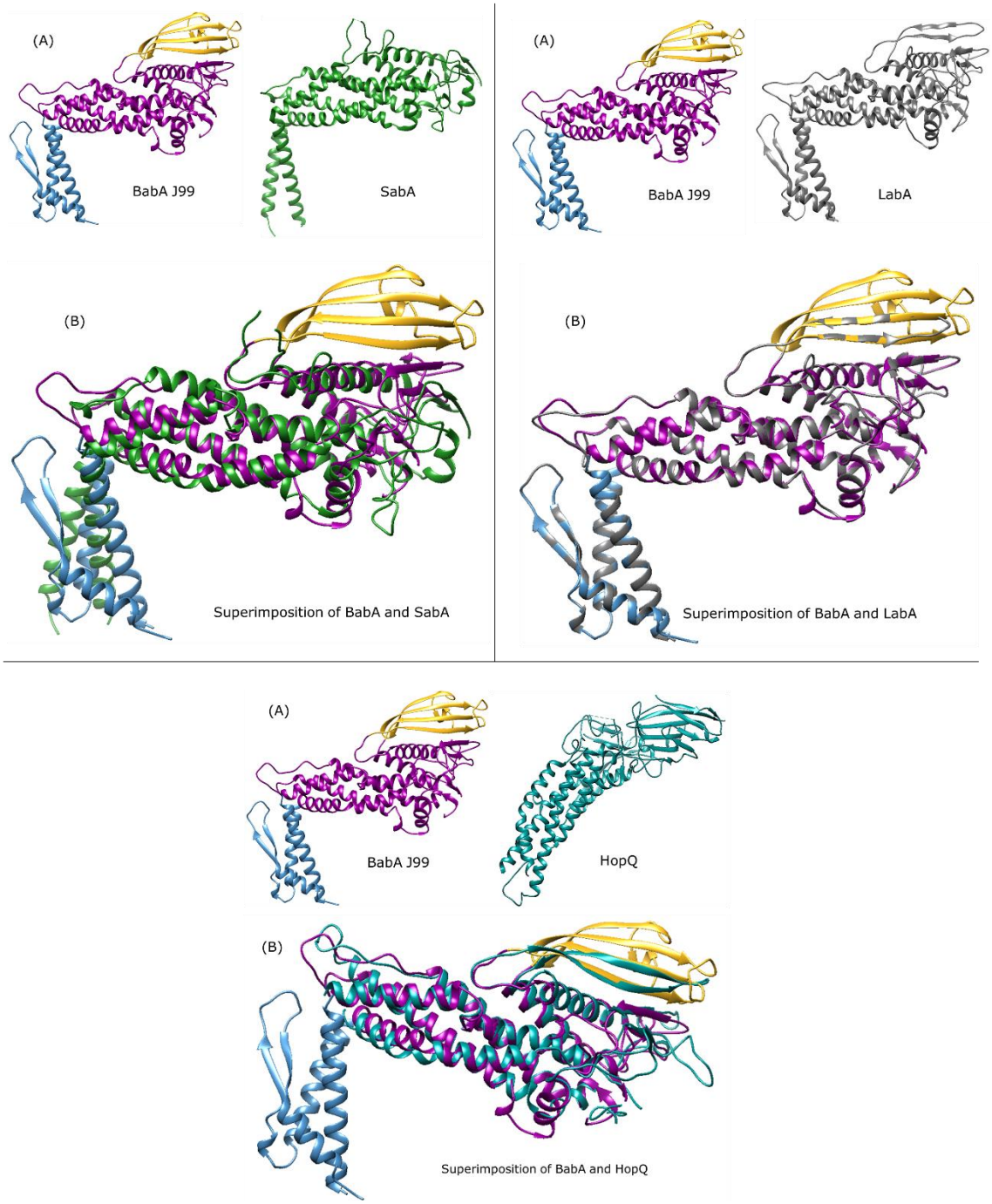


Figure 1.11 Comparison of BabA J99 with SabA and LabA adhesins using Phyre2

A) Ribbon representation of extracellular domain of the protein
B) Superimposition of BabA and other adhesin

The Crown domain is present in BabC and LabA but not in SabA. BabB shows one beta strand predicted to be a Crown. HopQ and LabA display a shorter Crown sequence.

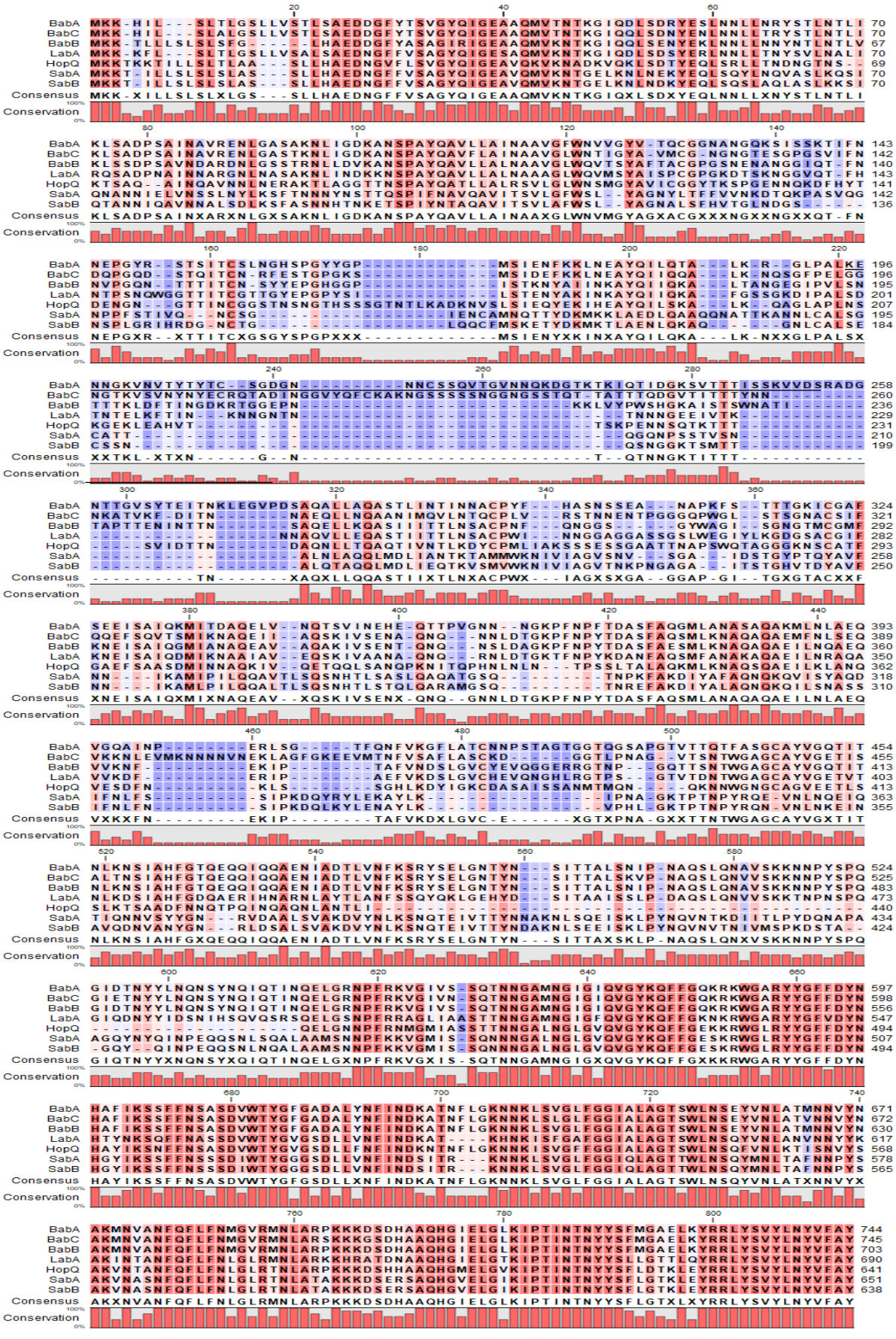


Figure 1.12 Sequence alignments of BabA with multiples adhesins

Alignment made using CLC Main WorkBench 8.1 (CLC bio, USA). The BabA-Crown sequence is underlined, which is a bit shorter and not conserved among the other selected adhesins. The sequence from Asparagine (N:618) is highly conserved among the adhesins. Variability occurs between Tryptophan (W:121) and Glutamine/Asparagine (504:Q/N).

BabA sequence variability substantially affects the specificity and binding strength (Kable *et al.,* 2017). Moreover, not all *H. pylori* strains express the BabA gene and not all of those that do can bind to Le^b. The variability in the binding sites (residues) is visible in the amino acid sequence alignment between two different strains, e.g. *H. pylori* J99 and *H. pylori* 17578 (Figure 1.13). The affinity of BabA-Le^b complex has been analysed by Scatchard method using whole bacteria. The data of the strain 17875 showed the affinity for Le^b with dissociation constant *(*K_d) value of 2 x 10^8 M^{-1} to 3 x 10^{11} M^{-1} (Aspholm-Hurtig *et al.,* 2004). However, using the same method, suspension of *H. pylori* J99 strain showed affinity as high as $K_d = 5\times10^{11}$ M^{-1} (Aspholm *et al.,* 2006). Subsequently, it was shown using dynamic force spectroscopy on single bacterial cells, the bond length was 0.86±0.07 nm (*Kd* 5x10^9 M^{-1}) (Björnham *et al.,* 2009). Using oblique-incidence reflectivity difference (OI-RD) microscopy, bacterial strain J166 exhibited a K_D to Le^b of 0.7x 10^{-15} M bonds (Fei *et al.,* 2011). Recently, isothermal titration calorimetry (ITC) revealed the monovalent binding between 17875 strain and Le^b with *Kd* of 80.0 ± 7.1 mM and 0.39 nM Kd for the full-length using surface plasmon resonance (Moonens *et al.,* 2016). However, BabA recombinant protein reported *Kd* of ~227 mM in acidic (pH 4.5) and *Kd* of ~252 mM in neutral (pH 7.4) conditions (Hage *et al.,* 2015a).

To ensure BabA is a suitable for carrying the formulation, a firm adherence to the cells needs to be achieved, in order to avoid clearance by mucus shedding and pepsin/acid proteolysis. This may be achieved by coating nano/microparticles with BabA, as the multiple repeats will increase the avidity while potentially conferring some degree of steric protection against proteolysis.

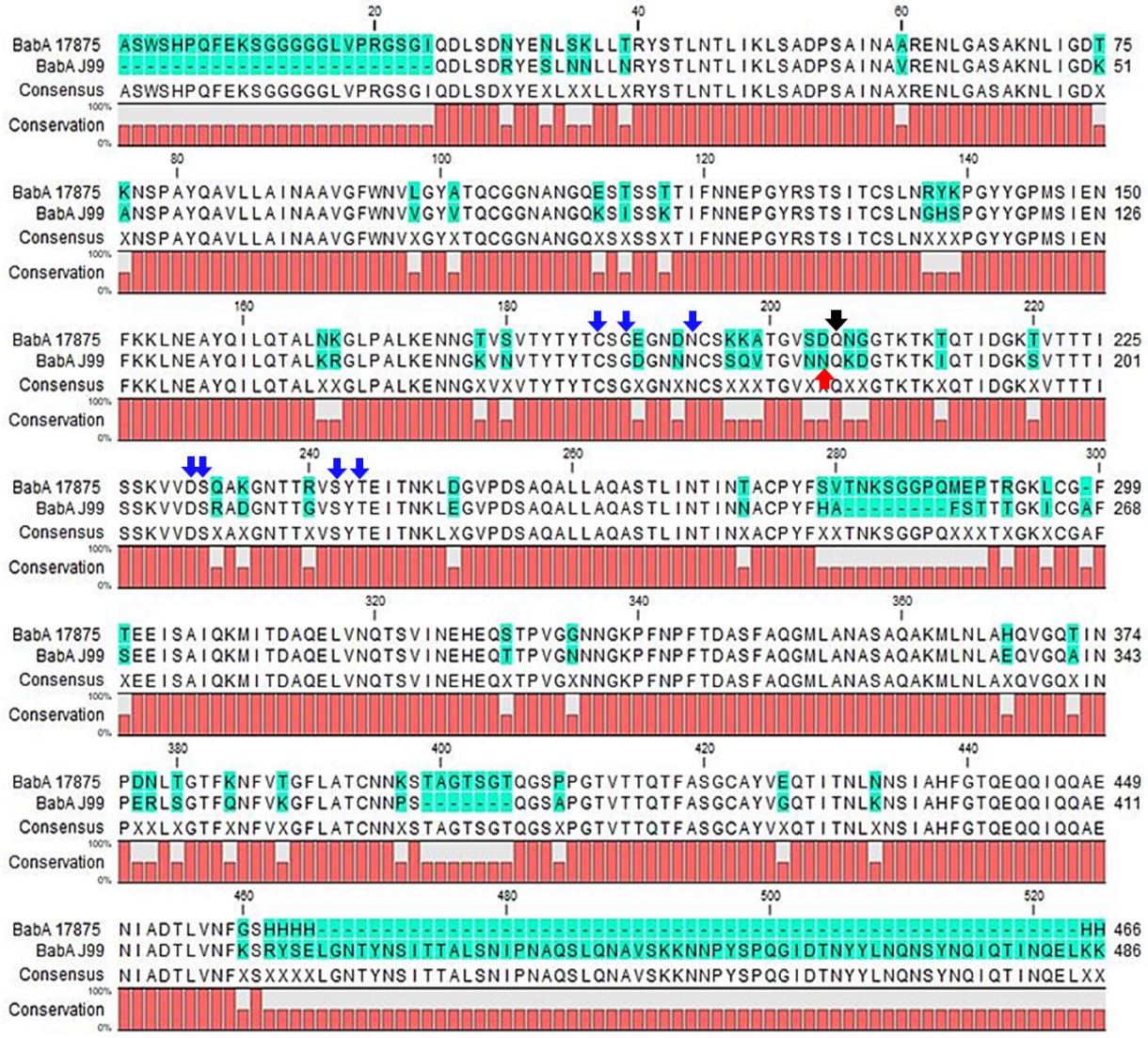


Figure 1.13 Sequence alignment of BabAJ99 with BabA 17875

Alignment made using CLC Main WorkBench 8.1 (CLC bio, USA). The Crown sequence in BAbA J99 is underlined and the Le^b binding sites are highlighted by blue arrows. The red arrow in BabA 17875 indicates Q:205 and the black one in BabA J99 indicates N:204 which both of them bind to Fucose 4 in Le^b.

From the aforementioned, it is apparent that *H. pylori*'s outstanding cytoadhesive properties may provide a suitable strategy for adhesion to gastric epithelial cells. To the best of our knowledge, no study has yet been published employing bacterial lectins as a biomimetic strategy to specifically target a drug to the same gastric glycans that *H. pylori* uses for adherence. Biomimicry of this natural bio-adhesive system, through usage of BabA as adhesin, may lead to a novel specific protein-glycan-binding targeting drug delivery system.

1.3.4 BabA-Crown domain- the drug moiety?

Elucidation of the Crown domain from BabA 3D-structure was a cornerstone for understanding the bacterial mechanism of attachment to Le^b. Although BabA was discovered in 1993, until 2015, no crystal structure was available. One of the issues was the lack of a stable, correctly folded recombinant version of BabA. The establishment of a protocol for its periplasmic expression in *E. coli* was an essential step to obtain a high amount of purified protein for crystallisation and detailed *in vitro* studies. The insertion of a stabilising and yield-increasing hexa-lysine tag at protein's carboxylic terminal led to successful expression and purification of BabA and subsequently crystallisation in the presence and absence of the physiological ligand, Le^b (Hage *et al.,* 2015b, Hage *et al.,* 2015a).

BabA-Crown displays marked variability between the strains particularly in two so-called hypervariable loops (Moonens *et al.,* 2016, Hage *et al.,* 2015a). Clarification of the binding interactions primed the thinking about using BabA-Crown as a mediator of *H. pylori* adherence to human fucosylated glycans ABO H-type-1 (Fucα2Galβ3GlcNAc) and Lewis b (Le^b) blood group antigen (Fucα2Galβ3(Fucα4)GlcNac) (Ilver *et al.,* 1998, Boren *et al.,* 1993). It is worth to note that this binding ability categorizes the bacterium into two strain categories, the 'specialist' vs 'generalist' strains. The former, mostly found in a population with blood group O phenotype such as in South America, recognise Le^b and H type 1 determinants (Benktander *et al.,* 2012). The latter strains bind to individuals with blood group $ALe^b/BLe^b/Le^b$ antigens (Cooke *et al.,* 2005). Binding preference is mediated by amino acid Leucine (L198) present in the BabA-Crown

hypervariable loop. Substitution of this Leucine (L) with Serine (S) 'generalises' the binding activity in the 'specialist' strains (Moonens *et al.,* 2016).

Individuals with group O are more susceptible to develop gastric ulcers than people with blood groups A (A-Le^b) and B (B-Le^b). This may be due to few of Le^b receptors available on their surface (Boren *et al.,* 1993), higher inflammatory response (Alkout *et al.,* 2000), larger gastric secretory-cell mass (Hanley, 1964) or the bacterial high affinity for group O-glycans (Sweeney and Guillemin, 2016).

Because *H. pylori* J99 is thought to be a generalist strain, its BabA-Crown as a glycan-binding domain is a suitable candidate for cytoadhesive drug delivery properties as it could be used for any ABO blood group. It could be retained in the stomach for a long duration, provided there is pepsin resistance. Using a shorter form of BabA also means fewer potential cleavage sites for pepsin, thus increased resistance to gastric juice. Therefore, assessment of the ability of the isolated Crown region to bind to its physiological ligand as proof-of-principle is crucial.

From the above mentioned, recombinant version of BabA-Crown possesses some characteristics which make it a potentially suitable adhesin for use as a gastric drug delivery moiety:

1. BabA as bacterial outer membrane protein is the most studied adhesin, predominantly expressed on the bacteria found in the stomach of healthy individuals.
2. The target physiological receptor is on the surface mucus cells, i.e. approachable.
3. BabA recombinant form retains the functionality of the native form.
4. Gastric drug delivery system can be developed using the specific cytoadhesive property of BabA-Crown and the nano/microparticles to carry the formulation.

1.4 Aim and objectives

The aim of this study is to generate a biomimetic drug delivery platform with micro/nanoparticles to specifically direct the drug to the gastric epithelial cells (Figure 1.15), which would increase the gastric retention time. Exploration of this system could elucidate two things, on one hand, may provide a novel biomimetic system for cytoadhesion based on *H. pylori* adhesion mechanism. On the other hand, characterising BabA-Crown functional properties, will give a clear insight into the mechanisms of the bacterial binding at the molecular level. If this approach succeeds, it will be a representative procedure for using the minimal binding domain as cytoadhesive protein.

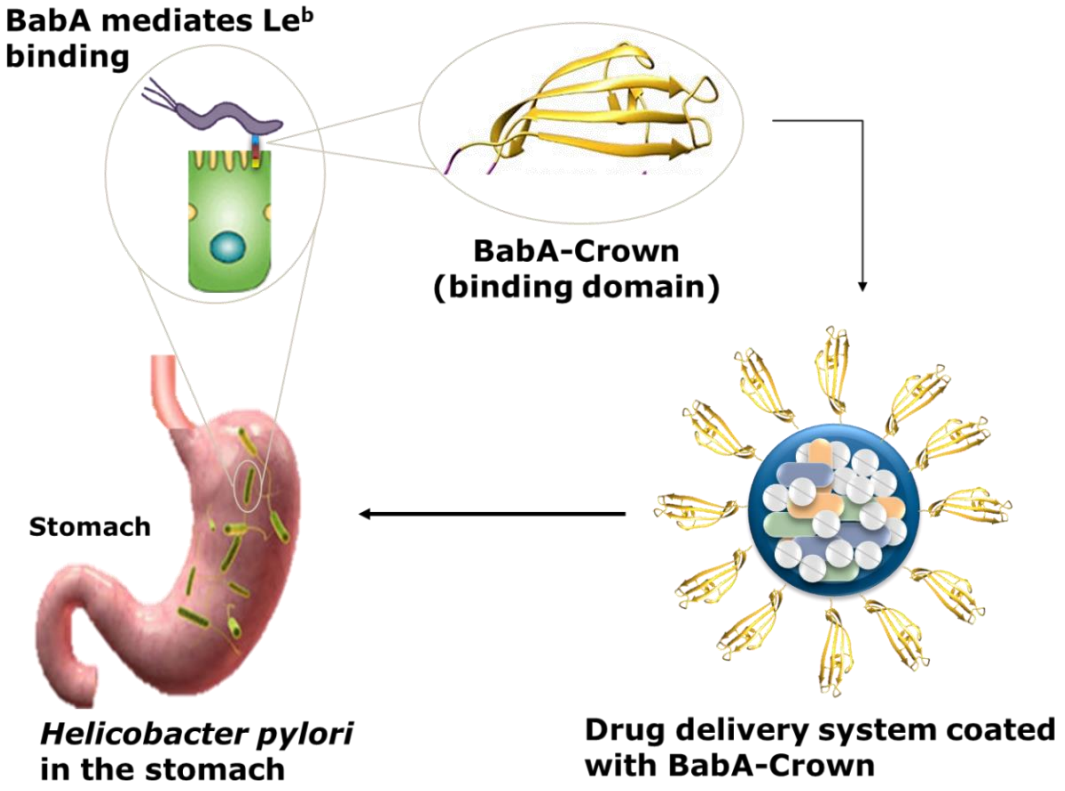


Figure 1.14 Schematic representation of the proposed biomimetic drug delivery system

BabA-Crown as minimal binding domain is intended to be used to coat nano/microparticle carrying antibiotics in order to specifically targeting the drug into the gastric epithelia cells.

To achieve the aim of this study, the following three objectives were set:

1. Generation of the recombinant form of BabA J99 Crown region as the minimal Le^b binding domain through cloning, expression an purification. This is essential to obtain BabA-Crown for subsequent characterisations and utilization as a targeting moiety (Chapter 3).
2. Characterisation of the BabA-Crown protein by testing its ligand-binding ability and its resistance to simulated gastric acidity or peptic digestion (Chapter 4). This is a crucial step in determining whether the minimal binding domain retains the whole BabA functionality and translate the applicability of being a target moiety in the gastric conditions. In case this objective is not achieved, alternative strategies will be applied (Chapter 5).
3. Development and evaluation of the biomimetic drug delivery carrier. This provides important insight about the ability of the protein to bind its ligand after coating the surface of the microparticles (Chapter 6). This also represents the final *in vitro*-step to explore the applicability of this cytoadhesive drug delivery system.

All of these objectives will give relevant insights into the adhesion mechanism used by *H. pylori* for inhabiting the gastric mucosa. Based on this knowledge, novel antimicrobial strategies could also be designed for future endeavours.

CHAPTER TWO

2. Experimental methodology (General overview)

2.1 Introduction

To address the objectives of this study and provide answers, empirically, a wide range of techniques were applied.

The first objective of this research was to construct an expression system having BabA minimal binding site, the Crown. To achieve this objective, general molecular biology techniques including polymerase chain reaction (PCR) and protein expression were carried out and extended to generate various recombinant proteins from BabA gene. After protein expression, purification was performed using chromatographic techniques, e.g. immobilised metal-ion affinity chromatography (IMAC). A brief description of the recombinant expression and the system (pOPE101 plasmid hosted by *E. Escherichia coli* XL10-Gold) used for both cloning and expression is given in Section 2.2. More details about the procedures conducted in this research can be found in Chapter 3.

The second objective was to characterise the purified protein for usage as drug delivery moiety. Firstly, assessment of protein resistance to acid/pepsin proteolytic activity was performed. Bioinformatics tools were used to model the protein stability based on its amino acid sequence. This is discussed in more detail in Chapter 4. Secondly, Enzyme-linked immunosorbent assay (ELISA) was employed to test ligand binding ability. Different types of ELISA were used and a general overview about each type is provided in Section 2.3.

Circular dichroism spectroscopy was employed to assess protein's secondary structure. An outline about the principle and mechanisms of the experimental processes is briefly described in Section 2.4.

The third objective was to evaluate the activity of protein-particle conjugates. This has been achieved through three steps, mutagenesis, biotinylation and conjugation with the particles.

Mutagenesis was carried out at the DNA level to insert an AviTag sequence. This sequence acts as a substrate for the bacterial enzyme (BirA) to add a biotin molecule into the protein sequence. This biotin is subsequently used to mediate protein interaction with neutravidin on the surface of the microparticles. The fundamental of the biotinylation and the method used are discussed broadly in Chapter 6. To study the colloidal stability and dispersity of protein-microparticle complexes, Dynamic light scattering (DLS) was used. The underlying biophysical principles and data interpretation are briefly described in Section 2.5.

2.2 Recombinant expression

Recombinant DNA technology offers the ability to synthetise any stretch of DNA encoding a protein of interest in order to study its structure, function or therapeutic ability. The general procedure applied follows the cut-paste-proliferate-select principle. This is followed by gene expression, which is commonly propelled by standard bacterial systems such as *E. coli* (Chen, 2012). This system was originally employed to produce massive amounts of recombinant proteins such as human insulin and erythropoietin using a simple carbon-source medium in a short-time and cost-effective way (Lomedico, 1982, Masson *et al.,* 2003, Baneyx and Mujacic, 2004).

The general steps for generation of recombinant DNA are summarized in Figure 2.1, using BabA-Crown fragment gene as a model. The first step is to amplify the chosen DNA sequence from a gene or genome, called the template. Then a set of short oligonucleotide sequences called primers is designed, one represents the sense or forward (5' - 3') and the other called the antisense or reverse primer (3' - 5'). The forward primer is complementary to the bottom strand in the 3' to 5'

direction the reverse primer is complementary to the top strand and reads from 5’ to 3’. The primers should include restriction enzyme sites which should also be present in the vector (e.g. plasmid) sequence, where the gene of interest will be inserted (Hoseini and Sauer, 2015).

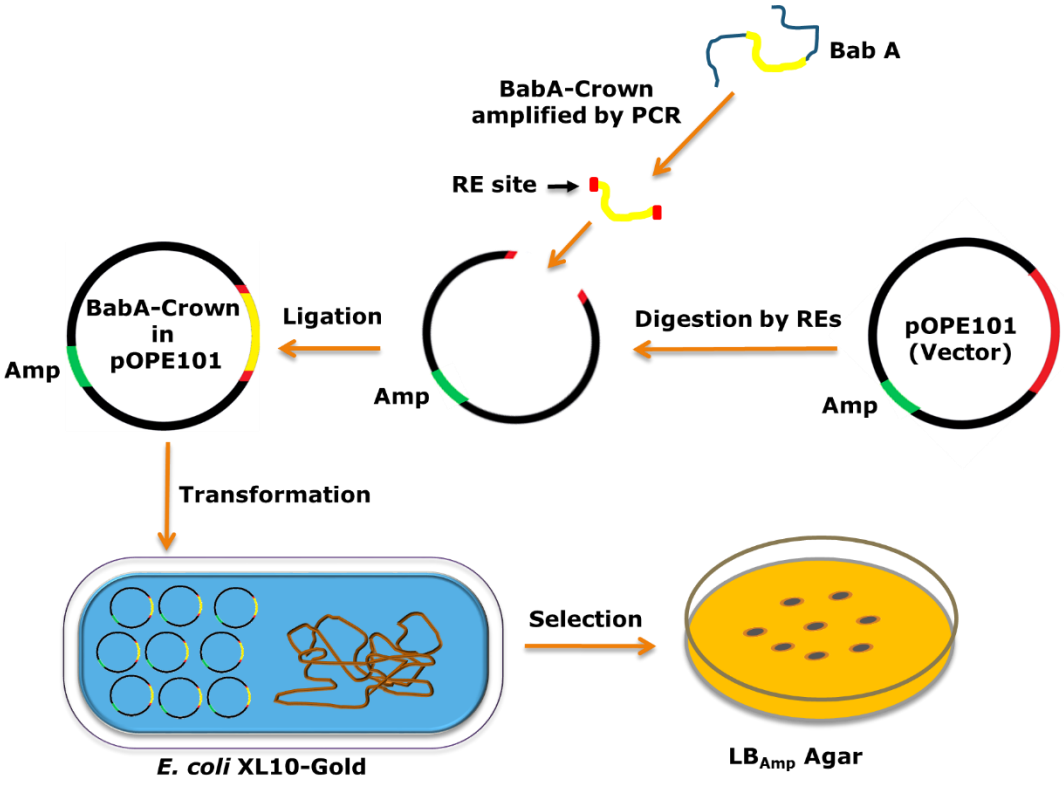


Figure 2.1 Schematic representation of recombinant technology methodology

Specific fragment of DNA, here the BabA-Crown coding DNA, is amplified by polymerase chain reaction (PCR) to obtain ample copies labelled with restriction enzyme (RE) recognition sites at both ends. A plasmid (pOPE101), with an antibiotic-resistance marker gene, ampicillin (Amp), is used for in-host replication after digestion with the same restriction enzymes. An intermediate step of ligation is applied to seal the DNA to be inserted into the vector. The ligated plasmid is introduced into a host, in this case “*E. coli* XL10-Gold bacterium”, to carry out the *in vivo* multiplication of the DNA fragment. The antibiotic corresponding to the selective marker on the plasmid is added in the growth medium (LB_{Amp}) for transformant selection.

For amplification of target DNA sequence through polymerase chain reaction (PCR), a thermocycler machine is usually used. It offers the choice for adjusting a number of cycles of different temperatures to carry out the amplification reaction in a relatively short time. Each cycle changes rapidly and consists of three steps:

1. Denaturation

High temperature (~94 - 98 °C) is used for unwinding double strands of DNA by breaking down the hydrogen bonds between the paired nucleotides.

2. Annealing

This step involves decreasing the temperature (usually between 50 - 72 °C) to enable the primers to bind to their complementary nucleotide sequence in the template.

3. Extension.

In this step the temperature is increased again (usually to 72 °C) and the DNA polymerase enzyme recognises the double stranded region, where the primers have annealed, and elongating the sequence in 5' to 3' direction to build up a copy of the complementary strand.

After PCR amplification, the PCR products are analysed by separation, according to the charge and size through agarose gel electrophoresis. These products are visualised through ultra violet (UV) light after staining with fluorescent dyes such as the intercalating agent ethidium bromide, which form a complex with the dsDNA and absorbs shortwave UV radiation (Garibyan and Avashia, 2013). After the amplification and confirmation, purification of the PCR products is conducted. The subsequent step involves introducing the purified DNA sequence/gene into a reproducing vector e.g. plasmid. This involves cleavage by specific restriction enzymes to target the sequence to a defined location within a vector DNA. To join these fragments together, enzymatic ligation is applied before transferring the ligated vector into a productive host organism following a process named transformation. After culturing in a selective growth medium, colonies having the incorporated gene of interest will be able to grow, as they will have acquired resistance to the selective antibiotic via the transformed plasmid. Afterwards, the selected clones, bearing the desired DNA sequence, will be harvested and used for protein expression (Topcu, 2000, Benoit *et al.,* 2006).

2.2.1 Recombinant protein expression in *E. coli*

Proteins can be expressed in prokaryotic vectors such as *E. coli* or in eukaryotic vectors such as yeast, insect, plant or mammalian cells. Each vector possesses specific advantages over the other one. Eukaryotic systems are ideal for expression of protein requiring post-translation modifications such as glycosylation. Prokaryotic systems offer rapid and inexpensive expression and the highest yields (Demain and Vaishnav, 2009, Majewska *et al.,* 2018).

There are several commercial strains of *E. coli* which can be used for protein expression. The choice is governed by the type of vector used, depending on several factors such as the presence of the desired multiple cloning site for insertion of the target gene, type of replicon and promoter (Rosano and Ceccarelli, 2014).

In the present study, *E. coli* strain (XL10-Gold) compatible with the plasmid pOPE101 was used. This plasmid was originally generated for the expression of single-chain Fv antibody fragment (scFv) to stabilise the disulphide bonds between the antibody fragments and facilitate its secretion into the periplasm, which constitutes an oxidizing environment, assisting in the formation of intra- or intermolecular disulphide bonds (Schmiedl *et al.,* 2000). Since then, pOPE101 has been continuously used with *E. coli* XL1-Blue (Minus Restriction) MR-derived strains e.g. *E. coli* XL10-Gold for soluble production of antibody heavy and light chains (Hust *et al.,* 2007) and for antibody multimerisation (Thie *et al.,* 2009). This expression system (pOPE101-*E.coli* Xl-10) proved to be an ideal expression system for recombinant BabA protein generated from two different *H. pylori* strains, J99 and 17875 (Fei *et al.,* 2011, Hage *et al.,* 2015b).

Protein expression of the gene of interest is regulated by lactose or *lac* operon. Transcription in the *lac* operon depends on two mechanisms, repression and induction. Repression occurs by lactose repressor *Lac*I which is activated by cyclic adenosine mono phosphate-carbon catabolite repression (cAMP-CRP) system. The catabolite activator protein is fundamental regulator of the *lac* operon. Induction happens through phosphoenolpyruvate (PEP) system (Deutscher *et al.,* 2006, Li and Young, 2014). For inducing protein expression, the most commonly used

inducer is isopropyl-β-D-thiogalactopyranoside (IPTG), which binds to the *lac* repressor and stimulate the transcription (Marbach and Bettenbrock, 2012, Marschall *et al.,* 2017).

In *E. coli*, protein expression occurs in the cytoplasm. It starts with transcription which involves RNA polymerase to transcribe the DNA into messenger RNA in order to be translated into a polypeptide. Translation of messenger RNA is aided by the ribosomes (Figure 2.2) and the resulting polypeptide, in case of periplasmic translocation, is tagged with a signal peptide at the amino terminal. If this specific N-terminal signal peptide was not present before translocation, it would lead to loss of direction and protein accumulation in the cytoplasm (Holland, 2004, Chatzi *et al.,* 2013). Protein periplasmic translocation is mediated by signal recognition particle (SRP), which is ribonucleoprotein complex, binding to the signal sequence and carry the protein into the inner membrane. In the inner membrane there is a membrane-bound SRP receptor which facilitates protein translocation and delivery into the periplasmic space (Luirink and Sinning, 2004). The periplasmic space provides an oxidative environment which allows formation of disulphide bonds in the protein. This helps the protein to reach a folding/conformation that favours its function. The cytoplasm is a reducing environment, posing a challenge for proteins containing cysteine in their amino acid sequence, as the susceptibility for forming inclusion bodies in the case of cytoplasmic expression is very high (Rosano and Ceccarelli, 2014). A protein failing to reach the correct conformation by itself or through folding-helper (chaperon) has two consequences: either accumulation into insoluble aggregates, forming what is known as inclusion bodies, or face enzymatic degradation (Goemans *et al.,* 2014). Therefore, there are many possible scenarios affecting the rate of recombinant protein expression compared to the cellular proteins which result in expression of the desired protein, formation of inclusion bodies or even not obtaining the protein.

As there are many endogenous proteins produced by the cells, purification of the desired protein from the mixture is an essential step. In the present study, purification was carried out in a two-step method. The first step relies on binding of the protein's hexa histidine tag to the nickel-nitrilotriacetic acid (Ni-NTA) resin. The second step is elution of the protein after washing out the unbound protein. Then size exclusion chromatography was applied for protein separation according to the size.

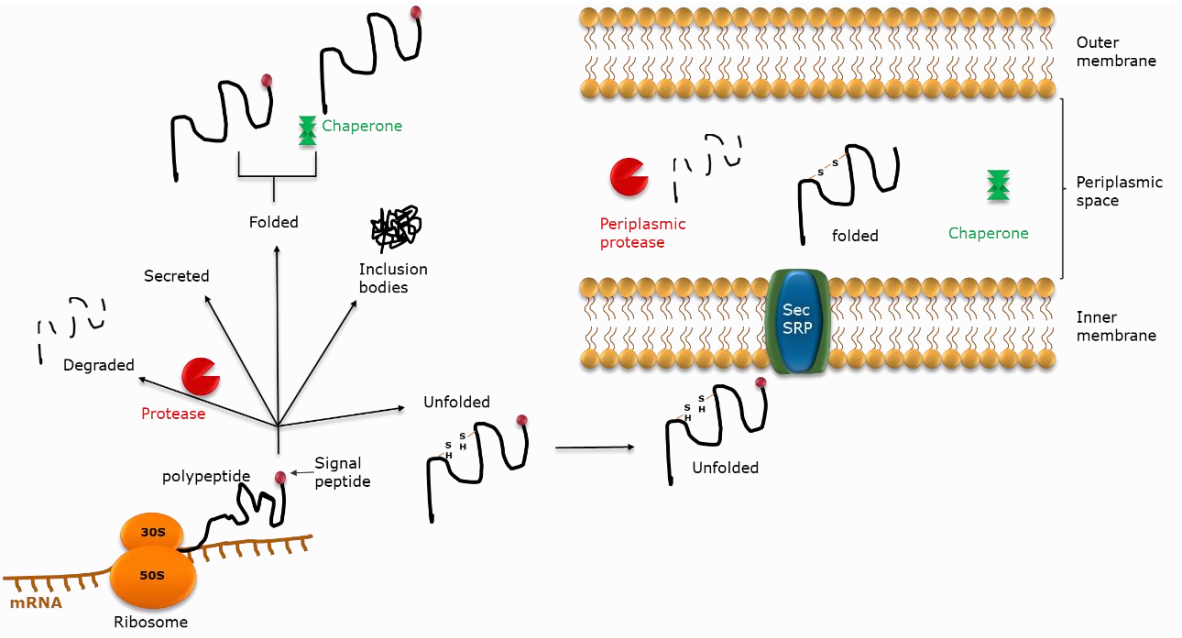


Figure 2.2 Schematic representation of recombinant protein fates after expression

After inducing expression of recombinant protein, messenger ribonucleic acid (mRNA) passes through ribosomes (consisting of 30S and 50S subunits) for translation. The transcript can be tagged with a signal leader which directs the protein to the periplasmic space. The possible scenario for this protein depends on protein composition (amino acid sequence), rate of expression and surrounding environment. If the protein is not folded properly, it will be aggregated in the cytoplasm forming insoluble inclusion bodies or degraded by cytoplasmic proteolytic system. The nascent protein either self-folded or folded with a co-helper (chaperon). The nascent protein passes through secretory recognition particle (SRP) receptor to be delivered into the periplasmic space. In some cases, protein undergoes further modification such as disulphide bonding in periplasmic space where oxidizing environment to reach its functional conformation. However, the same cytoplasmic regulation mechanisms such as degradative enzymes and chaperons are applied.

2.2.2 The expression vector (pOPE101)

The plasmid pOPE101 is sold by PROGEN Biotechnik GmbH, Germany (Figure 2.3). This cassette vector contains *lac* operon operator, which is IPTG-inducible, upstream to the synthetic *lac* promotor P/A1/04/03. Downstream to the operator there are:

1. Pectate lyase B (pelB) leader sequence
   pelB is a signal peptide sequence for periplasmic targeting. It encodes the amino acid sequence MKYLLPTAAAGLLLLAAQPAMA, which begins with methionine (M), where the protein translation is started. Then pelB is cleaved by signal peptidase in the inner membrane (Choi and Lee, 2004).
2. Multiple cloning site (MCS) in which many restriction endonuclease sites such as *Nco*I and *BamH*I are used to allow insertion of the gene of interest.
3. Short sequences code for two tags, Hexa-histidine tag and c-myc tag. Hexa-histidine commonly used for protein purification (Ferrer-Miralles *et al.,* 2011). While, c-myc tag which is part of proto-oncogene contains a product for epitope (EQKLISEEDL) that is recognised by mouse monoclonal antibody Myc1-9E10 (Hilpert *et al.,* 2001). This tag is used for protein immunodetection.
4. Transcription terminator T7, sequence from the *E. coli* ribosomal RNA (rrnB) gene, to terminate the transcription (Roßmanith *et al.,* 2018).

This plasmid also contains origin of replication, *ColE*1, and a gene for ampicillin resistance (selectable antibiotic marker).

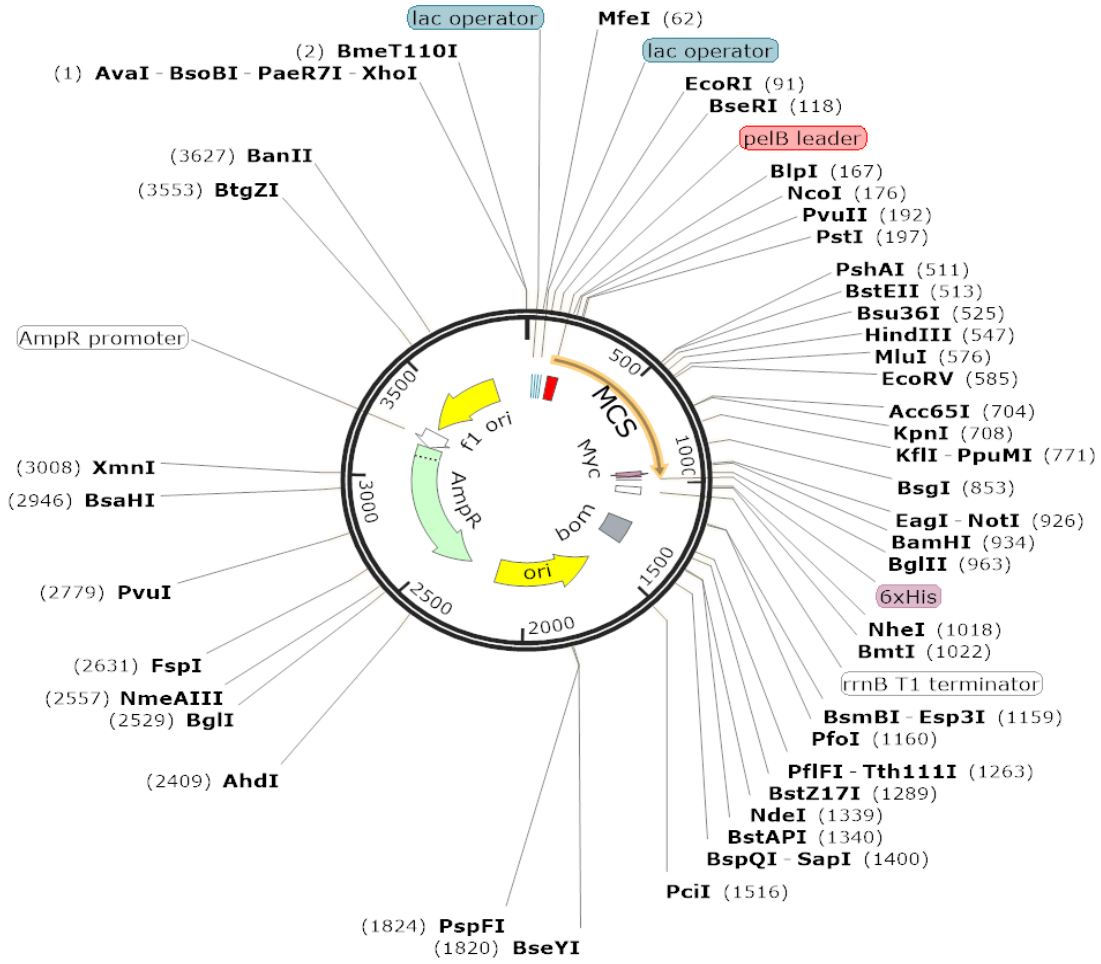


Figure 2.3 Circular map of the plasmid pOPE101

The orange arrow shows multiple cloning site (MCS), where the desired gene is inserted. Upstream to this site, pelB leader and *lac* operators are located which are marked red and blue, respectively. Downstream to MCS there are sequences for c-myc and Histidine tags. Ampicillin resistance (AmpR) gene has a separate promotor for protein expression. Ori indicate the origin of replication.

2.2.3 The expression host

The expression host used in this work is *E. coli* XL10-Gold Ultracompetent cells which was purchased from Agilent Technologies, USA. This XL2-Blue MRF derivative bacterium is highly efficient in large plasmids and ligated DNA transformation as it exhibits the Hte (high transformation efficiency) phenotype. It also has the following characteristics:

1. Deficient in restriction modification systems
   Restriction modification system is a defence system to degrade any foreign DNA by restriction enzymes. Deficiency in this system maintains the plasmid DNA safe (Vasu and Nagaraja, 2013).
2. Endonuclease deficient (endA1)
   Endonuclease A is a DNase enzyme producing DNA breakages. Mutation in this gene increases insert stability (Itaya *et al.,* 2012).
3. Tetracycline and chloramphenicol resistance.

This bacterium enhances production of recombinant membrane proteins based on plasmids using T7 RNA polymerase-based expression system (Dilworth *et al.,* 2018). These cells usually used for transformation because of the high efficiency in taking up large plasmids. Even though protein expressed in this host can result in high purity (Li *et al.,* 2012), this cell has high susceptibility to be infected by bacteriophages that resemble φ80 phage which require bacterial ferrichrome outer membrane transporter/phage receptor (Kamal *et al.,* 2013). Based on previous experience, this bacterium proved to be an optimal host for the protein production of pOPE101 and resulted in sufficient yields of functional BabA, whereas, other strains e.g. B-12, were less successful. Moreover, its periplasmic space provides an oxidising environment for disulfide bonds formation an ideal place for protein extraction after post-translational modification.

2.3 Enzyme-linked immunosorbent assay

Immunoassays follow the fundamental principle of specific antigen-antibody binding reaction. This principle can be traced back to 1890, when Behring and Kitasato discovered a substance in the blood which has the ability to neutralise diphtheria toxin. This neutralising substance was termed antibody, while the substance which acts as inducer was termed antigen (Gao *et al.,* 2018).

Enzyme-linked immunosorbent assay (ELISA) is a solid plate-based immunoassay invented independently by two research groups in 1971 (Engvall and Perlmann, 1971, Van Weemen and Schuurs, 1971). They modified the radioimmunoassay (RIA) method by employing enzymes instead of the radioactive iodine-125 (^{125}I) to quantify the binding reaction between target antigen and specific antibody (Aydin, 2015). Detection of this reaction can be through colour changes or fluorescence. There are different variations of the main principle to quantify a specific substance such as direct, indirect, competitive and sandwich ELISA (Grange *et al.,* 2014). In the present study, three types were applied (direct, indirect and sandwich) to study protein binding ability. More details about these types and their advantages and disadvantages have been reviewed in (Aydin, 2015, Shah and Maghsoudlou, 2016).

In general, ELISA consists of five main phases separated by washing step using phosphate buffer saline supplemented with Tween 20 to increase the specificity of the assay and remove any unbound substances.

1. The ligand was coated or immobilised, in this case glycoconjugates, using alkaline buffer (pH at least 9) to allow passive absorption to the well.
2. The unbound area was blocked using a non-reactive protein such as casein-rich milk to prevent non-specific binding and increase the specificity.
3. Protein of interest was added to test its binding ability.
4. A layer of primary antibody which is sometimes conjugated with biotin was added. This may be followed by secondary antibody/ streptavidin conjugated with horseradish peroxidase.
5. The substrate which react with the enzyme was added, following by measuring the change in colour which indicate the presence of the target substance.

2.3.1 Direct enzyme-linked immunosorbent assay

Direct ELISA is the simplest type which used to detect protein directly. Briefly, after coating the 96-well plate with an antigen, primary antibody conjugated with enzyme is added to interact with the antigen, then a substrate for the enzyme is added. Then the reaction is stopped, and a microplate reader is used for analysis.

In the present work, as illustrated in Figure 2.4, two modifications were made for the purpose of adapting the technique and to increase the specificity.

1. Neoglycoconjugates, which act as ligands for the protein, were immobilised onto the surface of the 96-well polystyrene plate.
2. Instead of using primary antibody with a conjugated enzyme, Nickel nitrilotriacetic acid-Atto 488 (Ni-NTA-Atto 488) (Sigma-Aldrich, UK) was used.

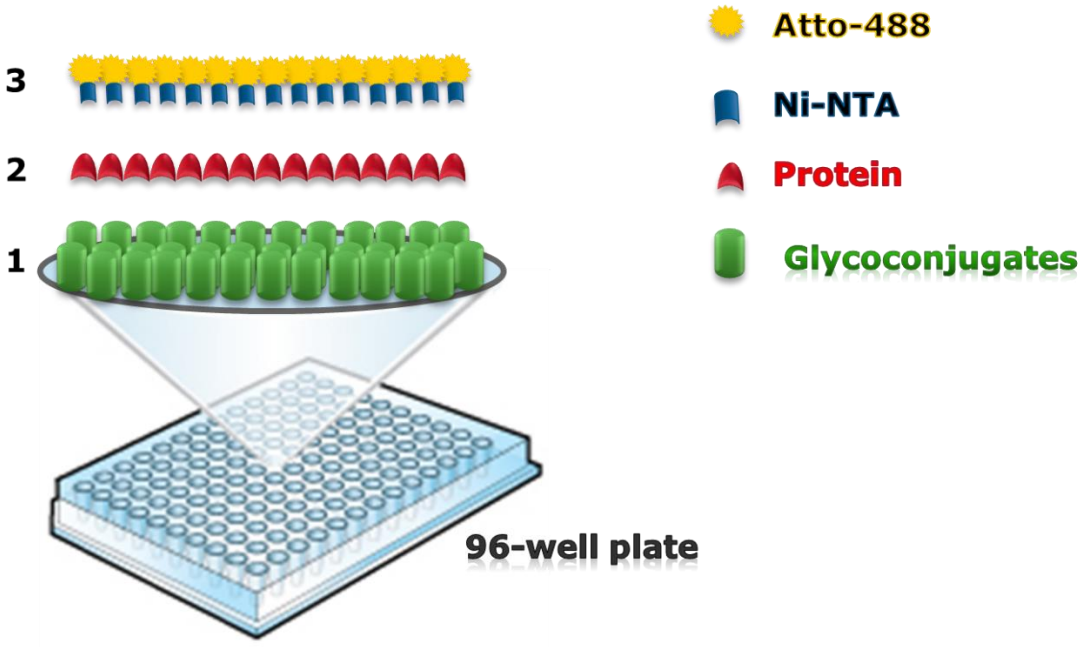


Figure 2.4 Schematic representative of a direct ELISA

The number indicates the order of the steps, which are 1. Coating the 96-well plate with glycoconjugates. 2. Adding the protein. 3. Adding the detection agent which is Nickel-nitrilotriacetic acid (Ni-NTA) conjugated with Atto 488.

2.3.2 Indirect enzyme-linked immunosorbent assay

Indirect enzyme-linked immunosorbent assay was used to reveal the binding of biotinylated protein to the glycoconjugates immobilised on the plate. The overall steps are demonstrated in Figure 2.5.

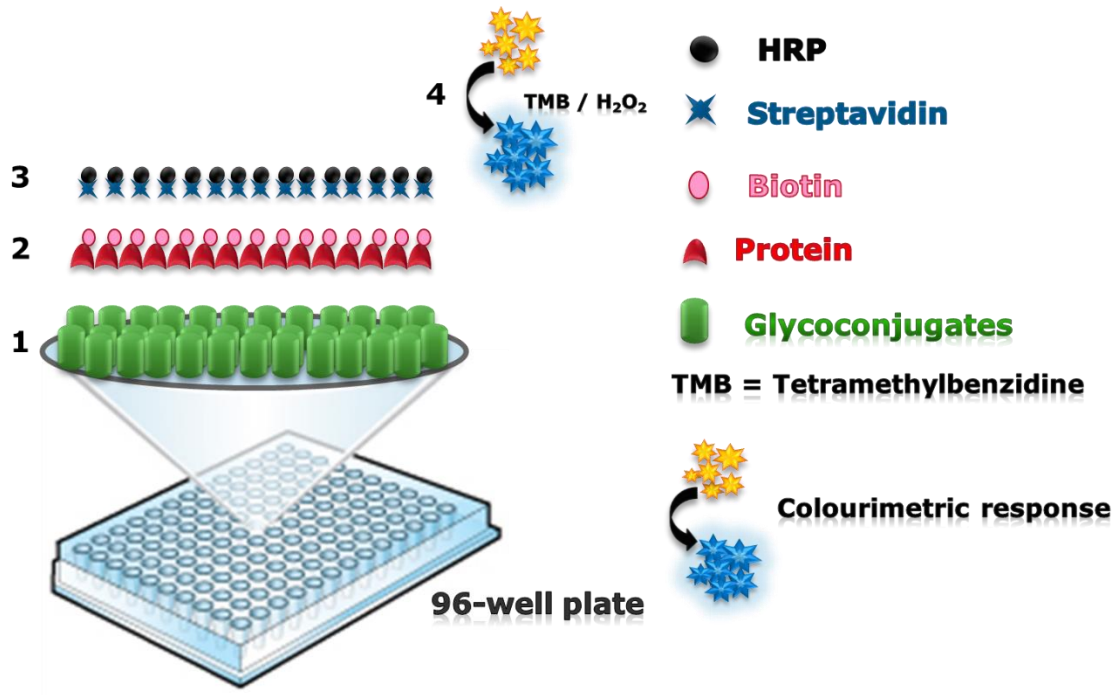


Figure 2.5 Schematic representative of indirect ELISA

The number indicates the order of the steps, which are 1. Coating the 96-well plate with glycoconjugates. 2. Incubating the plate with protein. 3. Adding streptavidin conjugated with Horseradish peroxidase (HRP). 4. Developing the reaction using the substrate tetramethylbenzidine (TMB) and H_2O_2.

2.3.3 Sandwich enzyme-linked immunosorbent assay

In the present study, a modification of sandwich ELISA was developed. Instead of trapping an antigen between two antibodies in the original method, the protein was sandwiched between a ligand (glycoconjugate) and a primary antibody. This modification provides high specificity for detecting the protein as the immobilised ligand capture the protein. The principle steps were demonstrated in figure 2.6.

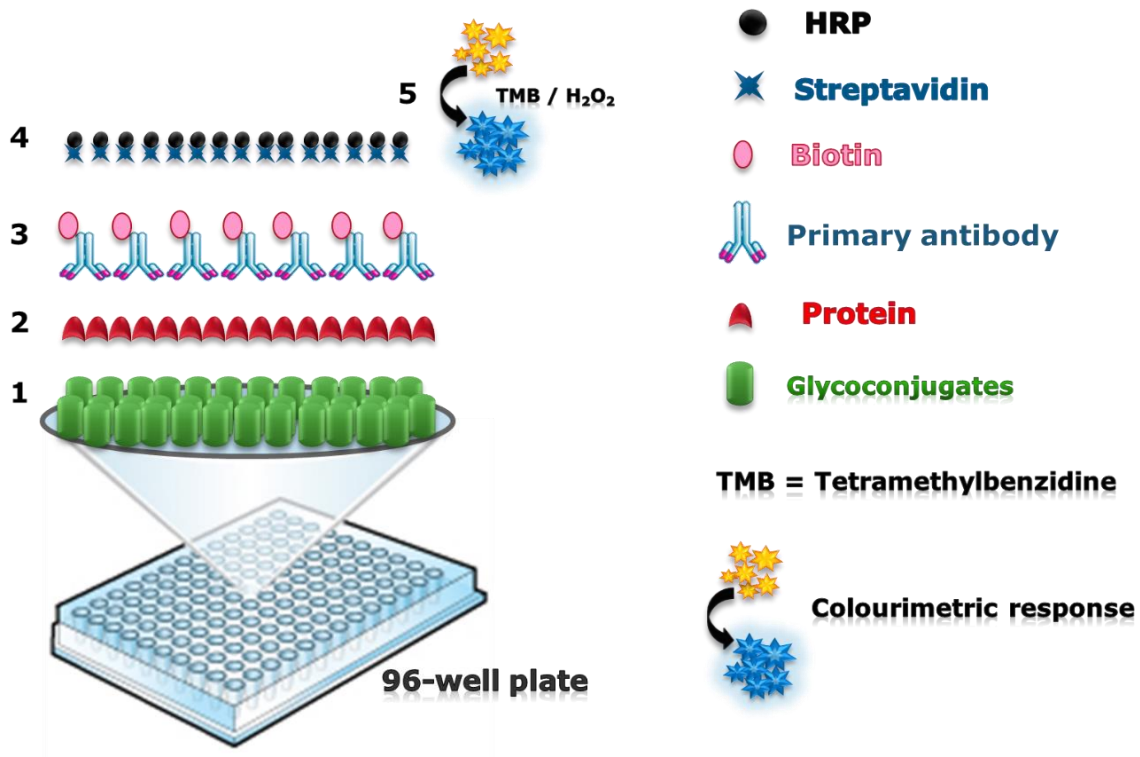


Figure 2.6 Schematic representative of sandwich ELISA

The number indicate the order of the steps, which are 1. Coating the 96-well plate with glycoconjugates. 2. Adding the protein. 3. Adding primary antibody conjugated with biotin. 4. Adding streptavidin conjugated with Horseradish peroxidase, which act as secondary antibody. 5. Developing the reaction using tetramethylbenzidine (TMB) and H_2O_2.

2.4 Circular Dichroism spectroscopy

Circular dichroism (CD) spectroscopy is a quick method for exploring protein secondary structure, dynamics, folding property or conformation (Greenfield, 2006). Circular Dichroism occurs when left-handed and right-handed circularly polarized light are absorbed differentially by chiral molecules such as nucleic acids or proteins. The basic principle underlying this spectrometric technique is the measurement of the differential magnitude of the left-handed and the right-handed absorption in ellipticity (θ) units (Kelly *et al.,* 2005).

In case of protein, characteristic CD spectra arise from the asymmetric peptide bonds, which act as chromophores for the circularly polarised light. The consequence of the interaction between the polarised light and the chiral molecules at distinctive wavelength results in distinguished CD spectra. Different secondary structures e.g. alpha helix, beta sheet (parallel or antiparallel), or turns are determined by CD spectra between 180 and 250 nm in the far-Ultraviolet wave length (Kelly and Price, 2000). Information about protein tertiary structure is provided from the aromatic amino acids (tryptophan, phenylalanine and tyrosine), which act as chromophores in the near-UV wavelength range between 250 and 320 nm (Miles and Wallace, 2016).

There are various kinds of circular dichroism spectroscopy, such as conventional electronic, magnetic, fluorescence detected and vibration CD. For more details about the difference types and their uses, review (Ranjbar and Gill, 2009, Kelly *et al.,* 2005). Indeed, these new types of CDs benefit from the new computational programmes and the advance in bioinformatics methods to improve not only structural analysis of the protein secondary structure but also to include symmetric, asymmetric substances and nanostructures (Ranjbar and Gill, 2009).

Different protein secondary structures (Figure 2.7) as explained in (Greenfield, 2006) are:

1. **α- Helices** show two negative and at 208 nm and 222 nm and a strong positive band at 193 nm
2. **β- pleated** sheets are characterised by the presence of a positive band at 195 nm and negative band centered around 216-219 nm.
3. Proteins with **random coil** or disordered conformation show a strong negative ellipticity below 200 nm and weak positive band above 210

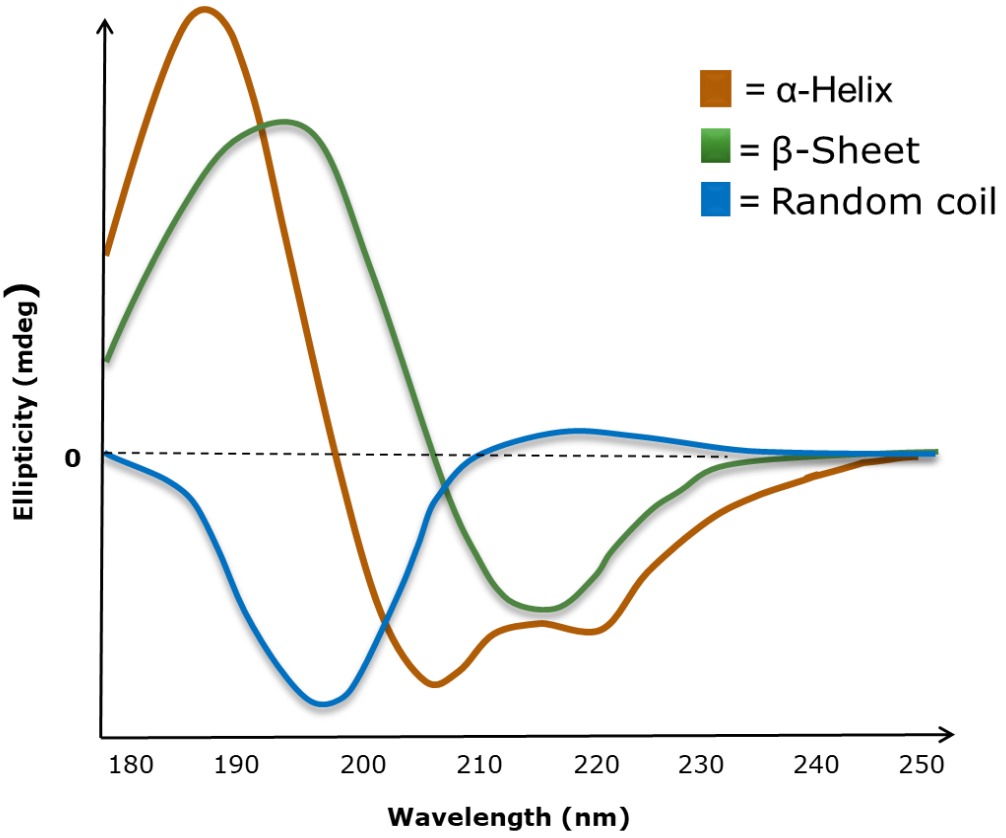


Figure 2.7 Far-UV circular dichroism spectra associated with the various protein secondary structures

Circular dichroism spectra of α-helices protein indicated in (brown), β-sheets (green) and disordered protein displayed in (blue). Modified from (Greenfield, 2006).

2.5 Dynamic light scattering (DLS)

Dynamic light scattering (DLS), also known as photon correlation spectroscopy (PCS) or quasi-elastic light scattering, is a classical technique to measure particles hydrodynamic size in suspension (Stetefeld *et al.,* 2016). Therefore, it can be a useful technique to study colloidal stability of protein conjugated to microparticles, i.e. not aggregated.

DLS measures particle size by calculating their velocity or Brownian motion (particles random motility in a suspension) and relate this to equivalent hydrodynamic size which is imparted through the frequent shifts of the scattered light over the time (Figure 2.8).

The principle of DLS based on the changes in light scattering pattern when a beam of monochromatic light is directed into a solution of particles. This change occurs due to the translations, motions and rotations of the particles and diffusion in the solvent. Each particle also acts as a refractive index to the other. Thus, the diffusion occuring randomly, termed Brownian motion, and proportional to the particles size and time. Small particles diffuse faster than the larger ones, as a result, the rate of changes in the light scattering pattern fluctuate more (Brar and Verma, 2011). These fluctuations in scattered light intensity are recorded by a detector and calculated depending on the velocity of Brownian motion over time. This time-dependent motion is termed the diffusion coefficient and related to the particle hydrodynamic size. See reviews by (Stetefeld *et al.,* 2016, Hassan *et al.,* 2015) for more explanation. For spherical particles, the hydrodynamic radius (R) is obtained from the translational, using autocorrelation function, diffusion coefficient (D) using Stokes-Einstein equation: $D = \frac{kT}{6\pi\eta R}$

Where D= diffusion coefficient

k= Boltzmann constant

T= absolute temperature (in Kelvin)

η= dispersant viscosity

R= radius of spherical particle

For nonspherical particles, the radius is taken as equivalent sphere radius. That means an average hydrodynamic dimeter calculated and size distribution are analysed to state the polydispersity of the sample.

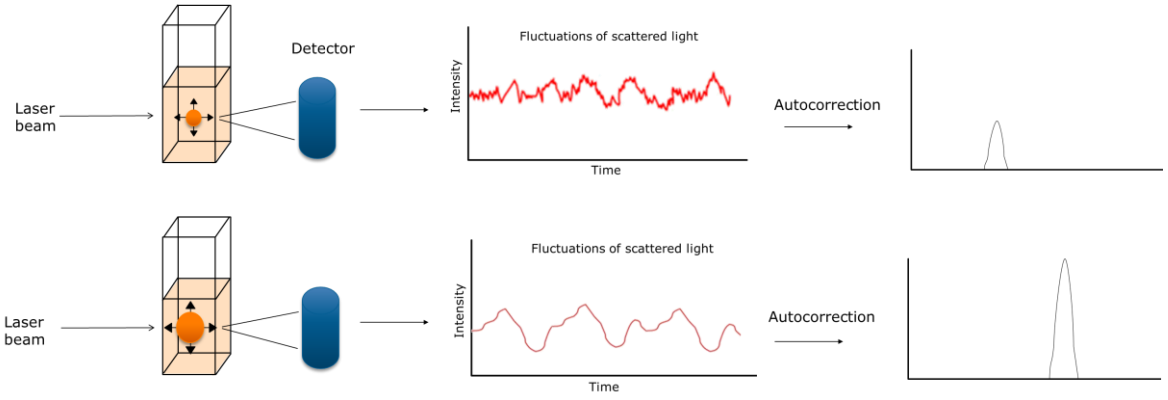


Figure 2.8 Schematic representation of the principle of dynamic light scattering

A laser light is directed through a cuvette containing a solution of particles, then data displayed depending of the speed of Brownian movement. Particles of small size move faster than the larger ones. A detector records the change in the light fluctuations over a time scale, then a software translates this data to display the graph. ✣ = represents random motility.

CHAPTER THREE

3. Cloning and expression of BabA J99 Crown region as the minimal Le^b-binding domain

3.1 General overview

The objective of this chapter was to use recombinant DNA technology to express BabA J99 Crown domain. The research hypothesis, based on crystallography, was that the Crown as a separate domain is able to perform the binding function independently. Thus, two goals were set:

1. Constructing the expression cassette of BabA-Crown domain through DNA amplification from an existing recombinant BabA J99 construct, clone the gene into an expression vector, pOPE 101, then transform the plasmid into a competent cell strain, *E. coli* XL10-Gold, for protein expression.
2. Developing a method to obtain soluble recombinant protein to be used for downstream experimentations.

BabA is a member of the outer membrane protein family or adhesin proteins. Its structure consists of cleavable N-terminal signal sequence, followed by passenger domain and translocator β-barrel-shaped domain at the C-terminal. The signal peptide, about 20 residues, leads the protein via Secretory (Sec) system across the inner membrane into the periplasmic space, where it is cleaved at A↓EDDG (arrow↓ marks the cleavage site) (Alm *et al.,* 2000). After post-transcriptional modifications, the translocator domain is embedded into the outer membrane and facilitates translocation of the passenger domain into the cellular outer membrane. The passenger domain is predicted to have a sequence acting as specific-protein functional domain that differentiates the adhesins (Coppens *et al.,* 2018).

In the light of the published BabA crystal structures (Moonens *et al.,* 2016, Hage *et al.,* 2015a), three regions were predicted and named in analogy to SabA, the first crystallised *H. pylori* adhesin. These three regions are the Handle, located at the C-terminus, followed by the Head and then the Crown, residing at the top of the other domains. The boundaries between these regions, as shown in BabA (pdb: 4ZH7) (Figure 3.1) are:

1. Handle between Q27 and K529
2. Head between P56 and N462,
3. Crown between G179 and V255

The Crown domain interacts with two beta sheets located in the Head domain through Hydrogen bonding e.g. two Hydrogen bonds in Crown's Serine (S190) interact with Lysine (K119) in the Head domain. This interaction may support the structure of the Crown or enhance its folding ability.

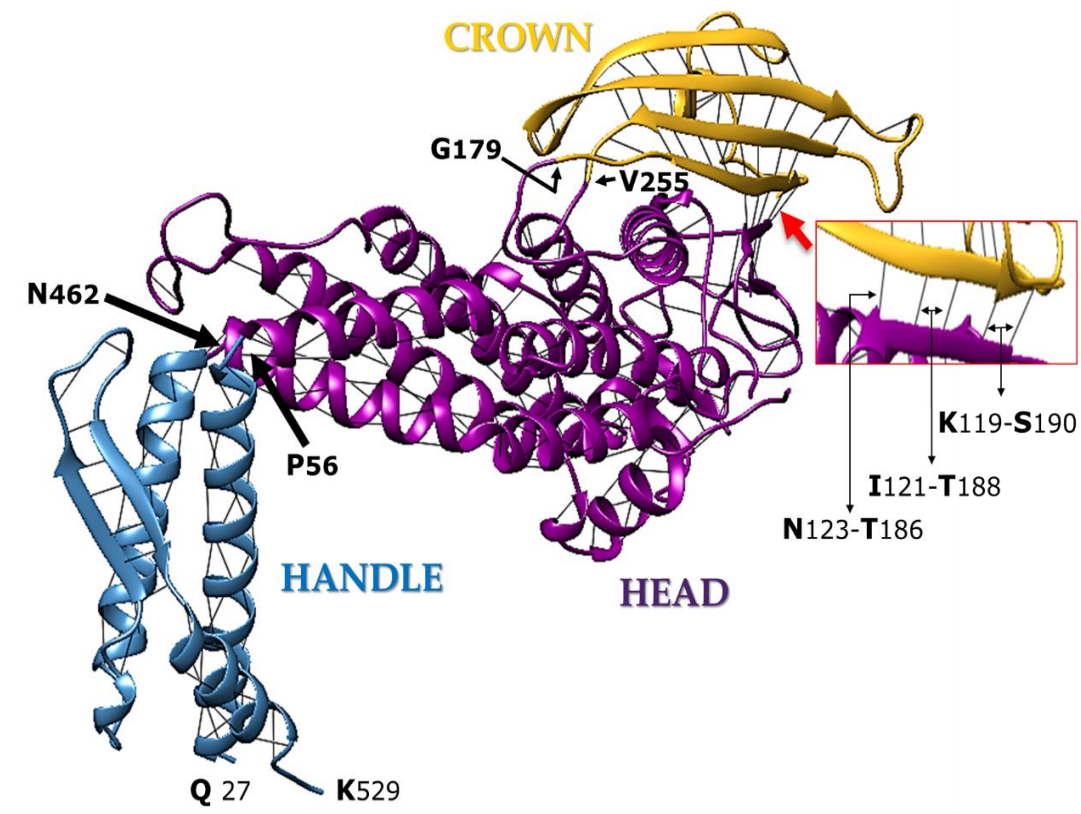


Figure 3.1 crystal structure of BabA (pdb:4ZH7) showing the boundaries between the domains and the Hydrogen bonds.

The Crown is the functional domain, specifically, the adhesin-receptor for Le^b (Figure 3.2). The mechanism of this β-sheet domain folding and orientation in the outer membrane is not known, but paired cysteine formation (Figure 3.3) is essential for functional requirement (Letley *et al.,* 2006, Dautin and Bernstein, 2007) through forming a disulphide-clasped loop which increases the association with Le^b (Moonens *et al.,* 2016). Even though the Crown interacts with the head domain, at this stage, an attempted was made to use it as the minimal binding site.

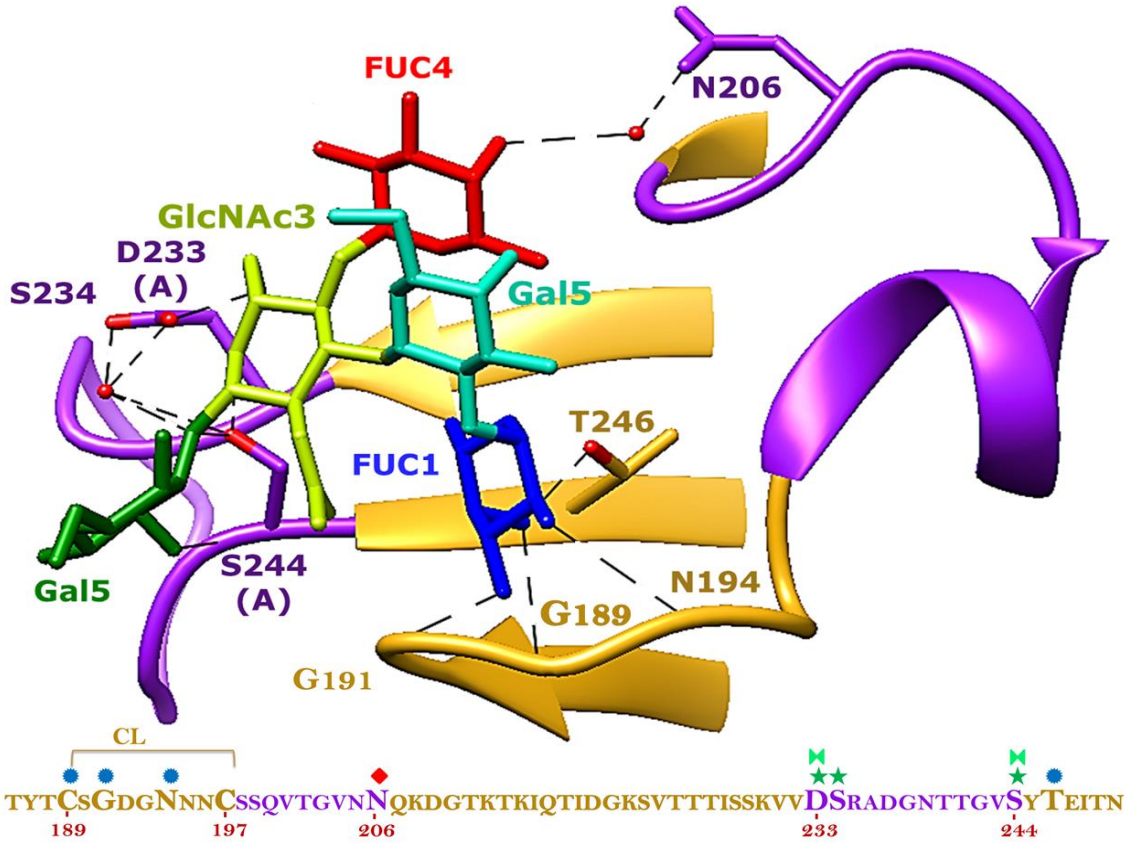


Figure 3.2 Crystal structure of BabA-Crown molecular interactions with Le^b.

Fucose1 ("FUC1") ( ) forms hydrogen bonds with the carbonyl backbone groups of C189, G191, and N194, and the hydroxyl group of the T246 side chain. Fucose 4 ("FUC4") ( ) interacts with the hydroxyl group of the N206 side chain through a water-mediated hydrogen bond. N-acetyl-glucosamine ("GlcNAc3") ( ) residue forms two hydrogen bonds with the carboxyl and hydroxyl side-chain groups of D233 and S244, respectively. Dual mutation ( ) in these two positions result in nonbinding activity and thus used as a BabA mutant protein. Purple sequence indicates hypervariable loops.

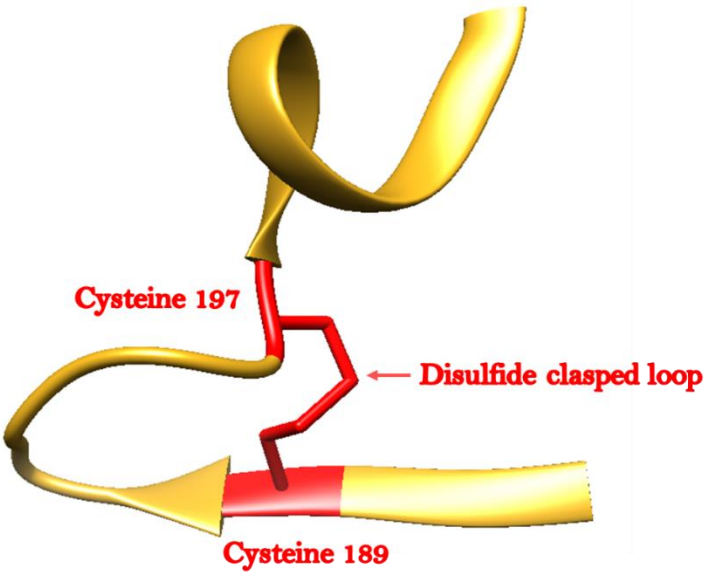


Figure 3.3 Detail of the BabA-Crown showing the Cysteine location

BabA-Crown (gold) has two Cysteine residues (red) forming a disulphide bond between C197 and C189. This disulphide clasped loop stabilises the structure of the ligand binding site (Moonens *et al.,* 2016).

The interactions between the Crown amino acids and Le^b residues depend on a network of Hydrogen bands, in part water-mediated. As demonstrated in Figure 3.4, S244 and D233 side chains of the Crown play a major role in binding, by two hydrogen bonds, with the N-acetylglucosamine (GlcNAc3) residue of Le^b. Substitutions in these sites result in a complete loss of binding affinity (Hage *et al.,* 2015a).

To achieve the goals of this chapter and based on BabA X-ray crystal structure (pdb: 4ZH7) which revealed the fine interactions between the Crown as a binding region and Le^b as the physiological glycan ligand on gastric cells, two different sequences of BabA-Crown (wild-type and mutant) were chosen for expression. The wildtype corresponds to the expressed fragment used in X-ray crystallography, while the mutant contained two substitutions (D233A/S244A) intended to be used as a negative control in binding assays.

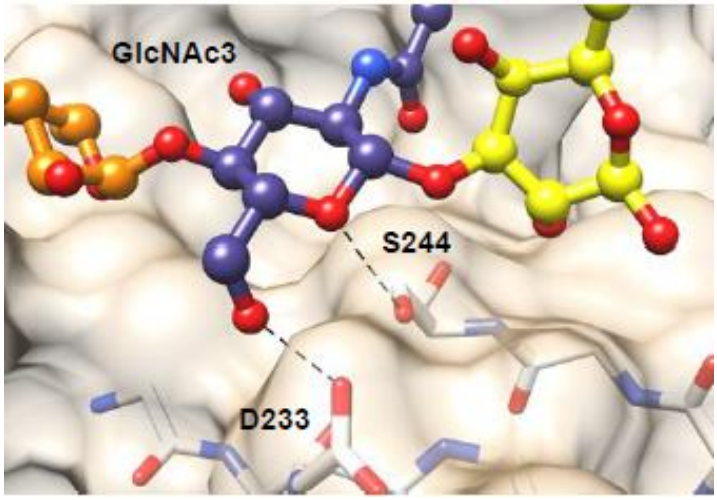


Figure 3.4 Interactions of N-acetylglucosamine in Le^b with BabA-Crown

N-acetylglucosamine (GlcNAc) of Le^b forms hydrogen bonds with carboxyl side chain of D233 and hydroxyl side chain group of S244 (Hage *et al.,* 2015a). Replacement of D233 and S244 with Alanine result in BabA loss of binding ability.

3.2 Experimental procedures

3.2.1 Generation of BabA-Crown expression construct

3.2.1.1 BabA-Crown gene

Nucleotides 528–766 bp corresponding to BabA-Crown amino acids 177-255 were used for generating the construct. The BabA coding sequence (GenBank accession no AE001439.1) was initially amplified from *H. pylori* J99 genomic DNA, a kind gift from Prof. John Atherton, University of Nottingham.

All of these sequences were inserted into the pOPE101 expression vector as shown in Figure 3.4.

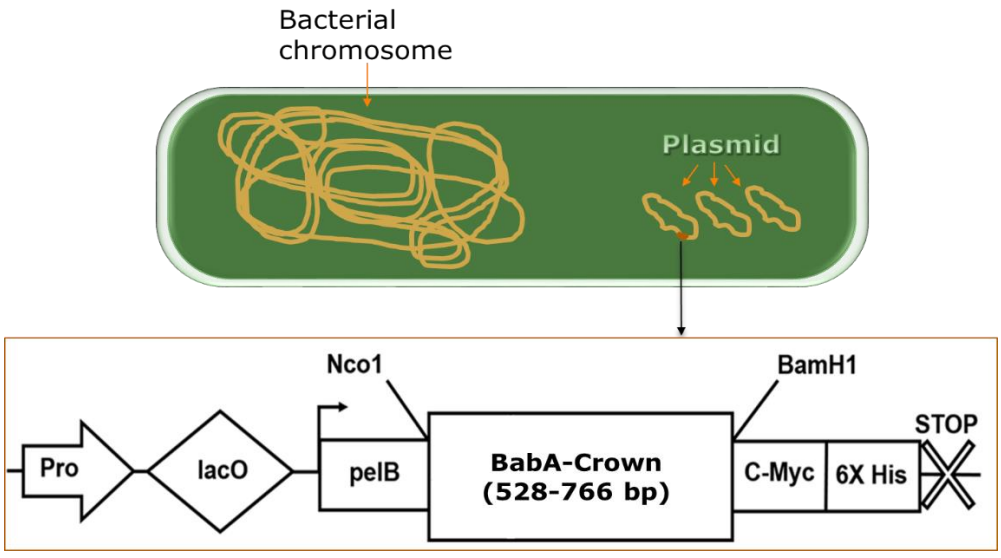


Figure 3.5 Schematic representative of the expression cassette

Pro: synthetic lactose promoter. **LacO**: IPTG-inducible lactose operator. **Arrow**: represents the start codon. **PelB**: leader sequence to target the protein into the periplasmic space. **c-Myc** tag for immunodetection. **6X His**: Histidine tag for protein purification. ***BamH*1** and ***Nco*1** are restriction sites.

3.2.1.2 Polymerase chain reaction amplification

BabA-Crown DNA sequence was amplified from previously produced recombinant BabA plasmid. This gene fragment encoded amino acids 177- 255 of mature BabA J99 (The Crown). The primers (shown in Table 3.1) contained a six-nucleotide overhang, terminal restriction sites that enabled insertion of the BabA-Crown sequence into a pOPE101 vector. PCR amplification was performed using KOD Hot Start Master Mix (Merck Millipore, Germany). The cycling conditions were performed as described in (Table 3.2).

Table 3.1 Primers for gene amplification

The primer name combined the names of the target gene sequence, restriction enzyme used which are underlined in oligonucleotide sequence, and whether it is a sense (FOR) or antisense (REV). The hexa-overhang nucleotides (AATATG & GCCGCC), are located up-stream of the underlined restriction sites *Nco*I and *Bam*HI.

Primer name	**Primer Sequence (5' → 3')**
BabA-Crown_*Nco*I FOR	AATATGCCATGGCAAACAACGGGAAAGTCAATG
BabA-Crown_*Bam*HI REV	GCCGCCGGATCCCACACCTTCTAATTTGTTGGTG

Table 3.2 Thermocycling conditions

Step	Temperature and time
1. Polymerase activation	95 °C for 2 min
2. Denaturation	95 °C for 20 seconds
3. Annealing	60 °C for 10 seconds
4. Extension	70 °C for 10 seconds

Cycles (steps 2 to 4) were repeated 30 times

3.2.1.3 Cloning

3.2.1.3.1 Digestion

After PCR amplification, the products were separated by agarose gel electrophoresis using 1 % agarose gel and running buffer TBE (0.5x Tris-Borate-EDTA). Then purified using Wizard® SV Gel and PCR clean-up system (Promega, USA). Two Eppendorf tubes contain 500 ng of purified PCR products and pOPE101 plasmid (Progen Biotechnik, Germany) were separately digested using 1X of each of the restriction enzymes, *Nco*I-HF and *BamHI*-HF (New England Biolabs, USA). The mixtures were incubated at 37 °C for 1 hour then the enzymes were deactivated by heating at 80 °C for 20 minutes. The digested PCR products and pOPE101 vector were combined together at molecular ratio of 20 ng of vector to 3-fold of the insert and incubated with 1X T4 DNA ligase (New England Biolabs, USA) for 20 minutes on ice.

3.2.1.3.2 Bacterial transformation

To propagate BabA-Crown recombinant plasmid in a bacterial host, transformation was carried out. From each of the ligation mixture which contain the engineered plasmids, 2 µL (containing about 50 ng of DNA) was added to 100 µL of *E. coli* XL10-Gold cells (chemically competent *E. coli*, Agilent Technologies, USA). This bacterium was also used as the expression host. The products were first incubated on ice for 30 minutes, followed by heat shock in a water bath at 42 °C for 30 seconds before incubating on ice for 2 minutes. Then the transformed cells were grown in super optimal broth with catabolic repression (SOC) medium for 1 hour at 37 °C. Afterwards, the transformants were plated at different concentrations on lysogeny broth (LB, Sigma-Aldrich, UK) agar plates treated with ampicillin (100 µg/mL) (herein named LB_{amp}) and incubated overnight at 37 °C. The next day, single colonies were picked from overnight culture plates and each colony was resuspended in 20 µL of LB_{amp}. The selected colonies were, individually, subject to PCR screening to check for the presence of the inserted gene within the plasmid sequence. This was done using the ReadyMix™ Taq PCR Reaction Mix (Sigma-Aldrich, UK) pOPE101 promotor/ terminator primers (Table 3.3) following protocol on Table (3.4).

Table 3.3 Primers for colony PCR screening and confirmatory DNA sequencing

Promotor and terminator indicate transcriptional sites for *Lac* operon gene between which the gene was inserted, FOR and REV are the sense and antisense primers, respectively.

Primer Name	Primer Sequence (5′ → 3′)
pOPE101_Promoter FOR	TTGACTTGTGAGCGGATAAC
pOPE101_Terminator REV	ATGTGTCAGAGGTTTTCACC

Table 3.4 Thermocycling conditions for colony PCR

Step	Temperature and time
1. Initial denaturation	95 °C for 2 minutes
2. Denaturation	95 °C for 30 seconds
3. Annealing	58 °C for 30 seconds
4. Extension	72 °C for 2 minutes
5. Final extension	72 °C for 2 minutes

Cycles (steps 2 to 4) were repeated 35 times

The PCR products were detected using agarose gel electrophoresis and colony samples/clones corresponding to the expected size were incubated in 5 – 10 mL LB_{amp} broth media supplemented with Ampicillin at 37 °C overnight. Afterwards, plasmids were extracted using a Wizard®*Plus* SV Miniprep DNA purification system (Promega, USA) following the manufacturer's protocol. The concentration and purity (OD 260/280 nm) of the plasmids was measured using Nanodrop2000 (Thermo Scientific, USA). Finally, to confirm the DNA sequence was in frame with the plasmid DNA sequence, i.e. pelB leader, samples were sent to Source Bioscience Life Sciences (Nottingham, UK) for sequencing using pOPE101 promotor primers (Table 3.3). After sequence confirmation, transformants having the correct insert sequence were aliquoted. Equal volume of bacterial culture to 60% glycerol was added in a vial, mixed gently, vortexed and incubated for 1 hour at – 40 °C before being stored at – 80 °C for later experiments.

3.2.2 Protein expression (small-scale)

3.2.2.1 BabA protocol

To investigate the suitability of the protocol used for BabA expression (Hage *et al.,* 2015b) and prior to large-scale expression of the confirmed engineered products, a small-scale experiment was conducted. This protocol is designed to extract the protein from the periplasmic space in *E. coli* XL10-Gold using an osmotic shock method (Schmiedl *et al.,* 2000). *E. coli* XL10-Gold cells harbouring the BabA Crown expression constructs were used for both plasmid propagation and protein expression.

From the glycerol stock, 10 µL was inoculated into 5 mL of LB_{ATG} medium (LB Broth containing 100 µg/mL Ampicillin, 12.5 µg/mL Tetracycline hydrochloride, 0.1 M D-Glucose) and grown overnight at 37 °C. Next day, 100 µL from the starter culture was inoculated into 20 mL of fresh LB_{ATG} culture medium, then grown at 37 °C until optical density (OD_{600}) of 0.6 was reached. At this point, before adding isopropyl β-D-1-thiogalactopyranoside (IPTG) to induce protein expression, 1 mL from the culture was taken to be used as total protein fraction. IPTG (0.1 mM) was added to the culture medium to a final concentration of 100 µM then incubated at 24 °C for 12 - 16 hours. Other samples e.g. the periplasmic extract were prepared, as described below, for the investigation of the expression and were subject to sodium dodecyl sulphate polyacrylamide gel electrophoresis (SDS-PAGE) analysis using Coomassie stain or Western blotting for detection of expression and confirmation of identity, respectively.

3.2.2.2 Preparation of total cell protein fractions

After the grown culture reached an OD_{600} of approximately 0.6, 1 mL of the culture was placed in 1.5 Eppendorf tube, centrifuged at 10,000 g for 1 minute at room temperature to harvest the bacterial cells, supernatant discarded, pellet dissolved in 100 µL Phosphate buffer saline (1X PBS) followed by 100 µL of non-reducing sample buffer (2X NRSB), which consisted of 100 mM Tris-Cl (pH 6.8), 0.2% bromophenol blue, 4% SDS and 20% glycerol. The solution was vortexed, sonicated on ice using probe sonicator about 5 seconds bursts at 10 - 20 % power in ultrasonic homogeniser (Bandelin sonopuls HD 2070) with the sample on ice,

then kept in the freezer until use. Immediately before running in SDS-PAGE, the sample was heat denatured at 100 °C for 5 minutes.

3.2.2.3 Periplasmic extraction and spheroplast fraction preparation

For preparing the periplasmic fraction, cells were harvested by centrifugation at 10,000 g for 10 minutes at 4 °C. The pellet was resuspended in 1/10 culture volume using cold Spheroplast solution [Tris-Cl 200 mM (pH 8), sucrose 20%, ethylenediaminetetraacetic acid (EDTA) 1%] supplemented with cOmplete®EDTA-free protease inhibitor cocktail tablets (Roche, USA), shaken gently on ice on an orbital platform shaker for 30 minutes, then centrifuged at 10,000 g for 10 minutes at 4 °C. The supernatant, which contained the periplasmic fraction, was collected and stored at 4 °C for further processing, while the pellet was resuspended in cold 5 mM $MgSO_4$, centrifuged at 10,000 g for 10 minutes and again the supernatant was collected. Afterwards, 250 µL of Trichloroacetic acid solution (TCA) was added to 1 ml of each of the obtained supernatants for protein precipitation, and centrifuged (10,000 g for 5 minutes) after incubation for 10 minutes on ice. The protein pellet was washed with 200 µL of cold acetone and centrifuged again at 10,000 g for 5 minutes. This step was done twice before the acetone was discarded and the pellet was finally spun at 10,000 g for 5 minutes. The residual acetone was allowed to evaporate. The obtained pellet was dissolved in 100 µL of 2x non-reducing sample buffer (2X NRSB) and an equal amount of 100 µL PBS, vortexed, heat-denatured prior to running in SDS-PAGE.

3.2.3 Plasmid DNA purification and measurement

During bacterial growth for protein expression, 1 mL from the growth culture was collected, hourly, to measure both OD_{600} and plasmid DNA concentration. For the later, samples purified with QIAprep® Spin Miniprep Kit–Qiagenl. The concentration of the purified pDNA was measured using Nanodrop2000 (Thermo Scientific, USA).

3.2.4 Subcellular fraction analysis

3.2.4.1 SDS-PAGE

From samples prepared for subcellular fractions preparation, 12 - 15 µL of each sample was loaded onto mini-PROTEAN TGX 4 - 20% (Bio-Rad, USA) precast gels for vertical gel electrophoresis in Mini-PROTEAN™ tetra Cell (Bio-Rad, USA) running for about 35 minutes at 200 Volt.

3.2.4.2 Coomassie stain

Following SDS-PAGE, Tri-glycine gels were stained with Coomassie staining (Instant Blue, Expedeon, USA) for at least 1 hour at room temperature to obtain good visualized protein bands, then destained with deionised water.

3.2.4.3 Western blot analysis

To specifically detect the presence of the recombinant BabA-Crown protein in the prepared subcellular fractions, Western blotting was performed. After SDS-PAGE, a 0.2 µm nitrocellulose membrane (Thermo Scientific, USA) was used for blotting the Tris-glycine gels. The gel was sandwiched between two ion reservoir stacks, one containing the blotting membrane, then laid in the centre of a cassette base and covered. Trans-Blot® Turbo™ Blotting System (Bio-Rad, USA) was used for blotting the gel onto the nitrocellulose membrane. Afterwards, the membrane was blocked, by incubating for 1 hour at room temperature, in 5% non-fat milk powder (Marvel, Premier Foods, UK) dissolved in TBS-T (Tris-buffered saline, pH 7.4, supplement with 0.1% Tween-20) buffer. Next, freshly prepared blocking buffer containing primary antibody was added to the membrane and incubated at 4 °C overnight under constant shaking. The primary antibody used was either

1. A biotinylated mouse anti-c-Myc antibody (Clone 9E10, AbD Serotec, USA) or
2. A monoclonal mouse anti-His-Tag antibody (GE Healthcare, USA)

Both antibodies were diluted in freshly prepared TBS-T buffer at a ratio of 1:5000.

The following day, the membrane was washed four times with TBS-T buffer for 15 minutes before incubation for 1 hour with secondary antibody diluted in blocking buffer at the same 1:5000 ratio and incubated at ambient temperature. The secondary antibody used was either

1. Streptavidin-Horseradish peroxidase (HRP) conjugate (AbD Serotec, USA) for c-Myc immunodetection or
2. Goat anti-mouse IgG HRP conjugate (GE Healthcare, USA) for hexa histidine detection.

After washing four times with TBS-T buffer for 15 minutes, the membrane was exposed to commercial chemiluminescent reagents (Pierce™ ECL Western Blotting Substrate, Thermo Scientific, USA). The composition of the reagents for detection used is proprietary.

Imaging was performed with a charge coupled device (CCD) camera (Fujifilm LAS-4000) using the high binning resolution setting.

3.3 Results

3.3.1 Construction of the BabA-Crown region

3.3.1.1 Crown region amplification

The initial step for generating BabA-Crown expression constructs was to amplify the BabA gene fragment encoding the Crown region and its variant (BabA-Crown$_{_D233A/S244A}$). PCR products gave single bands under 300 base pairs (bp) on agarose gel after gel electrophoresis. Considering that the gene length is 238 bp together with the restriction sites on both C- and N-termini (11 bp) in addition to the extra 12 bp flanking on each end, totalling 261 bp, it was assumed that successful amplification of both BabA-Crown gene fragments had been achieved (Figure. 3.6).

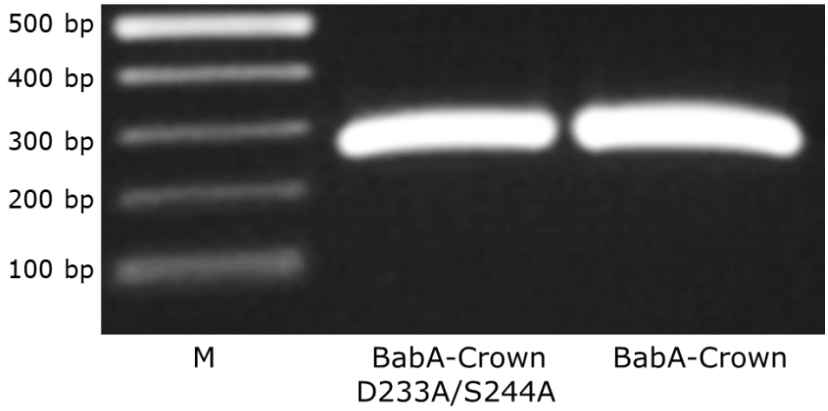


Figure 3.6 Gel electrophoresis of BabA-Crown gene

BabA-Crown$_{_D233A/S244A}$ and BabA-Crown were amplified from previously constructed recombinant BabA plasmid. The expected size of this PCR product is 261 bp including *Nco*I and *BamH*I restriction sites and hexa-nucleotides overhang at both 3’ and 5’ ends. The marker (M) used was 100 bp DNA ladder (Bio-Labs, UK).

3.3.1.2 *E. coli* XL10-Gold Transformation

Agarose gel electrophoresis demonstrated positive transformants (Figure 3.7) in lanes 1 and 2. These PCR amplicons revealed, based on size, that the recipient vector's multiple cloning sites hosting the target sequences. While the negative ones, lanes 3 and 4 seemed to have variable lengths corresponding to around 500 bp and were therefore discarded.

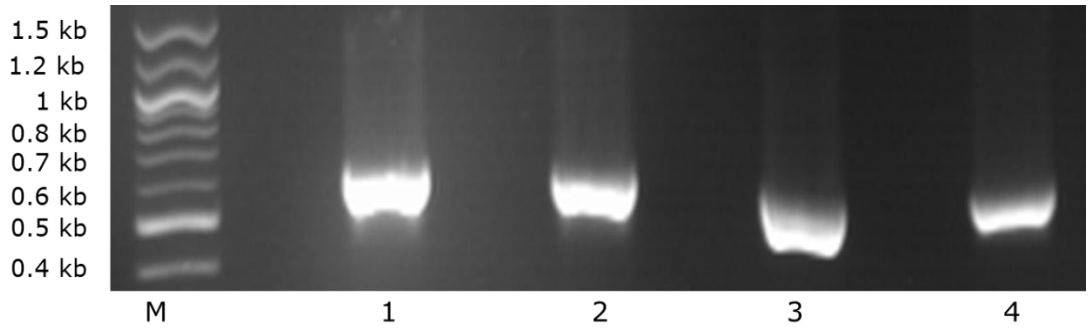
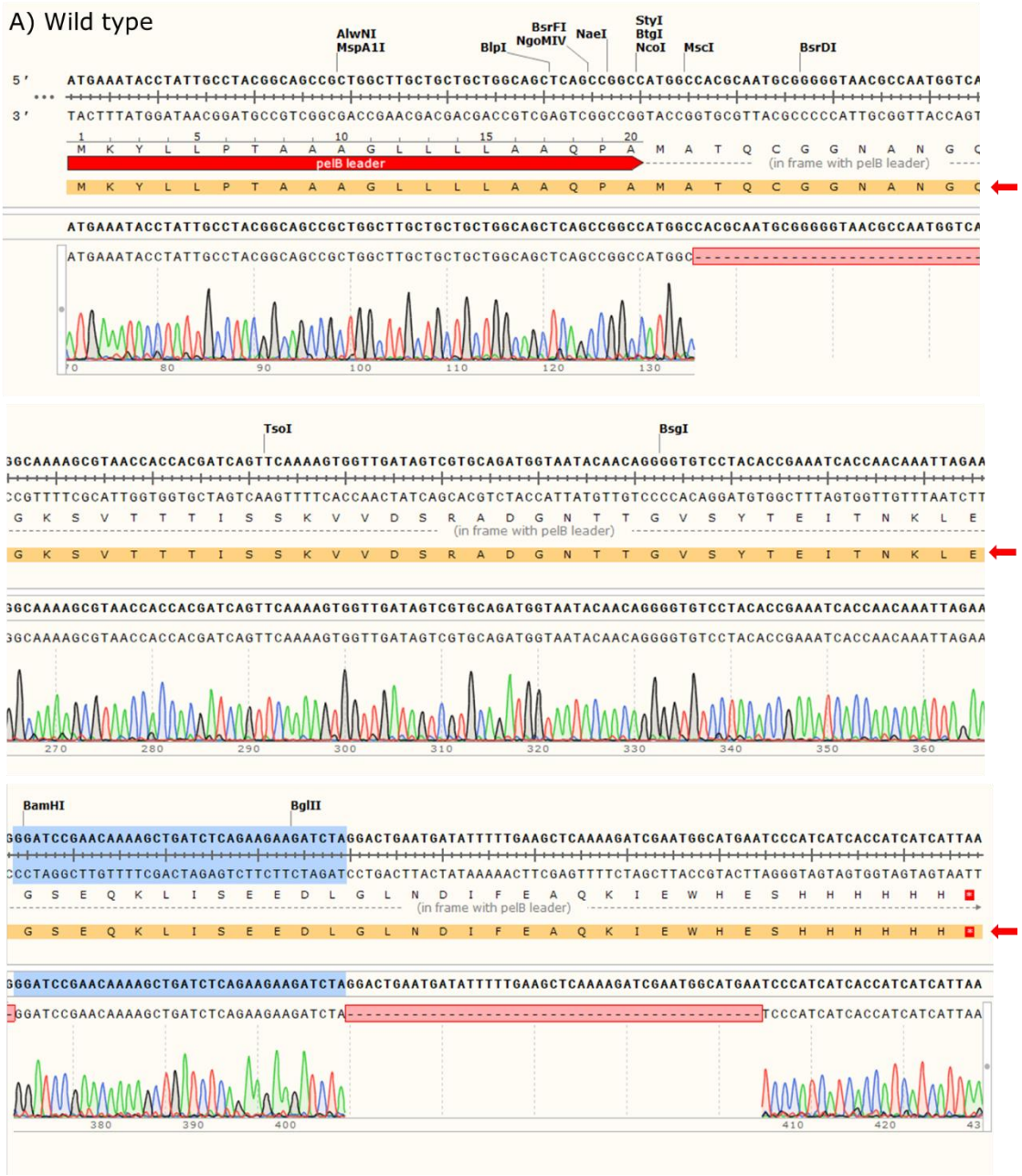


Figure 3.7 PCR colony screening for an inserted BabA-Crown gene into pOPE 101

BabA-Crown$_{D233A/S244A}$ and BabA-Crown were amplified, digested and ligated into a cloning vector, pOPE101. Agarose gel shows representative verification of vector PCR-amplified multiple cloning sites from different bacterial colonies harbouring positive pOPE101 constructs, either corresponding to the expected size of pOPE101 multiple cloning sites of ~ 615 bp as seen in lanes 1and 2 after the marker (M), or not as seen in lanes 3 and 4.

3.3.1.3 Confirmatory sequencing

DNA sequencing confirmed there was no mutation in the DNA sequences and that BabA-Crown was in frame with the vector's pelB leader sequence, the c-Myc and 6X-Histidine tags, as well as the stop codon (Figure 3.8).



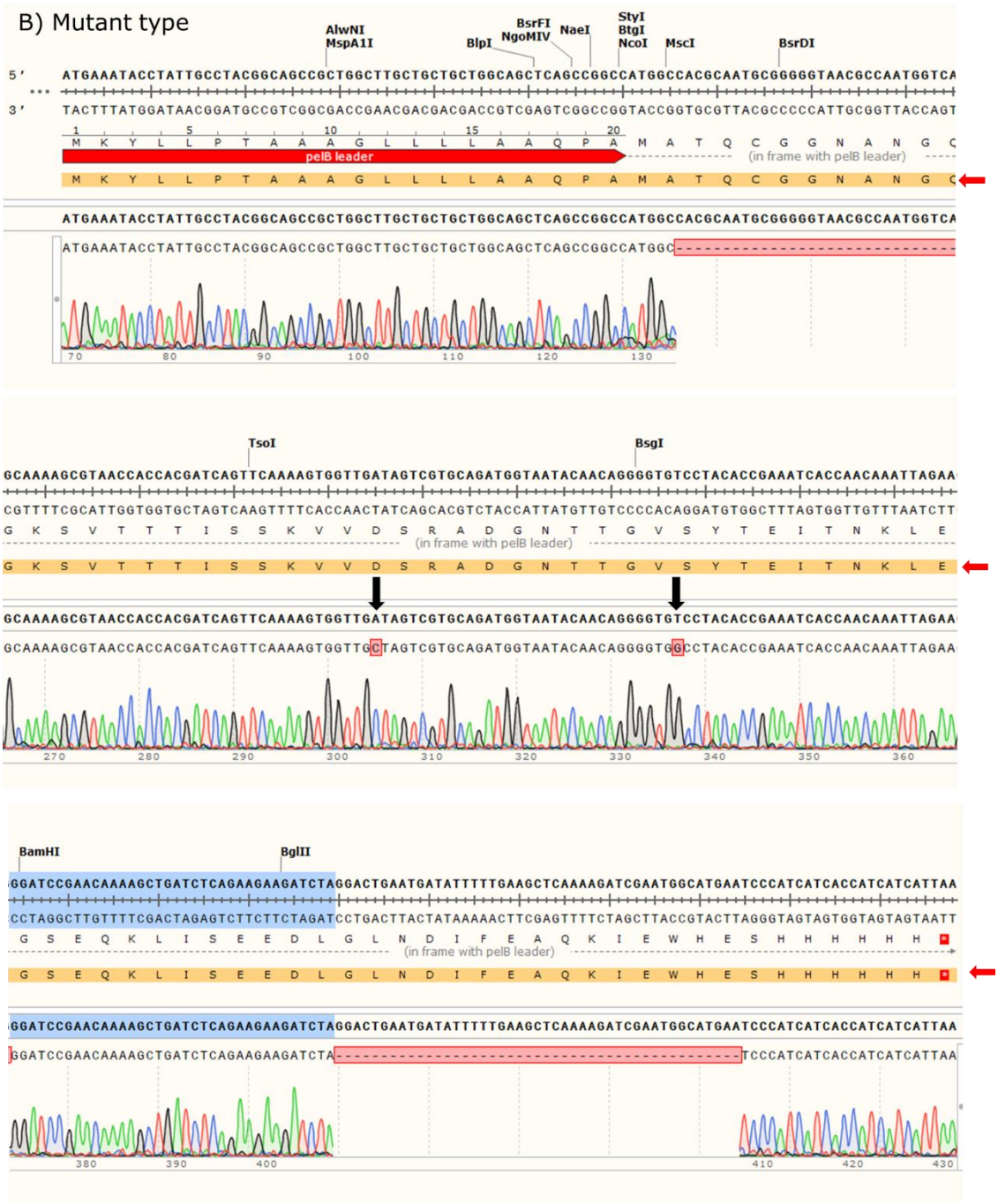


Figure 3.8 DNA sequencing analysis

Chromatogram showed sequences in frame with plasmid pelB leader of (A) BabA-Crown wildtype and (B) mutant type (BabA-Crown$_{D233A/S244A}$). The highlighted nucleotides encoded c-myc tag and downstream to it, after the red highlighted dashes, is the 6X Histidine tag. The black arrows in the mutant shows the two mutations. The red arrows indicate BabA amino acid sequence, which used as actual control to know if the sequence aligned with it.

3.3.2 Protein expression

3.3.2.1 BabA protocol

Bacteria harbouring pOPE101_BabA-Crown and BabA-Crown_D233A/S244A, were tested for expression. The cellular fractions were analysed by Coomassie staining and Western blot. However, no band at the expected molecular weight size of ~13 kDa was observed (Figure 3.9). Bands of ~20 kDa were observed in all protein lysates. These could be the endogenous biotin carboxyl carrier protein (BCCPL) in *E. coli* (Fall *et al.,* 1971). BCCPL acts as efficient carboxyl acceptor and donor in the biotin carboxylation and transcarboxylation reactions (Fall and Vagelos, 1972). It is therefore detected by the Streptavidin-HRP construct used as a secondary detection reagent in Western Blot.

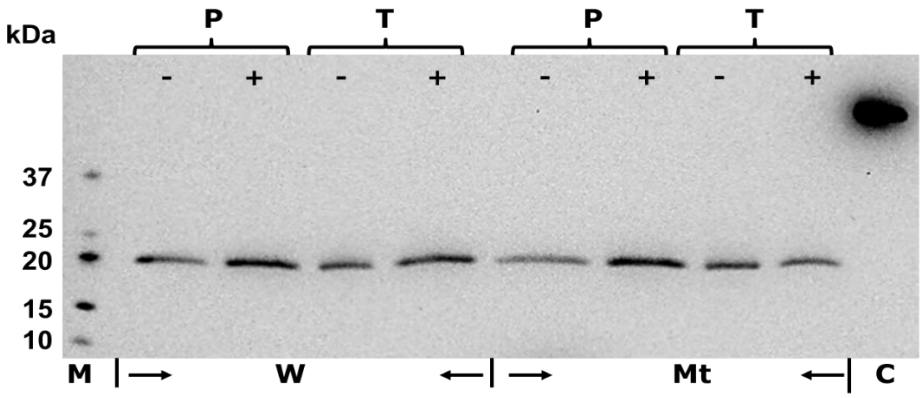


Figure 3.9 Protein expression of BabA-Crown

Western blotting showing only bands in 20 kDa all lanes, except the control (expected size 13 kDa), indicating no/very low expression. These bands represent the endogenous bacterial biotinylated protein (BCCPL). **M**= Molecular weight marker, **-** = not induced by IPTG, **+** = induced by IPTG, **P**= periplasmic extract, **T**= total cell protein extract, **Mt**= BabA-Crown$_{_D233A/S244A}$, **W**= BabA-Crown, **C**= recombinant BabA was used as a positive control for Western blotting.

3.3.2.2 Addition of chloramphenicol

To optimise the conditions for protein expression, chloramphenicol (Merck) at concentration of 170 µg/L (527 µM) was added into LB_{ATG} medium in attempt to increase the plasmid copy number (Andriushchenko *et al.,* 2011). This addition was made without any additional change in the protein expression/extraction procedure. Ultimately, BabA-Crown was found in the soluble fraction of the cell lysates, which contains both soluble cytoplasmic and periplasmic proteins (Figure 3.10). A dense band was observed in the periplasmic extract, which indicates successful protein targeting by pelB leader into the periplasm. However, overexpression was seen in the cytoplasmic soluble extract. Putative dimers (bands of around 26 kDa) were noticed in both cell lysates, periplasmic and total cell protein extracts. Dimers may result from disulphide bond formation between the two cysteines residues present in BabA-Crown sequence (Figure 3.3).

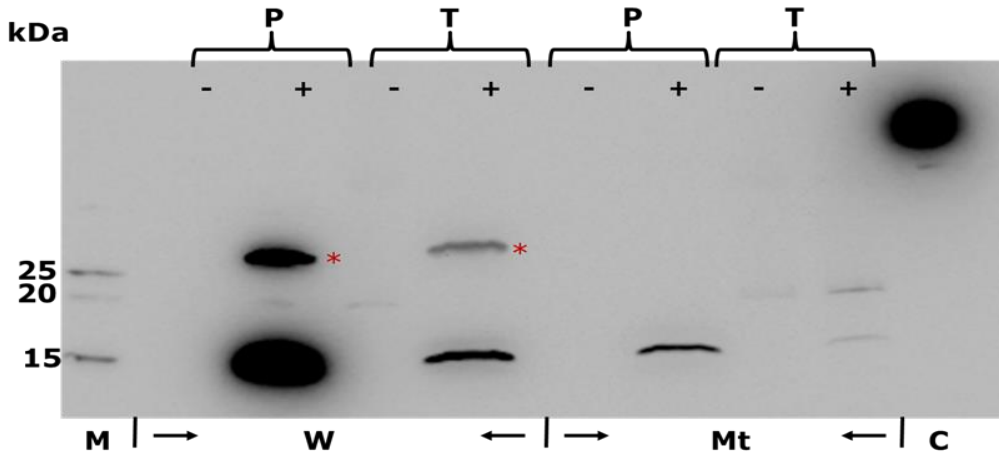


Figure 3.10 Effect of addition of chloramphenicol to LB_{ATG} media

Western blot showing protein bands at molecular weight size of about 13 kDa in both soluble lysates after induction. Periplasmic extracts, in **P+** lanes, indicate localization of the protein in the periplasmic space. Putative dimers at about 26 kDa (red asterisks) were found in both periplasmic, **P+**, and soluble total cell protein, **T+**, extracts using the non-reducing sample buffer (2X NRSB). The wildtype shows more dense bands compared to the mutant. BabA-Crown proteins could be also detected in the cytosolic extracts **T+**. **M**= Molecular weight marker, **-** = not induced by IPTG. **+** = induced by IPTG, **P**= periplasmic extract, **T**= total cell protein extract, **Mt**= BabA-Crown_D233A/S244A, **W**= BabA-Crown, **C**= recombinant BabA was used as a positive control for Western blotting.

To confirm that this recombinant protein forms dimers, besides non-reducing sample buffer (2X NRSB), a reducing sample buffer (2X RSB) was used. The purpose of dithiothreitol (DTT), present in 2X RSB, is to provide reducing conditions i.e. breaking the protein disulphide bridges, as a result, separating the subunits as it can be seen in the SDS-PAGE gel (Figure 3.11), whereas this bridge connection is conserved when using non-reducing conditions. Thus, only one band of the recombinant protein extract corresponding to the monomeric size (13 kDa) appeared in 2X RSB compared to two bands in the 2X NRSB.

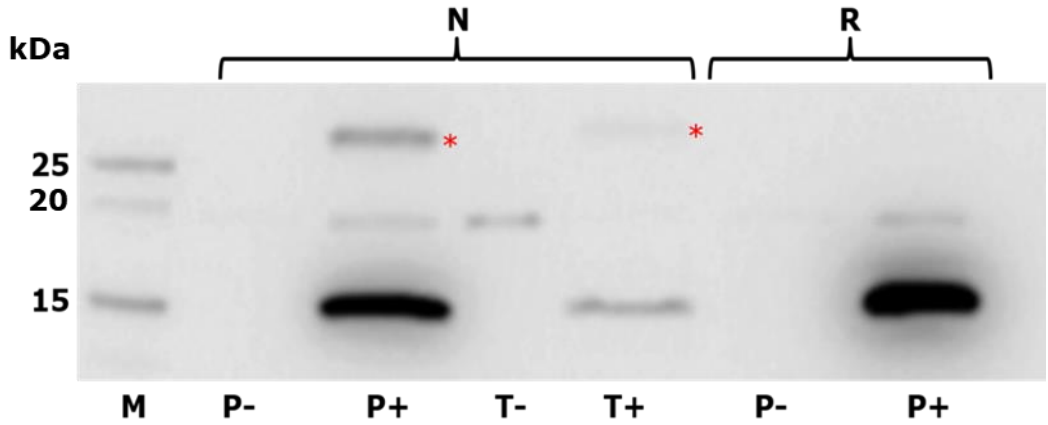


Figure 3.11 Expression in reducing and non-reducing conditions

Reduced and non-reduced sample buffer was used to confirm the presence of disulphide bonds in the recombinant protein expressed. In induced periplasmic extract (P+), three bands were visualised BabA-Crown monomer corresponding to 13 kDa, the 20 kDa endogenous BCCP protein and BabA-Crown dimer (red asterisk). The later was disappeared when the reducing condition was applied. No protein dimer is seen in the expected size using non-reducing sample buffer, while one band was observed under reducing conditions. **M**= Molecular weight marker, **-** = no IPTG induction, **+** = induced by IPTG, **P**= periplasmic extract, **T**= total cell protein extract. **N**=non-reducing sample buffer, **R**= reducing sample buffer.

To reduce the amount of the inducer, IPTG at two different final concentrations of 30 and 100 μM were used. This aimed to slow down protein translation and localization into the periplasmic space as well as minimising potential toxicity (Malakar and Venkatesh, 2012). Induction with low concentration (Figure 3.12), was still helping in protein expression, but not as potent as with higher IPTG concentration.

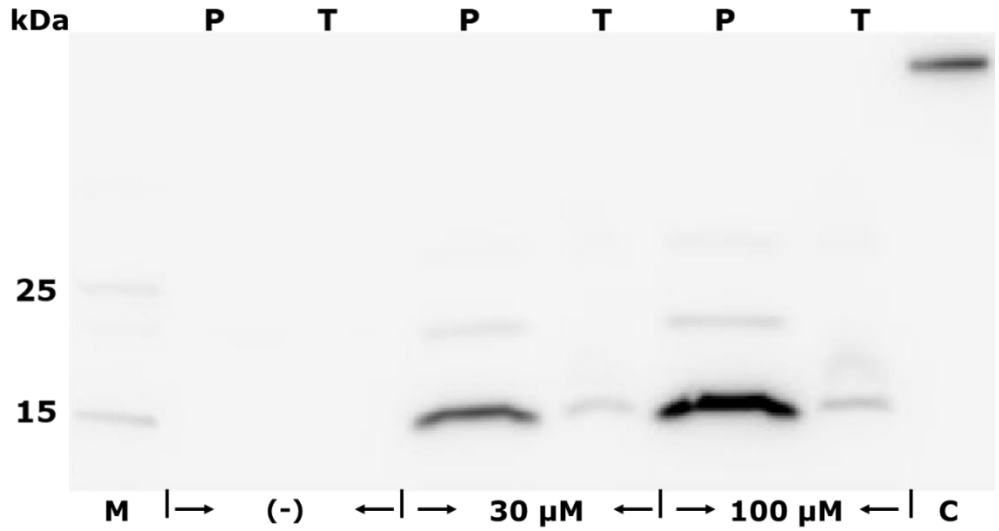


Figure 3.12 Expression in different concentrations of inducer (IPTG)

Western blotting using c-Myc immunodetection showing periplasmic extracts, **P**, after protein induction in two different concentrations of IPTG **30 μM** and **100 μM**. Protein induction using IPTG at concentration of 100 μM shows denser band compared to **30 μM**. (**-**) = not induced by IPTG. **P**: periplasmic protein extract, **T**: total cell protein extract, **C:** control, **M**= Molecular weight marker.

A trial was made to confirm that chloramphenicol can increase the protein expression besides testing intermediate (0.1 mM) and high (1 mM) concentrations of IPTG. As shown in Figure 3.13, no significant differences were noticed in the soluble lysates in LB_{ATGC} medium. The final IPTG concentration of 0.1 mM was favourable over 1 mM to avoid the toxicity.

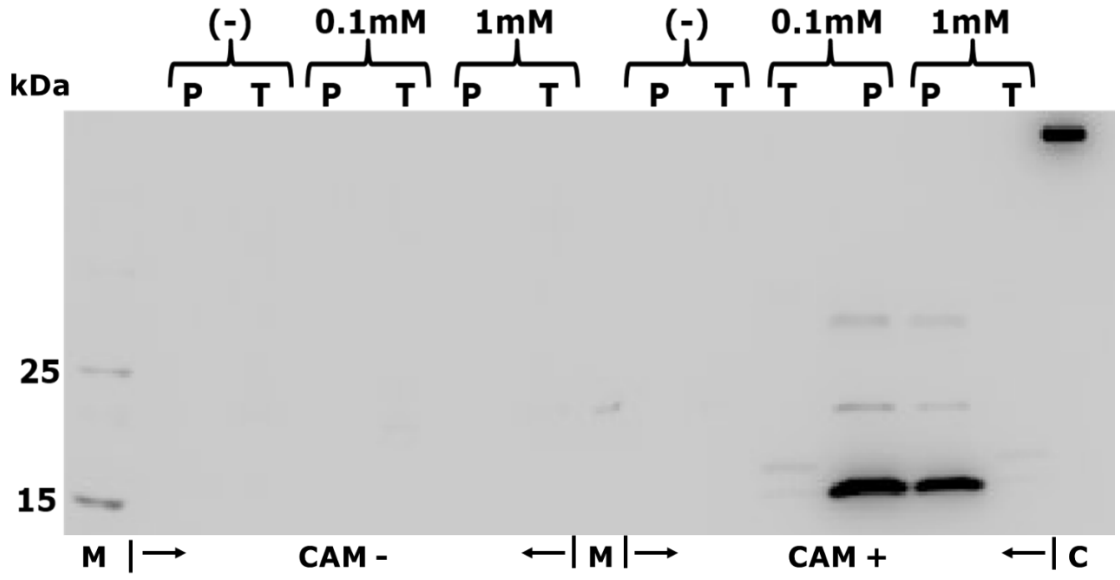


Figure 3.13 Different IPTG concentrations in the presence and absence of Chloramphenicol

Western blotting using c-Myc immunodetection showing the BabA-Crown in two different media, right, contained chloramphenicol (CAM) and left without. Periplasmic extracts in medium with CAM and induced with IPTG at concentration of 0.1 mM and 1 mM were seen. This indicate that BabA-Crown protein expression was obtained in the presence of CAM media. (**-**) = no induction by IPTG, **T:** total cell protein. **P**: periplasmic protein. **0.1 mM** and **1mM** show different concentrations of IPTG. **C:** control.

3.3.3 Chloramphenicol confines bacterial cell growth and increases the intracellular plasmid DNA concentration

Samples (1 mL) were collected from two different media (A) LB_{ATG} and (B) LB_{ATGC} every hour to measure the bacterial growth through the optical density (OD_{600}) and to monitor plasmid (pOPE101) replication through measuring the increment in its DNA concentration (Figure 3.14A and 3.14B). In LB_{ATG} medium, an increase in the optical density began after 1 hour from inoculation before entering the logarithmic phase after more 2 hours. At this point, the bacterial growth at LB_{ATGC} medium start increasing slowly for 7 hours from the time of inoculation. Then the cell entered a growth phase. Between hour 3 and hour 7, there is steady multiplication in the bacterial growth in media with chloramphenicol but not in the medium without chloramphenicol, which lasts for 4 hours (Figure 13.4C). This difference in time represents an intermediate phase between the bacterial growth in these two different media, thus, named the 'confinement period' (**CP**). During which plasmid concentration steady increase with gradual multiplication in the cell mass in LB_{ATGC} medium (Figure 13.4D). In LB_{ATG} medium, the cell mass was raised with less plasmid concentration. This suggests the effect of the chloramphenicol in confining the growth and, thus, may give the plasmid the opportunity to be harboured by each divided bacterium. After 4 hours from the inoculation, bacterial density in LB_{ATGC} medium reached the density of ~0.6 at OD_{600}, with higher plasmid DNA concentration (25 µg/mL). While bacterial growth in LB_{ATG} reached ~0.6 in OD_{600}, two hours earlier with plasmid concentration about 10 ng/µL.

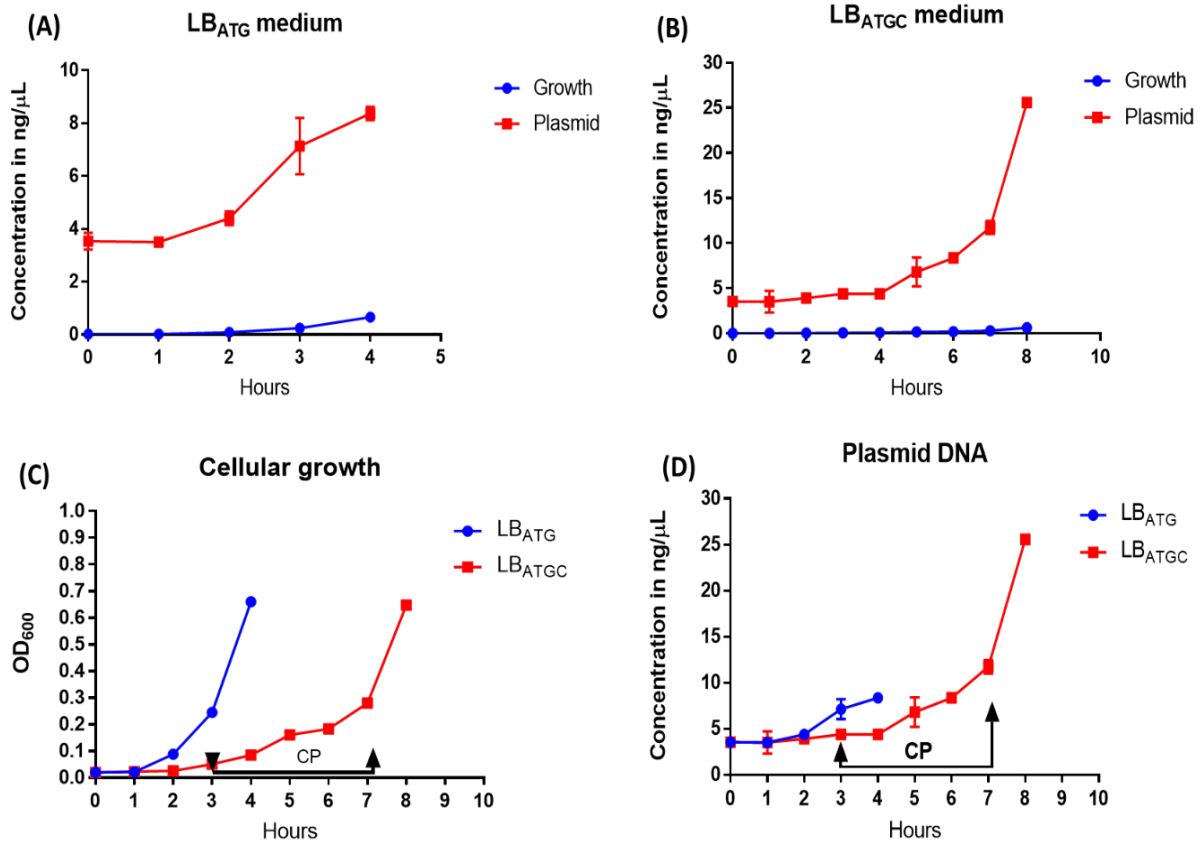


Figure 3.14 Bacterial growth and plasmid replication

The relationship between the bacterial growth and plasmid replication in LB_{ATG} (A) and LB_{ATGC} (B). Cellular growth in LB_{ATG} takes about 4 hours to reach OD600 0.6, while LB_{ATGC} needs about 8 hours to reach the same optical density. The plasmid in LB_{ATG} duplicated after 1 hour from inoculation while in LB_{ATGC} media begins after 4 hours and steady increment takes about 3 hours before sharp rising after 1 hour later. During these four hours, it was thought, plasmid multiplicated while the growth was confined, thus termed confinement period (**CP**). The cellular growth in LB_{ATG} and LB_{ATGC} was compared in (C), while the plasmid replication was compared in (D). Error bars represent the standard error of the mean (n=3).

3.4 Discussion

The basic objective of the work described in this chapter was to use recombinant DNA technology to generate the interacting length of the *H. pylori* adhesin (BabA) with human gastric glycan carbohydrate, (Le^b). To approach this objective, BabA gene, as a template for PCR amplification, was derived from *H. pylori* J99 which represents a generalist strain (Nell *et al.,* 2014), with binding affinity for its neoglycoconjugate ligand (Hage *et al.,* 2015a).

An important feature of pOPE101 vector is the presence of the N-terminal pelB leader sequence immediately before the insertion site for the gene of interest. This leader sequence directs the recombinant protein to the periplasmic space, facilitating recombinant protein extraction (Choi and Lee, 2004). Cellular periplasmic environment is a key point in BabA-Crown protein maturation and structure stabilisation, because of the necessity to form a clasped loop by the two-cysteine interaction (Moonens *et al.,* 2016). Another plasmid feature is the existence of IPTG-inducible *Lac* operator, which regulates protein expression and two C-terminal tags, c-myc and Hexa-Histidine, which facilitate protein immunodetection and purification, respectively (Ferrer-Miralles *et al.,* 2011, Hilpert *et al.,* 2001). The bacterium *E. coli* XL10-Gold harbouring pOPE101 which used in this study to obtain soluble BabA protein from the periplasmic space, was previously used for BabA expression from *H. pylori* 17875 (Fei *et al.,* 2011) and J99 strains (Hage *et al.,* 2015b).

The construction of BabA-Crown expression cassette was applied following the classical restriction/ligation-dependent cloning (Celie *et al.,* 2016). This starts with PCR amplification of DNA sequence of BabA-Crown followed by digestion of the products by specific restriction enzymes, then sealing the digested DNA within the plasmid nucleic acids sequence. The overall procedure depends on the availability of unique restriction sites available in both the insert and vector. These sites were taken into account when primers were designed to avoid inconvenient gene selection and digestion (Liu *et al.,* 2018b).

The use of the high-fidelity DNA polymerase (KOD DNA Polymerase) contributed to the successful results. Its ability to proofread the errors during amplification led to the specific product without further optimization. The sequence was in frame

with the pelB leader, which provided the start AUG start codon. The occurrence of mutations would potentially cause a frameshift in the resulting protein sequence (Benoit *et al.,* 2006). Sequencing of the full insert on each clone is important to confirm the integrity from the 5’ end of the promoter to the 3’ end of the terminator and are in the reading frame (van den Ent and Lowe, 2006).

Primers designed with restriction enzyme sites act as adaptors for cohesive ends production in the PCR products. These ends resulted from the added nucleotides at the 3’ end of the DNA strands by the polymerase (Topcu, 2000). The restriction reaction is usually carried out at 37 °C for 60 minutes. This can make it difficult to control the reaction and may result in sticky ends or non-site-specific cutting ‘star activity’ (Du *et al.,* 2011). The ligase derived from bacteriophage T4 is the most commonly used enzyme in recombinant DNA technology. T4 DNA ligase forms phosphodiester bonds between the 5'-phosphoryl and 3'- hydroxyl ends group in double-stranded DNA. After digestion, the sticky ends helps the ligase to covalently join the circular plasmid DNA (Celie *et al.,* 2016). The optimum ratio for ligating the insert to pOPE101 was 1:3. This gave rise to high recombination efficiency as stated by (Topcu, 2000) and favoured BabA-Crown insertion over plasmid re-circularisation. The successfully ligated plasmids were subject to further selection process which involve bacterial transformation for proliferation.

Naturally, bacteria can obtain the genetic information through one of these three mechanisms; conjugation (pilus-direct transference between two strains), transduction by bacteriophage injection, and transformation through cell membrane-bound uptake mechanism (Rahimzadeh *et al.,* 2016). Artificial transformation of the ligated PCR product or exogenous plasmid DNA into bacterial cells is a crucial practice in genetic engineering. This occurs by heat shock, i.e. a sudden temperature change from 0 °C →42 °C→ 0 °C for a number of seconds in the presence of divalent cations like $CaCl_2$ (Bergmans *et al.,* 1981). Transformation depends on adjusting the heat-shock incubation time (45 seconds). Increasing the time to 1 minute result in poor growth. Then the viability and selection of the recipient cells (transformants) were achieved by growing in the presence of Ampicillin (plasmid antibiotic marker). However, during bacterial potential reproduction, the constructed plasmid is propagated as well, but due to unequal distribution within the bacteria, some were lost throughout the continuous segregation (Camps, 2010). Moreover, the bacteria may harbour plasmids without

insert due to quick re-joining mechanism, if sticky ends on either end of the vector were not achieved or the ends are not compatible with each other. This might also occur due to setting very low amount of T4 ligase or short incubation time (Topcu, 2000). Thus, the resulted transformants were screened by sub-culturing them into LB media containing ampicillin (pOPE101 marker) followed by DNA sequencing as essential quality control steps before starting protein expression of the selected transformants.

Some *E. coli* strains, such as XL-10 Gold, were generated to take-up large DNA molecule. This achieved by counter-ion mechanism which reduces the electrostatic repulsion (Lipfert *et al.,* 2014). However, the exact mechanism underlying bacterial cell permeability for DNA entry is not fully elucidated, since free passage of very large molecules through the cell wall into the cytoplasm is not known so far. DNA is a hydrophilic negatively charged macromolecule, due to the phosphate backbone and *E. coli* has a negative surface charge due to the presence of phosphorylated lipid A in the outer LPS (Hepp and Maier, 2016). Recent research suggested that a mutation in gene *trg*A (transformation related gene A) could increase bacterial efficiency to take up plasmid DNA (Ortiz-Velez *et al.,* 2018). Recently, transformation has been facilitated through nanoparticles (arginine-glucose functionalized hydroxyapatite nanoparticle) in one step (Deshmukh *et al.,* 2019).

According the protocol used in this study, transformation depends on adjusting the heat-shock incubation time (45 seconds). Increasing the time to 1 minute resulted in poor growth. Then the viability and selection of the recipient cells (transformants) were achieved by growing the bacteria in the presence of Ampicillin (plasmid antibiotic marker) in the growth media. However, during bacterial potential reproduction, the constructed plasmid is propagated as well, but due to unequal distribution within the bacteria, some were lost throughout the continuous segregation (Camps, 2010). Moreover, the bacteria may harbour plasmids without insert due to quick re-joining mechanism, if sticky ends on either end of the vector were not achieved. This might also occur due to setting very low amount of T4 ligase or short incubation time (Topcu, 2000). Thus, the resulted transformants were screened by sub-culturing them into LB media containing ampicillin (pOPE101 marker) followed by DNA sequencing as essential quality control steps before starting protein expression of the selected transformants.

Generally, protein expression is achieved by inserting a foreign DNA sequence downstream of a highly efficient plasmid promoter. Lactose (lac) operon from *E. coli* is a well-established staple in molecular biology research. Induction of *lac* operon promotor by lactose or its non-hydrolysable analogue (IPTG) is common practice in protein production. However, this production could be hindered if a readily metabolized carbon source as glucose exists in the medium due to "carbon catabolite repression" (CCR) (Görke and Stülke, 2008). This term refers to favouring of utilization of rapidly metabolise (e.g. glucose) carbon source represses expression of genes encoding essential proteins for operating secondary carbon source such as lactose (Deutscher, 2008). This global transcriptional regulatory phenomenon controls lac operon expression (Bruckner and Titgemeyer, 2002). It is mediated by catabolite repressor protein A, which is a pleiotropic regulator of many cellular processes (Chen *et al.,* 2018a).

The presence of glucose in the growth medium (LB_{ATG}) represses the operon and the outcome is non-detectable recombinant protein in LB_{ATG} medium. Glucose depletion increases expression of T7 RNA polymerase and subsequently the expression of the recombinant protein (Ahmad *et al.,* 2018) which is located downstream to *lac* operon. T7 RNA polymerase gene is controlled by lac repressor and only transcribed after induction. When transcription begins, it will be predominant over cellular proteins synthesis (Graslund *et al.,* 2008). This affects the cellular metabolism and plasmid replication and, as a result, produces variation in plasmid copy number or plasmid-free cells (Camps, 2010). Thus, IPTG places a high metabolic burden on the bacterial cells and can lead to protein aggregation in the cytoplasm or formation of inclusion bodies (Wurm *et al.,* 2016). This mechanism could explain how BabA protein was obtained before inserting the hexa-lysine tag to increase the solubility in the original protocol used. In the present study, IPTG induction at different concentrations (30 µM – 1 mM) showed no alteration in BabA-Crown protein expression and failed to add an advantage in LB_{ATG} medium. High inducer concentration results in increased synthesis rate with a severe reduction in growth rate (Donovan *et al.,* 1996). This may also lead to high accumulation in the periplasmic space, bacterial bursting, and cells death (Dvorak *et al.,* 2015). It was demonstrated that IPTG concentration of 1 mM was not optimal to obtain the highest expression compared to lower concentrations (0-0.5 mM) (Ahmad *et al.,* 2019).

It is proposed that lower temperatures reduce bacterial replication rate, thus extending the logarithmic growth phase, in which protein is constitutively expressed (Kelley *et al.,* 2010). Inducing protein expression at low temperature together with bacterial growth significantly enhances protein expression (San-Miguel *et al.,* 2013), maximizes protein yield, and minimizes combining growth complications, such as activation of proteolytic enzymes associated with the stationary phase (Graslund *et al.,* 2008). Moreover, the decreased growth rate at low temperature supports correct folding of the recombinant protein (Krause *et al.,* 2010).

The resulting BabA-Crown protein showed dimerization, as confirmed by using reducing against non-reducing sample buffers. It is a property of native BabA to form a cysteine clasped loop to stabilize its structure (Moonens *et al.,* 2016). Dimer formation is explained by the presence of two cysteine residues in the amino acid sequence. Cysteine-pairing is formed by thiol group (SH) oxidation resulting in a covalent bond between two cysteine residues. Disulphide bond is formed in the periplasm by disulphide bond formation (Dsb) proteins which include DsbA and DsbB (Nakamoto and Bardwell, 2004). Bacterial periplasm has a very high efficiency in providing an oxidative environment for bridging the two cysteines (Siurkus and Neubauer, 2011). Similarly, dimer formation (mis-pairing) may be attributed to the incapability of the host's secretory system machinery to properly export the protein into the periplasm. This in turn can lead to protein jamming and accumulation and ultimately misfolding and aggregation which ultimately result in low protein yield or inclusion bodies (Berkmen, 2012).

Chloramphenicol is a broad-spectrum antibiotic acting principally as a potent bacterial protein synthesis inhibitor by binding to the 50S ribosomal subunit. This blocks the peptidyl transferase, which transfers the nascent peptide, from interacting with the aminoacyl-tRNA 3' end to form new peptide-bonds (Dinos *et al.,* 2016). This interference with translation is not bactericidal as it only competes with the incoming aminoacyl-tRNA in the A site (Tereshchenkov *et al.,* 2018). Chloramphenicol also stimulates RNA synthesis (Fraenkel and Neidhardt, 1961, Schlunzen *et al.,* 2001). Addition of chloramphenicol to the growth medium increased protein yield to a detectable level. However, *E. coli* XL10-Gold carries resistance plasmids for chloramphenicol and tetracycline.

The role of chloramphenicol in increasing the plasmid copy number and the relationship with the improved protein yield was investigated. Two types of growth media were used, one supplemented with chloramphenicol and the other without, to monitor the cell growth and plasmid amplification in these media. The hourly samples collected revealed increment in plasmid amplification/concentration, while the cellular growth remain in linear growth. In the first hours, steady elevation in the plasmid concentration occurred before reaching the OD_{600} of ~6.0. A time-delay difference of 4 hours was observed in bacterial growth in medium with chloramphenicol in comparison to the one without. Thus, this difference in time window termed confinement period to describe the phase when plasmid is amplified while cellular growth is inhibited. During this phase, simultaneous proliferation in plasmid copy number with efficient distribution may occurred during cellular segregation (Clewell, 1972, Andriushchenko *et al.,* 2011). This hypothesis based on the existence of plasmid colicinogenic factor E_1 (*ColE*$_1$) replication origin in pOPE101 plasmid (Inoue *et al.,* 1983). In the presence of chloramphenicol, *ColE*$_1$ enables the plasmid to continue replication, while cell mass and chromosomal DNA were slowly duplicated. This is due to chromosomal dependence on *de novo* protein synthesis (Clewell, 1972, Andriushchenko *et al.,* 2011), while plasmid replicate independently without requirement for initiator protein (Teich *et al.,* 1998), as it only utilises the residual protein present for several replication cycles (Tomizawa *et al.,* 1975). Replication of *ColE*$_1$ plasmid is autonomous and controlled by plasmid origin of replication (*ori*) which is regulated by RNA polymerase (RNAI and II), Rom (RNA one modulator) or Rop (repressor of primer) proteins, DNA polymerase I (Pol I) and RNase H (Wegrzyn, 1999, Brantl, 2014). Plasmid replication starts with synthesising antisense RNAI, using host polymerase (pol I), which interacts with pre-primer RNAII to form a hybrid with the single DNA strand at the origin. This RNA-DNA hybrid (R-loop) is stabilised by Rom protein until cleaved by RNase H which create a free 3'-OH end. DNA polymerase (pol I) use this end to initiate the leader strand synthesis forming a D-loop. Initiation of plasmid replication is positively regulated by antisense RNAII system which maintains plasmid copy number and negatively by RNAI and Rop protein (Wang *et al.,* 2007, Brantl, 2014). Therefore, the ratio between these two systems or the capacity of the RNAI to join with its complementary RNAII determines the longevity of plasmid replication. For this reason, increment in plasmid amplification heighten the concentrations of the antisense-RNA system

which put much stress on the inhibited cellular growth (Brantl, 2014) also plasmid replication increases cellular glucose uptake (Wang *et al.,* 2006).

Because *E. coli* XL10-Gold cells carry plasmids having *cat* gene which encodes chloramphenicol acetyltransferases (CATs) for chloramphenicol resistance, it takes time to restore the partially inhibited resistance machinery, i.e. protein synthesis, but never die (Huang *et al.,* 2017). Moreover, the inhibitory effect of chloramphenicol on peptidyl transferase activity is reversible, but concentration-dependent (Frenkel and Bremer, 1986). It was shown that high concentration of chloramphenicol can outcomes in special translation-arrest at specific sites, which lead to reorganisation of the ribosomes on mRNA (Marks *et al.,* 2016). At high chloramphenicol concentrations (> 100 µg/mL), the chloramphenicol will be in excess over the peptidyl transferase to saturate bacterial 50S ribosomal subunit and show high binding affinity to the ribosome (Dinos *et al.,* 2016). This high concentration may make XL-10-Gold cells sensitive to chloramphenicol, in addition to pOPE101 plasmid propagation was not potentially high due to, in line with (Siibak *et al.,* 2008), chloramphenicol severely inhibitory effect on ribosomal assembly. The concentration of the chloramphenicol seems to be bacterial strain or vector specific factor. In the literature, different final concentrations (10-300 µg/mL) were used to increase the protein expression. Final concentrations of chloramphenicol (10-20 µg/mL) was used to maximise the amplification and replication of colicinogenic factor E_1 (*Col*E_1-type) plasmids (pB322 and pB327) up to 10 fold in K12 strains, while higher concentrations (100 µg/mL) using pB329 in *E. coli* RR1 were reported to have similar effects (Frenkel and Bremer, 1986, Bentley *et al.,* 1990).

Overall the DNA concentration of pOPE101 plasmid was increased during bacterial growth in medium containing chloramphenicol compared to bacterial growth in medium lacking this antibiotic and was estimated to be more than 3 fold. Therefore, plasmid propagation within bacterial cells coupled with its distribution into the offspring are two essential boosters for increasing protein expression. Consequently, modifying the contents of the growth medium by adding chloramphenicol result in successful BabA-Crown protein expression. This modification could be a simple alternative method to the genetic modification (6X lysine tag insertion) which recently applied to increase BabA protein expression.

3.5 Conclusion

This work showed the successful construction of recombinant BabA-Crown plasmid and transformation into *E. coli* XL10-Gold, which was used for both plasmid propagation and protein expression. Recombinant protein expression was not possible without chemical modification of growth medium by adding chloramphenicol.

CHAPTER FOUR

4. Testing BabA-Crown protein functional properties as a moiety for gastric drug delivery

4.1 General overview

BabA is the most studied adhesin in *H. pylori* as a virulence factor. In this chapter, an innovative step towards translating the applicability of BabA minimal binding domain to be used as the proteinaceous moiety for gastric drug delivery system was attempted. Thus, the aim of this chapter was to characterise BabA-Crown protein functional properties in simulated gastric conditions. In this context, two main assessments were addressed

1. The ability of BabA-Crown domain to bind to its ligand
2. The resistance of BabA-Crown protein to peptic digestion/simulated gastric acidity.

So far, two crystal structures for BabA from two different *H. pylori* strains (17875 and J99) have been published (Moonens *et al.,* 2016, Hage *et al.,* 2015a). These structures gave detailed information about the molecular association mechanisms between BabA as bacterial adhesin and Le^b as gastric cellular receptor. The data revealed that the bacteria seems to undergo variable mutations in the adhesin sequence to interact with the gastric cellular receptor according to the host conditions. These substitutions occur constitutively in two regions termed the

hypervariable loops (Figure 3.2), which give rise to highly diverse sequences determining the binding ability and/or the strength of attachment. The binding residues (Figure 4.1) are the same in both strains except in *H. pylori* 17875 strain, binding to Le^b-Galactose is mediated by Glutamine (Q:207) (Moonens *et al.,* 2016), while in *H. pylori* J99 strain binding to Fucose 4, instead of Galactose 2, occur through Asparagine (N:206) (Hage *et al.,* 2015a). This substitution may give rise to difference in the overall binding strength as the dissociation constant (*Kd*) in 17875 is (80.0 ± 7.1 μM) about three times stronger than in J99 (*Kd* ~252 μM) (Moonens *et al.,* 2016, Hage *et al.,* 2015a).

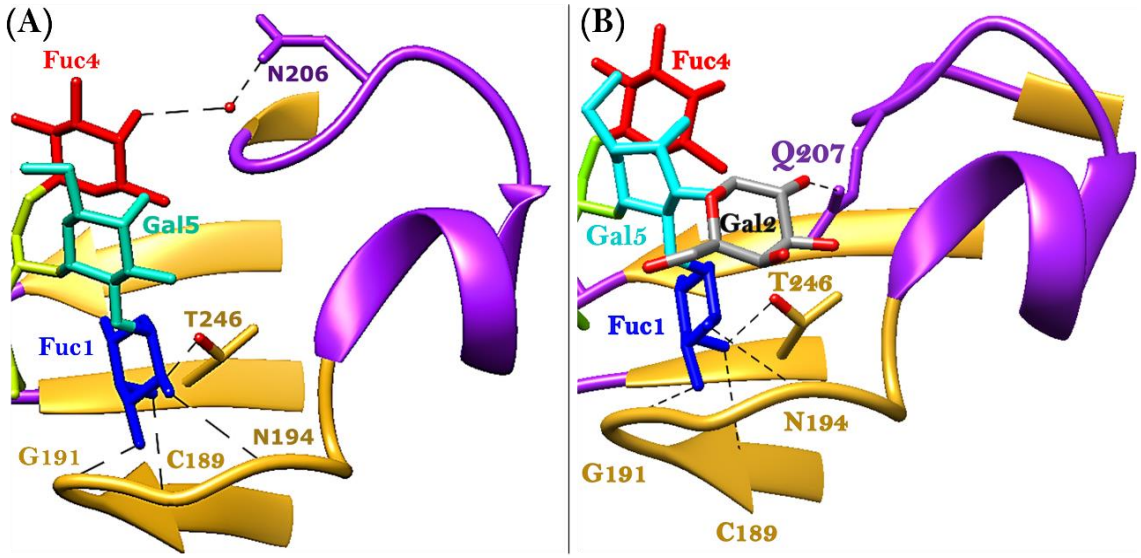


Figure 4.1 Molecular determinant of BabA preferences to Le^b binding

BabA-Crown crystal structures from BabAJ99 (A) pdb: 4ZH7 and from BabA17875 (B) pdb: 5F7W which explain different binding preference of the bacterial strain. (A) N206 in BabAJ99 binds to Fucose 4 in Le^b while in 17875 strain (B) the binding is mediated by G191 binding to Galactose 5. The two residues (G191 and N209) are located in the hypervariable loop (marked in violet).

The knowledge gained from these binding interactions could be rationalised to include polymorphic BabA sequences from other bacterial strains to spot how attachment and non-binding states occur. As shown in Figure 4.2, BabA contains some conserved residues such as C24, G26, N31, S87 and T89 to determine the binding ability and D76, S77 to determine the non-binding status, while shift in N44/Q45 reduce or increase the binding strength as demonstrated in bacterial strains J99, 17875. BabA in strains like J116 and 92-26 is non-functional (Hennig *et al.,* 2004), due to three substitutions in the hypervariable loop such as having E50 instead of N/D/I, besides replacing DS with GW/QS in sites 82 and 83, respectively. In specialist strains e.g. Peruvian strain (P448) the binding residues such as N50 and Q51 with S and S in 83 with G. Although BabA mediates bacterial binding to Le^b, some *H. pylori* strains such as J166 developed a mechanism for BabA-independent Le^b-binding. The dissociation constant of J166Δ*babA* mutant whole cells to Le^b was 9.2 X 10^{-15} M bonds and 0.7 X 10^{-15} M for the wild-type (Fei *et al.,* 2011).

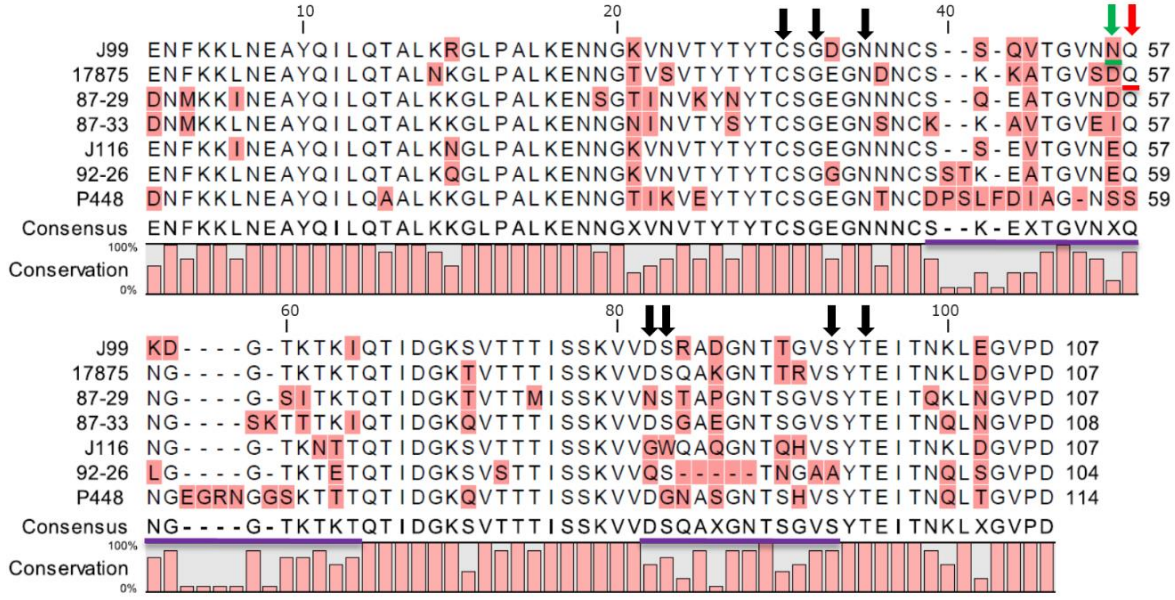


Figure 4.2 Multiple alignment of Crown sequences

Alignment of BabA amino acid sequence from selected *H. pylori* strains. Strains with functional BabA are 87-33, 87-29, J99 and 17875, while J116 and 92-26 represent strains with non-binding BabA. Strain P448 represents BabA specialist phenotype. The similar binding sites in both strains were marked by black arrows, while the green and red lines to mark the differences in the binding sites in two crystallised BabAJ99 and BabA17875, respectively. The underlined purple lines represent the hypervariable loop.

In order to persist in the gastric epithelium, *H. pylori* tends to undergo dynamic processes in attachment (to gain nutrients) and detachment (escaping from the luminal acidity and pepsin). These processes are modulated by BabA loss/gain mechanism through phase variation/switching to express other paralogues or adhesins (Ansari and Yamaoka, 2017). Loss of BabA expression is reversible and independent of the host immune response but may be host determinant (Moore *et al.,* 2011, Kable *et al.,* 2017). A recent study revealed that binding of BabA to Le^b-glycoconjugates is a critical negative feedback mechanism in response to the mucins as binding inhibits bacterial proliferation and decreasing BabA expression limited subsequent aggregation on the epithelial surfaces (Skoog *et al.,* 2017).

For the sake of potential oral therapeutic systems, pH-responsive carrier offer two things, formulation stability in the stomach and controlled release of the drug after specific adherence (Liu *et al.,* 2017a). *H. pylori* besides developing variable sequences to adapt to the surrounding gastric environment, creates systems for sensing the harsh situations. BabA as acid sensitivity system (Figure 4.3) is one example that provide insights for the ultimate goal of this study as it elucidates the bacterial mechanism of acid resistance. Based on the rate of binding and disassociation (on/off rate), which decreases or increases the binding affinity in the acidic conditions, BabA as acid sensitivity system was predicted to explain the pH-responsive adherence (Bugaytsova *et al.,* 2017). The structural composition of this system mainly consisted of three domains, which are Crown (called carbohydrate binding domain or CBD by the Boren Group), Velcro and stalk domains. The Crown is the ligand binding domain, the Velcro domain is composed of three helices and determines BabA avidity through forming low affinity monomers of high avidity multimers. The switching between these different conformations is determined by a key position E/D 207 and assisted by one residue, key position 199, which is located on one of the two hypervariable loops. D198/R207 is predicted to be acid-responder forms salt bridge which either relax the binding site or fast tighten it to decrease binding affinity. This bridge is disrupted at pH <4 and alter the folding to exclude fucose 1 from binding to the cysteine clasped loop, thus increases the off-rate. Finally, Stalk domain, mostly Beta-sheets, is responsible for connecting BabA extracellular part to the membrane-anchored domain in the outer membrane.

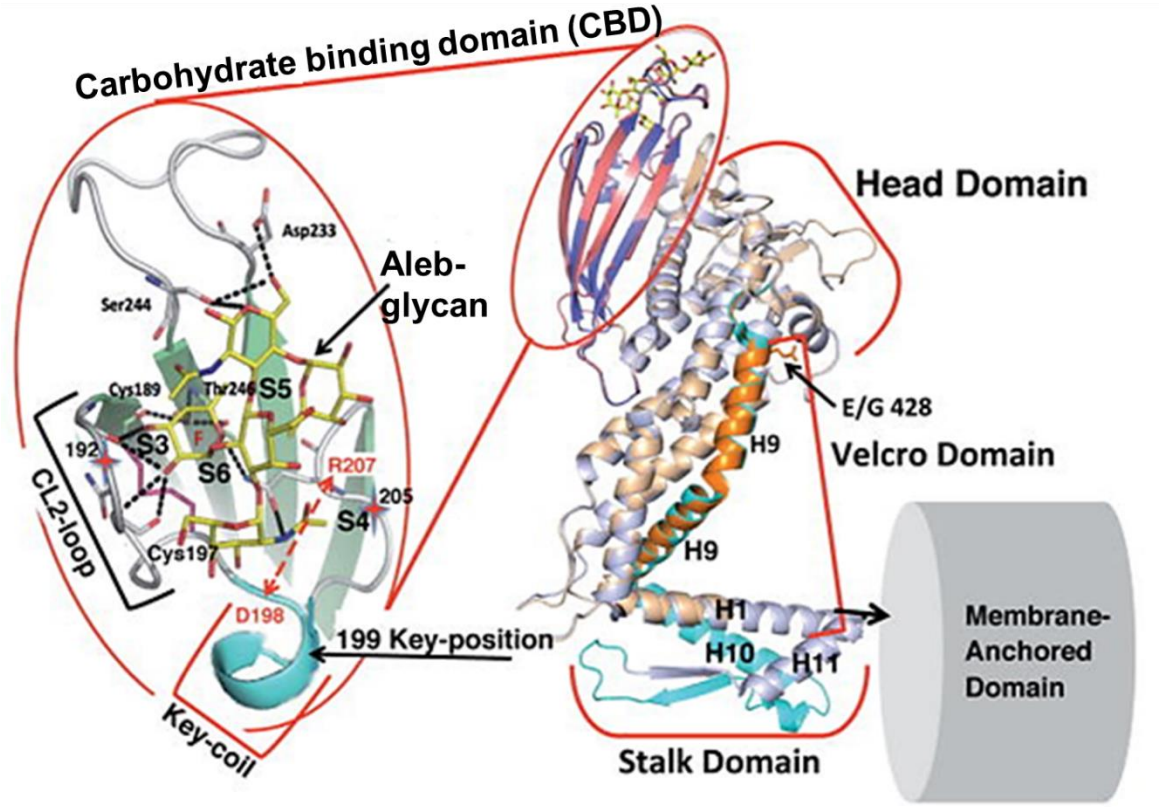


Figure 4.3 Structural organisation of the acid sensitivity system

Acid sensitivity structural organisation classified BabA into direct binding domain, Crown, Velcro domain which controls BabA multimerisation to increase binding avidity and Stalk domain which links the extracellular domain with the membrane-anchored domain in the outer membrane. Red arrow connecting R207 and 198 predicted to form salt-bridge, which joins the key coil at high acidity and is disrupted at pH <4 through the key-position 199. The position E/G 428 was suggested to play a direct role in acid-responsive effects. H= helical (Moonens *et al.,* 2016).

4.2 Experimental procedures

4.2.1 Mutagenesis to introduce AviTag™ sequence

Site-directed mutagenesis was performed using Q5™ high-fidelity DNA polymerase (New England Biolabs, USA) to insert an AviTag™. Primers shown in Table 4.1 were designed to introduce the AviTag™ sequence encoding the amino acid sequence (GLNDIFEAQKIEWHE) between pelB leader in the plasmid and the Crown complementary DNA region. This sequence will act as a substrate for BirA ligase, which adds a single biotin molecule into the protein sequence. Introducing this tag will offer specific site for enzymatic biotinylation (see Chapter 6) and thus reduce or eliminate aggregation when incubated with Streptavidin-coated nanoparticles (Beckett *et al.,* 1999, Fairhead and Howarth, 2015). PCR thermocycling was set up as described in Table 4.2. Afterwards, plasmids were extracted, transformed into *E. coli* XL-10 Gold and sequenced as described in Section 3.2.1.3.2.

Table 4.1 AviTagTM forward and reverse primers

Primer name	Primer Sequence (5' → 3')
AviTag-Crown For	CAAAAGATCGAATGGCATGAAAACAACGGGAA AGTCAATGTAACCTATACTTACACATGC
AviTag-Crown Rev	AGCTTCAAAAATATCATTCAGTCCTGCCATGGC CGGCTGAGCT

Table 4.2 Thermocycling conditions for mutagenesis

Step	Temperature	Time
1. Initial Denaturation	98°C	30 seconds
2. Denaturation	98°C	10 seconds
3. Annealing	72°C	30 seconds
4. Extension	72°C	30 seconds
5. Final Extension	72°C	5 minutes

Cycles step 2-4 repeated 30 times

4.2.2 Protein expression

4.2.2.1 Large-scale protein expression

The same protocol used for small-scale in section 3.2.2 was adjusted to be used for large-scale expression.

40 µl of *E.coli* XL-10 Gold cells were grown in 20 mL of LB_{ATG} medium at 37 °C overnight. From this starter culture, 2 mL was used to inoculate 1 L of LB_{ATG} medium grown in a 2 L Erlenmeyer flask at 37 °C. When the OD_{600} reached ~0.6, cells were induced with 0.1 mM IPTG and the incubation temperature lowered to 24 °C for 12-16 hours. Bacterial cells were harvested through spinning for 20 minutes at 10,000 g at 4 °C. The supernatant was kept at 4 °C after filtration through a 0.22 µm filter to exclude cell debris and large aggregates. The pellet was dissolved in 1/10 culture volume of spheroplast solution [Tris-Cl 200 mM (pH 8), sucrose 20%, ethylenediaminetetraacetic acid (EDTA) 1%] and mixed gently for 1 hour, centrifuged for 1 hour at 14000 g (4 °C). The new pellet was re-suspended in 1/10 culture volume of 5 mM $MgSO_4$, shaken gently for 1 hour, then centrifuged (20 minutes at 10,000 g, 4 °C). The supernatant was again filtered (0.22 µm filter) and mixed together with the previous one. 1 tablet of protease inhibitor cocktail (cOmplete® EDTA-free, Roche, USA) was added to every 25 mL of the periplasmic extracts before extraction.

4.2.2.2 Protein purification

Protein purification was conducted by either the automated purifier system, ÄKTA Start chromatography system (GE Healthcare, UK), or manually using gradient elution (gravity-flow chromatography). In manual purification, the periplasmic extracts were combined with 1 mL of cOmplete His-Tag Purification Resin (Roche, USA) and loaded into a PD-column holder (Econo-Pac® chromatography columns, Bio-Rad) after one-hour incubation. The solution was drained at a flow rate not greater than 2 mL/min, then the flowthrough was collected. The column was washed with 5 column-volumes (CV) of wash buffer (20 mM Tris-HCl, pH 7.4, and 300 mM NaCl) and protein was eluted stepwise with different percentages (5%, 10% 25%, 50% and 100%) of 500 mM imidazole in wash buffer. All of the purification fractions collected were analysed by SDS-PAGE and InstantBlue-staining.

Using ÄKTA Start chromatography system (GE Healthcare, UK) facilitated by UNICORN start system control software, periplasmic extract was loaded onto a 1 mL HisTrap-HP histidine-tagged protein purification column. A gradient elution program was set to run at a flow rate of 1 mL/min. The running buffer consisted of 20 mM Tris-HCl (pH 7.4) and 300 mM NaCl and the elution buffer contained 20 mM Tris-HCl (pH 7.4), 300 mM NaCl and 500 mM imidazole. Eluted fractions were loaded onto 4 - 20% Mini-PROTEAN® TGX™ Precast Gels for SDS-PAGE and InstantBlue-staining.

4.2.3 Tryptic peptide mapping

Experimental procedures performed by University of York

Peptide mapping is a technique for protein identification. Enzymatic digestion with Trypsin is applied to obtain constituent peptides. Trypsin cleaves the peptide bonds at the C-terminal of Arginine and Lysine if not followed by Proline (Heissel *et al.,* 2019, Olsen *et al.,* 2004). These peptides are then identified using mass spectroscopy and a database. Purified BabA-Crown was gel-electrophoresed and the band corresponding to the expected molecular weight was excised and placed into Eppendorf tube containing sterile molecular biology grade water before sending it to the University of York. Procedures are outlined below in brief.

After washing the samples with 50% (v:v) aqueous acetonitrile, gel pieces were vacuum dried, then rehydrated with trypsin solution for 10 minutes followed by addition of 25 mM ammonium bicarbonate solution to cover the gel pieces. Digestion was carried out using trypsin at a concentration of 0.02 mg/mL and incubated overnight at 37 °C. Resulting fragments were analysed by matrix-assisted laser desorption/ionization (MALDI) system. Bruker ultraflex III in reflectron mode was used to obtain Positive-ion MALDI mass spectra. Mascot program (Matrix Science Ltd.) version was used for Tandem mass spectra data analysis through Bruker ProteinScape interface (version 2.1).

4.2.4 Characterization of peptic digestion

4.2.4.1 Pepsin cleavage sites modelling

To predict the gastric pepsin digestive sites, bioinformatics tools were used. This was performed by submitting BabA-Crown amino acid sequence to ExPASy PeptideCutter (Swiss Institute of Bioinformatics), then mapping the potential predicted cleavage sites onto the BabA crystal structure for modelling simulation. Pepsin cleaves peptide bonds at hydrophobic amino acids, in particular, the aromatic residues (Tyrosine, Phenylalanine, and Tryptophan) if not before Proline (Kamatari *et al.,* 2003).

4.2.4.1.2 Peptic digestion test

To test the protein resistance to peptic digestion, a modified protocol from (Thomas *et al.,* 2004) was used. 2 µL of recombinant BabA-Crown protein at concentration of 1 mg/mL was added to 8 µL of 50 mM KH_2PO_4 (pH 4.5) or with NaCl 100 mm (pH 1.2) containing 750 units/mL pepsin from porcine gastric mucosa (Sigma-Aldrich, USA). Samples were incubated at 37 °C for variable times, then the reaction stopped at the indicated time points by adding 10 µL of quenching solution, 1 M Tris-HCl (pH 10.0). Afterwards, 20 µL of 2x NRSB were added to each sample and heat-denatured for 5 min at 100 °C. Subsequently, samples were loaded into Tris-Glycine gradient (4-20%) mini-PROTEAN TGX gels (Bio-Rad, USA), separated by SDS-PAGE and analysed by various techniques as described below. Protein reference sample for time point zero was primed with the quenching solution before mixing with the pepsin solution.

4.2.5 Sample analysis

Samples were analysed as described in section 3.2.2. However, silver stain was applied to increase the detection sensitivity.

4.2.5.1 Silver staining

Gels containing digested BabA-Crown samples were analysed using silver stain kit (Sigma-Aldrich, USA) following the manufacturer's instructions.

After electrophoresis the gel was immersed for 40 minutes in 100 ml of fixing solution (50 mL absolute ethanol, 10 mL acetic acid in 40 mL ultrapure water), then washed with 100 mL 30% ethanol for 10 minutes. To remove the ethanol, the gel was washed for 10 minutes with 200 mL ultrapure water, then incubated for 10 minutes with 100 mL sensitiser solution (1 ml of ProteoSilver Sensitizer in 99 ml of ultrapure water) and washed twice with ultrapure water. The gel was equilibrated for 10 minutes with 100 ml of the Silver solution (1 ml of ProteoSilver Silver solution in 99 ml of ultrapure water), then incubated for 1 min with 200 ml ultrapure water. After water removal, 100 ml of freshly prepared Developer solution (5 ml ProteoSilver Developer 1 in 95 ml of ultrapure water) was added. This was incubated for 3 - 7 mins and the reaction stopped with 5 mL of the ProteoSilver Stop Solution (0.1 mL ProteoSilver Developer in 95 mL of ultrapure water) to the developer solution to stop the developing reaction and incubated for 5 minutes. The Developer/Stop solution was then decanted and the gel washed for 15 minutes with 200 ml of ultrapure water. The gel was stored in fresh, ultrapure water.

4.2.6 BabA-Crown binding ability

Sandwich Enzyme-linked immunosorbent assay (ELISA) was used to test the ability of BabA-Crown protein to perform the function of whole BabA in binding to Le^b. Human serum albumin (HSA) (Sigma Aldrich), HSA-Le^a, HSA-Le^y and HSA-Le^b glycoconjugates (Isosep AB, Sweden) were immobilized by direct absorption to Nunc MaxiSorp®flat-bottom 96-well plates (Thermo Scientific, Denmark) at a concentration of 5.0 µg/mL dissolved in sodium carbonate (pH 9.6) buffer. BabA-Crown protein was diluted to different concentrations (10 - 20 µg/mL) and

incubated overnight at 4 °C. Then, the plate was washed three times with phosphate buffer saline (PBS) supplement with 0.05% Tween 20 (PBS-T). Next, mouse anti-c-Myc: Biotin clone 9E10 antibody (AbD Serotec, USA) diluted (1:2000) in PBS-T was applied and incubated for 2 hours at room temperature. After three washes, the step of the primary antibody was repeated with streptavidin-horseradish peroxidase (AbD Serotec, USA). Subsequently, binding was detected by solution contains chromogenic substrate 3, 3', 5, 5' Tetramethylbenzidine (TMB), sodium acetate/acetic acid buffer (pH = 6.0) and, before applying to each well, H_2O_2 was added to the solution to reach a final concentration of 0.03%. After 10 minutes of incubation, the reaction was stopped by adding 50 µL H_2SO_4 (2 M). Absorbance was measured at 450 nm on a microplate reader (Tecan, Spark™ 10M multimode microplate reader).

4.2.7 Single-chain fragment variable recombinant antibody

Specific anti-BabA Single-chain fragment variable (ScFv) antibody was used to directly detect the presence of BabA-Crown protein. It was generated after screening of phage-displayed recombinant single-chain fragment variable recombinant library for antibodies reactive with a recombinant BabA. This selected one was named K22, kindly provided by Professor Tim Cover's group (Vanderbilt University, USA). Therefore, it was used for direct identification (tags-independent recognition) of the recombinant binding domain (BabA-Crown). BabA-Crown detection method was applied according to Hennig *et alet al.* (2004). In brief, after separation by SDS-PAGE, samples were blotted onto nitrocellulose membrane. The membrane was blocked with PBS + 0.1% Tween 20 (PBS-T) for 90 minutes. It was then probed for 2.5 h with E-tagged ScFv present in solution (18 mM Tris pH 8.0, 0.6 mM EDTA, 12% w/v sucrose, 0.1% Tween 20 and 0.1% Triton X100). After washing with PBS-T for 30 minutes, the membrane was incubated with the secondary anti-E tag polyclonal antibody conjugated with HRP (Abcam, UK) at a dilution of 1:4,000 in PBS –T, for 90 minutes at room temperature. After washing for 30 minutes washes with PBS-T, the membrane was detected as described in section 3.2.3.3.

4.3 Results

4.3.1 Introducing the AviTag™ sequence

To generate a specific region for AviTag-mediated site-specific monobiotinylation, purified plasmids (wild and BabA-Crown$_{D233A/S244A}$ mutant types) were subjected to site-directed mutagenesis. This tag will offer specific site for enzymatic biotinylation and thus reduce protein aggregation when incubated with streptavidin-coated particles (detailed in chapter 6). The construct contained the AviTag directly after the pelB signal peptide and before the Crown sequence (Figure 4.4). AviTag PCR products were generated in both BabA-Crown constructs using specific sets of primers and screened by gel electrophoresis (Figure 4.5).

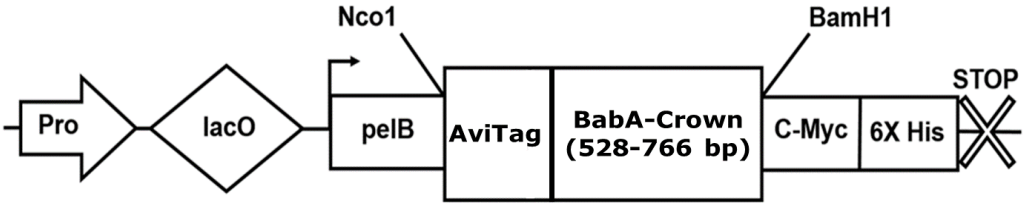


Figure 4.4 Location of the AviTag in the expression cassette of the Crown construct BabA-Crown after mutagenetically cloned, by restriction enzymes ***NcoI*** and ***BamHI***, into the cloning vector pOPE101. **Pro**: Lactose promoter (synthetic P/A1/04/03); **LacO**: lactose operator; **arrow**: represents the start codon; **pelB**: leader sequence for protein transference into the periplasm; **6x Lys**: Hexa-lysine peptide to increase protein expression and solubility; **c-myc** and **6x His**: tags for immunodetection and protein affinity purification, respectively; **X/STOP**: stop codon.

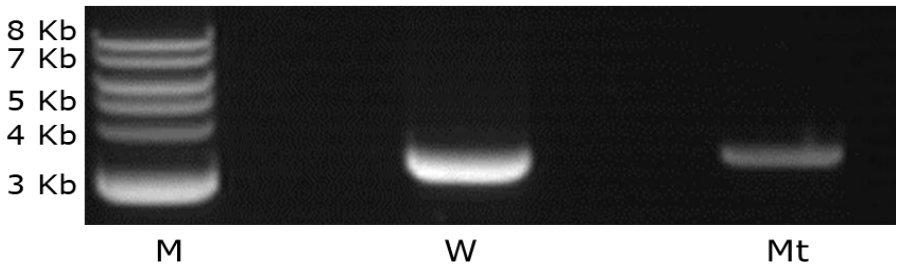


Figure 4.5 Representative PCR products of a mutagenised BabA-Crown construct Agarose gel of PCR-amplified samples. The wildtype (W) and mutant (Mt) BabA-Crown$_{_D233A/S244A}$ constructs were successfully amplified from the BabA-Crown plasmid. M = marker

4.3.2 Confirmatory sequencing

To ensure the AviTag sequences were upstream of BabA-Crown DNA and in frame with the pelB signal peptide, the plasmid was purified and sent for sequencing. There was no frameshift produced as seen in the chromatogram viewed by Snapgene software (Figure 4.6).



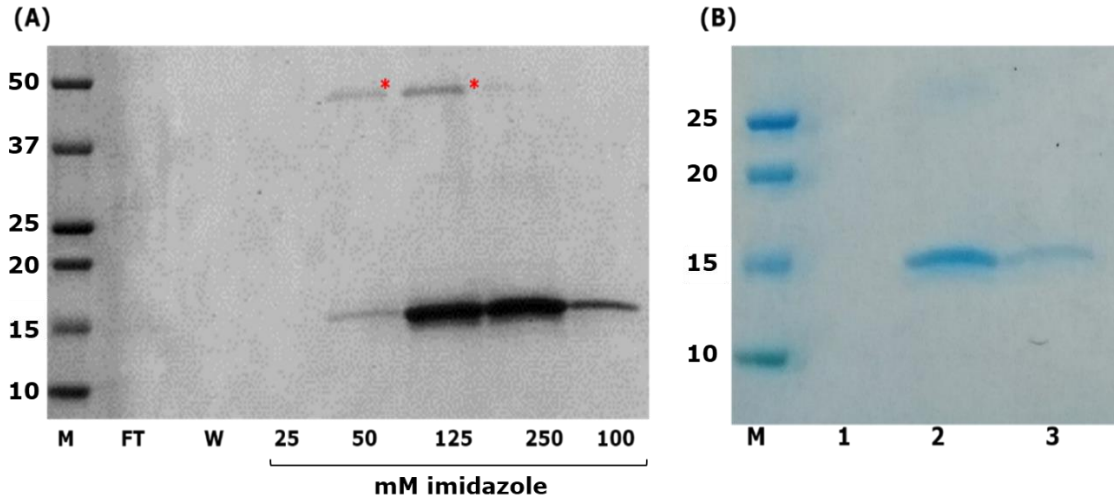
Figure 4.6 Representative DNA sequence of BabA-Crown construct

Chromatogram trace of BabA-Crown construct sequence showing AviTag™ sequence (highlighted in light blue). Left to it is part of pelB leader sequence and downstream to it, is BabA-Crown nucleotides. Underneath the DNA sequence is the corresponding amino acid sequence. The translation showed AviTag™ is in frame with pelB leader and BabA-Crown. Red arrow indicates BabA amino acid sequence.

4.3.3 Protein purification

After BabA-Crown protein expression, the recombinant protein was extracted from *E. coli* XL10-Gold periplasmic space and purified from the rest of the bacterial proteins using IMAC and analysed with SDS-PAGE and Coomassie stain. The hexa-histidine tag at the protein C-end was used for the IMAC purification. Based on the Coomassie stain, the protein was purified through manual (step gradient) and the automated IMAC (continuous gradient) purification methods using ÄKTA Start chromatography system (Figure 4.7). No protein appeared in the flow through. This suggested complete recombinant protein binding to the resin and high binding affinity of the histidine tagged-protein to the nickel-nitrilotriacetic acid (NTA) matrix present in the column. This is also supported by absence of the protein in the wash fractions.

Protein elution started with imidazole at concentration 50 mM and increased at higher concentrations 125 and 250 mM (Figure 4.7A). Thus, an imidazole concentration between 125 and 250 mM was chosen as the optimum range for harvesting purified protein in the automated system (Figure 4.7 B). Therefore, these amounts were concentrated and loaded onto a gel filtration column for further purification, based on the size of the protein (Fig. 4.7C). After Coomassie staining, the eluted fractions were pooled together and a 3 kDa molecular weight cut-off centrifugation was applied to remove most of the imidazole as well as to concentrate the protein.



(C)

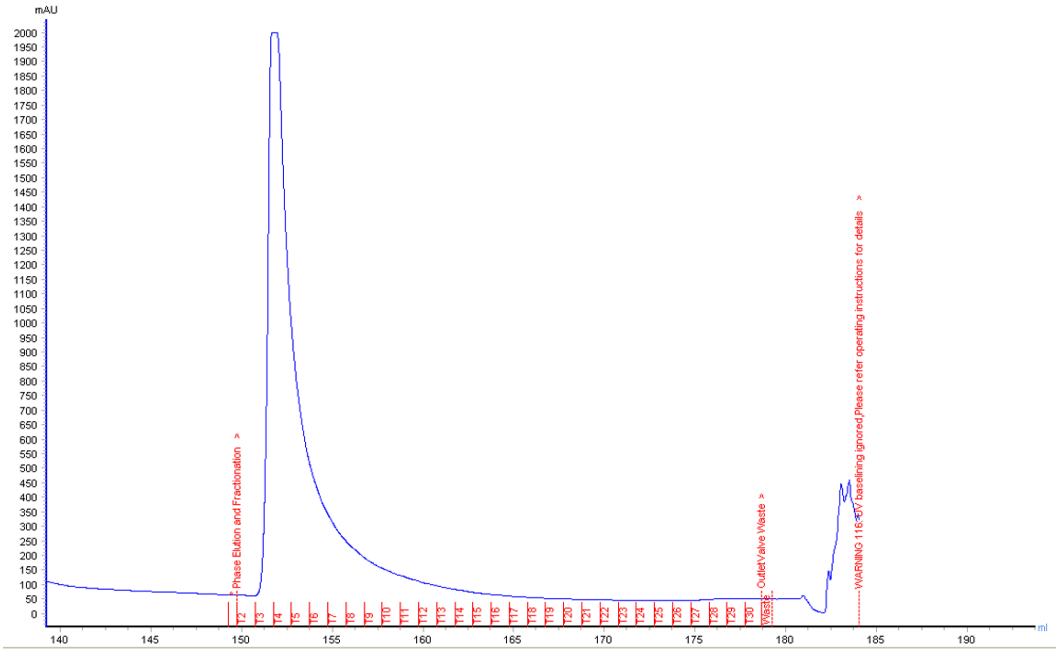


Figure 4.7 IMAC chromatogram of the purification of BabA-Crown

Different IMAC-elution fractions were collected, separated by SDS-PAGE and analysed via Coomassie staining. Manual gradient IMAC purifications (A) show fractions elution using imidazole at different concentrations 50 -250 mM of imidazole. Lane FT in (A) and lane 1 in (B) show no purified protein was detected in the flowthrough. Lanes 2 – 3 in (B) represent the purified BabA-Crown periplasmic extracts, using imidazole concentration between 120 to 250 mM, after pooling the tubes having the eluted fractions corresponding to the peaks displayed in (C) with the automated ÄKTA Start chromatography system. M= Molecular weight marker. FT= flow through. W= wash-out sample. Red asterisk (*) indicates possible protein tetramer formation.

4.3.2 Tryptic peptide mapping

To verify the identity of the protein obtained after purification, peptide mapping was performed from the excised gel slice. Beforehand, tryptic mapping (Figure 4.8) was performed using ExPASy PeptideCutter to determine the potential trypsin cleavage sites. The mapped peptides obtained by tryptic digestion contained about 99% of BabA-Crown residues.



(B)

1 **GLNDIFEAQKI** ↓ **EWHENNGKVNVTYTYTCSGDGNNNCSSQVTGVNN** 45
46 **QKDGTKTKIQTIDGKSVTTTISSKVVDSR** ↓ **ADGNTTGVSYTEITNK** ↓ **LE** 93
94 **GVGSEQK** ↓ **LISEEDLSHHHHHH** 113

Figure 4.8 Schematic indicating tryptic potential sites

A) Schematic indicating tryptic potential sites Trypsin cleaves the C-terminal of Lysin (K) or Arginine (R) if next residue is not Proline (P). Tryps=trypsin

B) BabA-Crown amino acid fragments identified in peptic fragmentation. Brown arrows indicate the site of cleavage.

4.3.3 Pepsin digestion

To assess the potential pepsin cleavage sites within BabA-Crown amino acid sequence, a prediction model for peptic digestion was generated (Figure 4.9) using ExPASy PeptideCutter. These potential cleavage sites were mapped onto BabA-Crown crystal structure (Figure 4.9A). Out of all of BabA-Crown binding residues, it was predicted that Serine (S:83) (S244 in BabA) is the only binding-site residue that can be affected by pepsin digestive activity (Figure 4.9 B). As shown in (Figure 4.9C) the potential peptic cleavage sites were intense in the AviTag™ sequence at the N-terminal and the two tags (C-myc and 6X Histidines) at the C-terminal sites.

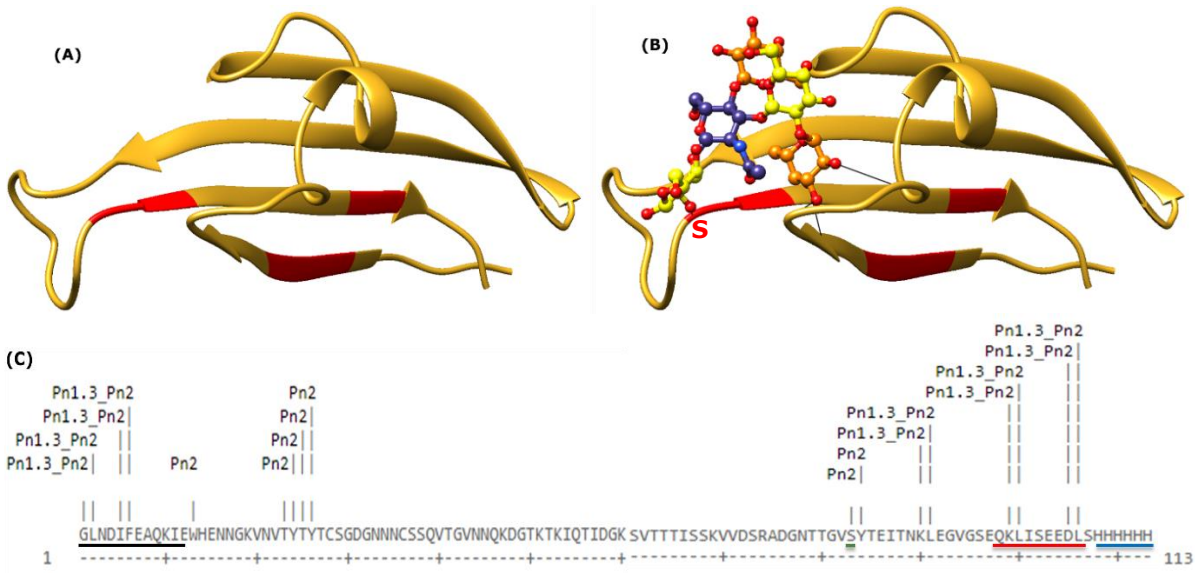


Figure 4.9 BabA-Crown protein predicted model

(A) Side view of BabA-Crown, the potential cleavage sites highlighted in red.

(B) Side view showing BabA-Crown binding to Le^b.
Serine is one of the residues which involved in binding interactions.

(C) BabA-Crown sequence showing pepsin predicted cleavage sites
The residue Serine (S: 83), underlined with green, participates in binding interactions, predicted to be cleaved. The first 15 residues underlined are the AviTag™ sequence. The two lines at the C-terminal are C-myc tag and Histidine tag in red and blue respectively. **Pn:** indicate pepsin digestion sites, **Pn**1.3 = pepsin (pH 1.3), **Pn**2 =pepsin (pH>2).

To experimentally determine the outcome of pepsin digestion on ligand binding, BabA-Crown protein was subjected to peptic digestion at two different pH values. One represents pepsin in partial activity at pH 4.5 (Figure 4.10) and the other at maximal activity at pH 1.2 (Figure 4.11). After incubation with pepsin in a time course trial, samples were analysed through SDS-PAGE and Coomassie stain. Firstly, at pH 4.5, the analysis revealed that BabA-Crown can withstand up to more than 5 minutes and less than 15 minutes in the simulated gastric fluid containing pepsin (Figure 4.10A). However, using the same samples in the same conditions and analysed by more sensitive staining method i.e. silver staining, BabA-Crown sustained pepsin digestion up to 45 minutes (Figure 4.10B). But two apparent bands were visible as patterns from BabA-Crown protein. The obtained pattern is consistent with pepsin cleavage as the larger MW band may result from cleavage of the sequence between T23 and S73, while the small one may represent the degraded bands from the Crown and the three tags.

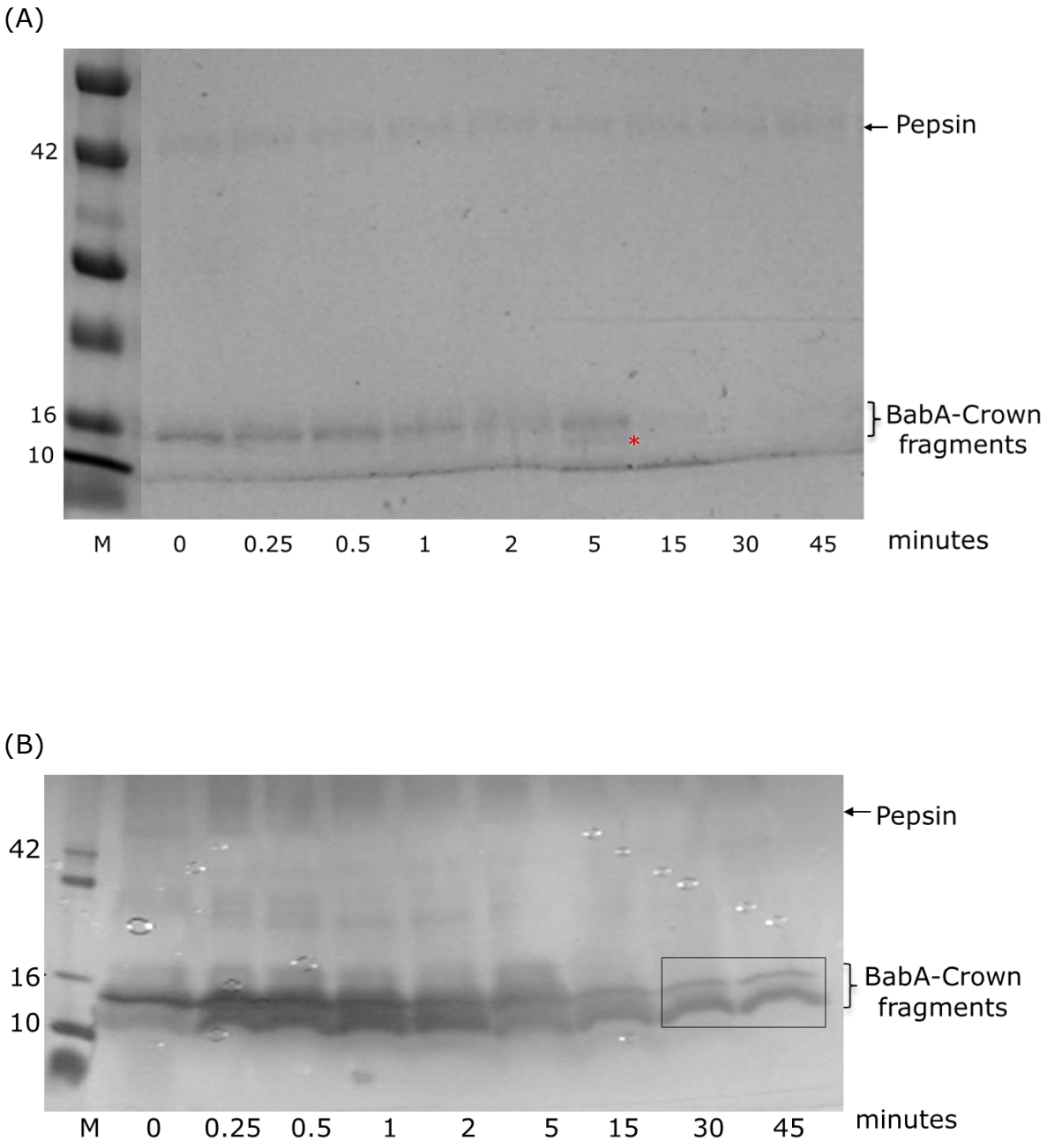


Figure 4.10 BabA-Crown after pepsin digestion at pH 4.5

A time course of BabA-Crown peptic digestion at pH 4.5 as analysed by SDS-PAGE and stained by (A) Coomassie stain and (B) silver staining. Pepsin cleaves BabA-Crown into two parts (boxed). M= molecular weight marker. Numbers indicate time points in minutes. Red star indicates the presence of the second the band.

Secondly, BabA-Crown was tested at the pepsin maximal activity, pH 1.2. This reaction was analysed by Coomassie stain. This showed that BabA-Crown is resistant for less than 5 minutes before complete degradation (Figure 4.11).

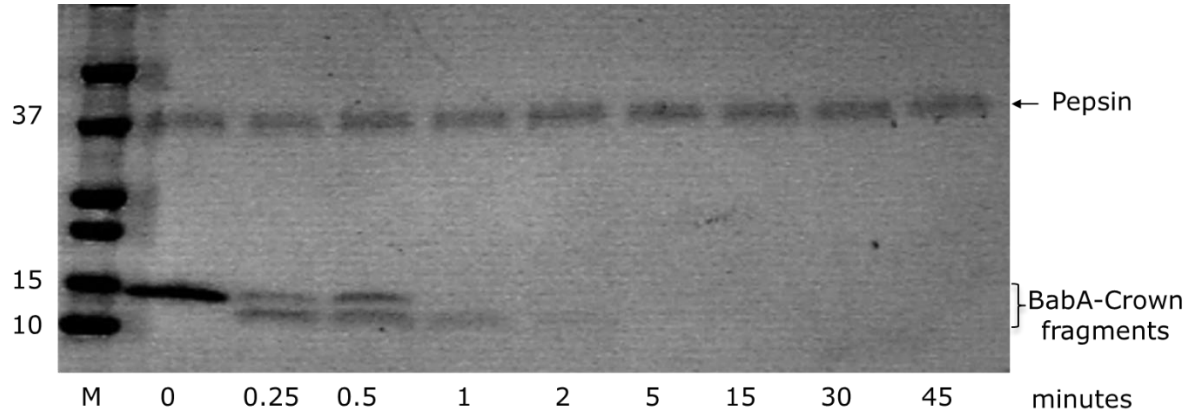


Figure 4.11 Coomassie stain for BabA-Crown after pepsin digestion

A time-course of BabA-Crown peptic digestion at pH 1.2 analysed by SDS-PAGE and Coomassie stain. Pepsin initially cleaves BabA-Crown into two parts starting from 15 and 30 seconds, with no protein visible after 5 minutes. Numbers indicate time points in minutes.

The result obtained from pepsin digestion was used to anticipate the state of BabA-Crown on *H. pylori* surface. The potential pepsin digestion sites at BabA were modelled onto the crystal structure (Figure 4.12). This would suggest that BabA is a very fragile protein in the presence of pepsin at low pH. This appears counterintuitive in a bacterium which has evolved to cope with the acidic conditions present in the stomach. Thus, we propose (Figure 4.13) that only part of the Crown motif is exposed to the harsh gastric environment, with the rest of BabA domains protected by the lipopolysaccharide (LPS) chains forming the bacterial outer membrane. This provides a possible protecting barrier from pepsin digestion in the stomach. The length of the LPS in *H. pylori* is not known but it was estimated to be more of less than *E. coli* which is between 7- 46 nm, while BabA estimated to be between 6.2 and 7.4 nm.

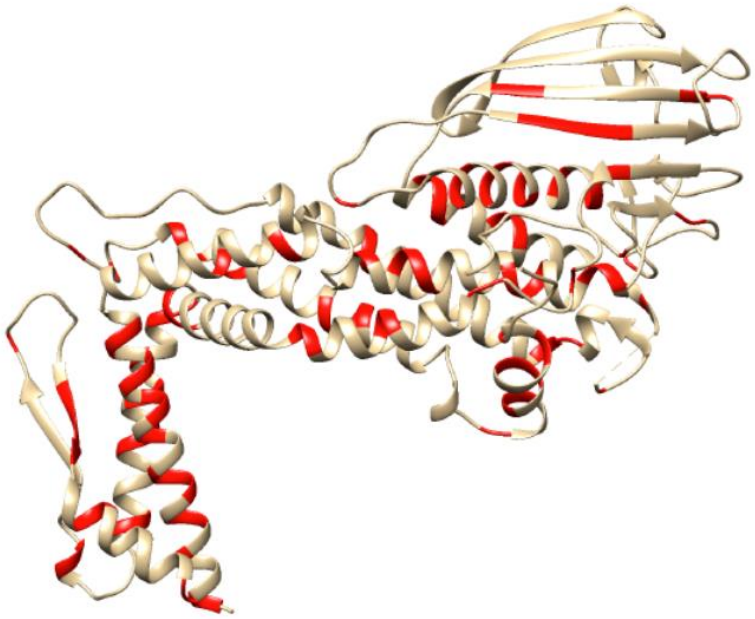


Figure 4.12 BabA crystal structure showing pepsin cleavage sites

The predicted potential pepsin digestive sites (shown in red) were mapped onto BabA crystal structure. The prediction was performed based on the probability of pepsin peptide bond cleavage on the BabA amino acid sequence.

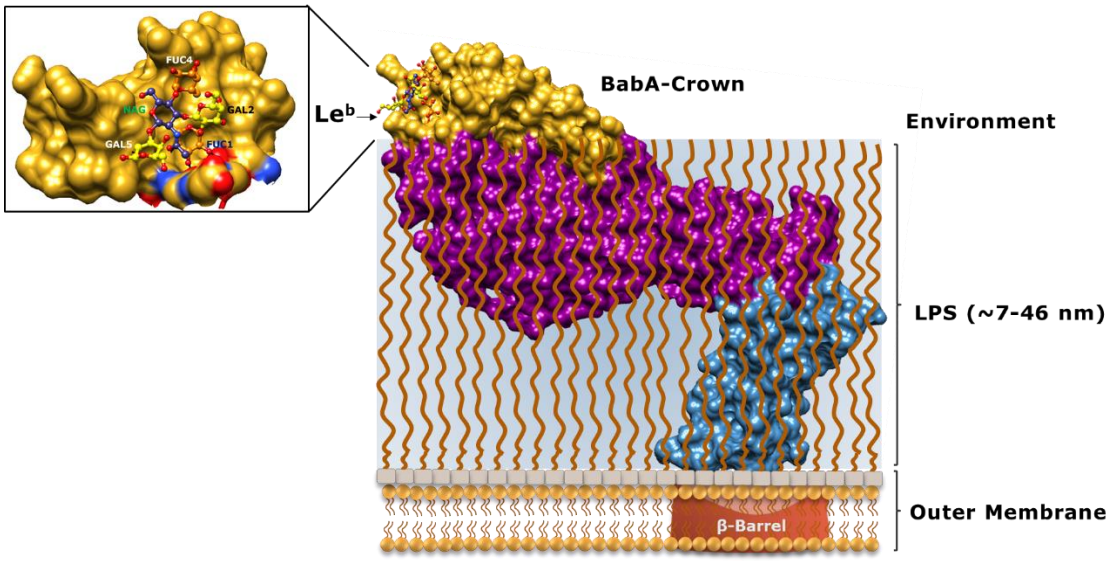


Figure 4.13 Prediction of BabA-Crown status on *H. pylori* surface

The Crown motif predicted to be embedded in a lipopolysaccharides (LPS) layer, which estimated to be 7 - 46 nm (Strauss *et al.,* 2009), extended from the bacterial (OM) outer membrane.

4.3.4 Assessment of binding ability

4.3.4.1 Enzyme-linked immunosorbent assay

To test Bab-Crown protein functionality after expression and purification, various ABO/Le blood group antigens were used for binding evaluation (Figures 4.14). Specific binding was observed in $BabA_{527K}$ (wildtype), while no binding was seen in BabA-Crown, which could be attributed to either improper protein folding or an unknown issue with detection. As expected, $BabA\text{-}Crown_{D233A/S244A}$ mutant type proved to be inactive, as it possessed two mutations in the binding residues (D233A and S244A). The absence of binding between Le^a and both of $BabA_{527K}$ and BabA-Crown validated the experiment. Le^a does not contain Fucose1, which is an essential sugar in BabA binding interactions, forming H-bonds with C189, G191, N194 and T246 in the protein. Interestingly, BabA-Crown mutant type showed a little elevation in binding to Le^a, which is one of SabA's ligands.

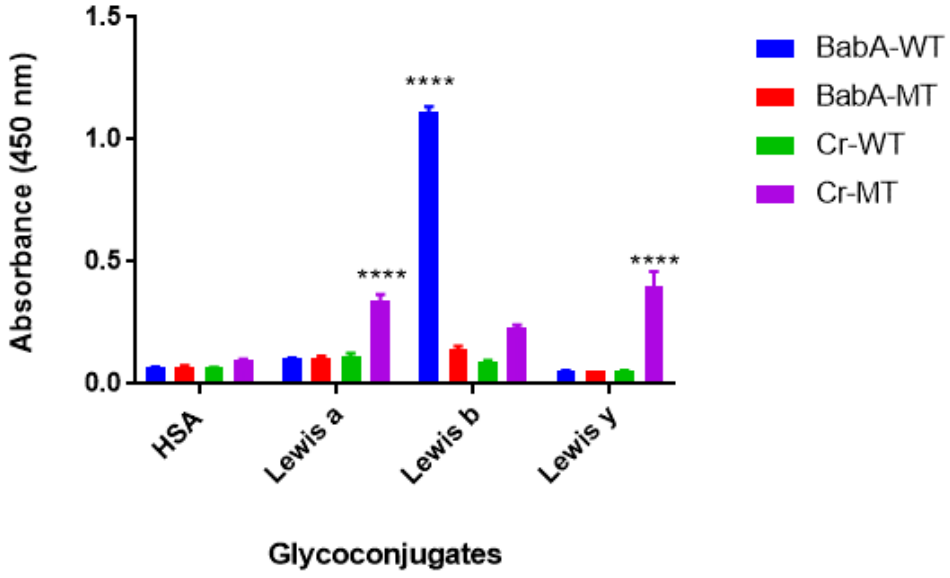


Figure 4.14 Binding of BabA-Crown using sandwish ELISA

BabA, as a positive control, binds to Le^b while BabA-Crown has not shown any affinity. BabA-Crown mutant variant ($BabA\text{-}Crown_{D233A/S244A}$) shows weak binding to Le^a and Le^y. Standard error of the mean was represented by error bars from triplicate readings from three independent experiments (n=3), asterisk (*) = significant difference, error bars represent the standard error of the mean, P <0.001) using 2way ANOVA for multiple comparisons followed by Tukey post-hoc test.

4.3.4.2 ELISA using Nickel nitrilotriacetic acid-Atto 488 for direct detection

This is a direct ELISA assay in which Nickel nitrilotriacetic acid-Atto 488 (Ni-NTA-Atto 488) was used to bind directly to the tag and reveal the binding if present. Fluorescent light was applied to excite Atto-488 at 485 nm and emission measured at 535 nm. As shown in Figure (4.15), convincing binding was seen in $BabA_{527K}$ (wildtype), while BabA-Crown still remained non-functional. This result indicated that BabA-Crown protein could not perform the binding functionality independently, possibly, due to improper folding. However, unexpectedly, BabA-$Crown_{D233A/S244A}$ binding to Le^a was again noticed.

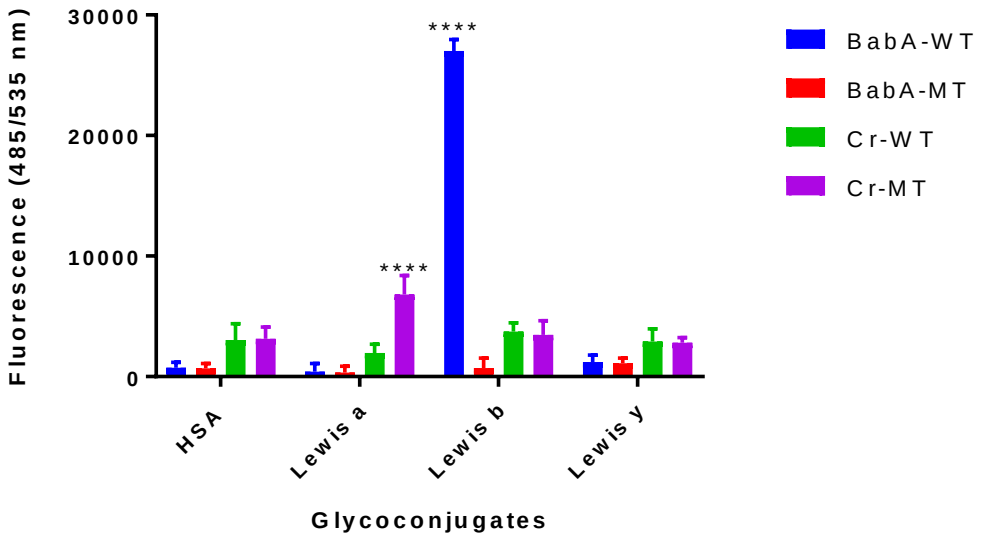


Figure 4.15 ELISA using Ni-NTA-Atto-448 for direct detection of BabA-Crown binding

BabA which bound to Le^b was used as a positive control and BabA mutant as a negative control. While BabA-$Crown_{D233A/S244A}$ form shows an affinity to Le^a, BabA-Crown has not bound to all of the glycoconjugates tested. Error bars represent the standard error of the mean from triplicate readings, n = 3, asterisk (*) = significant difference, ($p > 0.001$), using 2way ANOVA multiple comparisons followed by Tukey post-hoc test.

4.3.5 Phage-displayed ScFv recombinant antibody

This was performed to check whether the E-tagged K22 ScFv binds to the Crown directly as tag-independent recognition agent. K22 was immunoblotted with BabA (wild and mutant types) and BabA-Crown (wild and mutant types) and was detected using HRP-Anti E-Tag antibody. The K22 antibody recognised only BabA but not BabA-Crown, $BabA_{D233A/S244A}$ or $BabA\text{-}Crown_{D233A/S244A}$ (Figure 4.16).

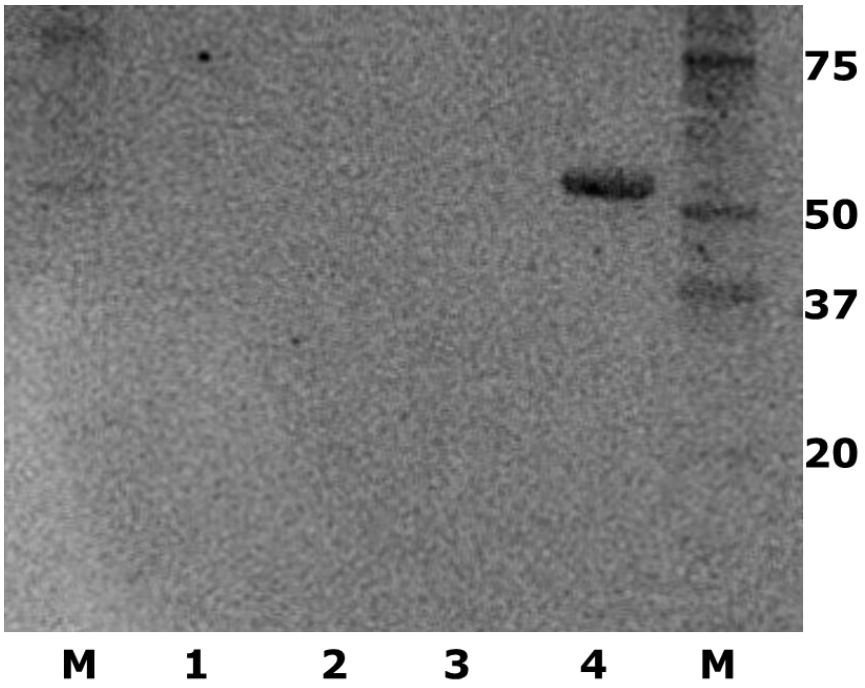


Figure 4.16 Immunoblotting of Bab-Crown with K22

BabA-Crown proteins and $BabA_{527K}$ (each Wildtype and mutant) were separated by SDS-PAGE, relocated into nitrocellulose membrane before immunoblotted with K22 (recombinant ScFv antibody). Binding of this anti-BabA antibody was detected by HRP-Anti E-Tag antibody. 1. BabA-Crown 2. $BabA\text{-}Crown_{D233A/S244A}$ 3. $BabA_{527K}$ mutant 4. $BabA_{527K}$. M= Molecular weight marker.

4.4 Discussion

Following successful expression and purification of BabA-Crown, assessments toward usage as a gastric–target moiety were addressed. Two objectives were set in this chapter to obtain relevant insights. Firstly, to assess the stability of BabA-Crown protein against acid/pepsin digestion. Secondly, measuring its binding affinity and specificity.

To direct BabA-Crown to the glycan on the surface of the gastric epithelial cells, where it is supposed to bind and increase drug retention time, the protein has to sustain the conditions prevalent in the stomach lumen. However, the stomach is a harsh acidic-denaturing milieu mediated by digestive gastric juice. This fluid consists mainly of proteolytic enzyme, i.e. pepsin, and hydrochloric acid. Hydrochloric acid secreted in the stomach display the pH values, which vary according to the prandial status. In the fasted state, it reaches pH ~ 1.5 and ranges from 2 - 7 in the fed state (Russell *et al.,* 1993, Mudie *et al.,* 2010). In the stomach, a gradient difference in the acidity is exited from the acidic lumen to the near-neutral mucosal epithelial surfaces due to bicarbonate secretion (Feldman, 1983). This secretion results in a rapid rise in the alkalinisation to pH ≥4 within less than 10 seconds (Kenny *et al.,* 2008). Additionally, the mucus layer, which protects the epithelial cells from luminal acid and pepsin, contains the bacterial BabA-Crown ligand Le^b (Allen and Flemstrom, 2005). Thus, to mimic the stomach acidic environment, simulated gastric fluid at pH values of 4.5 and pH 1.2 were used, at which the pepsin partial activity (70%) and full activity (100%) reached, respectively (Piper and Fenton, 1965). Even though pepsin is inactive at pH ≥ 6.5, it remains stable until near neutral condition (pH 8.0). At which the activity can be restored if the pH is reduced to 3.0 (Johnston *et al.,* 2007). Thus quenching solution at pH 10 was used to stop pepsin activity.

To the best of our knowledge, the susceptibility of BabA or its components to peptic digestion has not been described in the literature. Therefore, bioinformatics tools were used to predict pepsin cleavage sites within the BabA-Crown.

It is very necessary to know whether the protein could interact with pepsin, how the interaction could occur and what effect would be. Knowledge derived from such interaction would improve the safety drug usage when come to clinical

practise (Zeng *et al.,* 2014a). Pepsin as a globular digestive protease in the stomach is secreted by the chief cells in order to degrade the dietary proteins into peptides (Schubert and Peura, 2008). Structurally, pepsin is composed of two homologous domains. The catalytic site is formed by two Aspartates (one is protonated, while the other is not) present in a cavity between the two domains. Active site protonation to reach maximum activity occurs in pH range from 1.5–2.5 (Yue *et al.,* 2019). Pepsin cleaves mainly the peptide bonds between hydrophobic amino acids, in particular, those containing the aromatic group (Mohseni-Shahri *et al.,* 2018). Pepsin is less specific compared to trypsin (Kamatari *et al.,* 2003). The outcome of the peptic fragmentation depends on many factors such as pH, time or length of exposure and concentration (Ahn *et al.,* 2013). Pepsin hydrolysis activity at pH > 2 is less specific as it cleaves at either site of N- or C- terminals of the aromatic residues or Leucine, if not before Proline (Kamatari *et al.,* 2003). While this specificity is increased at pH 1.3, the cleavage occurs only at the amide bonds in the hydrophobic residues such as Leucine and Phenylalanine. Pepsin at rare occasion cleaves after Histidine and Lysine if not adjacent to Phenylalanine and Leucine (Ahn *et al.,* 2013).

Experimentally, BabA-Crown showed partial resistance to peptic digestion. SDS-PAGE analysis revealed a pepsin resistance to up to 5 minutes, while using the more sensitive silver staining, a small amount of BabA-Crown was detected after more than 45 minutes without complete degradation. As predicted, two main fragments were visualised in the gel after staining, one could represent most of the BabA-Crown sequence and the other one, as was mapped within the peptic zone, may include the AviTag™ sequence, which present in the N-terminal. This may affect the binding ability as one of the binding residue (S: 244). Moreover, pepsin hydrolysis may include the biotin conjugation residue (Y: 245), which is prerequisite for biotin-strept(avidin) interaction for coating nano/micro-particles. Thus, pepsin cleavage may lead to undesired protein conformational folding and affect the functionalization of the non/micro-particles used for drug delivery.

The use of a bioinformatic resource for prediction of pepsin digestion, i.e. peptide cutter, is not completely appropriate due to the limited ability to perform high efficient substrate prediction (Bhagwat *et al.,* 2018) and sometimes may give unrealistic results as demonstrated in (Pickles *et al.,* 2014). The data obtained from BabA sensitivity to peptic digestion could suggest the position/exposure of

the binding site, in bacterial (*H. pylori*) surface, to the surrounding environment. It is assumed that BabA-Crown is embedded in the outer membrane and extruding from the lipopolysaccharide (LPS). This makes only the Crown in the exposed arena and enclosed BabA-head and handle parts into the cell membrane. This assumption was based on the presence of the LPS with variable lengths in the outer membrane of some Gram-negative bacteria (Slomiany and Slomiany, 2017). Lipopolysaccharides constitute most of the outer membrane in Gram-negative bacteria and provide a protective layer against the host immune system. It contain three parts (1) lipid A which is anchored in the cell wall (2) oligosaccharides core and (3) O-antigen domains (O'Donoghue *et al.,* 2017). The exact Lipopolysaccharides structural organisation in *H. pylori* still remains to be determined, and its width as well. It has been proposed to be linear composed of short inner core of hexasaccharide (Glucose–Galactose–Heptose-III–Heptose-II–Heptose-I–keto-deoxyoctulosonate) linked through Heptose-III to outer core comprised of trisaccharides (GlcNAc–Fucose–Heptan) and decorated with Lewis antigen at the outermost part (Li *et al.,* 2018, Li *et al.,* 2017). The length of the lipopolysaccharides in *E. coli* strains having O-antigen is varied from 17 ± 10 to 37 ± 9 nm and about 3 ± 2 to 5± 3 in strains without O-antigen. However, this is correlated between the bacteria and the type of the host cell or tissue (Strauss *et al.,* 2009), e.g. LPS in *Salmonella enterica* expressing O-antigen estimated to be 16 – 46 nm. This length of LPS provide a protective role against complement and phagocytosis. Resistance was suggested to be due to a conformational change or the very long length of LPS may led to epitopes dispersion (Murray *et al.,* 2006). The length of BabA was suggested to be about 6.2 nm, however, as LPS structure in *H. pylori* is not determined, this suggestive model could be determined if other techniques such as *in vitro* model or high-resolution magnetic resonance imaging technique (Eida *et al.,* 2016), Cryogenic electron microscopy (Cohen *et al.,* 2017) or atomic force microscopy (Strauss *et al.,* 2009) were used. The study of the length and composition of *H. pylori* was set as a future plan.

The result obtained in this chapter could be promising if the gastric-targeting moiety was aimed to be located in a distal area from the acidic lumen or in a proximal to the pH-neutralised micro-environment found on the epithelial cell surfaces. Even though, this would restrict the application of BabA-Crown, if used, to the fed state only (Scott *et al.,* 1998, Pflock *et al.,* 2004). However, the

susceptibility of one of the Crown binding site to the pepsin digestion is a major drawback as well as the binding inability. One possible strategy to decrease the proteolytic digestion could be achieved by fluorinating the amino acids such as leucine and isoleucine, and as a result, interfere with the enzyme binding site (Huhmann *et al.,* 2017). This strategy can be applicable assuming that fluorination does not interfere with ligand binding. Another possible techniques is to add amides such as N-Methyl- and N-ethyl-amides to the carbohydrate, as amidation was suggested to increase the binding affinity (Miller-Podraza *et al.,* 2008).

To achieve the goal of developing drug delivery system, BabA-Crown adhesion to gastric epithelial cells is a fundamental property. Therefore, it is of paramount importance to ensure that recombinant BabA-Crown is folded correctly and as a minimal binding site can retains glycan-binding ability. Binding was assessed *in vitro* using glycoconjugates (HSA-Le^b and HSA-Le^a) through sandwich ELISA. As BabA is derived from generalist strain (*H. pylori* J99), it can, as recorded in the literature, interact with type 1 Le^b/ABO blood group antigens with variable binding affinities to Le^b (Nell *et al.,* 2014). However, no attachment to type 2 (corresponding to ABO/ Le blood group antigens) is expected. This lack of binding to type 2 is due to the difference in the type of the glycosidic linkage between the galactose and *N*-acetylglucosamine residues, Galβ1-3GlcNAc and Galβ1-4GlcNAc linkages in type 1 and 2, respectively (Hage *et al.,* 2015a).

In the present experiments, Le^b was used as the target ligand and Le^a as a negative control for binding. Although both of these ligands are from the same type, Le^a lacks Fucose 1 residue which forms hydrogen bonds with four of the eight binding residues (Cysteine 189, Glycine 191, Asparagine 194 and Threonine 246) in BabA-Crown (Moonens *et al.,* 2016, Hage *et al.,* 2015a). Anti-C-Myc tag antibody against the protein's C-terminal c-Myc tag was used to detect the binding interaction between BabA-Crown and Le^b, which was immobilized to a Maxisorp®plate. BabA-minimal binding site in comparison to BabA showed no binding activity. However, binding of BabA-$Crown_{D233A/S244A}$ mutant to one of type 1 ABO/Le blood group antigens, le^a, was not expected. This binding was reproducible using Ni-NTA-Atto-448 which interacts directly with the His-tag in the protein. Atto-488 is a commercial name for a rhodamine derivative (Konrad *et al.,* 2016). This water-soluble fluorescent dye is recommended for protein labelling because of its photostability (Zhang *et al.,* 2017). BabA-$Crown_{D233A/S244A}$ mutant binding activity

could undergo further confirmation if tested against a positive control such as SabA.

It worth noting that in ELISA assay, the positive control ($BabA_{K57}$) validated the interaction with Le^b. The lack of functionality may be due to protein aberrant conformation or the inability of the detecting antibody to access the detection tags. Thus, an attempted to use the specific anti-BabA antibody (K22), which does not detect any tags was carried out. K22 is a phage-displayed single-chain fragment variable (ScFv) recombinant antibody generated to identify BabA (Hennig *et al.,* 2004). It was selected after screening a phage-displayed ScFv recombinant antibody library that was specifically reactive to recombinant BabA protein (jhp0833) (GenBank accession number AAD06409), comprising amino acids 128-310, from *H. pylori* J99. This sequence is closely related to the construct $BabA_{CHPL}$ (review chapter 5) which comprising amino acids from 124 - 296. It was suggested that K22 recognised an epitope within BabA in a well-conserved sequence among different *H. pylori* bacterial strains (Hennig *et al.,* 2004). However, the exact binding sites between this antibody and BabA were not defined from multiple alignment of amino acid sequences. Interestingly, Hennig *let al.,* (2004) referred the variation in binding abilities to the heterogeneity in the Crown hypervariable loops as one of the strains (*H. pylori* 87-33) that binds to Le^b and K22 has a mutation in N209E (Hennig *et al.,* 2004). Later, BabA crystal structures revealed that a change in one of the binding sites (N209A) reduced the binding affinity and dual mutations or a disruption of the folding using redox-active pharmaceutic N-acetylcysteine to cleave the Cysteine bridges, can produce non-binding activity (Moonens *et al.,* 2016, Hage *et al.,* 2015a).

In this experiment, K22 was used for direct reactivity with BabA-Crown, recombinant $BabA_{K57}$ (wildtype) and the mutant ones. K22 antibody proved to be reactive with $BabA_{K57}$ without detecting the other proteins including BabA-Crown. This reinforced our view of BabA-Crown structural misfolding as the cause of non-functionality. The performance and specificity of the recombinant antibodies is determined by the nature of the recognition sites or the epitopes, which can be divided into linear or conformational. Linear epitopes bind to antibodies via a stretch of connected amino acids. Conformational epitopes are amino acids forming an epitope joint together because of protein folding (Forsström *et al.,* 2015, Forsstrom *et al.,* 2014). Hage *et al*, (2015) demonstrated that dual

substitutions in BabA (D233A/S244A) did not change the secondary structure (Hage *et al.,* 2015a). This was proved in the experimental done by Hennig *et al.,* (2004) as one of the strains (*H. pylori* 92-26) has a dual mutation in D233Q and S244A. Therefore, as the folding of BabA was not the cause of K22 non-detection, the specificity of K22 was probably due to the epitopes that either laid outside of BabA-Crown amino acid sequence or these epitopes are within the sequence but BabA-Crown did not reach the right conformation/folding to be detected by the K22 antibody. Circular dichroism was set as a future step to know if the secondary structure of BabA-Crown still retains the mostly β-sheets structure.

To investigate the causes of BabA-Crown non-functionality, additional factors were considered as stresses such as the role of the added Chloramphenicol in accelerating protein production. Increasing the plasmid copy number might negatively affect the bacterial (*E. coil* XL10-Gold) gene transcription rate or cause imbalance between protein production and localisation in the periplasm (Li *et al.,* 2014). This alteration could adversely affect the bacterial cellular functions in terms of interference with the transcription levels as more mRNA is synthesised to produce more recombinant protein (Schendel *et al.,* 1989). The high copy number up-regulated the rate of expression and/or protein accumulation in the periplasmic space (de Marco, 2009). Therefore, intensification of protein expression may not work in harmony with secretory mechanisms and adjustment of gene expression levels with the flow of cellular metabolism was not as required (Baumgarten *et al.,* 2018). This ultimately may result in protein accumulation in the periplasmic space, which subsequently extracted and used. Thus, to minimise the stress arose from the added chloramphenicol, protein expression in low or chloramphenicol free media should be tried.

Another factor which may interfere with binding ability could be dimer formation (multimerisation). The Crown, as revealed in the crystal structure is mostly β-antiparallel sheets and the interacting sites are stabilised by cysteine clasped loop, however, as a minimal binding site, asymmetric structure could result and alter the orientation of the interacting residues (Brown, 2006) dimerization may also occur on the membrane surfaces (Lin *et al.,* 2014) to render the hydrophobicity (Arnaouteli *et al.,* 2017) and increase the binding affinity or the conformation (Bugaytsova *et al.,* 2017).

The dimers could be gained from three-dimensional domain swapping, a mechanism by which exchange of identical elements occurs between two or more protein to form dimer or oligomers (Baiesi *et al.,* 2016). Therefore, it is useful to use separating techniques such as size exclusion chromatography to isolate the monomer from the dimer based on the difference in the size and use each of the two protein in binding assay to confirm which one attained the correct folding (Hong *et al.,* 2012). Size exclusion chromatography is analytical technique routinely used for protein separation based on the difference in the mass and for analysing protein aggregation (Busch *et al.,* 2017). However, it may give inappropriate mass estimation because the retention time relies on hydrodynamic radius and molecules interaction with the stationary phase may occur (Amartely *et al.,* 2018). Protein secondary structure or aggregation can be characterised by another methods such as Circular dichroism (Miles and Wallace, 2016), nuclear magnetic resonance spectroscopy (Sugiki *et al.,* 2017) and solid-state nuclear magnetic resonance spectroscopy (Mandala *et al.,* 2018), but protein refolding (multimerization) may occur again after purification or during storage due to some environmental factors such as pH, salt and temperature (Brusotti *et al.,* 2018). Thus, reducing condition is required to maintain the monomer and prevent further dimer or oligomer formation (Dombkowski *et al.,* 2014). However, the use of reducing agent may impact the BabA-Crown binding ability to the ligand.

A recent study justified the need for 'Velcro' domain to support BabA structure and thus influence binding property (Bugaytsova *et al.,* 2017). The study proposed that Velcro domain comprised of one helix in the head and two helixes in the handle forming a trio of helices. This domain was suggested to play a part in controlling BabA multimerisation and mediate acid-responsive adherence and thus determine binding affinity. Substitution of glycine in amino acid 428 with glutamic acid in Velcro domain, which is diametrically (~ 40 A$^{\circ}$ away) opposite the Crown, resulted in lower binding capacity. Moreover, there is an undefined link between this domain and two amino acids (D198 and R207), located in one of the hypervariable loops, the one immediately after the disulphide clasp (between C189 and C197) in acid responses. These two residues form a salt bridge and stabilise the disulphide clasp and seemed to act as a pH sensor. Bridge disruption at pH 1- 4 (less than 4) leads to loss of the Crown's ability to hold Le^b and thus binding activity. It was also suggested that Velcro domain helps BabA forming a

multimeric structure in native BabA at pH around 5.5 and at less pH dissociated into oligomer before come to a monomer structure at lower pH. Trimeric form of BabA was suggested to be of the highest binding affinity and the natural topological form (Bugaytsova *et al.,* 2017, Moonens *et al.,* 2016). However, this study did not include BabA protein from *H. pylori* J99, which does not have D198 and R207 in its amino acid sequence. Thus, the role of Velcro domain as a pH sensor or in multimerisation may reflect the need for a similar chaperon-like domain, within BabAJ99, to bring BabA-Crown conformation into a proper functionality.

The term chaperon was originally introduced for a separate class of proteins expressed upon an unfavourable shift in the surrounding environment (i.e. heat shock proteins) (Motojima, 2015). This term appeared to be more descriptive for protein family having a domain in its sequence to participate in protein folding, stabilisation, degradation and yield increasing (Kyratsous *et al.,* 2009). Therefore, a postulation that an intraspecific sequence which maybe encoded in BabAJ99 amino sequence was considered as an important point to solve the binding functionality issue. It is proved that proteins perform their biological function after reaching their native specific three-dimensional structures structure which is encoded in their amino acid sequences (Díaz-Villanueva *et al.,* 2015). The next steps, concluded from the data obtained in this chapter, are to confirm whether the BabA-Crown protein has the native secondary structure using circular dichroism, modify the expression conditions to exclude the Chloramphenicol from the growth medium and look for a chaperon-like domain within BabA protein. There is an evidence that VacA, as autotransporter, has an intramolecular chaperone sequence which played a role in assist the folding during or after translocation (Letley *et al.,* 2006) or stabilising the adhesin tertiary structure and functionality (Heim *et al*, 2014). This integral part is prone to the surrounding changes such as pH or temperature which may disrupt the native structure and lead to loss of function (Motojima, 2015). Even though the length of DnaJ is small compared to the other intramolecular chaperones, its function maybe like *Streptococcus mutans* adhesin P1, which is double in length and assists in protein folding and stabilising the tertiary structure (Heim *et al.,* 2014).

4.5 Conclusion

The Crown region is not sufficient to bind/recognise the ligand of BabA. Further optimization is required in terms of optimising expression conditions or structural modifications, with an aim to ensure that it is folded properly.

CHAPTER FIVE

5. Alternative strategies for BabA-Crown expression

5.1 General overview

The main objective of this chapter was to apply alternative strategies to solve the issue of BabA-Crown's lack of binding functionality. This started with considering the effect of adding chloramphenicol in order to achieve the recombinant expression. It was hypothesised that chloramphenicol increased the plasmid copy number and this could push the (chloramphenicol-resistant) bacteria to accelerate protein synthesis. This burden may affect the folding machinery and result in non-functional protein (discussed in chapter four). To address this issue, two strategies were applied: the first one was to adjust the growth media in an attempt to reduce or exclude the chloramphenicol. The second strategy was performed at the molecular level by adding additional nucleotides to extend the length of the minimal binding domain and constructing various different truncates as well.

As previously explained in Chapter three, BabA X-ray structure revealed Hydrogen bonding interactions (Serine 190 to Lysine 119, Isoleucine 121 to Threonine 188, and Asparagine 123 to Threonine 186) between BabA-Crown and two beta sheets located in the Head domain. These beta sheets are not themselves involved in ligand binding. However, they may support the folding/binding of the Crown region. Accordingly, the length of the Crown domain was adjusted to include them, i.e. amino acids 124-296. This new truncate (Figure 5.1) was named BabA-Crown-Head-Partial-Length ($BabA_{CHPL}$). Secondly, as a precautionary process, the complete sequence (amino acids 55- 462) of both BabA's Crown and the Head

(Figures 5.2) was recombinantly constructed and called BabA-Head-Crown-Handle-Free ($BabA_{HCHF}$).

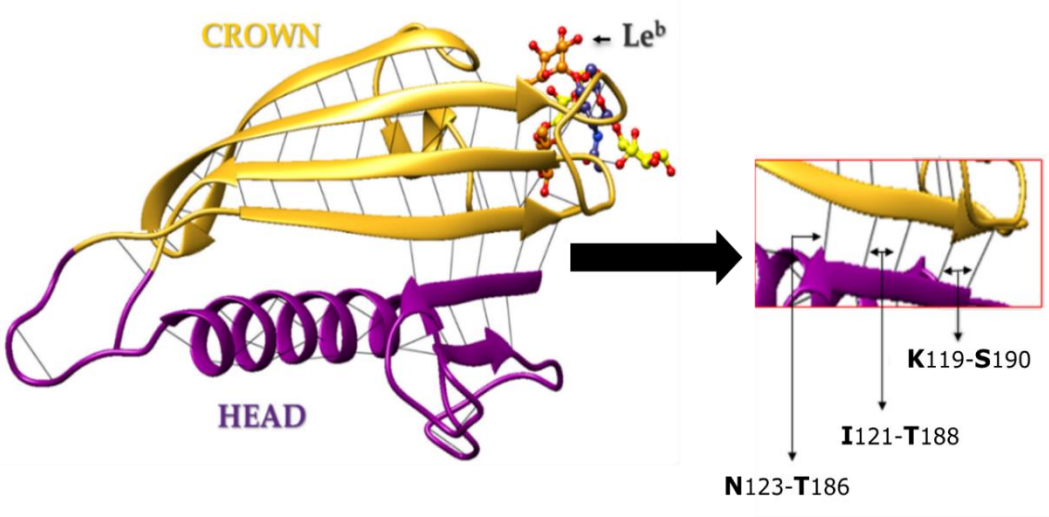


Figure 5.1 Crown-Head-Partial-Length (CHPL)

3D ribbon structure of BabA J99 strain showing the Crown (Gold) with part of the Head (dark magenta), this covers amino acids 124-296. Two beta sheets from the Head and Crown domains interact through several Hydrogen bonds K119, I121 and N123 on the Crown to S190, T188, and T186 on the Head domain, respectively. These interacting residues may support/stabilise the structure.

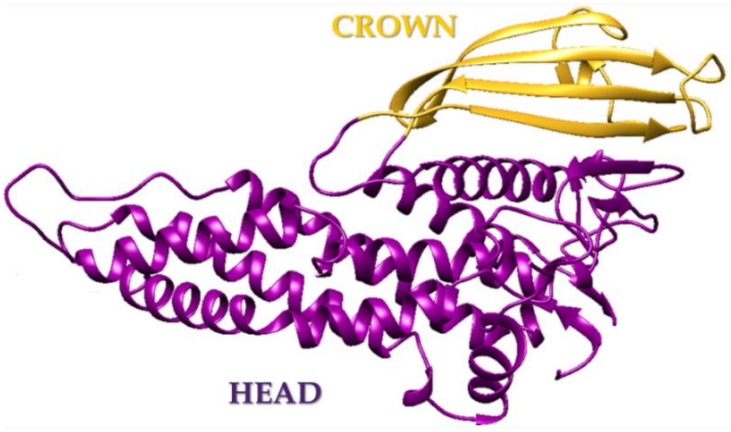


Figure 5.2 structure of BabA-Crown and the Head

3D structure of BabAJ99 showing Head (dark magenta) and Crown (Gold) domains which comprise amino acids 55- 462, forming the truncate BabA-Head-Crown-Handle-Free (HCHF).

Subsequently, a mutagenic step was carried out in the BabA coding sequence to incorporate nucleotides encoding protease-recognition sites in the DNA sequence (382 - 400 and 634 - 645 bp). After protein expression, these cleavage sites will be cut precisely by the protease enzyme. Notably, Factor Xa (Stuart-Prower factor) is the most used protease to remove a tag from any fusion protein (Jenny *et al.,* 2003). Thus, a Factor Xa endo-protease recognition sequence (Ile-Glu/Asp-Gly-Arg) was introduced into recombinant BabA sequence in the loops located immediately up- and downstream of the Crown domain. Factor Xa sequence Ile, Glu, Gly and Arg replaced L171, P172, A173, L174 (loop1) at the Crown N-terminal amino acids and (loop2) G254, V255, P256, D257 at the C-terminal amino acids. The idea behind this construct, named $BabA_{Fxa}$, (Figure 5.3), was to allow accurate folding of BabA-Crown protein within the full length of BabA protein synthesis. Then after protein expression and purification, incubate with Factor Xa protease to release the Crown.

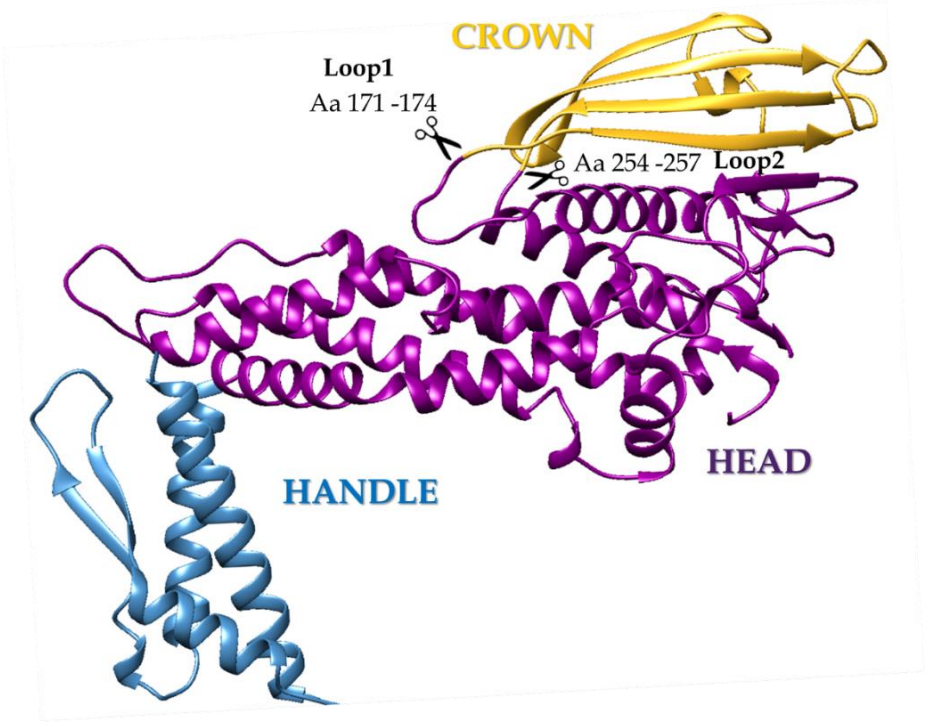


Figure 5.3 Crystal structure of J99-BabA protein

BabA-Crown (Gold), Head (dark magenta) and Handle (blue). Scissors showing places where two Factor Xa restriction sites at the N-terminal amino acids (Aa) 171-174 and at the C-terminal amino acid 254-257 were aimed to be inserted and where to cut after expressing the protein.

In a further attempt, an additional new version of a recombinant construct was generated to include BabA-Crown plus DnaJ sequence linked to one more copy of BabA-Crown at the N-terminal, thus termed Cr-DnaJ-Cr (Figure 5.4). This truncate was though to act as Velcro domain in BabA 17578 and to be the divalent form of BabAJ99. The four cysteine residues were assumed to form two clasps and bring the binding sites together, while the DnaJ domain as a helix region provides a hinge-like structure. Crown1 comprises the Avitag at N-terminal and amino acids (N177 - A259), while Crown 2 include G143-A259 besides the DnaJ domain.

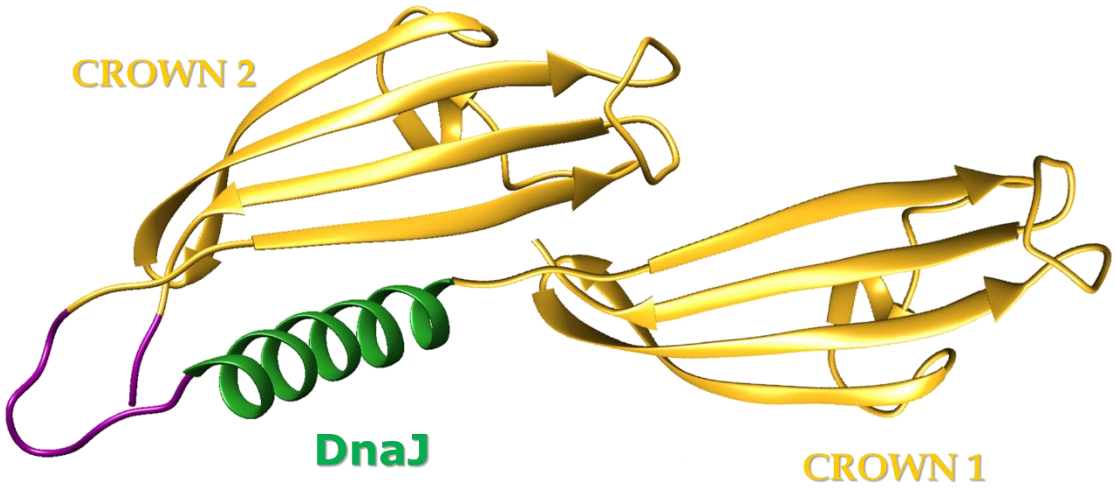


Figure 5.4 Cr.DnaJ-Cr

Schematic ribbon representation of two BabA-Crown (Gold) domains separated by DnaJ (forest green) and loop from the Head (dark magenta). Crown 1 include the AviTag sequence at the N-terminal followed by sequence from the Crown N177-A259. Crown 2 starts with G143-A259 and include the DnaJ domain.

5.2 Experimental procedures

5.2.1 Generation of truncated BabA expression constructs

Based on the aforementioned lack of glycan binding, four different truncates of BabA were generated from plasmid coding sequence of BabA from *H. pylori* J99, except Cr-DnaJ-Cr, as summarized in Table 5.1.

1. $BabA_{CHPL}$: Gene fragment 371 - 888 bp encoding amino acid sequence 124 - 296
2. $BabA_{HCHF}$: Gene fragment 163 - 1386 bp encoding amino acids 55 - 462
   These constructs contain DNA sequence encoding hexa-lysine tag, which was originally used for increasing BabA expression and solubility (Hage *et al.,* 2015b), was included to be expressed at the C-terminals of these proteins (Figure 5.5).
3. $BabA_{Fxa}$: site-mutagenesis was used to incorporate two proteolytic cleavage at two loops behind an after the Crown domain encoding loop1 (amino acids 171-174) and loop2 (amino acid 254-257).
4. Cr-DnaJ-Cr: cDNA synthesized by Invitrogen (GeneArt Gene Synthesis, USA) encoding two copies of BabA-Crown domain linked by a short sequence of DnaJ superfamily domain.

All of these constructs were generated after subsequent gene amplification, double digestion, ligation and transformation as described in Section 3.2.1.

Table 5.1 BabA truncated expression constructs

The abbreviation used in naming BabA constructs were detailed in the main text

Construct Name	Vector Backbone	Cloning Host
$BabA_{CHPL}$	pOPE101	*E. coli* XL10-Gold
$BabA_{HCHF}$	pOPE101	*E. coli* XL10-Gold
$BabA_{Fxa}$	pOPE101	*E. coli* XL10-Gold
Cr-DnaJ-Cr	pOPE101	*E. coli* XL10-Gold

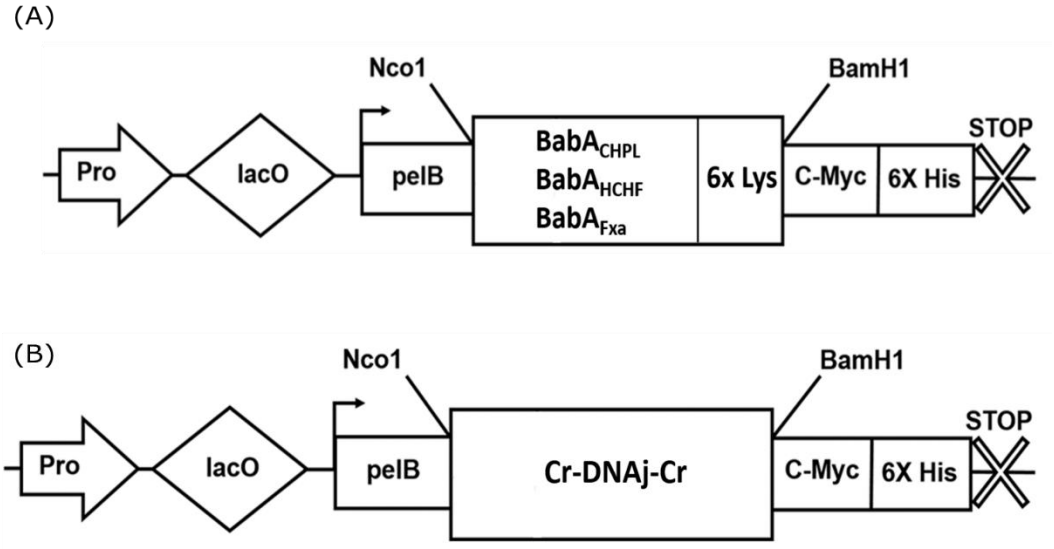


Figure 5.5 Schematic diagram representing the expression constructs built in pOPE101 vector

A. The cDNAs encoding $BabA_{CHPL}$, $BabA_{HCHF}$, $BabA_{Fxa}$ in addition to B. Cr-DnaJ-Cr were cloned, by restriction enzymes *Nco*I and *BamH*I, into the cloning vector pOPE101. Pro: Lactose promoter (synthetic P/A1/04/03); *Lac*O: lactose operator; arrow: represents the start codon; pelB: pectate lyase B leader sequence for periplasmic targeting; 6x Lys: Hexa-lysine peptide to increase the expression of the protein; c-myc and 6x His: tags for immunodetection and protein purification, respectively; X/STOP: stop codon.

5.2.1.1 Gene design - PCR amplification

PCR was performed using Q5™ high-fidelity DNA polymerase (New England Biolabs, UK) for fragment amplification following the manufacturer's protocol. The constructs listed in Table 5.1 were engineered from previously formed recombinant plasmids using the designed primers shown in Table 5.2.

Cr-DnaJ-Cr synthesised by GeneArt (ThermoFischer Scientific, UK) was sub-cloned into pOPE101 and transformed into *E. coli* XL10-Gold as described in Section 3.2.1.3. PCR products were analysed on 1% agarose gel buffered by Tris-Borate-EDTA (TBE).

Plasmid confirmatory sequencing was carried out by Source BioScience, Nottingham using primers listed in Table 3.3. SnapGene® software (GSL Biotech LLC, USA) was used for alignment of the obtained DNA sequences with BabA J99 (GenBank accession no. AAD06409).

Table 5.2 BabA truncated expression constructs

The oligonucleotide primer name comprises the names of the target gene sequence, restriction enzyme sequence and whether it is a sense (FOR) or antisense (REV). Nucleotides of the restriction sites (CCATGG & GGATCC), underlined, are located downstream of the hexa-overhang nucleotides. The reverse primer contained the hexa-lysine peptide, bold font, at downstream to *BamH*I restriction site. The primers used for constructing $BabA_{Fxa}$_pOPE101 through site-direct mutagenesis were designed to insert nucleotides encoding cleavage sites sequences for Factor Xa protease. Loop 1 and 2 referred to the positions where the cleavage sites introduced into BabA-Crown N-and C-termini, respectively.

Vector backbone	Primer name	Primer Sequence (5'- 3')
pOPE101	$BabA_{CHPL}$_*Nco1* For	TCGCATCCATGGCCACGCAATGCGGGGGTAAG
pOPE101	$BabA_{CHPL}$_*BamH1* Rev	GCTGCTGGATCC**CTTCTTCTTCTTCTTCTTT**GCGTTGTTGATGGTGTTA
pOPE101	$BabA_{HCHF}$_*Nco1* For	TCTGATCCATGGACCCGAGCGCGATTAAT
pOPE101	$BabA_{HCHF}$_*BamH1* Rev	CGAGTTGGATCC**CTTCTTCTTCTTCTTCTT**ATTCACCAGAGTGTCAGCG
pOPE101	$BabA_{Fxa}$_Loop1 For	ATCGAGGGTCGTAAAGAAAACAACGGGAAAGTCAATGTAACC
pOPE101	$BabA_{Fxa}$_Loop1 Rev	GCCTCGTTTTAAAGCCGTTTGGAGGATCT
pOPE101	$BabA_{Fxa}$_Loop2 For	ATCGAGGGTCGTAGCGCTCAAGCGCTCTTAGCGCAAGC
pOPE101	$BabA_{Fxa}$_Loop2 Rev	TTCTAATTTGTTGGTGATTTCGGTGTAGGACACCCCTG

5.2.2 Protein expression

To check the possibility of obtaining BabA-Crown recombinant protein using a growth medium with minimal concentration of chloramphenicol or chloramphenicol-free medium, three different kinds of media LB_{AT} medium, which have no glucose or chloramphenicol (LB Broth containing 100 µg/mL Ampicillin, 12.5 µg/mL Tetracycline hydrochloride), LB_{ATG} medium, which only contains glucose (LB_{AT} medium supplement with 0.1 M D- Glucose) and LB_{ATGC} medium (LB_{ATG} medium supplement with 34 µg/mL chloramphenicol) were prepared. Small-scale expression was performed as described in (Section 3.2.2) to examine the likelihood of achieving soluble protein in the periplasmic space in *E. coli* XL10-Gold cells.

5.2.3 Circular Dichroism Spectroscopy

All BabA-Crown CD experiments were performed by Dr Geoff Holdgate at AstraZeneca, while Cr-DnaJ-Crown CD experiments were performed by collaborator at CBS, University Of Nottingham.

In the present research, J-810 Spectrophotometer (Jasco, USA) and Pi Star-180 Circular Dichroism Spectrophotometer (Applied Photophysics, UK) were used for detecting protein spectra.

Sample (1 µM) was placed in a buffer consisting of 20 mM Tris-HCl (pH 7.5). Using a quartz cell at 25°C measurements were made with a 0.1 cm path length at data pitch of 0.5 nm and a 100 nm/min scanning speed.

5.2.4 Enzyme-linked immunosorbent assay

ELISA was performed as described in Section 4.3.4.1.

5.2.5 Peptic digestion

This was carried out as described in Section 4.3.3

5.3 Results

5.3.1 Growth medium optimization

Three different types of growth media (LB_{AT}, LB_{ATG} and LB_{ATGC}) were examined to elucidate which one will be useful for producing soluble protein in the bacterial periplasm with low/zero concentration of chloramphenicol. BabA-Crown was successfully expressed in LB_{AT} medium but not in LB_{ATG} or LB_{ATGC} media (Figure 5.6). *E. coli* endogenous ~20 kDa protein was present in the cytosolic extracts in LB_{ATG} and LB_{ATGC} media, while a small amount of this protein was observed in LB_{AT} medium together with BabA-Crown putative dimer.

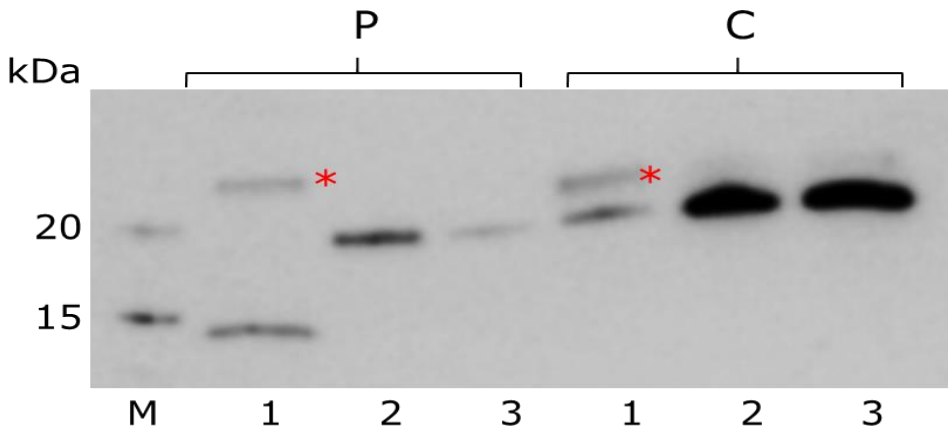


Figure 5.6 Comparison between different LB media

Western blot showing protein bands in Lane 1 at molecular weight size of about 13 kilo Dalton (kDa) in both soluble lysates, periplasmic extracts (**P**) and cytoplasmic extract (**C**), with the presence of putative dimers, red asterisk (*) at about 26 kDa. Bands appeared in molecular weight 20 kDa, lanes 2 and 3 in P and C, are the bacterial endogenous biotin carboxyl carrier protein (BCCPL). 1. LB_{AT}, 2. LB_{ATG}, 3. LB_{ATGC} media, M= Molecular weight marker. Numbers (15 and 20) indicate the marker molecular size in kDa.

Next, to study the effect of the inducer on protein expression, a wide range of IPTG concentrations were applied (Figure 5.7). This did not result in marked differences in the soluble cellular lysates containing recombinant BabA-Crown. The final IPTG concentration of 100 µM was considered the most favourable as it showed the highest level of expression with the lowest bacterial endogenous biotin carboxyl carrier protein (BCCPL) expression.

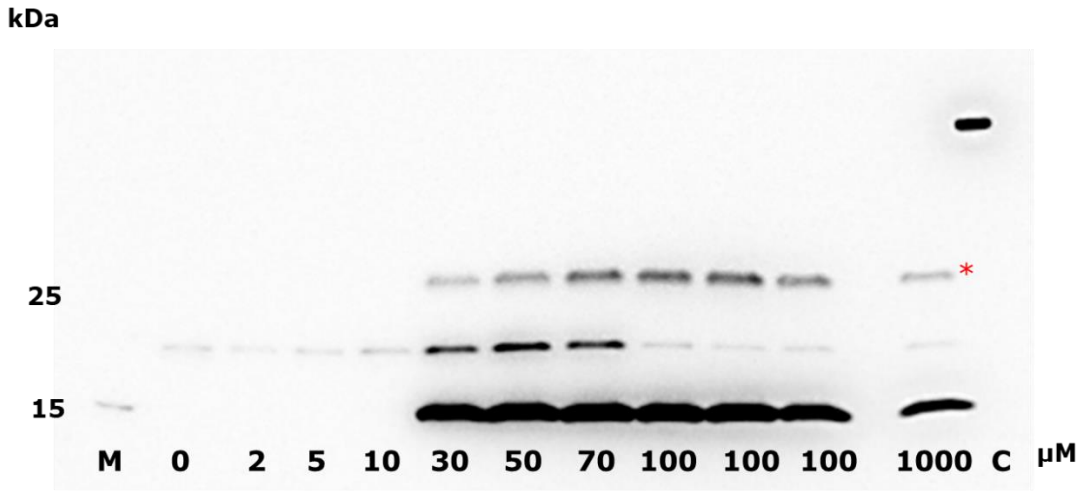


Figure 5.7 Effect of different IPTG concentrations

Western blot showing protein bands after induction. Different IPTG concentrations were used (2 - 1000 µM) for induction. Dimers at about 26 kDa (red asterisk) were seen in periplasmic extracts induced by IPTG from 30 -1000 µM. Bands corresponding to the molecular weight 20 kDa are the bacterial endogenous biotin carboxyl carrier protein (BCCPL). **M**= Molecular weight marker, **C**= control for Western blotting. Numbers indicate the IPTG concentrations (µM).

Interestingly, after expressing both BabA-Crown protein having AviTag sequence and the one without AviTag, in parallel and under identical conditions, we observed that, after loading same amount of protein (10 µL) onto the gel, protein with AviTag sequence appeared more concentrated than the one without (Figures 5.8). This was also noticed after purification during immunodetection method using anti-c-myc antibody (Figure 5.9). The bands in both lower and higher imidazole concentrations were more pronounced compared to the protein not having the AviTag sequence as well as the putative tetramer in ~50 kDa.

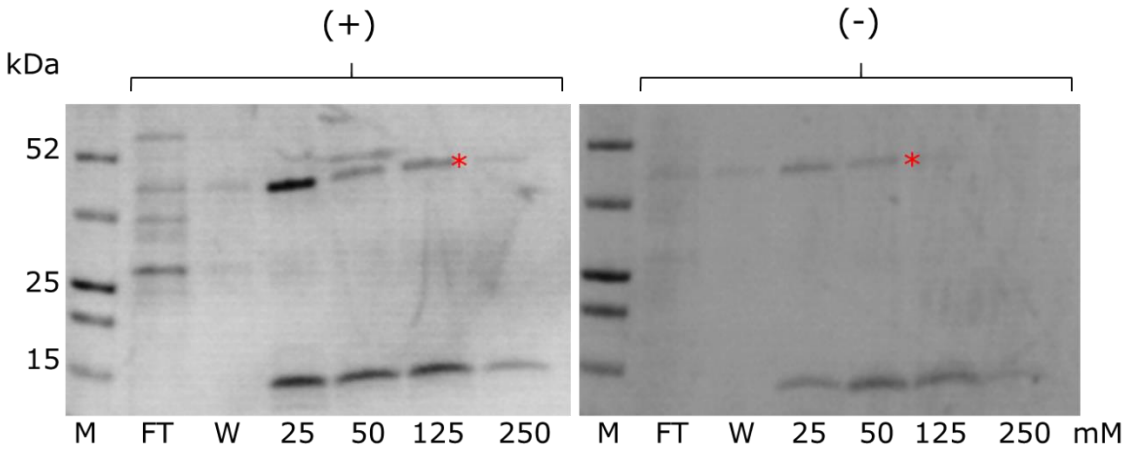


Figure 5.8 Comparison between the presence and absence of AviTag sequence after purification

Coomassie staining showing protein bands at molecular weight corresponding to about 13 kDa after purification in protein extracts with or without AviTag sequence. Protein was eluted with imidazole at concentration ranging from 25 - 250 mM. Tetramers at about 50 kDa (red asterisk) have been seen in all of the elutions **M**= Molecular weight marker, **FM** = protein flow through, **W** = wash before elution. Numbers are the molar concentrations of the imidazole used. **mM**= mille molar.

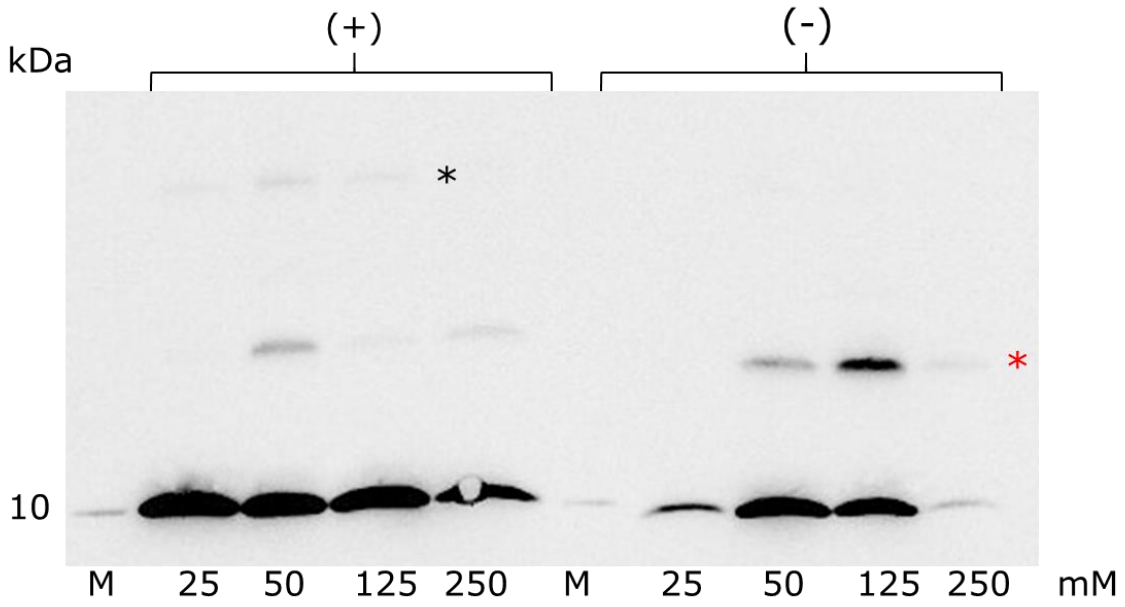


Figure 5.9 Western blotting comparing purified BabA-Crown protein in with or without an AviTag

Bands at ~13 kDa represent purified BabA-Crown protein, with (**+**) or without (-) AviTag sequence. Protein was eluted with an imidazole gradient ranging from 25 - 250 mM. Tetramers with a molecular weight size of about 50 kDa have been marked in **black** asterisk, while the putative dimers are labelled with red asterisk. **M**= Molecular weight marker. Numbers are the molar concentrations of the imidazole used in purification. **mM**= millimolar.

5.3.2 DNAJ domain

DnaJ is a member of the heat-shock protein 40 (Hsp40) molecular chaperone family. It binds to Hsp70 and stimulates ATPase activity (Walsh *et al.,* 2004). This region of the DnaJ superfamily appeared upon delta-blasting (using NCBI website) of BabA-Crown and Head residues (Figure 5.10).

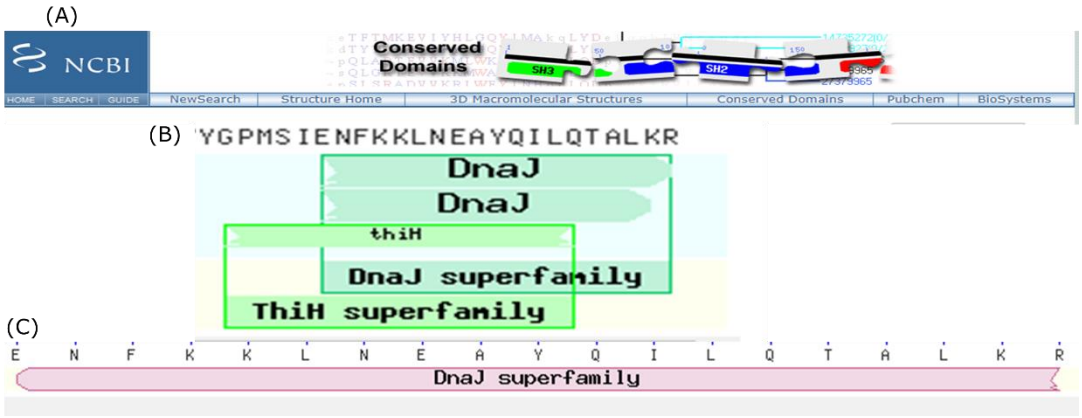


Figure 5.10 Screenshots of DnaJ sequence from National Center for Biotechnology Information (NCBI) website.

A. DELTA-BLAST (NCBI website).
B. Blasting part of BabA amino acid sequence showing the presence of a DnaJ domain (cyan box) in the green box reviewed ThiH superfamily (for thiamine biosynthesis protein).
C. Detail of the DnaJ sequence as appeared in NCBI conserved domain after blasting.

Obtaining these 19 amino acids sequence as part of DnaJ superfamily hinted to a possible role for folding/translocation or acting as a chaperone-like region (Qiu *et al.,* 2006). Even though it is not highly conserved in BabA of all *H. pylori* strains (Figure 5.11), online blasting restricted its existence to only being available within BabA Helicobacter sequence. DnaJ, together with part of the loop before N-terminal of BabA-Crown sequence, form a consensus of a Lysine-Leucine rich repeat sequence (X**KK**XNXAYQI**L**XXA**LK**G**L**PX**L**).

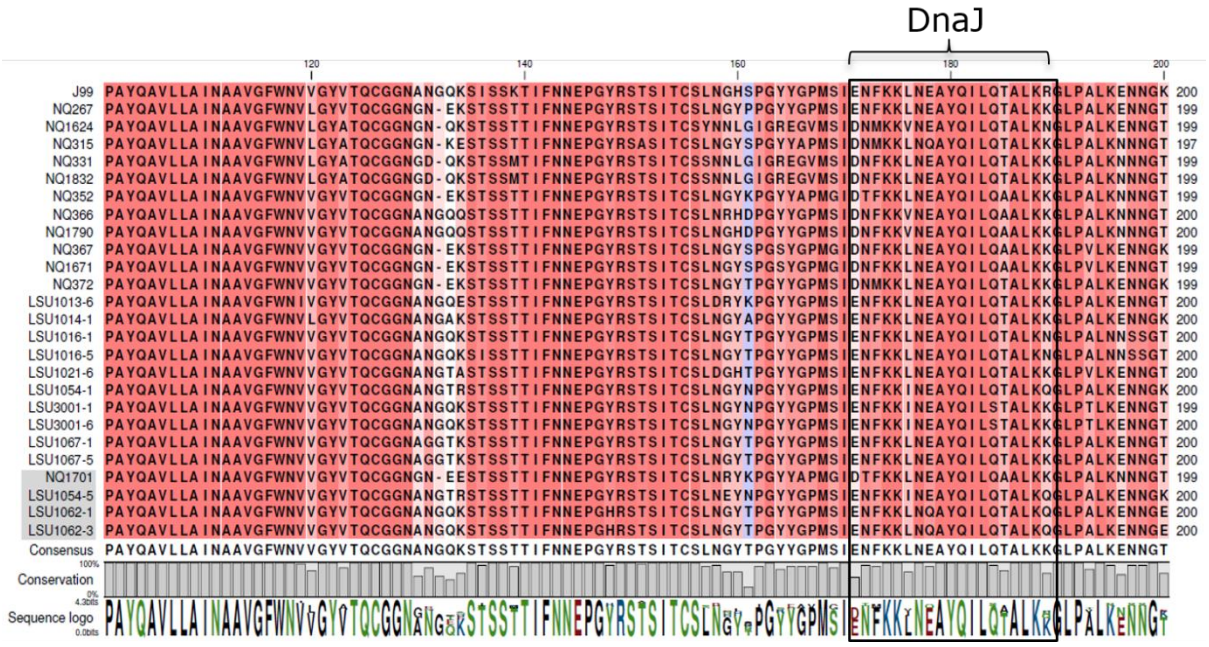


Figure 5.11 Segment of BabA residues showing the DnaJ sequence

Amino acid sequence alignment of BabA from several Helicobacter strains showed the semi-conserved DnaJ sequence, which is highlighted in the black box.

5.3.3 Circular Dichroism Spectroscopy

Circular dichroism spectroscopy was used to examine if the loss of BabA-Crown binding affinity was due to improper folding. Different protein concentrations were assessed in both buffer and water. The crystallography data displays BabA-Crown (Figure 5.1), as mostly β-sheets with few loops (see chapter three for more details). Therefore, it was expected to have a corresponding secondary structure when analysing by CD spectrum.

BabA-Crown did not show the expected secondary structure, neither in buffer nor in water. Although in water at 0.51 mg/ml (Figure 5.12) and 0.16 mg/ml (Figure 5.13), the conformation suggested the existence of a few of β-sheets, most of the secondary structure was random folding with some α-helical structure.

On the other side, the CD spectra of Cr-DnaJ-Cr revealed its secondary structure as mostly β-sheet (Figure 5.14). This result is in accordance with expected original nature of the Crown domain as mostly β-sheets with two loops.

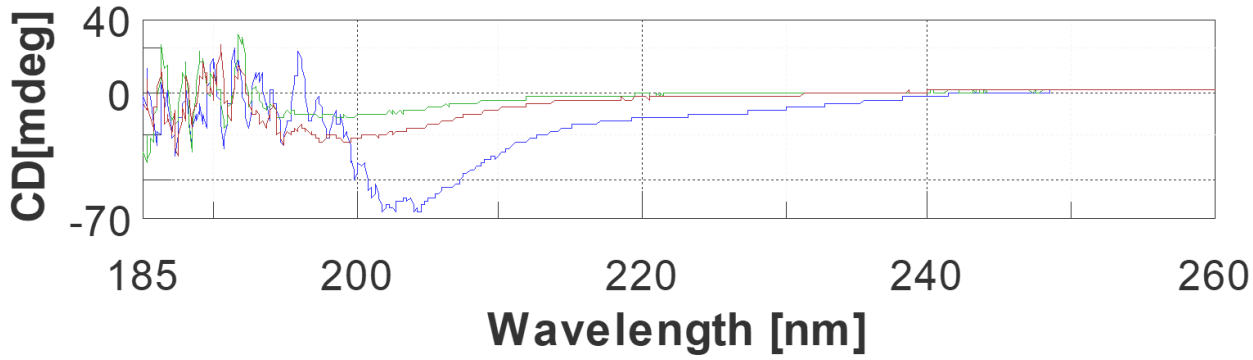


Figure 5.12 Secondary structure, thermal stability and absorbance of BabA-Crown

BabA-Crown protein was tested in water at concentrations of 0.51 (blue) which demonstrates a positive band in about 195 nm, which suggested to be α-Helices and a negative band between 202 and 207 nm, 0.16 which could be β-sheets and (red), 0.08 (green) mg/ml, both show high fluctuated bands, which suggested to be random coil.

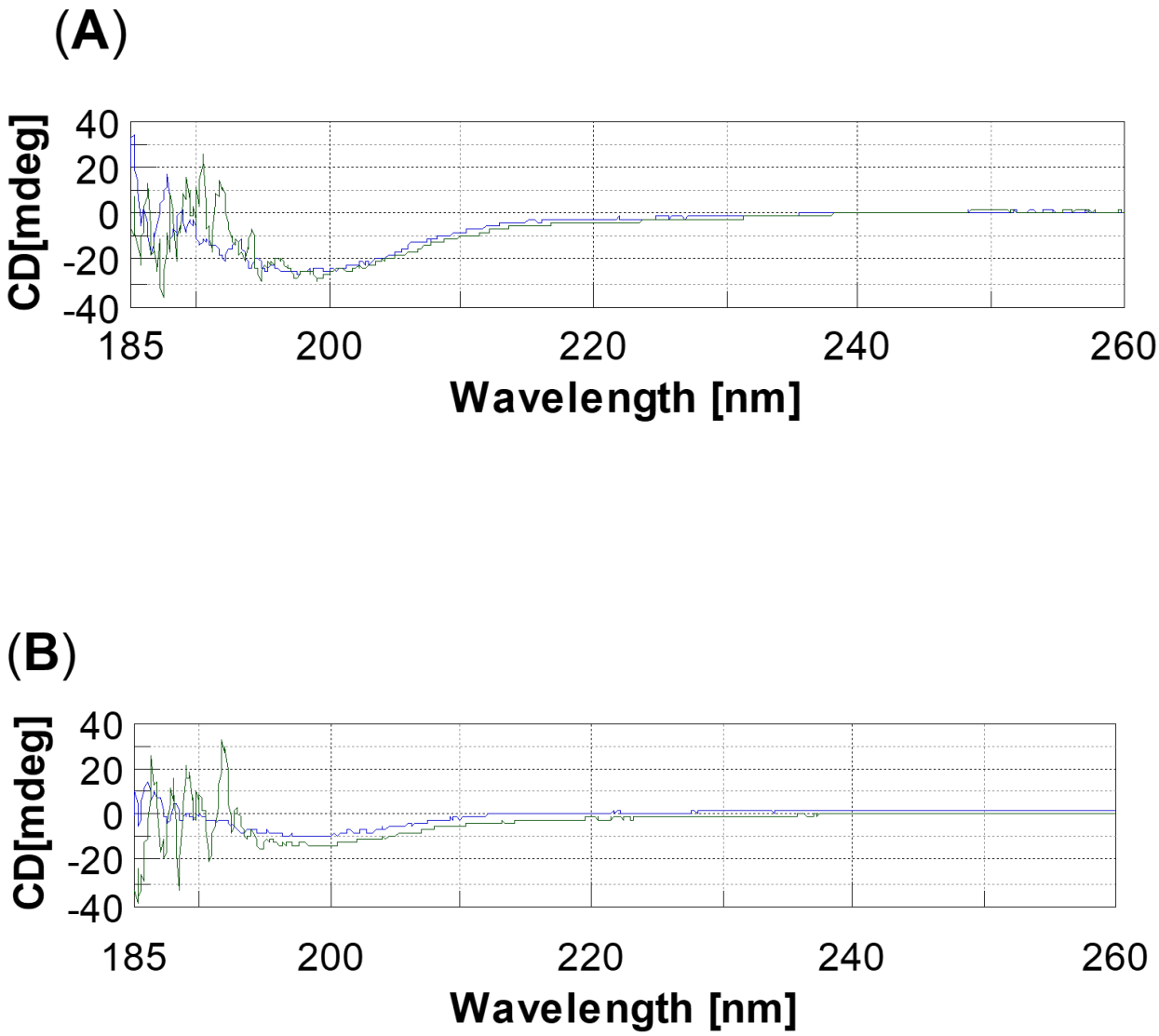


Figure 5.13: Secondary structure and absorbance of BabA-Crown

(A) Overlay of far-UV circular dichroism spectra in the buffer at 0.16mg/ml (blue) and in water (green). This spectrum shows band between 190 and 210 nm which suggests random coil.

(B) BabA-Crown at a concentration of 0.08 mg/ml in water (blue) and in the buffer (green). The spectrum illustrated weak band between 190 and 210 nm which indicates random coil.

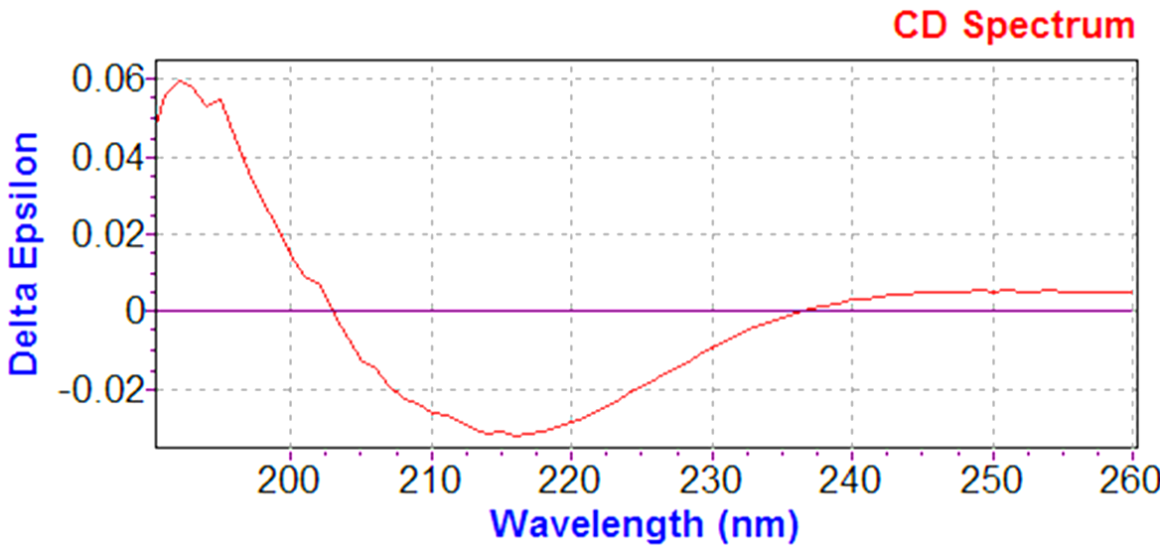


Figure 5.14 Secondary structure and absorbance of Cr-DnaJ-Cr

Spectrum of Cr-DnaJ-Cr protein showing a mostly β-pleats from three independent readings. The CD spectra displays a negative band between 210 and 220 nm, which is typically β-sheets.

5.3.4 Expression of BabA-variants

Analysis of BabA-Crown-Head-Partial-Length ($BabA_{CHPL}$) protein in the cellular extracts, using Coomassie staining (Figure 5.15) and the confirmation through c-Myc immunodetection, showed successful expression in the periplasmic extract after IPTG-induction overnight at 24°C (Figure 5.16).

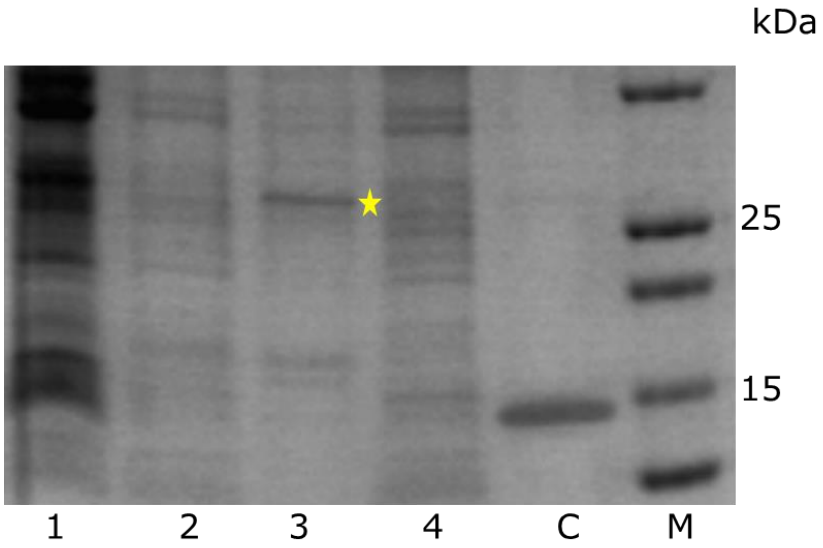


Figure 5.15 Expression of recombinant $BabA_{CHPL}$ protein in *E. coli* XL10-Gold

Coomassie staining showing protein bands with an apparent molecular weight of ~ 26 kDa (yellow star) in the periplasmic space extract, lane 3, which could be the target protein.

1 = protein extract before IPTG induction, **2 =** periplasmic extract in spheroplast buffer, **3** = periplasmic extract in $MgSO_4$ buffer, **4** = cytoplasmic extract, **C** = purified BabA-Crown extracted from *E. coli* XL10-Gold periplasmic extract was used as a positive control. **M** = Molecular weight marker.

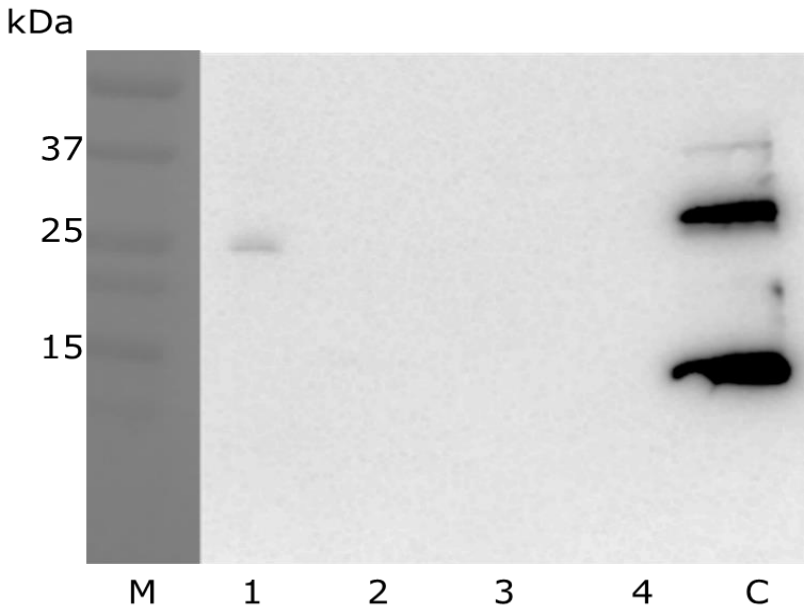


Figure 5.16 Immunodetection of recombinant BabA-CHPL protein in *E. coli* XL10-Gold

Western Blot showing protein weak band at molecular weight size of about 26 kDa in the periplasmic space extract, lane 1.

1 and **2** = periplasmic extracts using $MgSO_4$ and spheroplast buffers, respectively. **3** = cytoplasmic extract, **4** = protein extract before IPTG induction, **C** = purified BabA-Crown extracted from *E. coli* XL10-Gold periplasmic extract was used as a positive control, **M**= Molecular weight marker.

After immobilized metal ion affinity chromatography (IMAC), $BabA_{CHPL}$ protein showed two bands corresponding to 26 and 16 kDa (Figure 5.17). The second (lower) band may be due to intra-molecular disulphide bond formation between two Cysteines.

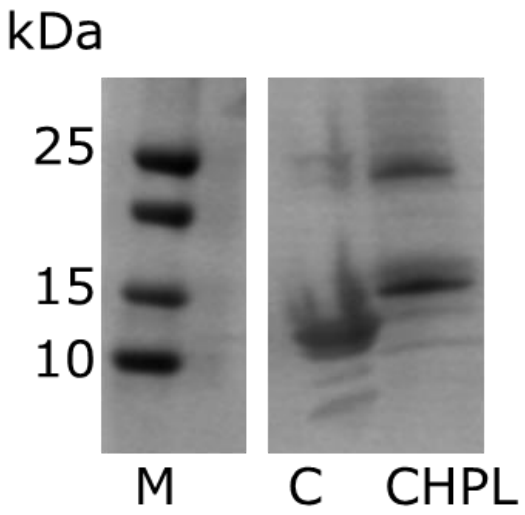


Figure 5.17 IMAC of recombinant $BabA_{CHPL}$ protein

Coomassie staining revealed $BabA_{CHPL}$ protein bands at molecular weight size of about 16 kDa and 26 kDa in the periplasmic space extract. **C**= BabA-Crown was used as a positive control, **M**= Molecular weight marker.

However, BabA-Head-Crown-Handle-Free ($BabA_{HCHF}$) was not detected in any of the extracts (Figure 5.18). This lack of expression was reproducible using different expression methods such as induction at variable temperatures including 37°C and harvest 2 hours later.

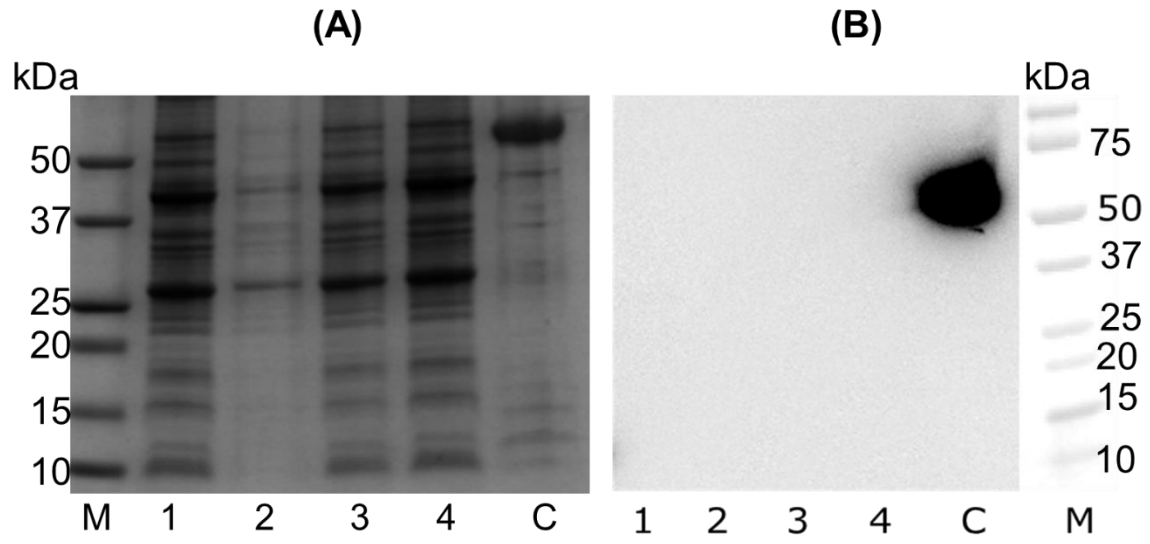


Figure 5.18 Analysis of recombinant $BabA_{HCHF}$ protein

(A) Coomassie staining and (B) Western Blot showing no expression of $BabA_{HCHF}$ protein. 1= protein extract before induction, 2 periplasmic extract in spheroplast buffer, 3= periplasmic extract in $MgSO_4$ buffer, 4= cytoplasmic extract, **C**= purified BabA protein extracted from *E. coli* XL10-Gold periplasm was used as a positive control for Western blotting, **M**= Molecular weight marker.

After overnight IPTG-induction at 24°C, Cr-DnaJ-Cr protein was successfully expressed in the periplasmic space of *E. coli* bacteria. c-Myc immunodetection of this duplicated version of the Crown showed high expression in both the soluble and insoluble cytoplasmic extracts (Figure 5.19).

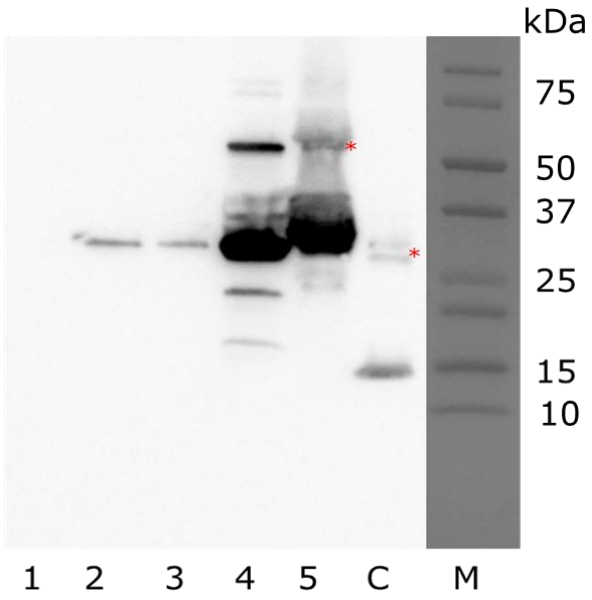


Figure 5.19 Expression of recombinant Cr-DnaJ-Cr protein

Western Blot showing Cr-DnaJ-Cr protein after c-Myc immunodetection. The protein is present in the periplasmic and cytoplasmic extracts, but mostly in the cytoplasmic.
1= protein extract before induction, **2** and **3**= periplasmic extracts in spheroplast and MSO_4 buffers, respectively, **4** and **5**= cytoplasmic soluble and insoluble extracts, respectively. The red asterisk (*) = represents a putative dimer, **C**= purified BabA-Crown protein extracted from *E. coli* XL10-Gold periplasm was used as a positive control for Western blotting, **M**= Molecular weight marker.

5.3.5 Testing the capabilities of BabA truncates for the drug delivery moiety

Assessment of Cr-DnaJ-Cr protein resistance to peptic digestion was carried out in a time-course experiment at pH 4.5 Afterwards, the samples were analysed through SDS-PAGE and Coomassie staining.

Crown-DnaJ-Crown was able to withstand the peptic hydrolysis for about 2 minutes (Figure 5.20). Even though after initial rapid cleavage of this duplicated version of BabA-Crown, the cleavage products resisted further pepsin digestion for at least 45 minutes, as two fragments corresponding to BabA-Crown protein molecular size were visualised in Coomassie staining. This result reproduced what was obtained in a similar experiment, under identical conditions, performed to test BabA-Crown protein resistance to peptic digestion (Figure 4.10).

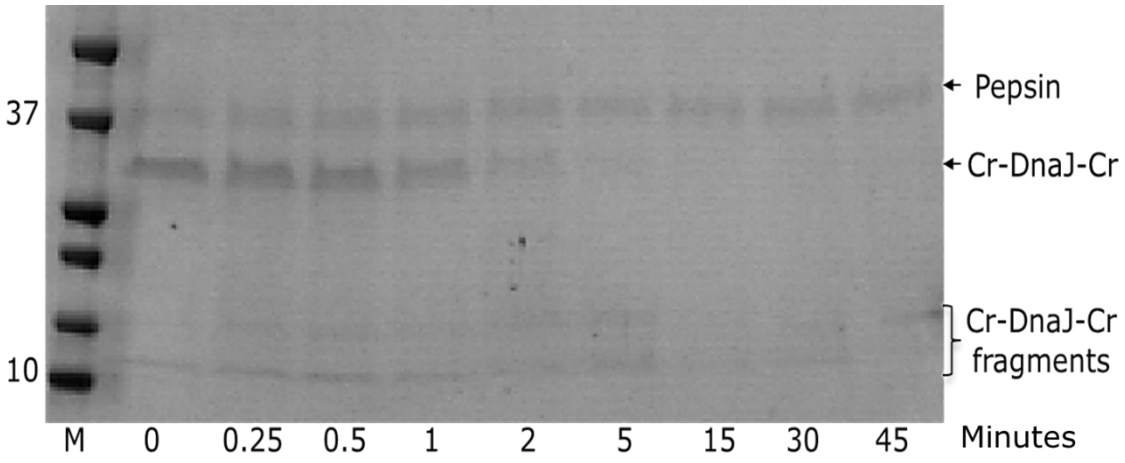


Figure 5.20 Coomassie staining for Crown-DnaJ-Crown after pepsin digestion at pH 4.5

A time-course (0 – 45 minutes) of Cr-DnaJ-Cr peptic digestion at pH 4.5 analysed by SDS-PAGE and Coomassie stain. Pepsin cleaves Cr-DnaJ-Cr into fragments. **M**= Molecular weight marker.

As described in Section 1.3, BabA mediates the attachment of *H. pylori* to fucosylated Histo-blood group antigens. To further characterize the binding specificity, molecular interactions were applied between $BabA_{CHPL}$ and Cr-DnaJ-Cr proteins, with the other BabA-Crown proteins and several glycoconjugates e.g. Le^a, Le^b and Le^y. These neoglycoconjugates were immobilised in a Maxisorp plate and c-Myc tag immunodetection was carried out (Figure 5.20).

As shown in Figure 5.21A, $BabA_{527K}$ (wildtype) bound specifically to Le^b, while some of the proteins such as BabA-Crown and Cr-DnaJ-Cr proteins show non-specific binding. This occurred upon changing the primary antibody to non-biotinylated c-Myc monoclonal antibody and the detecting secondary antibody to anti-mouse IgG (whole molecule peroxidase conjugate) antibody instead of streptavidin-HRP. Additionally, a reduction of $BabA_{527K}$ (wildtype) binding ability to almost half of the strength was observed (see Figure 3.15). Unexpectedly, BabA-$Crown_{_D233A/S244A}$ mutant type showed binding ability to the glycoconjugates at pH 6 (Figure 5.21B). This could be attributed to either specific binding or non-specific binding.

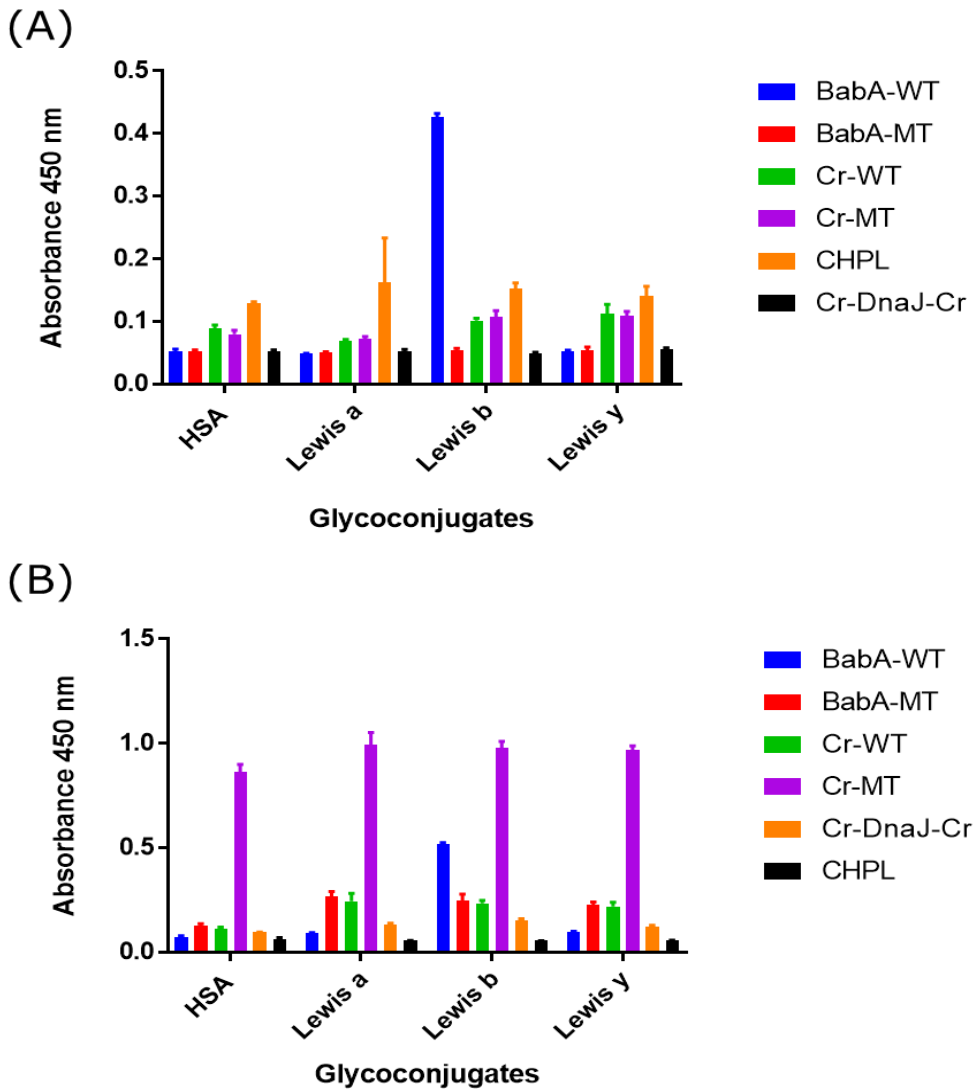


Figure 5.21 ELISA binding assays for BabA and BabA truncates proteins

BabA variants proteins binding to immobilised HSA, HSA glycoconjugates (Le^a, Le^b and Le^y) were assessed by sandwich ELISA. (A) $BabA_{527K}$ (wildtype) as a positive control binds to Le^b, while BabA-Crown did not show the same affinity. Even though BabA-Crown (wildtype and mutant) proteins show together with $BabA_{CHPL}$ show non-specific binding to HSA-Le^b and HSA-Le^y. The latter protein also shows nonspecific affinity to HSA and Le^a. (B) binding assessment was performed at pH 6. Still no binding affinity for BabA-Crown was observed. However, the interactions with the glycoconjugates were similar to BabA mutant type. While BabA-Crown (BabA-$Crown_{D233A/S244A}$) mutant variant displays attachment to all of the glycoconjugates, no binding was observed using Cr-DnaJ-Cr and $BabA_{CHPL}$ (n=3, error bars represent the standard error of the mean, $P < 0.001$) using 2way ANOVA for multiple comparisons followed by Tukey post-hoc test.

5.4 Discussion

The main objective of this chapter was to develop substitution methods to solve the issue of BabA-Crown's lack of ligand binding. To solve this dilemma, special consideration was given to adjusting the length of the interacting binding domain and optimising the conditions used for protein expression, in particular, the composition of the growth medium used.

E. coli is the most commonly used bacterium for obtaining high amounts of recombinant protein in a fast and inexpensive way (Murray *et al.,* 2012). Many factors influence this goal, including growth/induction temperature, type of inducer, concentration, the time point of induction, as well as the duration of induction (Fernández-Castané *et al.,* 2012, Larentis *et al.,* 2014, Shirano and Shibata, 1990). Therefore, the possibility of protein expression in a low or chloramphenicol-free medium was investigated. Accordingly, three different culture media were prepared. LB_{AT} medium, which have neither glucose nor chloramphenicol, LB_{ATG} medium, which only contains glucose and LB_{ATGC} medium, which was supplement with chloramphenicol 34 µg/mL. LB_{ATGC} medium contains 5 times lower chloramphenicol concentration compared to the one initially used for improved BabA-Crown protein expression (Section 3.3.2.2). This alternative growth medium resulted in a non-detectable protein, which in turn, support the need of high amount of chloramphenicol for plasmid (pOPE101) multiplication and BabA-Crown protein synthesis. Though, the effect and the concentration of chloramphenicol varied depending on plasmid and host bacteria. Even though it was reported that chloramphenicol at concentrations from 10 - 300 µg/mL were used to increase colicinogenic factor E_1 multiplication and protein expression, low final concentrations of chloramphenicol (about 15 µg/mL) demonstrated to have the same effect as concentration up to 300 µg/mL depending on the plasmid type and host used (Frenkel and Bremer, 1986, Bentley *et al.,* 1990). It was also verified that under normal growth condition, each cell harbours about 24 copies of *ColE*1 plasmid (Hershfield *et al.,* 1974, Clewell, 1972).

The inhibitory effect of chloramphenicol on the cellular metabolism is reversible but concentration-dependent. At high chloramphenicol concentrations (>100 µg/mL), plasmid propagation was minimal due to severe chloramphenicol

inhibitory/blocking effect on peptidyl transferase binding ability to bacterial 50S ribosomal subunit. This inhibit peptide bond formation and consequently lead to very low protein synthesis (Dinos *et al.,* 2016), but at low chloramphenicol concentration (<100 µg/mL), increment in plasmid propagation was not very high in relA mutant strains such as XL10-Gold (Frenkel and Bremer, 1986). However, in this study, BabA-Crown protein expression in LB_{ATGC} (34 µg/mL) medium was not achieved. This could be, beside low plasmid copy number, due to either catabolite repression or metabolic burden.

Catabolite repression occurs, in general, when glucose is present in the growth medium, it represses the transcriptional machinery of *Lac* promotor, by decreasing the level of intracellular cAMP (Donovan *et al.,* 1996, Li and Young, 2014). While the expression system depends on *Lac* operon for transcription, which is regulated by catabolite activator protein, catabolite repression could be triggered as a result of inducer exclusion (Deutscher, 2008). It is proposed that binding of catabolite activator protein to the promotor increase the affinity for RNA polymerase, which in turn, enhanced by increased levels of cyclic adenosine monophosphate (cAMP) level. Protein expression under *Lac* promotor control was affected by the level of glucose. Whereas, catabolite gene activator protein serves to maintain certain level of carbon (Bruckner and Titgemeyer, 2002). Thus, the presence of glucose in the medium could repress the transcription and cause catabolite repression because of the low level of cAMP (Donovan *et al.,* 1996), which consequently affecting plasmid amplification and protein expression (Teich *et al.,* 1998). Even though, glucose downregulates protein expression which is guided by *Lac* operon, using 0.1% glucose is used to give optimal results and glucose-free media is the common practice (Kirsch *et al.,* 2005).

The metabolic burden is used to describe a change in the host metabolism due to the introduction of foreign DNA into a host, which may impair the host normal metabolic process (Wu *et al.,* 2016). The occurrence of the metabolic load may lead to plasmid instability, i.e. loss of a part of the plasmid DNA or gene of interest deletion (Glick, 1995). This is true with the high plasmid copy number, however, using a higher concentration of chloramphenicol which reversely, increases plasmid-encoded protein synthesis (Bentley *et al.,* 1990), gives the plasmids the opportunity to be maintained while the cell slowly divided. As a consequence, expression of the recombinant protein exploits the cell's resources (e.g. ATP, rRNA

or amino acids) which reduces the quantity of the recombinant protein produced (Wu *et al.,* 2016). To avoid this unwanted stress, LB_{AT} as a glucose-free medium was used, this outcome in obtaining soluble protein lysates from both bacterial periplasm and cytoplasm.

One of the best strategies for achieving higher protein-yield by inducing at high cell density, mid-logarithmic phase. This is followed by decreasing the growth temperature to slow down the growth rate, lessen proteolytic enzyme activation and support protein folding as well as prolong the induction period (Krause *et al.,* 2010, Larentis *et al.,* 2014, Fernández-Castané *et al.,* 2012). In this study, different IPTG concentrations (2 µM - 1 mM) used for BabA-Crown protein showed no alteration in protein expression. The results obtained are in parallel with the minimal concentration (25 µM) sufficient for gene expression (Dvorak *et al.,* 2015) and the maximum activity achieved at IPTG concentration above 40 µM (Fernández-Castané *et al.,* 2012). Even though, it is difficult to compare density between different strains, plasmids or expression systems. However, due to the expression of the bacterial endogenous biotin carboxyl carrier protein (BCCPL), a higher amount of IPTG was used to allow the target protein to be predominant over the bacterial protein.

After optimizing the growth conditions, the expression of BabA variants was investigated. Both $BabA_{CHPL}$ and Cr-DnaJ-Cr proteins were both successfully exported into the bacterial periplasmic space, while Cr-DnaJ-Cr was extracted from both periplasm and the cytosol in an insoluble form. These proteins contain the N-terminal pelB signal sequence which directs the protein into the periplasmic space where two actions occur. Firstly, cleavage of pelB signal by signal peptidase, secondly, the oxidative condition provides a favourable milieu for the oxidase DsbA and isomerase DsbC to catalyse disulphide bond formation (Ruiz *et al.,* 2010). Presence of insoluble Cr-DnaJ-Cr protein in the cytoplasm was unexpected. This can be a result of an imbalance between translocation efficiency and secretion levels (Le Calvez *et al.,* 1996). Protein transportation from the cytoplasm needs a specific transport signal for recognition of the corresponding inner membrane translocon, defined structure or folding for both entry/ crossing and energy for effective transport/refolding, if needed. Insoluble Cr-DnaJ-Cr protein can also result from overcrowding of the newly synthesised recombinant polypeptides in the reducing environment, the cytoplasm, forming inclusion bodies (Baneyx and

Mujacic, 2004) coupled with the incompetency of pelB leader in transporting the protein into the periplasmic space.

The absence of the first 16 N-terminal residues in BabA was reported to affect the assembly and proper folding (Coppens *et al.,* 2018). If synthesis of the transport signal was completed and modified before translocation, it would lead to protein aggregation in the cytoplasm and inclusion body formation (Chatzi *et al.,* 2013, Holland, 2004).

Inclusion bodies are insoluble aggregates resulting from a cellular stress reaction to many factors, such as high IPTG concentration, a shift in pH or temperature (Slouka *et al.,* 2018). Inclusion bodies need complicated processes for denaturation and refolding to get biologically active protein (Singh *et al.,* 2015). However, recent studies pointed out that protein obtained from inclusion bodies still preserve its biological activity (de Groot and Ventura, 2006), if a short hydrophobic self-assembling peptide GFIL8 (GFILGFIL) was inserted into the carboxylic terminal of the target protein (Wang *et al.,* 2015), or if formed in the absence of chaperone DnaK (Gonzalez-Montalban *et al.,* 2008).

Chaperones provide an excellent auxiliary for protein refolding and transportation to its destination. After blasting difference sequences of BabA, a part of DnaJ domain was noticed in BabA, then it was anticipated to play a part in folding or multimerisation. Therefore, this part together with two Crown domains was constructed to make a divalent version of BabA.

Cheetham and Caplan (1998) divided DnaJ family based on the primary amino acid sequence into three types.

Type I (same like *E. coli* DnaJ) has four recognised domains:

1. J domain consists of 70 amino acid forming α-helical domain at the N-terminus
2. Gly/Phe rich region.
3. Cys rich domain (CXXCXGXG), and
4. Diverse C-terminus sequence.

Type II has a longer Gly/Phe sequence replacing the Cys rich domain.

Type III contains only the J domain.

DnaJ protein is responsible for binding substrate polypeptides and its J domain interacts with Hsp70/DnaK to enhance the ATPase activity and location of the polypeptides to Hsp70 chaperone (Cheetham and Caplan, 1998). J-domains are involved in protein biogenesis and delivery of newly synthesised proteins to be allocated into the membrane (Opaliński *et al.,* 2018).

Although, molecular chaperones assist in stabilizing or helping the nascent protein to reach the functionally active form, they are not present in the final protein produced (Hartl *et al.,* 2011). Moreover, a short stretch of amino acids (18 amino acids instead of 70 present in the J domain) originally present in BabA was incorporated. Thus, in this study, using the term "DnaJ'' in BabA variant might be misleading. However, each one of BabA-Crown sequence contains two cysteines which have a remote similarity with DnaJ central region. Overall, this stretch of amino acids is conserved in BabA species, so its presence may place BabA as a member of the DnaJ-like family. This stretch may also represent one additional folding step in the post-translation (Sarvas *et al.,* 2004).

From the data obtained from the circular dichroism, it was thought that DnaJ region may help the two Crown domains to form the expected β-pleated sheets. DnaJ region may also act as an auxiliary chaperone for BabA-Crown and/or may stabilise BabA trimer structure. In contrast with what was predicted by Bugaytsova *et al.,* (2017), it was expected that, rather than "Velcro domain", the helical structure of DnaJ together with the interacting Hydrogen bonds in the Head domain may gave a hinge-like structure and assist in determining the Crown binding status. This because BabA from J99 does not contain the salt bridge, as present in BabA from 17875, in order to form the "clamp-structure" between D198 and R207 in the "key-coil" (Bugaytsova *et al.,* 2017). Thus, Cr-DnaJ-Cr may surrogate the salt-bridge, while the helical hydrogen bonds serve to stabilise the structure and orientation of the amino acid chain in the acidic environment.

Interestingly, an AviTag sequence which was introduced to allow site-specific protein biotinylation, may participate in increasing protein expression. Ashraf's group reported two scenarios to explain this increment. Firstly, the increase in protein yield could, probably, have happened after extraction, i.e. during IMAC immobilisation phase, due to the biotin high binding affinity to the AviTag sequence during purification. Secondly, increment of protein expression occur

during protein expression and translocation (Ashraf *et al.,* 2004). As in this study, the metal ion Nickel was used in protein purification, the former scenario was excluded (Wang *et al.,* 2005). It was reported that a plasmid construct bearing AviTag sequence also activated gene expression and increase protein yield (Athavankar and Peterson, 2003). Overall, this interesting finding needs more investigation and was set as an objective in our future research studies.

Two BabA-variants were not successfully expressed, $BabA_{HCHF}$ and $BabA_{Fxa}$. As they were not detected in the cellular extracts, three assumptions were proposed to know the reason, i.e. not expressed, degraded or excreted into the medium. The latter assumption was investigated, and no protein was detected using Coomassie stain. Even though Coomassie staining is very efficient in protein visualisation, detected down to 50 ng, after separation by SDS-PAGE (Kahn and Rubin, 1975). Silver staining is more sensitive (100 times) in detecting proteins (Switzer *et al.,* 1979). However, in respect to this, visualising tiny amount of protein is not useful for the downstream experiments as used large scale (1 litre) was used for protein expression.

The degradation option is more likely to be occur in any part of the protein. Hage *et al.,* (2015b) reported that degradation of recombinant BabA protein could potentially be at both N-terminal and the C-terminal. To solve this issue hexa-lysine tag at the C-terminus was introduced and successfully result in protein expression. Therefore, it may act as a proteolytic defensive mechanism and enhance protein solubility (Hage *et al.,* 2015b). Hexa-lysine-tag provides an unexplained protective mechanism to the C-terminus, but still there is a loss in the first nine amino acids at the N-terminal, by a mechanism which remains unanswered in BabA (Hage *et al.,* 2015b, Subedi *et al.,* 2014) and in LabA as well (Paraskevopoulou *et al.,* 2019). However, $BabA_{HCHF}$ and $BabA_{Fxa}$ contain the C-terminal hexa-lysine tag. With this view, it was suggested that there are residues within $BabA_{527K}$ prone to periplasmic cleavage.

Secretion in Gram-negative bacteria follows Type V secretion system (van Ulsen *et al.,* 2014). Proteins are exported from the cytoplasm to the periplasm via secretory (Sec) pathway, which represents a ubiquitous and viable system in all living cells (Papanikou *et al.,* 2007), protein folded into the outer membrane through the heteropentameric β-barrel assembly machine (BamB) complex

(Mahoney *et al.,* 2016). Thus, the periplasm provides an environment for structural assembly of β-barrel proteins (Miller and Salama, 2018) such as BabA, which as a member of autotransporters, does not require an energy for translocation (Henderson *et al.,* 2004).

The bacterial periplasm contains about 20 periplasmic serine endoprotease (Merdanovic *et al.,* 2011), some of them, e.g. the dual activity chaperone-protease (DegP), are responsible for misfolded recombinant protein degradation, others serine protease, e.g. tail-specific protease (Tsp), for unfolded polypeptides with nonpolar C-termini (Silber *et al.,* 1992). This endopeptidase preferentially cleaves 2 alanine residues at the C-terminal positions (Lykkemark *et al.,* 2014), while other protease such as, High temperature requirement A (HtrA), degrades reduced unfolded protein containing two or three disulfide bonds (Kim *et al.,* 1999) and directly enhance the functionality of cell adhesion protein(Wessler *et al.,* 2017). It was envisaged that some of these proteolytic enzymes could be acting on BabA variants but this prediction is a subject for further verification. Alternatively, one of these proteases may act as transpeptidase in the presence of a nucleophilic probe such as Coenzyme A (Eom and Kim, 2018) and changed BabA primary amino acid sequence, which in turn leads to its degradation.

Furthermore, assembly of outer membrane proteins relies mainly on periplasmic folding factors, importantly, SurA, Skp and DegP (Soltes *et al.,* 2017). Generally, SurA is the primary chaperone that act on many of the outer membrane proteins and very critical factor for lipopolysaccharides transport machinery (Soltes *et al.,* 2016). Skp binds to the nascent protein in the early stage, while in Sec pathway, to prevent the aggregation (Lyu and Zhao, 2015). DegP as the principle chaperone regulator or gatekeeper defend the cell from protein folding stress (Peterson *et al.,* 2017). Therefore, it is hypothesised that there is a need for at least a part of the β-barrel present in the C-terminal of the Handle domain in BabA to facilitate the correct folding. This hypothesis was supported by the presence of stack domain in BabA from J99 strain (Hage *et al.,* 2015a) and the need of nano-antibody to stabilise the structure in BabA from 17387 strain (Moonens *et al.,* 2016). The presence of part of the J-domain, which may act as a substrate for one of these folding factors in BabA together with the presence of the poly-cationic lysine tag could be an additional reason for obtaining the full length of BabA J99 extracellular part. However, recent study revealed that recombinant form of BabA

J99 with partial length of the putative transmembrane β-domain was partially traversed through the outer membrane without affecting the binding property (Coppens *et al.,* 2018).

Introducing multiple tags into a recombinant DNA gene can enhance the versatility of the produced recombinant protein (Romero Pastrana *et al.,* 2017). Peptide tags are commonly employed as useful tools in molecular applications such as in increasing the protein purification affinity, acting as epitopes for immunodection or in protein visualisation as fluorescent substrates (Zordan *et al.,* 2015). Hexa-histidine tag (His-tag) is one of the widely applied tag in affinity chromatography purification because of their metal binding ability. Recently it was utilised to increase enzyme catalytic properties (Schoonen *et al.,* 2017). The location of the hydrophilic Hexa-histidine tag in one of the protein ends is important. In particular, when the C-terminal of a protein is directed to the periplasm, the Histidine tag may interfere with the protein traverse activity (Dilworth *et al.,* 2018). In other cases, the poly-His tag on the N-terminal may interfere with protein conformation structure or decrease its thermal stability (Booth *et al.,* 2018) and thus affecting its solubility (Zhu *et al.,* 2013). Hexa-Histidine tag position may also influence the arrangement of disulphide bonds without affecting the binding ability (Klose *et al.,* 2004). The existence of Hexa-Histidine tag in BabA did not affect the functionality. Even though, removal of this tag may shed a negative effect on the protein quality (Paraskevopoulou and Falcone, 2018), no experimental trial was made to cleave this tag to know if it interferes with the Crown binding ability.

An increasing consideration is recently given to add fusion tags to proteins in order to enhance protein solubility and to avoid the formation of inclusion bodies (Jong *et al.,* 2017). Recently, solubility enhancing peptide (SEP) tag, which consists of triplet of Arginine preceded by Glycine (GR3)3 was used for increasing the expression, solubility and yield of Tobacco Etch Virus (TEV) protease activity without affecting its functionality (Nautiyal and Kuroda, 2018). It was reported that tags with positively charged amino acids increase the protein solubility, whereas, very hydrophobic poly-Ile significantly reduced it. However, tag with poly-Aspartic acid- and poly-Glutamic acid can also increase solubility, due to side-chains ionization at pH 7.7 (Islam *et al.,* 2012). Hexa-Lysine tag was used to enhance recombinant BabA protein solubility (Hage *et al.,* 2015b) and recombinant Goat myosin light chain 6, anti-tumour peptide which promotes

cytotoxicity of Natural killer cells (Liu *et al.,* 2018a) without inhibiting the functionality of the target protein. Whilst, tri-lysine tag was utilised for purification of metalloproteins (Wijekoon *et al.,* 2016). An increment of protein solubility was ascribed to the repulsive intermolecular electrostatic forces occurring between the protein and the lysine tag (Jung *et al.,* 2011). However, introducing the lysine tag at the N-terminal may result in protein misfolding or aggregation if not neutralised by anionic functional groups of cationic exchanger (Kim *et al.,* 2012). In this study, the incidence of Hexa-Lysine tag at the C-terminal of BabA truncates had no effect in either elevating the solubility or enhancing protein expression. This result was supported recently using the same expression system for expressing LabA However, hexa-lysine tag increases thermal stability (Paraskevopoulou *et al.,* 2019).

$BabA_{Fxa}$ sequence contains two sites for Factor Xa introduced by site-directed-mutagenesis. Then expression trials were carried out to obtain mature BabA protein before purification and release of the Crown domain by incubation with Factor Xa protease. Unlike the $BabA_{527K}$ protein used for crystal structural study, this variant failed to be expressed. A similar trial was made to study BabA protein after inserting a thrombin protease cleavage site between BabA passenger domain and β-transmembrane domain. The expression of this protein was achieved but consistently co-eluted with the 6-Histidine tag, suggesting a stable folding/intimate connection had occurred (Coppens *et al.,* 2018).

Factor Xa as one of the serine protease family is commonly used for tag removal from fusion proteins. However, the exact location of the Factor Xa recognition sites in the recombinant protein is critical (Arnau *et al.,* 2006). Introduction of two cleavage sites may result in canonical conformation structure which act as a substrate for homologue serine protease in the bacteria (Ruiz-Perez and Nataro, 2014, Tyndall *et al.,* 2005). This postulation was rationalised by the common specificity shared by these class of serine protease enzymes and may led to protein degradation (Perona and Craik, 1995, Hsu *et al.,* 2008). However, to examine this assumption, it is useful to test the expression of $BabA_{Fxa}$ harbouring one single cleavage site and then try once more with the two cleavage sites. This will give more insight about the suitability of Factor Xa sequence introduced for protein expression. Alternatively, it may be better to choose other proteolytic cleavage enzymes such as Recombinant type 14 3C protease from Human

rhinovirus (HRV 3C), which is currently of great interest due to high sequence specificity and activity (Ullah *et al.,* 2016).

Protein secondary structure analysis was improved through the development in circular dichroism computational programmes, interpretational bioinformatics tools and accumulation of modern reference databases from resolved crystal structures (Whitmore and Wallace, 2008). Circular dichroism is good alternative method to study membrane proteins which have not been crystallised and whose structures are not known (Miles and Wallace, 2016). In the current study, it gave a better indication for protein secondary structure, as it suggested that the reason underlying the lack of ligand binding by the Crown was due to inappropriate folding. This could be extended to the other BabA truncates, but this has not been tried experimentally.

Cr-DnaJ-Cr was made to act as a bivalent binding site and still did not show any affinity toward the ligand Le^b, though the secondary structure was attained. Moreover, $BabA_{CHPL}$ protein, which contains the DnaJ as well, showed no affinity for binding the glycan. This unexplainable result needs further investigation in two ways, firstly confirming the secondary structure by another method such as Nuclear magnetic resonance spectroscopy (NMR) which can provide detailed data about the protein at atomic resolution (Sugiki *et al.,* 2017) or the more advanced solid-state nuclear magnetic resonance (SSNMR) spectroscopy which assist in elucidation of the protein structure and provide mechanistic insights (Mandala *et al.,* 2018). Secondly, testing the glycan-binding by another method such as Isothermal titration calorimetry (ITC) which may offer new insights. Otherwise, use of synchrotron radiation circular dichroism spectroscopy (SRCD) may overcome some of the conventional circular dichroism limitations and enable characterisation of protein dynamic and static states, determination of protein stability at lower wavelengths, study of protein complexes formation in a solution and high reduced signal-to-noise levels (Wallace and Janes, 2010). Additionally, SRCD has been recently used in characterising the membrane proteins conformational and ligand binding abilities (Hussain and Siligardi, 2016).

To use BabA as a moiety for gastric drug delivery system, it is useful to understand the adhesion strength of BabA-Le^b interactions in different environmental parameters. *H. pylori* presumably optimized its adhesion and deadhesion

properties, which are described by open/close transitions states, to allow regular migration to and from the cellular surfaces (Formosa-Dague *et al.,* 2018). Bugaytsova *et al.,* (2017) reported that BabA-attachment of *H. pylori* le^b binding strains to human gastric mucosal epithelium and MUC5AC gastric mucin was increased 2-fold at pH 6 compared to lower binding at pH 2. However, BabA undergoes reconstitution into a multimeric form. This finding suggested BabA as a pH sensor, mediating the bacterial detachment when the mucus and epithelial cells being shed into the acidic lumen (Bugaytsova *et al.,* 2017).

In healthy individuals, binding to Le^b receptor on MUC5AC is bacterial strain-dependent, as strain P466 bound to Le^b antigens but not to BLe^b structure (Lindén *et al.,* 2002). It was described that *H. pylori* strains expressing BabA, AlpA/B and SabA bound to MUC5AC and MUC6 at pH 3 and maximum binding at charge-dependent way to mucins containing chondroitin sulphate/dermatan sulphate side chains at pH 4-5, whereas at neutral pH only Le^b-positive strains (17875 and P466) bound to MUC5AC with high affinity and to H-type-1 structure on MUC1, which act may as a decoy mucins for the bacteria (Lindén *et al.,* 2004) and limiting bacterial colonisation (McGuckin *et al.,* 2007). Thus, MUC1 is upregulated in infection to reduce bacterial adhesion and *MUC1* gene polymorphism can increase the susceptibility for developing gastritis or gastric cancer (Quintana-Hayashi *et al.,* 2018). Some bacterial strains use BabA as a negative feedback mechanism to avoid bacterial propagation and subsequent accumulation on the epithelial ends. This suggest mucins antibacterial effect as inhibition and subsequent aggregation may force the bacteria to be in the epithelial apical surfaces, where terminal α1,4-GlcNAc residues act as growth inhibitor, or being washed out during the mucosal turnover (Skoog *et al.,* 2017, Kawakubo *et al.,* 2004).

In a study which used a microtiter plate-base assay to study *H. pylori* binding affinity to pig gastric mucins, it was found that the binding ability was affected by the change in temperature, pH, host and bacterial strain (Nordman *et al.,* 1999). Bacterial attachment to the stomach substantially depends on the anatomic site and gastritis status as *H. pylori* render BabA adhesion property to the inner gastric mucus layer at neutral pH during gastritis (Lindén *et al.,* 2008). However, at acidic conditions (pH 2 and 4), BabA was suggested to have a role in mediating *H. pylori* adherence to mucins, especially, in pediatric ulcerogenic strains (Rocha *et al.,* 2018).

In the current study, lowering the buffer pH did not change the BabA-Crown binding ability, although there was a slight increase in $BabA_{527K}$ (wildtype) binding affinity together with the increase in $BabA_{527K}$ (mutant type) and BabA-Crown. The pH change also did not improve the binding ability of $BabA_{CHPL}$ and Cr-DnaJ-Cr proteins. However, BabA-$Crown_{_D233A/S244A}$ mutant type binding activity for all of the glycoconjugates was increased, but this result need more investigations.

Ultimately, all the modifications attempted for overcoming the non-functionality, suggested that binding is not possible without full-length BabA (whereby full length meant the full extracellular region, without the transmembrane domain). However, comparative studies proved that BabA high binding ability is attained by the existence of a transmembrane domain (Moonens *et al.,* 2016). This domain stabilizes BabA full length and increases the binding avidity. Moreover, it was reported that BabA as monomer has a lower affinity in binding to Le^b ($\sim 2.2 \times 10^{10}$ M^{-1}) (Aspholm-Hurtig *et al.,* 2004). Therefore, in the interest of carrying on to the next step, changing the expression system was not pursued, instead protein binding to nano/microparticle was explored in the next chapter.

5.5 Conclusion

While suitable culture conditions allowing recombinant expression of sufficient amounts of protein for downstream experiments were successfully established, our attempts to define the minimal ligand binding region for the extracellular region of BabA remained unsuccessful. Truncated versions of BabA were either not expressed successfully, or did not show the expected Le^b-specific ligand binding patterns.

CHAPTER SIX

6. Proof-of-principle application: Development of biomimetic BabA–truncates microparticles

6.1 General overview

The potential use of efficient micro/nanoparticle delivery systems critically hinges on the specific binding interaction between the particles' surfaces and molecules. Modification of the particle surface by biological recognition molecules (protein, polypeptide or DNA) is an increasingly accepted practice (Malyala and Singh, 2010). One frequently explored surface modification is the interaction between biotin and (strept)avidin, which has been widely used for decades in biological applications (Liu *et al.,* 2017b).

Avidin, neutravidin and streptavidin are homotetrameric proteins sharing similar molecular weight of ~60 kDa, high affinity to biotin and are not present in mammalian tissues. Avidin, originally isolated from chicken egg white and also isolated as dimer from *Rhizobium etli* bacteria, is glycosylated containing N-acetyl glucosamine and mannose. Chemical deglycosylation of avidin results in neutravidin, while streptavidin is a non-glycosylated protein, secreted by the bacterium *Streptomyces avidinii*. These proteins are characterised by being heat-stable, resistant to denaturing agents and enzymatic hydrolysis action (Lesch *et al.,* 2010, Dundas *et al.,* 2013, Laitinen *et al.,* 2006, Helppolainen *et al.,* 2007, Jain and Cheng, 2017) and with the biotin forms the strongest non-covalent

interaction (K_d 4x10^{-14} to ~10^{-15} M) known in biology (Fogen *et al.,* 2015, Strzelczyk *et al.,* 2016).

Streptavidin has lower non-specific binding than lectins, longer half-life and is more negatively charged. These advantages made it more often used compared to its counterpart, avidin (Luong *et al.,* 2019). Streptavidin-biotin complex systems provide multipurpose applications such as, drug delivery, protein purification, diagnosis and immunoassays (Beloborodov *et al.,* 2018, Verma *et al.,* 2018, Singh and Mitragotri, 2019). Neutravidin was deglycosylated to lower binding non-specificity while preserving the biotin affinity, therefore, commonly used together with the streptavidin and captavidin (nitrated avidin) in biotin-based applications (Nguyen *et al.,* 2012, Buzid *et al.,* 2019).

For efficient site-specific protein functionalisation on different surfaces, labelling with biotin is a useful approach. Biotin (vitamin H) is an essential coenzyme for carboxylase enzymes present in most of the living organisms. Biotin carboxylases are fundamental enzymes in metabolic pathways such as gluconeogenesis and lipid biosynthesis (Chapman-Smith and Cronan, 1999, Jain and Cheng, 2017). Biotinylation is a highly specific post-translational modification, catalysed by biotin protein ligase (BPL). *In vitro* site-specific enzymatic biotinylation can be developed using the *E. coli* enzyme BirA (Sternicki *et al.,* 2017, Beckett, 2018). Then using the irreversible bonding between the biotin in the protein and the strep(avidin), for example on microparticles, for further applications.

This chapter describes development of biomimetic protein-microparticles complexes model. This model takes advantage of the ability to introduce a single biotin group, in a defined position of the protein via BirA-mediated enzymatic ligation and hence achieve system with strong biotin-streptavidin affinity interaction. Biotin-avidin based microparticles are easy to develop and have less effect on protein activity (Jain and Cheng, 2017). (Strept)avidin-coated polymeric particles are commercially available in different sizes and fluorescent chemistries, allowing flexibility with experiments. To the best of our knowledge, this is the first time to use neutravidin-coated particles for biotinylated protein from *H. pylori* and use such model for drug delivery.

The overall aim of this research was to develop biomimetic gastric targeted drug delivery system, answering the question of whether obtaining particles with surface 'corona' formed by the biotinylated BabA-crown can bind its physiological ligand, Lewis b. To achieve this aim, the choice of conjugating the protein to the microparticles and the orientation of the protein on particles' surface are two criteria should be considered. For the first criterion, the high affinity between the avidin and biotin was exploited by introducing Avitag sequence into the protein (chapter 4) and enzymatically conjugated a biotin to this sequence before immobilising on particle's surface. However, for the second criterion, i.e. the functionality of this system and the ability of binding should be empirically assessed.

6.2 Experimental procedures

6.2.1 Protein expression and purification

Protein expression was performed, using *E.coli* XL10-Gold grown in LB_{AT} medium, under the same condition described in Section 3.2.2. Purification was achieved using ÄKTA purification system as described in Section 4.2.2.2.

6.2.2 Protein biotinylation

In vitro enzymatic protein biotinylation was performed using *E. coli* BirA biotin ligase, which specifically adds biotin molecule to the acceptor domain (the 15 amino acid AviTag™ sequence GLNDIFEAQ**K**IEWHE) in the substrate. Specifically, the biotin is added to the lysine residue (bold and underlined above) in the Avi-tagged protein (Figure 6.1). BabA-Crown (Wildtype and mutant), Cr-DnaJ-Cr and $BabA_{CHPL}$ proteins were biotinylated using BirA biotin-protein ligase standard reaction kit (Avidity, USA), according to the manufacturer's protocol. Briefly, about 2 mg/mL (40 µM) was used as a substrate for BirA enzyme (1mg/mL) in the presence of Biomix A (500 mM Bicine, pH 8.3) and Biomix B (100 mM ATP, 100 mM MgOAc and 500 µM D-biotin). The mixture was mixed well before incubation at room temperature for 2 hours. Amicon Ultra-0.5 mL Centrifugal Filters with a molecular weight cut-off of 3 kDa (Merck Millipore, UK) were used for protein concentration. Verification of successful biotinylation of proteins was achieved by Western blotting technique using only streptavidin-HRP for biotin detection.

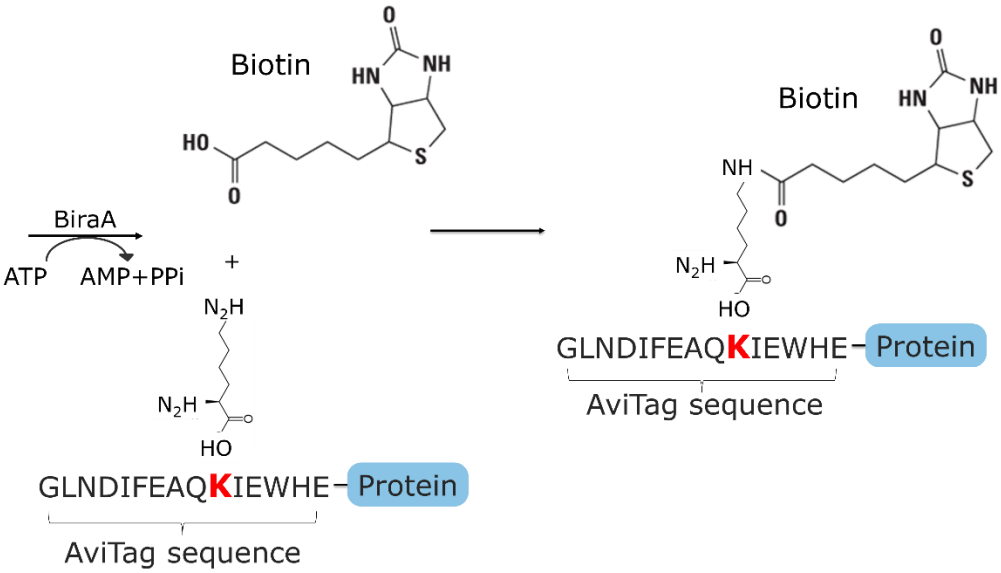


Figure 6.1 Schematic representation of the biotinylation

The lysine residue in the AviTag sequence (red) conjugated through its amine group facilitated by ATP-dependent BirA enzyme to a biotin molecule.

6.2.3 Conjugation of micro-particles to the proteins

Dynamic light scattering (DLS) also known as photon correlation spectroscopy (PCS) or quasi-elastic light scattering, is a 'classical' technique to measure particles hydrodynamic size in suspension, based on light scattering pattern of the sample used (Stetefeld *et al.,* 2016). More technical details can be found in Chapter 2 and on the Malvern website.

Microparticle hydrodynamic diameters and polydispersity indices (PDI) of samples of microparticles conjugated with proteins were measured by DLS using Zetasizer NanoZS instrument (Malvern, UK) at 25°C. Samples were measured in triplicates after dilution to 1% in deionised water (solids concentration of about 20 µg/mL).

6.2.4 Enzyme-linked immunosorbent assay (ELISA)

ELISA was applied as described in section (4.3.4.1) for quantification of the biotinylated protein binding. Detection was achieved using streptavidin-HRP only, at dilution of 1:10000, for biotin detection.

6.3 Results

6.3.1 Assessment of protein biotinylation

BabA-Crown proteins, $BabA_{CHPL}$ and Cr-DnaJ-Cr, were biotinylated using BirA enzyme. Samples were then run on SDS-PAGE and analysed by Coomassie staining and Western blotting. Using Coomassie stain, a shift was noticed in BabA-Crown protein size after biotinylation due to the protein's interaction with the streptavidin (lane 3, Figure 6.2A) compared with the biotinylated ones in the absence of streptavidin (lane 2, Figure 6.2A). This appeared in Cr-Dnaj-Cr (lane 3 compared to lane 2, Figure 6.3B). Bands around 55 kDa (lane 3 and 5, Figure 6.3A), indicated the presence of streptavidin in monomeric form. In Western blotting, the data indicate that the mutant type BabA-Crown$_{_D233A/S244A}$ tends to form more dimer than the wildtype BabA-Crown (Fig 6.2B). An excess of biotinylated protein over the streptavidin added to saturate the reaction was shown in lane 5 (Figure 6.2B) and in Cr-Dnaj-Cr in lane 3 (Figure 6.3B). As only streptavidin was used for detection, bands in Western blotting confirmed that proteins were successfully biotinylated.

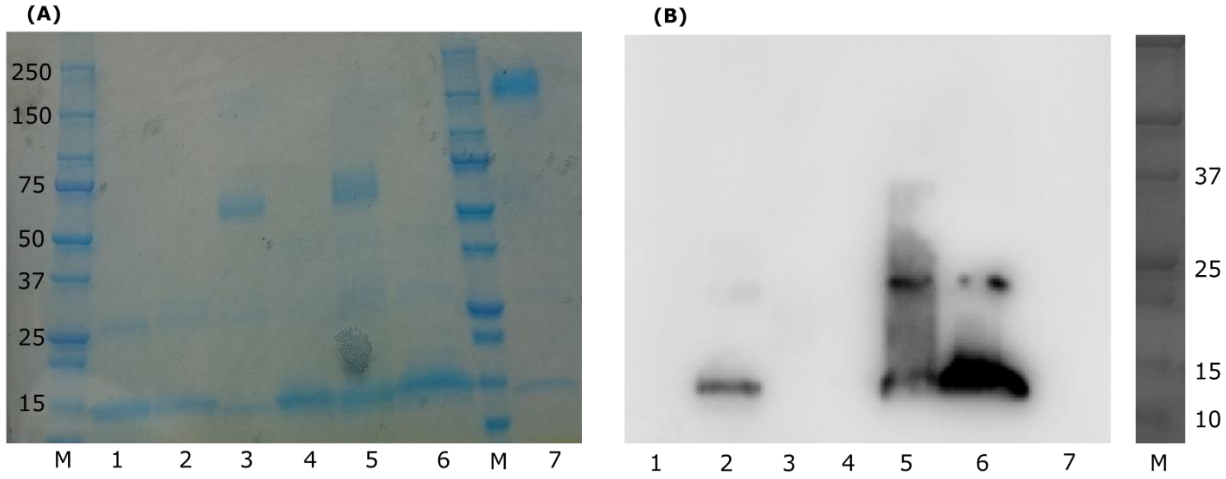


Figure 6.2 Biotinylation analysis of BabA-Crown proteins

(A) Coomassie-stained recombinant protein samples after SDS-PAGE separation. (B) Western blotting of the same samples. 1. BabA-Cr, 2. biotinylated BabA-Cr, 3. Biotinylated BabA-Cr conjugated with streptavidin, 4. BabA-Crown$_{_D233A/S244A}$, 5. A complex of biotinylated BabA-Crown$_{_D233A/S244A}$ with streptavidin 6. Biotinylated BabA-Crown$_{_D233A/S244A}$, 7. Streptavidin. M = molecular weight ladder (kDa).

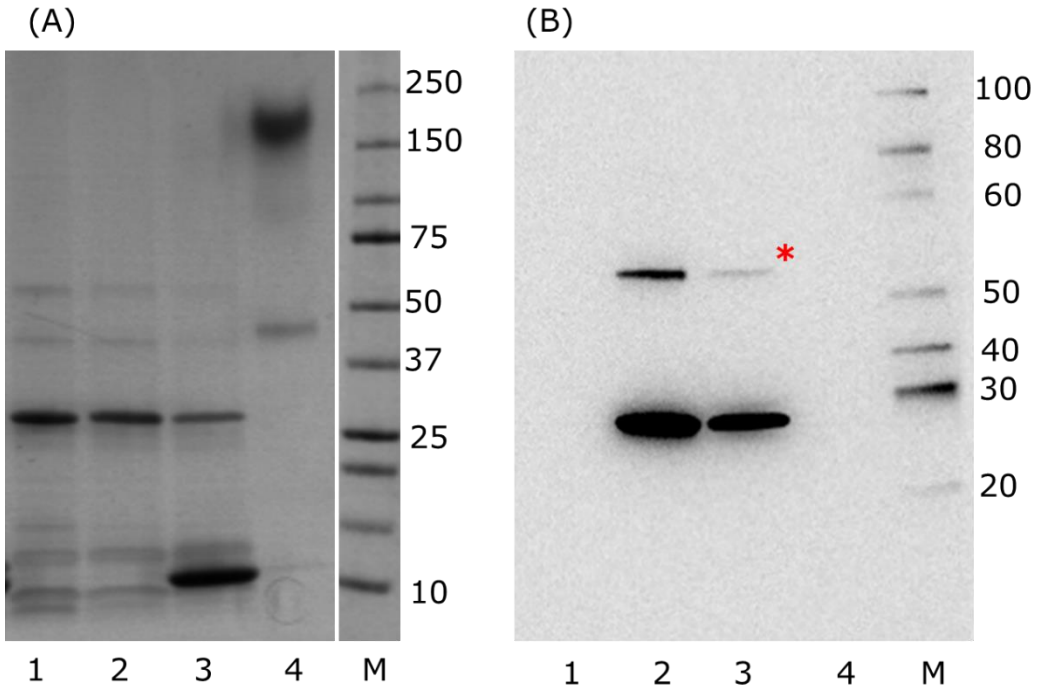


Figure 6.3 Biotinylation analysis of Crown-DnaJ-Crown protein

(A) Coomassie-stained recombinant protein samples after SDS-PAGE separation, and (B) After Western blotting.

1. Cr-DnaJ-Cr 2. Biotinylated Cr-DnaJ-Cr 3. Biotinylated BabA-Cr in complex with streptavidin 4. Streptavidin. M = molecular weight ladder (kDa).

Next, to ascertain whether adding biotin to the protein affects the protein's capacity to bind to its physiological ligand, ELISA was conducted, again using streptavidin-HRP for measurement of binding. As demonstrated in Figure 6.4, none of the expressed constructs bound to Lewis b, showing only weak non-specific binding. While only $BabA_{527K}$ wildtype, used as a positive control, confirmed that biotinylation did not interfere with the binding ability of the protein.

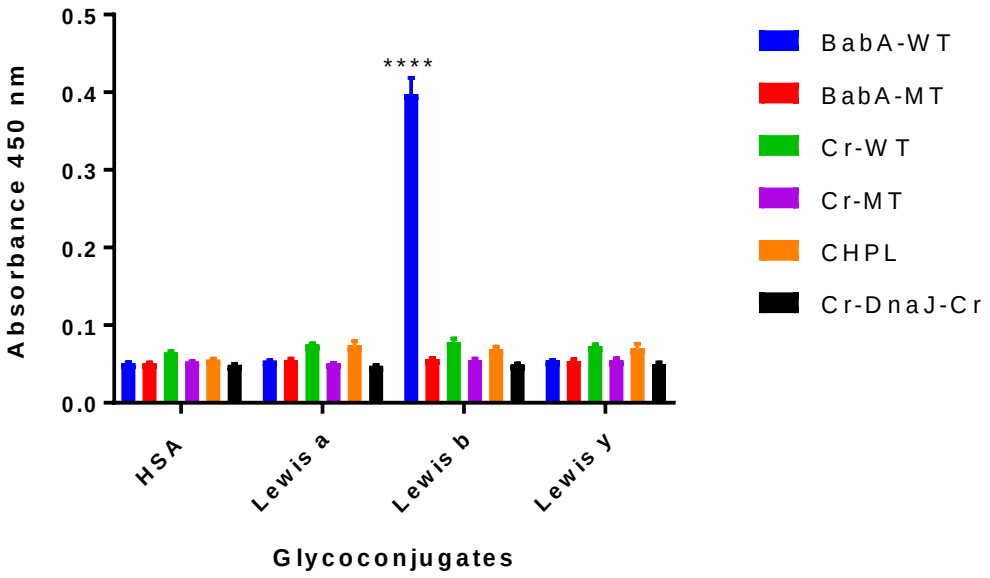


Figure 6.4 Biotinylation analysis using ELISA

Binding of biotinylated proteins to immobilised HSA, Le^a, Le^b and Le^y glycoconjugates in sandwich ELISA. Only $BabA_{527K}$ (BabA-WT) shows binding to Le^b. (n=4, error bars represent the standard error of the mean, $P < 0.001$) using 2way ANOVA for multiple comparisons followed by Tukey post-hoc test.

6.3.2 Functionality of protein-microparticles complexes and binding assessment

Biotin-avidin interaction was used to conjugate the microparticles to the proteins. The biotin on the protein mediate the bonding interaction with the immobilised non-glycosylated avidin (NeutrAvidin) on the microparticle surface. Various concentrations of biotinylated proteins were chosen and incubated with the microparticle to determine the best concentration for saturating the particle surface. The optimum amount chosen for saturating 50 µg of NeutrAvidin microparticle solids was 2 µg of each protein (Figure 6.5).

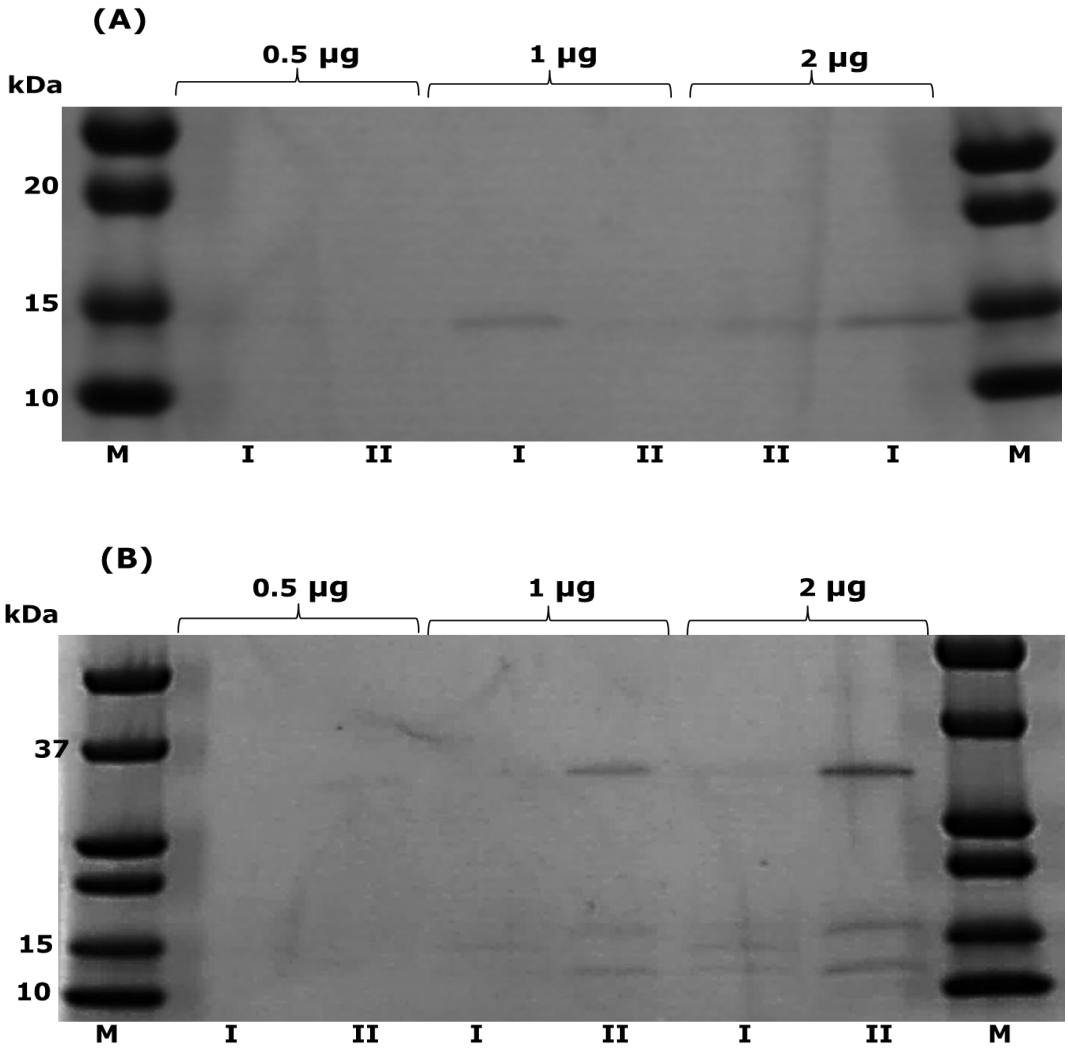


Figure 6.5 Optimisation of protein-microparticle complexation in Coomassie staining

Different amounts (0.5, 1 and 2 µg) of Cr-DnaJ-Cr biotinylated proteins were incubated with NeutrAvidin microparticles (50 µg) and analysed by Coomassie staining after SDS-PAGE. A) BabA-Crown B) Cr-DnaJ-Cr.

I. represents the unbound protein obtained from the supernatant of the protein-particle conjugates after centrifugation. II. represents the same stated amount of the protein before incubation with the microparticles (100% unbound protein).

After conjugating Neutravidin microparticle to the proteins, Dynamic light scattering was used to evaluate the change in the hydrodynamic diameter of the microparticles. The possible scenarios (Figure 6.6) were envisaged to anticipate the microparticle-protein interactions.

A) Proteins having the same size form monodisperse solution or polydisperse colloid in case of different sizes such dimers or tetramers.
B) Monodisperse solution bound to microparticle via the neutravidin on its surface and biotin molecule in the protein forming a layer, which could be measured, in case there is a relatively similar size/weight between the protein and the microparticle. Multiple measurements of this increase in size can be reproducible as the monomolecular formed is devoid of aggregation.
C) In case of polydispersity, upon protein interaction with particles, variable size distributions can be detected as the protein may form aggregates and then bind to neutravidin, which has 4 binding sites, in the microparticles forming complexes of multiple intensities or heterogeneous samples.

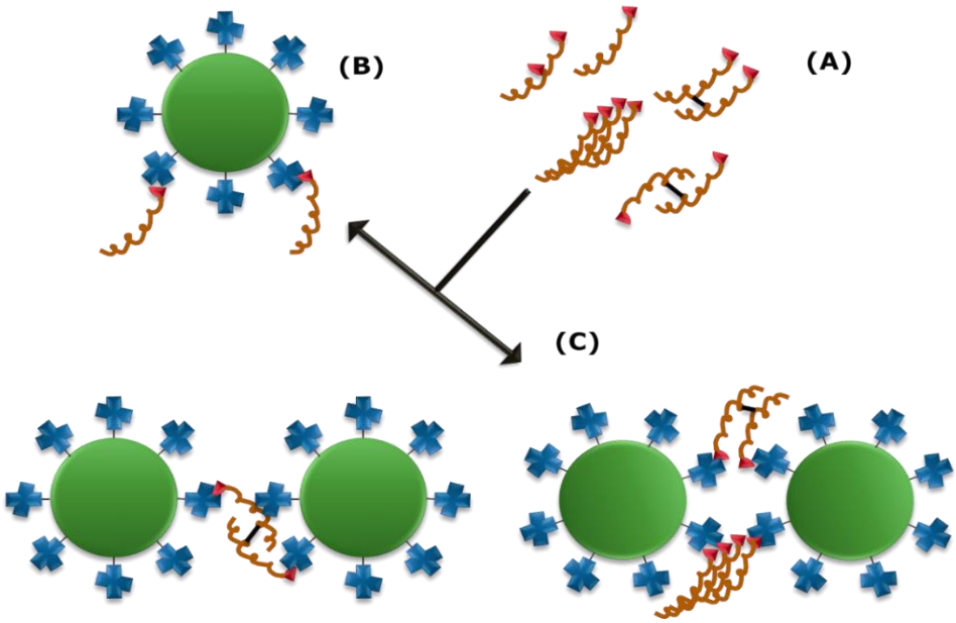


Figure 6.6 Schematic diagram shows the possible ways for microparticles size increasing/aggregation

(A) Proteins (brown strings) having single biotin (red triangle) present in monomer, dimer due to disulphide bridge (black line) or aggregates interact with neutravidin (blue tetramer) on the surface of the microparticles forming monodisperse solution (B), or cause particles aggregations (C) and result in polydisperse colloid.

The hydrodynamic size distribution by intensity for the Neutravidin microparticle-protein complexes at 50 µg/mL was investigated using DLS (Figure 6.7). An increase in the hydrodynamic diameter was recorded in microparticle-protein complexes, however, because of the difference in the size of the microparticle (~1.0 µm) and the protein (few nanometers), it is not possible to measure, accurately, the change in particles hydrodynamic diameter. Microparticle alone (Figure 6.7A) demonstrates two peaks around 1 µm in size for the three readings, suggesting particles size (~ 900 nm). BabA-Wildtype (Figure 6.7B) shows similar result to the microparticle alone with a subtle increase in size, however, there is a major peak combining all measurement suggesting no/less aggregation occurs. BabA mutant type (Figure 6.7C) illustrates different peaks from multiple runs e.g. one reading showed particles size of 1050 nm suggesting an aggregation as there are fluctuations in the size displayed, i.e. the complexes are not monomolecular (polydisperse). While, BabA-Crown-Wildtype (Figure 6.7D), BabA-Crown$_{_D233A/S244A}$ the mutant type (Figure 6.7E) and BabA$_{CHPL}$ (Figure 6.7F) display similar patterns, suggesting polydispersity due to the increase in the size distribution and particle radius to between 1050 - 1150 nm. Moreover, intensity measurement of BabA-Crown Wildtype and BabA$_{CHPL}$ indicates less heterogeneous samples, while BabA-Crown$_{_D233A/S244A}$ shows more variable sizes and this may be due to the tendency to form dimers more often than the other samples. Cr-DnaJ-Cr (Figure 6.7G) appeared to be bigger in size (~ 1200 nm) compared with BabA-Crown sample. Triple measurement of size distribution by intensity of these samples reveal multiple peaks, which are coincide with each other and displayed as two peaks, suggesting protein bivalency, which could be in part to dimer formation or cross-linking between the two Crown domains that forming the protein, which bind with different microparticles together. However, the reading look more similar, a side from the size and intensity, to BabA and microparticles.

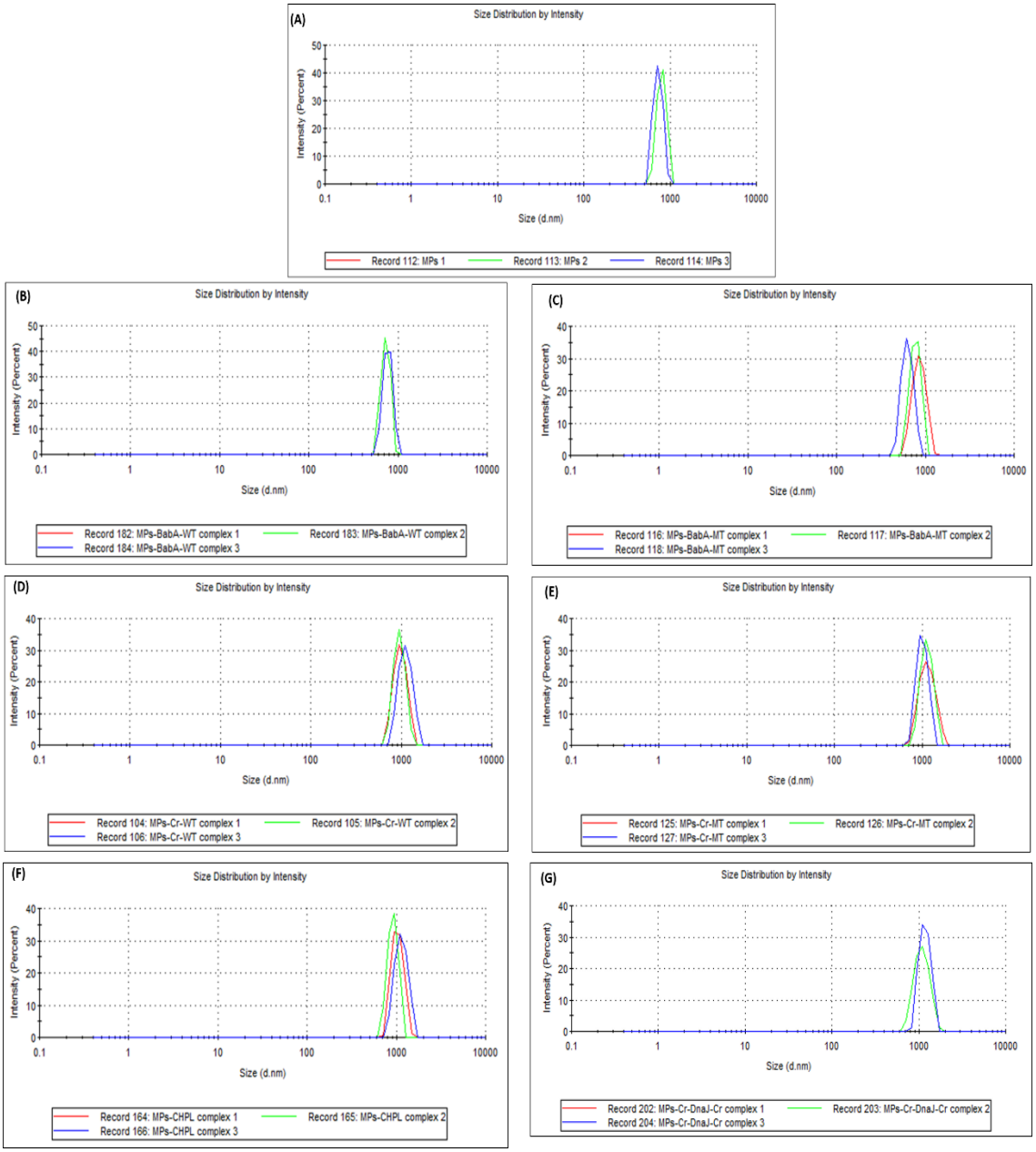


Figure 6.7 Evaluating homogeneity of protein solution

Measurement of hydrodynamic size distribution by intensity for Neutravidin microparticle-protein complexes disclose (**A**) Microparticle alone are around (~ 900 nm in size, which is approximately the same size of BabA-Wildtype in (**B**). While BabA mutant type (**C**) show fluctuations in the size distribution (900 – 1050 nm) which indicate particles aggregation or polydisperse solution. Similar patterns were noticed in BabA-Crown-Wildtype (**D**), BabA-Crown$_{_D233A/S244A}$ the mutant type (**E**) and BabA$_{CHPL}$ (**F**) suggesting polydispersity but to less heterogenecity due to size increment between (900 – 1100 nm) and less intensity percentages (~35 %). Size distribution in Cr-DnaJ-Cr (**G**) showed multiple coincided peaks which are combined into two peaks (900 – 1200 nm), suggesting protein bivalency.

For testing the binding ability of protein-microparticle complexes to the glycoconjugates, ELISA was performed. Labelling the microparticle with biotinylated protein and direct fluorescent detection revealed no binding activity for the tested proteins to the glycoconjugates except $BabA_{527K}$ or wildtype (used as positive control) which bound to le^b (Figure 6.8). The presence of nonspecific binding observed, mostly, in BabA proteins (wildtype and mutant) and Cr-DnaJ-Cr may be due to the interaction between the microparticle and the sugars as no antibody was added for binding detection.

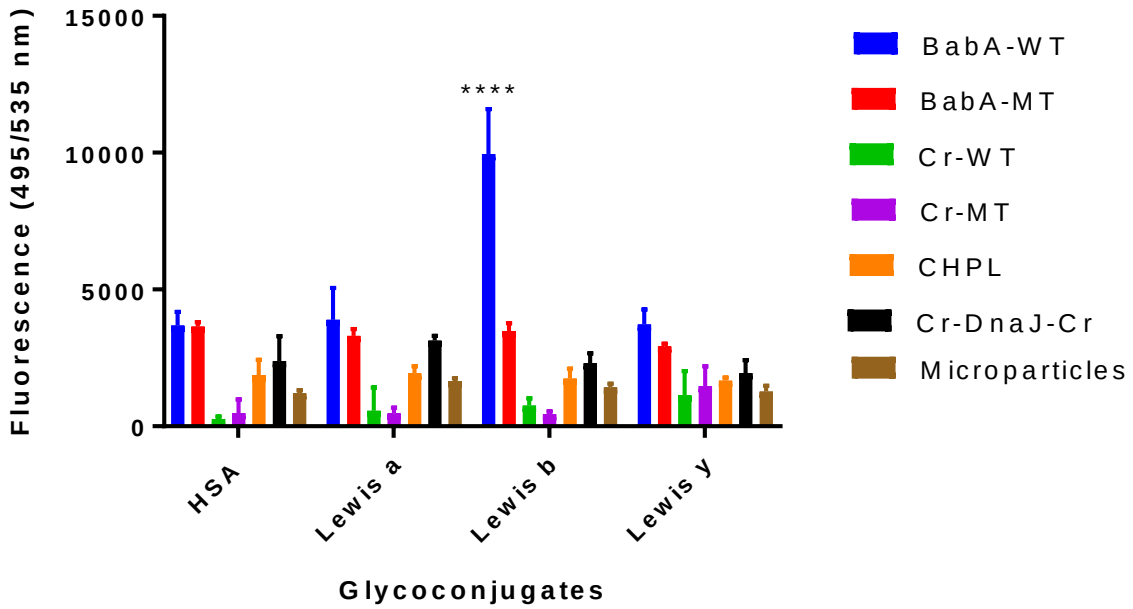


Figure 6.8 ELISA determination of binding of protein-microparticle complexes glycoconjugates

Binding of protein-microparticle complexes to immobilised HSA (negative control), HSA-Le^a, HSA-Le^b and HSA-Le^y glycoconjugates in sandwich ELISA. $BabA_{527K}$ (BabA-WT) conjugated with NeutrAvidin microparticles bound to Le^b. BabA proteins (Wildtype and mutant), Cr-DnaJ-Cr and to a lesser extent $BabA_{CHPL}$ show non-specific binding to the glycoconjugates (n=4, error bars represent the standard error of the mean, $P < 0.001$) using 2way ANOVA for multiple comparisons followed by Tukey post-hoc test.

6.4 Discussion

This chapter represents the final objective of this study which was to find the smallest binding domain of BabA before using it as a targeting moiety for drug delivery. For this purpose, microparticles were surface-modified with different BabA domains, applying biotin-avidin specific complexation approach. Biotinylated BabA domains were attached to Neutravidin microparticles. This attachment aimed to dually help the protein to be in an orientation similar to the bacterial surface and to assist in approaching the correct folding for binding.

Neutravidin-biotin interaction is the strongest non-covalent bonding known in nature. This interaction has been explored in several applications such as nucleic acid delivery, diagnosis/detection of surface antigen and monoclonal drug deivery are examplified below.

1. Nucleic acid delivery was exploited in developing small interfering ribonucleic acids (siRNA) coupled to monoclonal antibody to target podocytes (specialised cells in the kidneys) *in vivo*. Monovalent IgG was conjugated to neutravidin via sulfohydryl group. Then biotinylated protamine, polycationic nuclear protein used as adaptor for siRNA, was joined to the neutravidin (Hauser *et al.,* 2010). Neutravidin was used for delivery of biotin-labelled poly(rC) binding protein 2 (PCBP2) siRNA to hepatic stellate (HSC-T6) cells and rats (Jain *et al.,* 2017).
2. For diagnostic purposes, Avidin-nucleic acid nanoassembly system (ANANAS) assisted by confocal laser endomicroscopy was developed for diagnosis of inflammatory bowel disease in experimental model. The nucleic acids were coated by neutravidin forming toroidal structure and conjugated to biotinylated polyethylene glycol (Buda *et al.,* 2015). Streptavidin conjugated to highly luminescent quantum dots in combination with atomic force microscope and confocal laser scanning microscopy were used for detection of TrkB receptors distributed in cultured hippocampal neurons (Park *et al.,* 2010). Recently, streptavidin was conjugated to gold nanoclusters (Au-glutathione) to develop ultrasensitive fluorescent sensors for diagnosis of HIV infection in the early stages through detection of HIV-1 p24 antigen (Kurdekar *et al.,* 2018).

3. For monoclonal drug delivery, therapeutic IgG fusion protein with transferrin receptor monoclonal antibody was used for penetrating the blood brain-barrier through transferrin receptors (Pardridge, 2015). Anti-epidermal growth factor receptor antibody was integrated with avidin nucleic acid nano-assembly carrying doxorubicin for breast cancer therapy, *in vivo* using human breast adenocarcinoma cells, MCF-7 and MDA-MB-231 (Roncato *et al.,* 2018).

The use of neutravidin-biotin for intracellular protein drug delivery is a challenge as, generally, the proteins show low membrane permeability, limited target-specificity and stability (Jain and Cheng, 2017). Moreover, for microparticle encapsulation proteins need special consideration to keep the structural organisation stable and compatible to perform the function (Deshpande *et al.,* 2017). Here, for the first time, BabA was used from different point of view, i.e. instead of bacterial virulence factor, to achieve two aims. Firstly, developing BabA as a biomimetic moiety for gastro-retention drug delivery. Secondly, simulating bacterial BabA-binding to Le^b through modelling the bacterial surface using complete extracellular BabA-microparticle complex. This novel model demonstrated promising results as BabA retains the binding ability and suggesting better insight about its orientation on the bacterial surface.

The ultra-high affinity and selectivity of avidin-biotin binding has been extensively applied to modulate protein structure and function (Dundas *et al.,* 2013). For preparation of avidin-biotin complexes, protein (antibody or lectin) needs to be conjugated with biotin through a biotinylation process. This process can be exploited through biochemical or chemical reactions (Beckett, 2018). Biochemical (enzymatic) biotinylation is more site-specific as biotin ligase enzyme (BirA) adds a single biotin to the lysine residue in the protein substrate bearing the biotin acceptor, Avi-Tag sequence, in an ATP-dependent reaction (Fairhead and Howarth, 2015). A commonly used alternative to enzymatic (mono-)biotinylation is chemical biotinylation, e.g. *via* sulfo-*N*-Hydroxy sulfosuccinimide-(NHS)-esters. However, chemical biotinylation is not sequence-specific and will generate multiple biotinylations of any accessible lysine residue (Elia, 2008, Sternicki *et al.,* 2017). This happens because the primary amine on lysine is frequently surface-exposed, due to its positive charge, at physiological pH. Lysine modification does not usually

affect the protein biological activity (Elia, 2008). As the intention is to conjugate the biotinylated Crown to nano/microparticles, multiple biotinylation could create multiple particle binding, and thus, undesirable particle aggregation. In contrast, mono-biotinylation cannot induce clustering of nano/micro-particles surface modified with neutravidin. Neutravidin as a tetramer can use each of the four binding sites to capture a single biotinylated protein (monomer) without leading to aggregation (Dundas *et al.,* 2013), unless the binding protein is bivalent (dimer).

Biotinylation of BabA-Crown and other truncates was successfully performed using BirA enzyme. This step was confirmed by Western blotting and ELISA binding assay. However, these techniques confirmed that the biotin has been conjugated to the proteins, but did not show if the proteins are monobiotinylated proteins. Monobiotinylation can be specifically obtained by co-transforming a plasmid encoding BirA enzyme into the bacterial cell, then the expressed enzyme will target the AviTag sequence and monobiotinylated the protein of interest (Sung *et al.,* 2011). Other strategy, by transforming the plasmid of interest into *E. coli* containing biotin ligase encoding plasmid pBirACmu and extract the monobiotinylated protein from periplasm (Noor *et al.,* 2018).

Interestingly, there are two tags acting as a substrate for ligase BirA enzyme. The first is Avitag sequence which consists of 15 amino acids and the second is BioEase™ tag which has 72 amino acids and derived from the oxalacetate decarboxylase α subunit isolated from *Klebsiella pneumonia* (Kumano-Kuramochi *et al.,* 2017). Even with the difference in the length of the sequence and composition (Ala-Met-Lys-Met in BioEase™ and Ala-Gln-Lys-Ile in Avitag™), both share the same efficiency in being a substrate for BirA ligase *in vitro*. However, AviTag™ is preferable as a tag due to its small size (Tirat *et al.,* 2006, Kumano-Kuramochi *et al.,* 2017). While the benefit of monobiotinylated protein is the lack of aggregation of streptaviding particles, this could still be caused e.g. by dimers of biotinylated proteins formed by disulfide bridges present in BabA-Crown, Cr-DnaJ-Cr or other BabA truncates. These cannot be reduced (e.g. using DTT or beta-mercaptoethanol as reducing agents), as this step would impact the ligand binding ability of the BabA-Crown. Moreover, it was reported that disulfide bridge formed a cysteine-clasped loop in BabA is essential for its stability, binding interaction, and oligomer formation in response to the change in the stomach pH

(Bugaytsova *et al.,* 2017, Moonens *et al.,* 2016). Even though confirmation of protein biotinylation was conducted using tradtional Western blotting, which recently improved by using Streptavidin containing poly-horseradish peroxidase (Mishra *et al.,* 2019), further confirmatory techniques are required. Mass spectrometery to analyse the increment in protein molecular weight (biotin molecular weight is 0.226 kDa) will be beneficial for confirming the biotinylation. Direct detection of biotin-tagged protein (DiDBiT) method using mass spectrometry can increase detection of biotinylated proteins to about 200 fold (Schiapparelli *et al.,* 2014). Recent advances in liquid chromatography time-of-flight mass spectrometry (LC-TOF-MS) can provide more accurate estimation (Eeltink *et al.,* 2017).

Dynamic light scattering (DLS) is commonly used to estimate particle hydrodynamic size and the thickness of adsorbed layer. This is done by taking the average particle hydrodynamic radii before and after the modification (Tiraferri and Borkovec, 2015). In this study, microparticle was conjugated to proteins then measured using DLS. Measurement indicated an increase in particle size in BabA-Crown (Wildtype and mutant), Cr-DnaJ-Cr and $BabA_{CHPL}$ proteins. This enlargement could also be due to aggregated proteins bound to neutravidin in different particles. As DLS was used as a complementary approach for characterisation of the microparticle-protein complexes, further confirmatory tehniques such as electron microscopy can be advantageous. DLS is beneficial instrument in determining the protein-particle behaviour, particle homogeneity and estimation of the particle size (Stetefeld *et al.,* 2016). Furthermore, it is capable of studying the ability of the conjugates to remain as suspension, i.e. their resistance to any aggregation/ sedimentation (Gambinossi *et al.,* 2015). The measurement of the hydrodynamic size is calculated assuming that the particles are spherical in shape and can reveal more accurate measurement if there is single population in the sample. However, DLS has many limitations such as lacking the ability to separate the measurement of closely related molecules (e.g. monomer and dimer) (Stetefeld *et al.,* 2016). The main limitation is the difficulty of accurate quantification of the amounts of the aggregates. This is because the particles are usually considered to be spherical, which in case of heterogeneous size distribution, makes data interpretation more problematic (Brar and Verma, 2011). In this case, the presence of aggregates or polydispersity means that the

technique cannot accurately estimate the hydrodynamic thickness of the adsorbed layer on the particle surface as proposed by (Tiraferri and Borkovec, 2015). As it was intented to use the microparticle surface to obtain functional protein, particle aggregation can form heterogeneous layers. This would produce variable protein loads and thus different concentrations (Tiraferri and Borkovec, 2015).

It is worth emphasizing that NeutrAvidin microparticles are polystyrene-based and were used as proof-of-principle. Thus, their usage can be helpful in simulation of bacterial surface for protein functionalisation. Polystyrene is commonly used as model particles to study the surface effect on biological molecules activity. These particles are a convenient platform for proof-of-principle application but their non-degradability in biological environment restricts their usage *in vivo* (Loos *et al.,* 2014).

Testing protein binding ability using ELISA revealed that the aim to get a functional protein was not achieved. While the usages of microparticle to improve BabA-Crown functionality was not a successful strategy, $BabA_{527K}$ wild type still retains the binding ability to its physiological ligand, Le^b. This may suggest correct orientation of BabA on the surface of the particle and retaining of the binding functionality. However, in this case, it did not result in maximizing the binding strength/avidity.

The non-specific binding seen in case of using microparticles-protein complex maybe due to the neutravidin that coated the microparticle. This nonspecificity maybe as explained by (Wilchek and Bayer, 1988) as a result of the basicity of the neutravidin or traced to the affinity of the avidin to bind the sugar (neoglycans). The association between Biotin and neutravidin is mediated by a set of hydrogen bonds and van der Waals interactions. When biotin binds to neutravidin, it buries inside a β-barrel central pocket of the neutravidin which leads to a conformational change (Rosano *et al.,* 1999). This change may lead to the non-specific interactions when protein is absorbed onto a solid phase (Vermette *et al.,* 2003). As in the absence of biotin, the pocket in the neutravidin contains water molecules (Wilchek and Bayer, 1999). This may explain the protein-particle complexes' non-specific binding.

The protein can be immobilised directly on a solid-phase microplate to reduce the non-binding ability or facilitate antibody detection ability but this may produce

random orientation (Vermette *et al.,* 2003) or give rise to false-negative result due to buried protein ligands which make the epitopes of the antibody have no access to their targets. Moreover, protein covalent adsorption to solid surface leads to conformational change or denaturation and potentially loss of binding affinity (Butler, 2000). The concentration of the protein/ligand is additional critical factor (Nguyen *et al.,* 2012). High concentration can give rise to aggregation and increase the background signal, while low concentration reduces the amount of the exposed reactive receptors and lead to misinterpretation, giving false negative results (Güven *et al.,* 2014). Background noise can be eliminated by changing the buffer, e.g. ChonBlock™ buffer system, which was reported to substantially reduce these non-specific interactions (Waritani *et al.,* 2017). This mainly occurs because protein-ligand interactions are measured in soluble form. Isothermal titration calorimetry can provide more factual results with less background noise even when a minimal buffer concentration was used (Booth *et al.,* 2018). However, sample purity and preparation, protein and ligands concentrations need to be more precisely determined for accurate results (Duff *et al.,* 2011). Another sensitive techniques to analyse the binding of immobilised protein on microparticle to the ligand is surface plasmon resonance spectroscopy, which can provide real-time data (Masdor *et al.,* 2017). An alternative strategy is coating the microparticles with a layer of poly(ethylene) glycol, after protein adsorption, which provides antiadhesive characteristic and reduce particles aggregation. However, the density of the surfactant should be adjusted to preserve protein specificity and affinity (van der Wel *et al.,* 2017).

6.5 Conclusion

In summary, from the overall results obtained, coating the microparticle with $BabA_{527K}$ did not affect its glycan binding ability. This indicates that $BabA_{527K}$ retained the correct folding when attached to the microparticle surface. As the AviTag sequence is located at the C-terminal end of the recombinant protein, this may bring the orientation on the particle following complexation which exposes the crown facing outwards, similar to what is found on the *H. pylori* surface. This surface presentation could be used as a biomimetic vector for further studying of the binding affinity.

Unexpectedly, it also appears from the data that a reduction in the size of the extracellular domain of BabA molecule did not yield a functional protein, as none of the truncated forms resulted in binding to BabA's physiological ligand, Lewis B. Thus a strategy based on finding the smallest possible binding domain, followed by protein engineering to remove the last remaining pepsin cleavage sites, is not a viable option.

CHAPTER SEVEN

7. General discussion

7.1 Study impact and importance

The aim of this study was to develop a new system for cytoadhesive drug delivery, using *H. pylori* adhesin as a targeting moiety. While this remains to be accomplished, the work has defined some key challenges and desirable properties of such systems.

Concisely, the best cytoadhesive drug delivery system would need to increase gastric retention time by 1) direct binding to the gastric epithelial cells, 2) have the sustainability to withstand constant gastric mucus turnover and 3) be resistant to the combined action of gastric acidity and pepsin proteolytic activity (Streubel *et al.,* 2006b). Lectins are the best candidates which might help in achieving such characteristics as reviewed in these references (Oldenkamp *et al.,* 2018, Marcos Luciano, 2019, Devi and Basil-Rose, 2018, Coelho *et al.,* 2017, Brooks, 2017). However, no such specific lectin-based gastric drug delivery system has been described in the literature. This might be due to the potential of the lectins to be immunogenic and possibly toxic (Mbae *et al.,* 2018). Though, this gap in the knowledge could be filled by utilizing a similar model already existent in Nature, for example, inspired from gastric bacteria. *H. pylori* as a widespread gastric inhabitant represents a good model to be simulated. This research for the first time paved the way for the use of one of *H. pylori* lectins (BabA), which specifically interacts with gastric ligands, as a novel strategy. This biomimicry, if successful, would open a new frontier for new improved drug delivery systems.

The biomimetic system aimed to increase gastric retention time, and this poses a special challenge. This because targeting a proteinaceous moiety bearing a drug

to the gastric epithelium makes the system highly susceptible to the hostile acidic and proteolytic nature of the gastric digestive juices. Therefore, characterisation of the glycan binding abilities and its resistance to peptic digestion were important elements of this thesis.

Indeed, a recombinant form of BabA's full extracellular domain can be a candidate drug targeting moiety, but its sensitivity to proteolysis makes it a less suitable system. One possibility to avoid degradation by gastric pepsin would be to use the smallest possible binding domain of BabA. This would facilitate the creation of a targeting moiety without any pepsin digestion sites. Therefore, defining the minimal binding domain of BabA besides the empirical assessment of its properties in a simulated gastric environment were attempted. This has been done for the first time in this thesis.

Importantly, it must be stressed on the possible disadvantage of using such lectins for targeting the drug delivery system to gastric surface glycans *in vivo*. The possibility of premature or unavoidable binding to the mucins in the mucosal layer, rather than to the gastric epithelium could be a possible hindrance to this model. This could occur because BabA binds to a variety of ligands, shared with gastric mucus, starting from the oral cavity up to the secreted mucin MUC5AC found on the stomach epithelium. Thus, it is essential that this biomimetic system should be studied in a relevant physiological environment, i.e. not just *in vitro*, to achieve a more realistic evaluation of the feasibility of this approach.

An unexpected outcome of this work was the inability to express a functional, shorter domain of BabA. This initially appeared achievable, because knowledge gained from crystallography suggested that all binding interactions between BabA and its ligand were restricted to a small area of the adhesin, which was called the Crown domain. It is worth noting that, throughout this study many advances were achieved, not only in trying different BabA truncates and understanding the possibility in mediating the adhesion, but also in the elucidation of a pepsin digestion-resistant model and microparticle application, which was also a novel achievement applied in this thesis for the first time. Overall, new insights were obtained from the results of the experiments performed in this thesis and some are summarised and discussed below.

7.1.1 Improved periplasmic expression approach

Bacterial periplasmic space, as oxidising environment, is the site of choice for targeting recombinant proteins when formation of disulfide bonds is required for correct folding or functionality. It also makes isolation of the recombinant protein easier and could be used for developing strategies for improving protein yields (Selas Castiñeiras *et al.,* 2018, Ytterberg *et al.,* 2019).

While most of the experimental procedures used for protein expression were derived from the previous published strategy (Hage *et al.,* 2015b), the protocols had to be modified to obtain successful expression of truncated BabA versions. The use of chloramphenicol in the growth medium, instead of incorporating a hexa-lysine tag as originally used in the published study, resulted in a significant improvement in the expression yield. This strategy can be considered for future studies to increase the copy number of plasmids having *ColE*1 origin of replication (i.e. *ColE*1 family plasmids) such as pMB1, p15A and CloDF13 (Son *et al.,* 2016, Camps, 2010) and thus, increase protein periplasmic expression.

The introduction of hexa-lysine tag at BabA carboxylic terminal increased the solubility of the protein, through a yet to be explained mechanism, and protected it from partial N-terminal degradation (Hage *et al.,* 2015b). Recently, partial N-terminal degradation was also occurred in expression of LabA in the presence of hexa-lysine tag (Paraskevopoulou *et al.,* 2019). Albeit a significant increase in the protein yield was achieved, this method failed to produce two different BabA truncates. However, a pronounced band was observed after protein purification in BabA-Crown variant having AviTag™ sequence. In the literature, this 15 amino acids long sequence was usually used to generate a biotinylated protein through being a substrate for BirA enzyme-dependent biotinylation (Fairhead and Howarth, 2015). Little is known about the ability of this sequence to increase protein expression. Therefore, it would be interesting to determine if this sequence could, empirically, improve the expression also in other proteins.

7.1.2 Identification of the minimal binding mechanism

The molecular recognition of *H. pylori* adhesins and cellular receptors has been sought for a long time until recently established. Out of all of *H. pylori* adhesins, only two were co-crystallised with their ligands, BabA and HopQ (Hage *et al.,* 2015a, Javaheri *et al.,* 2016). BabA crystallisation led to elucidation of the mechanism these bacteria undertake to interact with Le^b and type 1 ABO/Le blood group, thereby, publicised initial gastric colonisation. The structural insight gained from this knowledge revealed the existence of the binding site, which is mostly stranded β-domain, termed the Crown. Application and understanding of such binding mechanism is critical, not only to elucidate the structural basis and how *H. pylori* mediates the attachment, but also for developing functional minimal binding site vectors, which could be rationalised to other adhesins.

This data shed a light on the usage of the Crown as a targeting moiety for drug delivery. It was assumed that the minimal interactive domain if used for surface modification of nano/microparticles, it would increase the avidity.

Indeed, the experimental trials conducted in this study have increased the knowledge about the characteristics of BabA protein, even though the binding issue has not been completely tackled. It is worth constructing different BabA sequences from different bacterial strains after comparing their binding affinity. This because of

1) BabA variants have different dissociation rates (Aspholm-Hurtig *et al.,* 2004).

2) The high diversity in the amino acid sequence may affect the functionally and binding properties (Bugaytsova *et al.,* 2017).

3) Some variants might tend to form oligomers (Moonens *et al.,* 2016).

For the sake of generating a prospective drug delivery moiety, it is useful to try other *H. pylori* adhesins as an additional/alternative targeting moiety. LabA or SabA are two possible lectin-based candidates having proved affinity towards specific ligand in the gastric glycans (Rossez *et al.,* 2014a, Pang *et al.,* 2014). LabA specifically adheres to lacdiNac motif, which is abundantly carried by healthy gastric mucosa. SabA binds to sialylated glycoproteins which are found on the

epithelium in an inflamed stomach. However, crystal structures of these adhesins with their ligands are not available, so far. Thus, more investigation is needed to know the binding molecular interactions between these adhesins and their ligands. The recently characterised *H. pylori* adhesin 'HopQ' could be a potential alternative as it was crystallised alone and co-attached with its ligand carcinoembryonic antigen-related cell adhesion molecule (CEACAM). Interestingly, the crystal structure shows the binding domain comprising of a small Crown region, β-domain consists of 2 strands instead of the 4 strands present in BabA (Javaheri *et al.,* 2016). Future comprehensive knowledge of these domains or molecular binding interactions could reveal better insights about the possible ways of enhancing cytoadhesive properties.

A further alternative approach could be sought to develop antimicrobial peptide to antagonise bacterial binding and/or inhibit the colonisation/invasion. The principle of anti-adhesion was applied through mannosides, small-molecular-weight compounds, which blocked uropathogenic *E. coli* (UPEC) adherence to the bladder epithelium through inhibiting bacterial FimH type 1 pilus lectin (Cusumano *et al.,* 2011). This orally administrated FimH antagonist demonstrated potentially promising new treatment for urinary tract infection in females. Moreover, a newly identified family of lectin 'odorranalectin' was the focus area of recent research. This 17-amino acid sequence was isolated from skin secretions of the frog of *Odorrana grahami*. It represents a promising candidate as anti-amphibian and in brain targeting drug delivery (Wen *et al.,* 2011a, Wu *et al.,* 2012, Li *et al.,* 2008, Wen *et al.,* 2011b). However, applying this new lectin or any of the family member for gastric drug delivery was not recorded, so far.

Recently, monoclonal antibody was used for gastric drug delivery such as programmed death-ligand 1 (PD-L1) monoclonal antibody. This antibody was conjugated with polyethylene glycol-poly-caprolactone nanoparticles to enhance Docetaxel delivery and showed chemotherapy efficacy in gastric cancer cells *in vitro* besides induced cell apoptosis and increase cell cycle arrest at Gap2/Mitosis phase *in vivo* (Xu *et al.,* 2018).

7.1.3 Creation of Crown-DnaJ-Crown

The observation of a sequence (ENFKKLNEAYQILQTALKR) representing a part of a molecular chaperon DnaJ within BabA has attracted our attention to its possible function. This semi-conserved 19-amino acid sequence is only present in *H. pylori* J99 strain. It may play a role in increasing the flexibility of the Crown folding or binding functionality. This assumption was derived from the role J-domain played in *Mycoplasma pneumoniae* in terminal organelle function protein (TopJ). Loss of this domain led to adherence-deficient phenotype (Cloward and Krause, 2009). Alignment of this sequence with other BabA allelic variants (Figure 7.1) shows the middle 11 amino acids are semi-conserved. Blasting these residues (NEAYOILQTAL) using NCBI protein bank displayed a matching (91% identity) with only BabA sequence. Yet the exact function, if any, is poorly understood and interpretation of its role is beyond the scope of this thesis.

```
BabB          KNYAIINKAYQIIQKALTA-    19
BabC          DEFKKLNEAYQIIQQALKN-    19
BabA-DnaJ     ENFKKLNEAYQILQTALKR-    19
BabA1         ENFKKLNEAYQILQTALNKG    20
BabB/BabA1    ENFKKLNEAYQILQTALNKG    20
              .::  :*:****:* **.
```

Figure 7.1 Multiple sequence alignment of BabA allelic variants

DnaJ sequence in BabA from J99 *H. pylori* has two different residues (K/N and R/K) from BabA1 (not expressed protein) and the chimeric BabB/BabA1. While there is 100% identity in BabA1 and BabB/BabA1, there is heterogeneity in BabC.

The presence of part of DnaJ domain in BabA may indicate one or both of these possibilities:

1. It may acts as chaperon-like or putative co-chaperone with DnaK sequence and help in folding/unfolding. This assumption derived from the role DnaJ protein plays in localising the protein to Hsp70 chaperon (Kampinga *et al.,* 2019). Or the role BabA 'key-coil' plays in monomer to trimer/oligomer transition in response to the variation in the pH (Bugaytsova *et al.,* 2017).
2. Has a signal transducing role intracellularly, such as a sensor for unknown element. This is suggestive explanation derived from the role DnaJ-like 'DjlA' protein plays in interaction with the membrane sensor kinase RcsC in *E. coli* (Castanié-Cornet *et al.,* 2014). Noticeably, DjlA does not contain the cysteine-repeat domain but only has the J-domain (Genevaux *et al.,* 2007).

Both of the above-mentioned possibilities need further investigation.

From J99 BabA crystal structure, DnaJ sequence appeared to form alpha-helix in the head domain. It located upstream to the Crown domain, between two cysteine-clasps. Its position is close to the Crown key-coil found in BabA from 17387 strain, in which D198 with R207 forms a salt-bridge clamp. This clamp, at low acidity, acts as a pH sensor, while maintaining the binding interactions (Bugaytsova *et al.,* 2017). As BabA J99 protein does not contain this key-coil, we suggested that DnaJ may acts as an alternative in this strain. Successful folding of Cr-DnaJ-Cr, as displayed in the CD experiment, may support the suggestive role DnaJ played in acting as a chaperon-like factor (Takayanagi-Kiya and Jin, 2016). This probably was made possible by bringing the two Crowns together to form Cysteine clamps. However, the inability of Cr-DnaJ-Cr protein to bind its ligand is far from being understood.

As the Cr-DnaJ-Cr is the divalent form which is made up of two Crowns, an interesting concern is raised about the nature of the Crown itself. The Crown as a domain could be either a native sequence evolved to mediate BabA attachment function, or it might be acquired from an external DNA source through e.g. transformation/transduction, and subsequent integration events. Upon blasting the Crown's DNA nucleotide and amino acid sequences, no significant homologue sequence was identified with any other organisms. This result was supported by two studies considering BabA-Crown as a unique (BabA-ID) sequence mainly

present to mediate the specific binding of *H. pylori* to the gastric histo-blood group antigens (Hage *et al.,* 2015a, Moonens *et al.,* 2016). Noticeably, the presence of two hypervariable loops sequences, complicated the choices of the blasting, as numerous sequences should be tested.

Searching for a similar protein/molecule share the same binding ability to Le^b to gain more insights, have led to two viruses that infect the stomach. These two viruses are from the Caliciviridae family, namely, Norovirus and Sapovirus. They are infecting most of the world's population and are the dominant cause of gastroenteritis (Atmar *et al.,* 2018). At least three human Norovirus genogroups are binding to histo-blood group antigens (HBGAs) including Le^b (Shirato, 2011), while Sapovirus bind only to sialic acids (Kim *et al.,* 2014). An association between infection with *H. pylori* CagA-positive strains and an increase in Norovirus (GII.4 strains) binding spectrum to the mucosal surface was reported (Ruvoen-Clouet *et al.,* 2014). It was proposed that the bacteria induce fucosyltransferase 1 (FUT1) expression in the gastric epithelial cells, thereby increasing the binding sites for Norovirus GII.4 virus. However, this association does not explain the competition between *H. pylori* and Norovirus in binding to the same gastric glycoconjugates.

Unexpectedly, it has been shown that *H. pylori* expresses glycoconjugates (e.g. Le^b) on its surface as part of the lipopolysaccharides (Li *et al.,* 2016a). If these Lewis antigens are used for immune evasion, then how the bacterium can differentiate between its own receptors and the ones expressed by the host cells? On one side, while some scientists, such as Chmiela *et al.,* determined that bacterial expression of Lewis antigen is host-mimicking mechanism and corresponded to the host phenotype at various conditions (Chmiela *et al.,* 2014, Chmiela *et al.,* 2018, Chmiela and Gonciarz, 2017), other scientists concluded that this expression has no definite role in host evasion and need more exploration (Matsuura, 2013) also expression of Le^b in *H.pylori* does not interfere with the bacterial adhesion capability (Zheng *et al.,* 2003). It is interesting that the bacteria can produce highly specific lectins to mediate the host attachment and at the same time express these lectins to be located on their surface. It was suggested that the bacteria can distinguish between these carbohydrate ligands based on the differences in the core structure (Falk, 2001).

Recently, it was revealed that BabA binding to Le^b inhibits bacterial proliferation. This negative feedback mechanism is regulated by histidine kinase sensor (ArsS) and leads to a decrease in *babA* gene expression (Skoog *et al.,* 2017). However, this finding complicates the situation, as some bacterial strains, e.g. *H. pylori* 26695, do not express functional BabA or SabA protein. This, in turn, raised two questions which remained unanswered.

1. Why is BabA expressed in some strains and not in others?
2. Does BabA have another function in addition to mediating the bacterial attachment?

In summary, knowledge of the Crown role is of great interest not only for developing a drug delivery moiety but also for understanding how *H. pylori* mediates the attachment and elucidation of BabA functionality. Although the crystal structure of SabA was solved before BabA, no Crown or comparable β-strand domain was revealed in SabA crystal structure (Pang *et al.,* 2014). Moreover, SabA was not co-crystallised with the sialyl-Le^x to know the binding domain. However, there is a shorter β-domain (2 strands instead of the 4 strands present in BabA) in the recently crystallised HopQ (Javaheri *et al.,* 2016). A comprehensive knowledge of these domains or molecular binding interactions could reveal better insights about the possible ways of enhancing cytoadhesive properties.

7.1.4 Discovery of partial BabA-Crown resistance to peptic digestion

What makes *H. pylori* a successful gastric inhabitant bacterium, is its ability to adapt to this hostile environment. This adaptation depends on several factors, including attachment to the gastric epithelial cells. This specific binding could be an advantageous characteristic for making a suitable moiety for gastric targeting, however, using proteinaceous moiety is a challenge.

BabA-Crown partial resistance to pepsin, aside from binding non-functionality, renders it as a model for drug delivery. This because the proteolytic sensitivity could be solved by mutagenic mutations to give a completely resistant form. Moreover, pepsin secretion into the gastric lumen occurs during digestion as a response to the meal's entry (Gritti *et al.,* 2000). This gives BabA-microparticles drug delivery system the opportunity to be administrated in the fasted state only. However, one limitation anticipated, BabA when conjugated to the surface of the microparticles could not be replaced continuously in response to the surrounding environment such in the case of being on the bacterial surface.

Even if the binding issue was solved and the resultant mutagenic model could resist the gastric acidity, still further *in vivo* assessment should be performed before it could be considered for use regardless of the prandial status. An alternative substitution strategy could be to use pepstatin to inhibit the pepsin activity (Kim *et al.,* 2018), providing a space of time for BabA activity. However, the potential interference of this intervention with the natural digestive processes would need to be considered carefully.

The experimental work proved that both recombinant BabA-Crown and Cr-DnaJ-Cr proteins were partially resistant to pepsin digestion at both low and full proteolytic activity phases. These results could be translated into a knowledge for elucidating the adhesin susceptibility to the gastric lumen during the course of *H. pylori* infection. In this context, it is useful to take into account that bacterial attachment/detachment does not only rely on adhesins but also on multiple other factors such as flagella and urease enzyme. The former propel the bacteria to escape from the harsh environment, while the latter is employed to neutralise the acidity in the surrounding microenvironment (Karkhah *et al.,* 2019). These two

factors cannot easily be applied with the drug system to give it additional advantages.

Of course, BabA is not the only adhesin expressed on the outer membrane. Other outer membrane proteins were also found on the bacterial cell surface (Kable *et al.,* 2017). At the same site, there is the lipopolysaccharide (LPS) which is the prevalent component of the outer membrane. LPS consists of lipid A, polysaccharide region and O-antigen chain. It was established that most of *H. pylori* strains have Lewis antigens, Le^x and Le^y, within the O-antigen region. This lead to variability in the structural organisation and length (Li *et al.,* 2018).

To know how the bacteria managed to use its adhesins to bind the gastric carbohydrate ligands in spite of the proteolytic and acidic environment, we anticipated that the oligosacchardies of the LPS are extended to cover most of the Crown. This could support BabA-Crown resistance to the acidity and pepsin digestion by providing a glycosylated microenvironment. However, measurement of the membrane thickness by electron microscopy, Attenuated Total Reflection Fourier Transfer Infra-Red (ATR-FTIR) spectroscopy (Bass and Freger, 2015) or indirectly through fluorescent lipid tension reporter (FliptR) (Colom *et al.,* 2018) should be done to confirm this finding.

7.1.5 Development of a novel glycan-binding drug using BabA-Crown

As emphasised throughout this thesis, the main object of this study was to develop functional glycan-binding particles which can increase the gastric retention time. Empirical *in vitro* and *in vivo* analysis to test the efficiency, viability and functionally of this drug delivery model are of great importance. However, due to the primary need to focus on tackling the glycan-binding issue, such experiments were limited in this thesis. It worth noting that, in this study, preliminary experiments were conducted using MUC5AC cell line as a gastric model. Unfortunately, these attempts required more optimisation to the cultural conditions to support the cellular expression of ABO/Le blood group antigens on their surface. More investigation is ongoing to establish this method, not only because of the need to confirm the outcomes obtained, but also to use a suitable *in vitro* model to study *H pylori* interactions with the human epithelium as proposed by (Boccellato *et al.,* 2019). Moreover, it will be required for future work to

1) Explore the properties of other adhesins as biomimetic vectors.

2) Investigate the particles' penetration ability and

3) Mechanisms of withstanding of these moieties against the frequent gastric mucus turnover.

Albeit there is no defined model developed for studying gastric mucin turnover, but the renewal rate of the mucus layer in the distal colon was studied (Johansson, 2012). Recently, mucus and glycocalyx turnover were analyzed in the small intestine by *in vivo* labeling of *O*-glycans with *N*-azidoacetylgalactosamine (Schneider *et al.,* 2018). These models could be applied/ optimised to be used for future experiments.

So far, using bacterial adhesin from *H. pylori* as specific lectin gastric-targeted drug delivery system has not been described in the literature. Other lectin candidates such as *Helix pomatia* (HPA) and *Ulex europaeus* agglutinin I (UEA-I) were tested toward blood group antigens and showed specificity to blood group A

and H antigens, respectively. However, cross-reactivity (non-specific binding) with other mucins was detected (Matsui *et al.,* 2001). Wheat germ agglutinin (WGA) interaction with pig gastric mucin (PGM) was studied. It was found that the WGA binding is specific to sialic acid and *N*-acetyl-glucosamine residues in PGM but fully reversible (Wirth *et al.,* 2002b).

In summary, it worth to keep trying with BabA-Crown or C-DnaJ-Cr to achieve proper folding and retain glycan-binding functionality by trying different expression system such as chaperone-fusion expression plasmid vectors (Kyratsous *et al.,* 2009) or try pMAL-c5X vector, which depends on maltose-binding protein (MBP) fusions (Lee *et al.,* 2015), then treating with Factor Xa for cleaving the protein from maltose-binding protein. Other strategy can be employed such as investigating BabA from different bacterial strains, assessing their binding capacity, then use the binding domain, the Crowns and/or BabA truncates for developing drug delivery system (more details below).

7.2 Future work

The experimentations presented throughout this thesis shed a light on some aspects that could be used for further development of gastroretentive drug delivery strategies. A future outlook could be drawn from unsuccessful attempts to generate fruitful outcomes.

1. Selecting a suitable form of BabA from different strains

H. pylori J99 strain does not possess a gene for *bab*C but contains one allele for each of *babA* gene (*jhp0833*) and *babB* gene (*jhp1164*). Homologous recombination between these genes leads to chimeric *bab*B/A gene. The resulting protein is active in Le^b-binding ability (Yamaoka, 2008). It would be interesting to try expressing the Crown domain from chimeric babA/B or *bab*B/A genes. This may give a general overview about sequence variations regarding BabA binding functionality and pepsin resistant ability. A published study (Fujimoto *et al.,* 2007) classified the bacterial binding ability through the level of BabA expression into three classes:

A. BabA-high producers (BabA-H), which includes strains that highly express BabA with high affinity to bind Le^b.
B. BabA-low producers (BabA-L), which include strains that express small amounts of BabA without binding to Le^b. These strains are highly associated with mucosal injury and duodenal ulcers.
C. BabA-negative strains, which include strains that do not possess a BabA gene and therefore do not express BabA protein.

This indicates that bacterial binding ability to the host cellular receptors does not only rely on the strength of BabA protein or oligomerisation, but also on the level of expression. Therefore, before selecting a Crown domain from any strain, it is better to investigate/quantify the strain level of BabA expression. Then produce the recombinant form by cloning and expression, followed by measuring the binding affinity. After selecting BabA proteins that of high affinities, the Crowns can be used for developing the drug delivery model. Moreover, since 17875 BabA appears to have 3x higher affinity than J99 BabA, it would an interesting candidate for drug delivery.

2. Confirming the mutant binding ability

BabA does not bind to Le^y because of the structural difference in Gal (β1-4)GlcNAc glycosidic linkage with Le^b and it is not a known receptor for *H. pylori* (Hage *et al.,* 2015a). To sustain the chronic colonization and evade the immune system, *H. pylori* mimics the host carbohydrates structures by expressing Lewis antigens on its surface (Leker *et al.,* 2017). Some of these glycans are expressed in deep gastric glands such as MUC6 type 2 antigens, which express Le^y and Le^x (Magalhães *et al.,* 2010). The result obtained in this work about the ability of the Crown mutant protein to bind to Le^y is interesting, and need to be considered for future research. In European population, expression of Le^y together with Le^x was found to be linked with atrophic chronic gastritis in *H. pylori* $VacA^+CagA^+$ strains more than strains expressing Le^a and Le^b (Broutet *et al.,* 2002). While in Asian patients, strains expressing $Le^{x,y}$ are associated with peptic ulcer but not with VacA and CagA expression (Zheng *et al.,* 2000). Le^y plays a role in angiogenesis and thrombomodulin domain 1 (TMD1), which acts as specific ligand (Kuo *et al.,* 2012) and enhances monocytes adhesion (Lin *et al.,* 2017). However, Le^y is associated with various forms of human tumours such as ovarian carcinoma, lung and colorectal adenocarcinomas and can be used for enhancing T cells anti-tumour activity or for immunotherapy (Westwood *et al.,* 2009). If the investigation revealed the ability of the Crown mutant form to specifically interact with Le^y, then a wide application could be followed. This will not only be the first lectin that discovered to bind to Le^y, but also could be used as a broad spectrum ligand for therapeutic or developing an effective drug delivery system.

3. Using cell culture model

Cell lines were used in this study but further optimization was needed, therefore, no result was included. This made a gap in knowledge and understanding of BabA-Crown binding capability which constituted one of the research limitations.

There is a pressing need for establishing an *in vitro* or *in vivo* gastric models for translational research as most cell lines are taken or transformed from gastric adenocarcinoma (Burkitt *et al.,* 2017). The knowledge derived from these types of cells have not comprehensively addressed *H. pylori* initial mechanism of infection in healthy patients. Therefore, several trials were conducted to establish a lab model to study how *H. pylori* initiate gastric colonisation. Gastric human

pluripotent stem cells have been used to form primitive gastric glands and led to identification of the association of CagA factor with c-Met receptor, which could enhance the initiation of cancer onset (McCracken *et al.,* 2014). New *in vitro* quasi-immortal tissue culture model was developed from spheroids and used as primary gastric cells to study the *H. pylori* mechanisms of infection (Schlaermann *et al.,* 2016). This place the gastric organoids as an emerging *in vitro* model system to study bacterial pathogenicity from the early stages. Different stem cell-derived organoid systems were recently reviewed in (Pompaiah and Bartfeld, 2017).

4. Mutagenesis of the cysteine residue

Cysteine is a conserved residue within BabA-Crown sequence and it could be an essential for binding and pH sensing abilities (Bugaytsova *et al.,* 2017). However, for the minimal binding domain it may not be essential, therefore, it worth to substitute the one which does not participate in binding with any other residues, such as Serine. It was established that changing Cysteine into Serine, by site-directed mutagenesis, in HopQ adhesin does not affect the binding functionality. Out of the six Cysteine residues, only 2 are essential for adherence and CagA delivery. Mutation in one of the disulphide bridges resulted in expression of HopQ in the periplasmic and outer-membrane fractions, while mutant *H. pylori* strain P12 having $HopQ_{C123S}$ bind to CEACAM1 molecules with the same strength as the wild type (Grzeszczuk *et al.,* 2018).

5. Use different techniques for investigating binding interaction

As most of the work performed in this study based on binding, other techniques could be used for future work to get more knowledge and better results.

A. Although ELISA was the predominant technique performed throughout this study, several techniques can be used to study the binding ability. This could be started with the newly reported ELISA-based method for detecting specific carbohydrates. This method utilised multivalent gold-nanoparticles conjugated with oligosaccharides for coating ELISA plates. This approach presented easy and high sensitive method for detection and quantifying the binding abilities (Chiodo *et al.,* 2013). This technique can be used as a

simple confirmatory test after coating gold nanoparticles with the glycoconjugates and test BabA-Crown interactions.

B. Isothermal titration calorimetry (ITC) is a biophysical tool for measuring the affinities and thermodynamic characteristic of binding interactions (Damian, 2013). This technique uses label-free protein and provides valuable data about the dissociation constants and thermodynamic parameters such as binding heat capacity, enthalpy and entropy (Boudker and Oh, 2015). ITC is useful tool in studying weak interactions (Ereño-Orbea *et al.,* 2018), therefore, it worth to study BabA-Crown binding affinities with this approach because it may detect transient binding ability to Le^b or demonstrate binding capabilities at human body temperature.

C. Surface plasmon resonance (SPR) is very useful technique for monitoring carbohydrate-lectin association and dissociation rate constants in real time (Thakur *et al.,* 2007). In this technique, only low amount of sample is needed (nM concentration) without labelling and can detect picomolar amount of analyte (Beseničar *et al.,* 2006). Recently, it has been used for glycan profiling of proteins using specific glycosidases (Wang *et al.,* 2017). It also very useful in investigating the dynamic dimeric assembly that blocks the lectin from binding to the cellular glycoreceptors as suggested by (Machida *et al.,* 2017).

D. Most of the mammalian cell surfaces are decorated by multiple glycans or glyco-conjugates, which play a role in defining the cell function. This elicits a continuous request to understand carbohydrates biological interactions in cell surface composition/function (O'Neil *et al.,* 2018). Glycan microarray is technique used to mimic these interactions and involves immobilising a large set of these glycans onto a solid-phase platform to be used for screening glycan-binding proteins (GBPs) such as lectins, antibodies or viruses (Song *et al.,* 2012). Even though this method needs small amount of protein, it is limited to the nature of the glycan and the enzymatic process used to generate the backbone components. It also provides little information about the protein binding specificity and ligand binding affinity (Leppänen and Cummings, 2010). The recently released method of assembly of cell-based glycan arrays offers a rapid and economic way for studying the interactions between the glycan and its binding protein. This array could be constructed using Chinese hamster ovary cell mutants Lec2

as a platform and through recombinant glycosyltransferases, sialic acid, fucose, and some monosaccharides analogues which are directly introduced on the cell surface (Briard *et al.,* 2018). Thus, it would be interesting to apply this recently developed technique as an alternative or additional technique in the future.

6. Glycosylation as a new look

Glycosylation is a common post-translation modification in the secretory pathway. It contributes in protein folding, intracellular trafficking and functional maturation in the eukaryotic cells (Xu and Ng, 2015). It is thought that about half of the secreted proteins are glycosylated to increase the stability, enhance the functionality and provide protection against proteolysis (Goettig, 2016).

The discovery of glycosylation in *Campylobacter jejuni* (Kelly *et al.,* 2006) unlocked the potential of post translation modifications in prokaryotic cells. The genes responsible for synthesising the N-linked glycosylation system were identified and demonstrated to be functional when transferred into *E. coli* (Wacker *et al.,* 2002). Until now, no such system was discovered in *H. pylori*, except the similar O-linked glycosylation system for flagella modification (Josenhans *et al.,* 2002). However, it was suggested by Champasa *et al.,* upon using mass spectrometry, that some of the bacterial proteins were glycosylated (Champasa *et al.,* 2013). These glycosylated protein may play a biological role such as in modulation of the host immune system (Gilbreath *et al.,* 2011). It was predicted that post-translational modification of surface adhesins form a protective conformational structures which enable the bacteria to be resistant to the hostile gastric environment (Szymanski and Wren, 2005). Some studies support this point, exemplified the presence of glycosylated proteins e.g. flagellar (Josenhans *et al.,* 2002), and the presence of fucosylated *N*-acetyllactosamine units in the lipopolysaccharides, which function to mimic surfaces glycoconjugates, that found in human gastric granulocytes (Aspinall *et al.,* 1996). Recently, *N*-linked protein glycosylation system was disclosed in *Helicobacter pullorum* and named HgpA (Jervis *et al.,* 2018). This glycan provides a bulky hydrophilic groups which may reduce protein dynamics but can stabilise the structure. It may also provide a precise conformation/oligomerization which influence the function (Jayaprakash

and Surolia, 2017). Moreover, *Yersinia kristensenii* and *Yersinia rohdei* used *N*-glycosylation to promote enzymes structure and function such as histidine acid phosphatase phytases. Through this mechanism, the bacteria can decrease pepsin's approachability to the active sites, enhancing proteins stability (Niu *et al.,* 2016). Thus, it would be very interesting to try expressing BabA-Crown in mammalian cells and test, if glycosylation can restore the Crown ligand binding ability.

7.3 Conclusion

The main objectives of this study were partially fulfilled, even though the ultimate goal is still ongoing. Below is a roadmap for the overall objectives.

1. Generation of the recombinant form of BabA J99 Crown region as the minimal Le^b binding domain through cloning and expression.

These molecular biological techniques used for establishing constructing an expression system for studying BabA-Crown for subsequent characterisation and its utilization as a drug targeting moiety. The protein was extracted from the periplasmic space of *E. coli* XL10-Gold, which was used for plasmid propagation and protein expression. The experimentations presented to achieve this objective demonstrated that optimising the growth conditions for a better expression could be achieved through 1) addition of the chloramphenicol to elevate the plasmid copy number and subsequently, successful protein expression. 2) Excluding the glucose from the growth medium restrain *Lac* operon repression which in turn led to protein synthesis and successful protein expression.

2. Testing the functionality of BabA-Crown protein

The ability of recombinant BabA-Crown protein to bind its host ligand (Le^b) and its resistance to simulated gastric acidity/peptic digestion were tested. These tests represented fundamental points in determining the minimal binding domain and to know if it could retain the binding functionality of whole BabA. It appeared that BabA-Crown as the minimal binding site was not able to render the adhesion functionality of BabA. Attempts to restore this loss of binding activity were performed using different truncates without solving the issue. In terms of testing pepsin digestion, BabA-Crown partial resistance to peptic hydrolysis could be the first milestone towards the successful generation of a protein/polypeptide for drug delivery. Full resistance could be developed, by point mutations in the Crown domain, for gastric targeting.

3. Developing a biomimetic drug delivery system.

While coating the microparticle with BabA-Crown to improve the binding functionality was not a useful process, $BabA_{527K}$ proved to retain the binding ability to its physiological ligand, Le^b. Overall, what has been achieved in this study laid a good foundation enabling further development of proof-of-principle for the use of BabA-Crown as the minimal binding site domain, also in the creation of a new gastric targeting drug delivery system which mimics *H. pylori* attachment mechanisms. As a final remark, encapsulating $BabA_{527K}$-microparticle with gastric-resistance polymer such as Eudragit S100 could reduce $BabA_{527K}$ sensitivity to peptic digestion (Beck *et al.,* 2008), provided that such encapsulation does not interfere with ligand binding properties. Other alternative way processe could be co-administration of pepsin inhibitors such as Pepstatin A. Otherwise, use natural additives such as sunset yellow food additive (sodium (E)-6-hydroxy-5-((4-sulfonatophenyl) diazenyl naphthalene-2-sulfonate), which is used as natural food, pharmaceutical and cosmetic colouring agent (Mohseni-Shahri *et al.,* 2018), or Nobiletin (5,6,7,8,3′,4′-hexamethoxyflavon), anti-inflammatory flavonoid found in citrus fruits, which were both suggested to inhibit pepsin activity (Zeng *et al.,* 2014b). Finally, as stated by Victor Hugo "we make the road, others will make the journey".

References

AHMAD, A. R., KAEWPUNGSUP, P., KHORATTANAKULCHAI, N., RATTANAPISIT, K., PAVASANT, P. & PHOOLCHAROEN, W. 2019. Recombinant human dentin matrix protein 1 (DMP1) induces the osteogenic differentiation of human periodontal ligament cells. *Biotechnology Reports,* 23**,** e00348.

AHMAD, I., NAWAZ, N., DARWESH, N. M., UR RAHMAN, S., MUSTAFA, M. Z., KHAN, S. B. & PATCHING, S. G. 2018. Overcoming challenges for amplified expression of recombinant proteins using Escherichia coli. *Protein Expression and Purification,* 144**,** 12-18.

AHN, J., CAO, M.-J., YU, Y. Q. & ENGEN, J. R. 2013. Accessing the reproducibility and specificity of pepsin and other aspartic proteases. *Biochimica et biophysica acta,* 1834**,** 1222-1229.

ALGOOD, H. M. & COVER, T. L. 2006. Helicobacter pylori persistence: an overview of interactions between H. pylori and host immune defenses. *Clin Microbiol Rev,* 19**,** 597-613.

ALI, A., NAZ, A., SOARES, S. C., BAKHTIAR, M., TIWARI, S., HASSAN, S. S., HANAN, F., RAMOS, R., PEREIRA, U., BARH, D., FIGUEIREDO, H. C. P., USSERY, D. W., MIYOSHI, A., SILVA, A. & AZEVEDO, V. 2015. Pan-genome analysis of human gastric pathogen H. pylori: comparative genomics and pathogenomics approaches to identify regions associated with pathogenicity and prediction of potential core therapeutic targets. *BioMed research international,* 2015**,** 139580-139580.

ALKOUT, A. M., BLACKWELL, C. C. & WEIR, D. M. 2000. Increased inflammatory responses of persons of blood group O to Helicobacter pylori. *J Infect Dis,* 181**,** 1364-9.

ALLEN, A. & FLEMSTROM, G. 2005. Gastroduodenal mucus bicarbonate barrier: protection against acid and pepsin. *Am J Physiol Cell Physiol,* 288**,** C1-19.

ALM, R. A., BINA, J., ANDREWS, B. M., DOIG, P., HANCOCK, R. E. & TRUST, T. J. 2000. Comparative genomics of Helicobacter pylori: analysis of the outer membrane protein families. *Infect Immun,* 68**,** 4155-68.

ALOMAR, M. J. 2014. Factors affecting the development of adverse drug reactions (Review article). *Saudi Pharmaceutical Journal,* 22**,** 83-94.

AMARTELY, H., AVRAHAM, O., FRIEDLER, A., LIVNAH, O. & LEBENDIKER, M. 2018. Coupling Multi Angle Light Scattering to Ion Exchange chromatography (IEX-MALS) for protein characterization. *Scientific Reports,* 8**,** 6907.

AMIEVA, M. R. & EL–OMAR, E. M. 2008. Host-Bacterial Interactions in Helicobacter pylori Infection. *Gastroenterology,* 134**,** 306-323.

ANDRIUSHCHENKO, S. V., BUKHARIN, O. V., PERUNOVA, N. B. & IVANOVA, E. V. 2011. [The increase of plasmid DNA copy number is a possible mechanism of the amplification of bacteria anti-lysozyme activity under the effect of chloramphenicol]. *Zh Mikrobiol Epidemiol Immunobiol***,** 8-13.

ANSARI, S. & YAMAOKA, Y. 2017. Helicobacter pylori BabA in adaptation for gastric colonization. *World journal of gastroenterology,* 23**,** 4158-4169.

ARNAOUTELI, S., FERREIRA, A. S., SCHOR, M., MORRIS, R. J., BROMLEY, K. M., JO, J., CORTEZ, K. L., SUKHODUB, T., PRESCOTT, A. R., DIETRICH, L. E. P., MACPHEE, C. E. & STANLEY-WALL, N. R. 2017. Bifunctionality of a biofilm matrix protein controlled by redox state. *Proc Natl Acad Sci U S A,* 114**,** E6184-e6191.

ARNAU, J., LAURITZEN, C., PETERSEN, G. E. & PEDERSEN, J. 2006. Current strategies for the use of affinity tags and tag removal for the purification of recombinant proteins. *Protein Expression and Purification,* 48**,** 1-13.

ASHRAF, S. S., BENSON, R. E., PAYNE, E. S., HALBLEIB, C. M. & GRØN, H. 2004. A novel multi-affinity tag system to produce high levels of soluble and biotinylated proteins in Escherichia coli. *Protein Expression and Purification,* 33**,** 238-245.

ASPHOLM-HURTIG, M., DAILIDE, G., LAHMANN, M., KALIA, A., ILVER, D., ROCHE, N., VIKSTROM, S., SJOSTROM, R., LINDEN, S., BACKSTROM, A., LUNDBERG, C., ARNQVIST, A., MAHDAVI, J., NILSSON, U. J., VELAPATINO, B., GILMAN, R. H., GERHARD, M., ALARCON, T., LOPEZ-BREA, M., NAKAZAWA, T., FOX, J. G., CORREA, P., DOMINGUEZ-BELLO, M. G., PEREZ-PEREZ, G. I., BLASER, M. J., NORMARK, S., CARLSTEDT, I., OSCARSON, S., TENEBERG, S., BERG, D. E. & BOREN, T. 2004. Functional adaptation of BabA, the H. pylori ABO blood group antigen binding adhesin. *Science,* 305**,** 519-22.

ASPHOLM, M., OLFAT, F. O., NORDEN, J., SONDEN, B., LUNDBERG, C., SJOSTROM, R., ALTRAJA, S., ODENBREIT, S., HAAS, R., WADSTROM, T., ENGSTRAND, L., SEMINO-MORA, C., LIU, H., DUBOIS, A., TENEBERG, S., ARNQVIST, A. & BOREN, T. 2006. SabA is the H. pylori hemagglutinin and is polymorphic in binding to sialylated glycans. *PLoS Pathog,* 2**,** e110.

ASPINALL, G. O., MONTEIRO, M. A., PANG, H., WALSH, E. J. & MORAN, A. P. 1996. Lipopolysaccharide of the Helicobacter pylori type strain NCTC 11637 (ATCC 43504): structure of the O antigen chain and core oligosaccharide regions. *Biochemistry,* 35**,** 2489-97.

ATHAVANKAR, S. & PETERSON, B. R. 2003. Control of Gene Expression with Small Molecules: Biotin-Mediated Acylation of Targeted Lysine Residues in Recombinant Yeast. *Chemistry & Biology,* 10**,** 1245-1253.

ATHERTON, J. C. & BLASER, M. J. 2009. Coadaptation of Helicobacter pylori and humans: ancient history, modern implications. *J Clin Invest,* 119**,** 2475-87.

AYDIN, S. 2015. A short history, principles, and types of ELISA, and our laboratory experience with peptide/protein analyses using ELISA. *Peptides,* 72**,** 4-15.

BÄCKSTRÖM, A., LUNDBERG, C., KERSULYTE, D., BERG, D. E., BORÉN, T. & ARNQVIST, A. 2004. Metastability of Helicobacter pylori bab adhesin genes and dynamics in Lewis b antigen binding. *Proceedings of the National Academy of Sciences of the United States of America,* 101**,** 16923-16928.

BAIESI, M., ORLANDINI, E., TROVATO, A. & SENO, F. 2016. Linking in domain-swapped protein dimers. *Scientific Reports,* 6**,** 33872.

BANEYX, F. & MUJACIC, M. 2004. Recombinant protein folding and misfolding in Escherichia coli. *Nat Biotechnol,* 22**,** 1399-408.

BANSIL, R. & TURNER, B. S. 2018. The biology of mucus: Composition, synthesis and organization. *Advanced Drug Delivery Reviews,* 124**,** 3-15.

BARDONNET, P. L., FAIVRE, V., PUGH, W. J., PIFFARETTI, J. C. & FALSON, F. 2006. Gastroretentive dosage forms: Overview and special case of Helicobacter pylori. *Journal of Controlled Release,* 111**,** 1-18.

BASS, M. & FREGER, V. 2015. Facile evaluation of coating thickness on membranes using ATR-FTIR. *Journal of Membrane Science,* 492**,** 348-354.

BAUMGARTEN, T., YTTERBERG, A. J., ZUBAREV, R. A. & DE GIER, J. W. 2018. Optimizing Recombinant Protein Production in the Escherichia coli Periplasm Alleviates Stress. *Appl Environ Microbiol,* 84.

BAUWENS, E., JOOSTEN, M., TAGANNA, J., ROSSI, M., DEBRAEKELEER, A., TAY, A., PETERS, F., BACKERT, S., FOX, J., DUCATELLE, R., REMAUT, H., HAESEBROUCK, F. & SMET, A. 2018. In silico proteomic and phylogenetic analysis of the outer membrane protein repertoire of gastric Helicobacter species. *Scientific reports,* 8**,** 15453-15453.

BECK, R. C. R., POHLMANN, A. R. & GUTERRES, S. S. 2008. Nanoparticle-coated microparticles: preparation and characterization. *Journal of Microencapsulation,* 21**,** 499-512.

BECKETT, D. 2018. Specificity and selectivity in post-translational biotin addition. *Biochem Soc Trans,* 46**,** 1577-1591.

BECKETT, D., KOVALEVA, E. & SCHATZ, P. J. 1999. A minimal peptide substrate in biotin holoenzyme synthetase-catalyzed biotinylation. *Protein Sci,* 8**,** 921-9.

BELOBORODOV, S. S., BAO, J., KRYLOVA, S. M., SHALA-LAWRENCE, A., JOHNSON, P. E. & KRYLOV, S. N. 2018. Aptamer facilitated purification of functional proteins. *Journal of Chromatography B,* 1073**,** 201-206.

BENKTANDER, J., ANGSTROM, J., BREIMER, M. E. & TENEBERG, S. 2012. Redefinition of the carbohydrate binding specificity of Helicobacter pylori BabA adhesin. *J Biol Chem,* 287**,** 31712-24.

BENOIT, R. M., WILHELM, R. N., SCHERER-BECKER, D. & OSTERMEIER, C. 2006. An improved method for fast, robust, and seamless integration of DNA fragments into multiple plasmids. *Protein Expr Purif,* 45**,** 66-71.

BENTLEY, W. E., MIRJALILI, N., ANDERSEN, D. C., DAVIS, R. H. & KOMPALA, D. S. 1990. Plasmid-encoded protein: the principal factor in the "metabolic burden" associated with recombinant bacteria. *Biotechnol Bioeng,* 35**,** 668-81.

BERGMANS, H. E., VAN DIE, I. M. & HOEKSTRA, W. P. 1981. Transformation in Escherichia coli: stages in the process. *J Bacteriol,* 146**,** 564-70.

BERGSTROM, K. S. & XIA, L. 2013. Mucin-type O-glycans and their roles in intestinal homeostasis. *Glycobiology,* 23**,** 1026-37.

BERKMEN, M. 2012. Production of disulfide-bonded proteins in Escherichia coli. *Protein Expr Purif,* 82**,** 240-51.

BERNKOP-SCHNÜRCH, A., GABOR, F., SZOSTAK, M. P. & LUBITZ, W. 1995. An adhesive drug delivery system based on K99-fimbriae. *European Journal of Pharmaceutical Sciences,* 3**,** 293-299.

BESENIČAR, M., MAČEK, P., LAKEY, J. H. & ANDERLUH, G. 2006. Surface plasmon resonance in protein–membrane interactions. *Chemistry and Physics of Lipids,* 141**,** 169-178.

BHAGWAT, S. R., HAJELA, K. & KUMAR, A. 2018. Proteolysis to Identify Protease Substrates: Cleave to Decipher. *PROTEOMICS,* 18**,** 1800011.

BIE, P., CHEN, L., LI, X. & LI, L. 2016. Characterization of concanavalin A-conjugated resistant starch acetate bioadhesive film for oral colon-targeting microcapsule delivery system. *Industrial Crops and Products,* 84**,** 320-329.

BIES, C., LEHR, C. M. & WOODLEY, J. F. 2004. Lectin-mediated drug targeting: history and applications. *Adv Drug Deliv Rev,* 56**,** 425-35.

BJARNASON, I., SCARPIGNATO, C., HOLMGREN, E., OLSZEWSKI, M., RAINSFORD, K. D. & LANAS, A. 2018. Mechanisms of Damage to the Gastrointestinal Tract From Nonsteroidal Anti-Inflammatory Drugs. *Gastroenterology,* 154**,** 500-514.

BJÖRKHOLM, B., ZHUKHOVITSKY, V., LÖFMAN, C., HULTÉN, K., ENROTH, H., BLOCK, M., RIGO, R., FALK, P. & ENGSTRAND, L. 2000. Helicobacter pylori

Entry into Human Gastric Epithelial Cells: A Potential Determinant of Virulence, Persistence, and Treatment Failures 1. *Helicobacter,* 5**,** 148-154.
BJÖRNHAM, O., BUGAYTSOVA, J., BORÉN, T. & SCHEDIN, S. 2009. Dynamic force spectroscopy of the Helicobacter pylori BabA–Lewis b Binding. *Biophysical Chemistry,* 143**,** 102-105.
BOCCELLATO, F., WOELFFLING, S., IMAI-MATSUSHIMA, A., SANCHEZ, G., GOOSMANN, C., SCHMID, M., BERGER, H., MOREY, P., DENECKE, C., ORDEMANN, J. & MEYER, T. F. 2019. Polarised epithelial monolayers of the gastric mucosa reveal insights into mucosal homeostasis and defence against infection. *Gut,* 68**,** 400.
BOOTH, W. T., SCHLACHTER, C. R., POTE, S., USSIN, N., MANK, N. J., KLAPPER, V., OFFERMANN, L. R., TANG, C., HURLBURT, B. K. & CHRUSZCZ, M. 2018. Impact of an N-terminal Polyhistidine Tag on Protein Thermal Stability. *ACS Omega,* 3**,** 760-768.
BOREN, T., FALK, P., ROTH, K. A., LARSON, G. & NORMARK, S. 1993. Attachment of Helicobacter pylori to human gastric epithelium mediated by blood group antigens. *Science,* 262**,** 1892-5.
BOUDKER, O. & OH, S. 2015. Isothermal titration calorimetry of ion-coupled membrane transporters. *Methods (San Diego, Calif.),* 76**,** 171-182.
BRANTL, S. 2014. Plasmid Replication Control by Antisense RNAs. *Microbiol Spectr,* 2**,** Plas-0001-2013.
BRAR, S. K. & VERMA, M. 2011. Measurement of nanoparticles by light-scattering techniques. *TrAC Trends in Analytical Chemistry,* 30**,** 4-17.
BRIARD, J. G., JIANG, H., MOREMEN, K. W., MACAULEY, M. S. & WU, P. 2018. Cell-based glycan arrays for probing glycan–glycan binding protein interactions. *Nature Communications,* 9**,** 880.
BRITANNICA, E. 2010. https://www.britannica.com/science/gastric-gland.
BROOKS, S. A. 2017. Lectin Histochemistry: Historical Perspectives, State of the Art, and the Future. *Methods Mol Biol,* 1560**,** 93-107.
BROUTET, N., MORAN, A., HYNES, S., SAKAROVITCH, C. & MEGRAUD, F. 2002. Lewis Antigen Expression and Other Pathogenic Factors in the Presence of Atrophic Chronic Gastritis in a European Population. *The Journal of Infectious Diseases,* 185**,** 503-512.
BROWN, J. H. 2006. Breaking symmetry in protein dimers: designs and functions. *Protein science : a publication of the Protein Society,* 15**,** 1-13.
BRUCE, M. G. & MAAROOS, H. I. 2008. Epidemiology of Helicobacter pylori infection. *Helicobacter,* 13 Suppl 1**,** 1-6.
BRUCKNER, R. & TITGEMEYER, F. 2002. Carbon catabolite repression in bacteria: choice of the carbon source and autoregulatory limitation of sugar utilization. *FEMS Microbiol Lett,* 209**,** 141-8.
BRUSOTTI, G., CALLERI, E., COLOMBO, R., MASSOLINI, G., RINALDI, F. & TEMPORINI, C. 2018. Advances on Size Exclusion Chromatography and Applications on the Analysis of Protein Biopharmaceuticals and Protein Aggregates: A Mini Review. *Chromatographia,* 81**,** 3-23.
BUDA, A., FACCHIN, S., DASSIE, E., CASARIN, E., JEPSON, M. A., NEUMANN, H., HATEM, G., REALDON, S., D'INCA, R., STURNIOLO, G. C. & MORPURGO, M. 2015. Detection of a fluorescent-labeled avidin-nucleic acid nanoassembly by confocal laser endomicroscopy in the microvasculature of chronically inflamed intestinal mucosa. *Int J Nanomedicine,* 10**,** 399-408.
BUGAYTSOVA, J. A., BJORNHAM, O., CHERNOV, Y. A., GIDEONSSON, P., HENRIKSSON, S., MENDEZ, M., SJOSTROM, R., MAHDAVI, J., SHEVTSOVA, A., ILVER, D., MOONENS, K., QUINTANA-HAYASHI, M. P., MOSKALENKO,

R., AISENBREY, C., BYLUND, G., SCHMIDT, A., ABERG, A., BRANNSTROM, K., KONIGER, V., VIKSTROM, S., RAKHIMOVA, L., HOFER, A., OGREN, J., LIU, H., GOLDMAN, M. D., WHITMIRE, J. M., ADEN, J., YOUNSON, J., KELLY, C. G., GILMAN, R. H., CHOWDHURY, A., MUKHOPADHYAY, A. K., NAIR, G. B., PAPADAKOS, K. S., MARTINEZ-GONZALEZ, B., SGOURAS, D. N., ENGSTRAND, L., UNEMO, M., DANIELSSON, D., SUERBAUM, S., OSCARSON, S., MOROZOVA-ROCHE, L. A., OLOFSSON, A., GROBNER, G., HOLGERSSON, J., ESBERG, A., STROMBERG, N., LANDSTROM, M., ELDRIDGE, A. M., CHROMY, B. A., HANSEN, L. M., SOLNICK, J. V., LINDEN, S. K., HAAS, R., DUBOIS, A., MERRELL, D. S., SCHEDIN, S., REMAUT, H., ARNQVIST, A., BERG, D. E. & BOREN, T. 2017. Helicobacter pylori Adapts to Chronic Infection and Gastric Disease via pH-Responsive BabA-Mediated Adherence. *Cell Host Microbe,* 21**,** 376-389.

BURKITT, M. D., DUCKWORTH, C. A., WILLIAMS, J. M. & PRITCHARD, D. M. 2017. Helicobacter pylori-induced gastric pathology: insights from in vivo and ex vivo models. *Disease models & mechanisms,* 10**,** 89-104.

BUSCH, F. M., SAHASRABUDDHE, A., VANAERNUM, Z., RIVERA, B. & WYSOCKI, V. H. 2017. Analysis of proteins and protein interactions by size exclusion chromatography – high resolution mass spectrometry. *The FASEB Journal,* 31**,** 926.9-926.9.

BUTLER, J. E. 2000. Solid Supports in Enzyme-Linked Immunosorbent Assay and Other Solid-Phase Immunoassays. *Methods,* 22**,** 4-23.

BUZID, A., HAYES, P. E., GLENNON, J. D. & LUONG, J. H. T. 2019. Captavidin as a regenerable biorecognition element on boron-doped diamond for biotin sensing. *Analytica Chimica Acta,* 1059**,** 42-48.

CAMPS, M. 2010. Modulation of ColE1-like plasmid replication for recombinant gene expression. *Recent Pat DNA Gene Seq,* 4**,** 58-73.

CARLSON, T. L., LOCK, J. Y. & CARRIER, R. L. 2018. Engineering the Mucus Barrier. *Annual review of biomedical engineering,* 20**,** 197-220.

CARVALHO, F. C., BRUSCHI, M. L., EVANGELISTA, R. C. & GREMIAO, M. P. D. 2010. Mucoadhesive drug delivery systems. *Brazilian Journal of Pharmaceutical Sciences,* 46**,** 1-17.

CASTANIÉ-CORNET, M.-P., BRUEL, N. & GENEVAUX, P. 2014. Chaperone networking facilitates protein targeting to the bacterial cytoplasmic membrane. *Biochimica et Biophysica Acta (BBA) - Molecular Cell Research,* 1843**,** 1442-1456.

CELIE, P. H., PARRET, A. H. & PERRAKIS, A. 2016. Recombinant cloning strategies for protein expression. *Curr Opin Struct Biol,* 38**,** 145-54.

CELLI, J. P., TURNER, B. S., AFDHAL, N. H., KEATES, S., GHIRAN, I., KELLY, C. P., EWOLDT, R. H., MCKINLEY, G. H., SO, P., ERRAMILLI, S. & BANSIL, R. 2009. Helicobacter pylori moves through mucus by reducing mucin viscoelasticity. *Proc Natl Acad Sci U S A,* 106**,** 14321-6.

CERDA, O. A., NUNEZ-VILLENA, F., SOTO, S. E., UGALDE, J. M., LOPEZ-SOLIS, R. & TOLEDO, H. 2011. tlpA gene expression is required for arginine and bicarbonate chemotaxis in Helicobacter pylori. *Biol Res,* 44**,** 277-82.

CHAMPASA, K., LONGWELL, S. A., ELDRIDGE, A. M., STEMMLER, E. A. & DUBE, D. H. 2013. Targeted identification of glycosylated proteins in the gastric pathogen Helicobacter pylori (Hp). *Mol Cell Proteomics,* 12**,** 2568-86.

CHAPMAN-SMITH, A. & CRONAN, J. E., JR. 1999. Molecular biology of biotin attachment to proteins. *J Nutr,* 129**,** 477S-484S.

CHARIFSON, P. S. & WALTERS, W. P. 2014. Acidic and Basic Drugs in Medicinal Chemistry: A Perspective. *Journal of Medicinal Chemistry,* 57**,** 9701-9717.

CHATZI, K. E., SARDIS, M. F., KARAMANOU, S. & ECONOMOU, A. 2013. Breaking on through to the other side: protein export through the bacterial Sec system. *Biochem J,* 449**,** 25-37.

CHEETHAM, M. E. & CAPLAN, A. J. 1998. Structure, function and evolution of DnaJ: conservation and adaptation of chaperone function. *Cell Stress Chaperones,* 3**,** 28-36.

CHEN, C., LU, Y., WANG, L., YU, H. & TIAN, H. 2018a. CcpA-Dependent Carbon Catabolite Repression Regulates Fructooligosaccharides Metabolism in Lactobacillus plantarum. *Frontiers in Microbiology,* 9.

CHEN, J., BLEVINS, W. E., PARK, H. & PARK, K. 2000. Gastric retention properties of superporous hydrogel composites. *Journal of Controlled Release,* 64**,** 39-51.

CHEN, L., YAN, C. & ZHENG, Z. 2018b. Functional polymer surfaces for controlling cell behaviors. *Materials Today,* 21**,** 38-59.

CHEN, R. 2012. Bacterial expression systems for recombinant protein production: E. coli and beyond. *Biotechnol Adv,* 30**,** 1102-7.

CHIODO, F., MARRADI, M., TEFSEN, B., SNIPPE, H., VAN DIE, I. & PENADÉS, S. 2013. High Sensitive Detection of Carbohydrate Binding Proteins in an ELISA-Solid Phase Assay Based on Multivalent Glyconanoparticles. *PLOS ONE,* 8**,** e73027.

CHMIELA, M. & GONCIARZ, W. 2017. Molecular mimicry in Helicobacter pylori infections. *World J Gastroenterol,* 23**,** 3964-3977.

CHMIELA, M., MISZCZYK, E. & RUDNICKA, K. 2014. Structural modifications of Helicobacter pylori lipopolysaccharide: an idea for how to live in peace. *World J Gastroenterol,* 20**,** 9882-97.

CHMIELA, M., WALCZAK, N. & RUDNICKA, K. 2018. Helicobacter pylori outer membrane vesicles involvement in the infection development and Helicobacter pylori-related diseases. *J Biomed Sci,* 25**,** 78.

CHOI, H. S. & FRANGIONI, J. V. 2010. Nanoparticles for biomedical imaging: fundamentals of clinical translation. *Mol Imaging,* 9**,** 291-310.

CHOI, J. H. & LEE, S. Y. 2004. Secretory and extracellular production of recombinant proteins using Escherichia coli. *Appl Microbiol Biotechnol,* 64**,** 625-35.

CHU, Y.-T., WANG, Y.-H., WU, J.-J. & LEI, H.-Y. 2010. IInvasion and Multiplication of Helicobacter pylori in Gastric Epithelial Cells and Implications for Antibiotic Resistance. *Infection and Immunity,* 78**,** 4157.

CLEWELL, D. B. 1972. Nature of Col E 1 plasmid replication in Escherichia coli in the presence of the chloramphenicol. *J Bacteriol,* 110**,** 667-76.

CLOWARD, J. M. & KRAUSE, D. C. 2009. Mycoplasma pneumoniae J-domain protein required for terminal organelle function. *Molecular microbiology,* 71**,** 1296-1307.

COELHO, L. C., SILVA, P. M., LIMA, V. L., PONTUAL, E. V., PAIVA, P. M., NAPOLEAO, T. H. & CORREIA, M. T. 2017. Lectins, Interconnecting Proteins with Biotechnological/Pharmacological and Therapeutic Applications. *Evid Based Complement Alternat Med,* 2017**,** 1594074.

COHEN, E. J., FERREIRA, J. L., LADINSKY, M. S., BEEBY, M. & HUGHES, K. T. 2017. Nanoscale-length control of the flagellar driveshaft requires hitting the tethered outer membrane. *Science,* 356**,** 197-200.

COLOM, A., DERIVERY, E., SOLEIMANPOUR, S., TOMBA, C., MOLIN, M. D., SAKAI, N., GONZÁLEZ-GAITÁN, M., MATILE, S. & ROUX, A. 2018. A fluorescent membrane tension probe. *Nature Chemistry,* 10**,** 1118-1125.

CONE, R. A. 2009. Barrier properties of mucus. *Advanced Drug Delivery Reviews,* 61**,** 75-85.

COOKE, C. L., HUFF, J. L. & SOLNICK, J. V. 2005. The role of genome diversity and immune evasion in persistent infection with Helicobacter pylori. *FEMS Immunol Med Microbiol,* 45**,** 11-23.

COPPENS, F., CASTALDO, G., DEBRAEKELEER, A., SUBEDI, S., MOONENS, K., LO, A. & REMAUT, H. 2018. Hop-family Helicobacter outer membrane adhesins form a novel class of Type 5-like secretion proteins with an interrupted beta-barrel domain. *Mol Microbiol,* 110**,** 33-46.

CORFIELD, A. P. 2015. Mucins: a biologically relevant glycan barrier in mucosal protection. *Biochim Biophys Acta,* 1850**,** 236-52.

CROXEN, M. A., SISSON, G., MELANO, R. & HOFFMAN, P. S. 2006a. The Helicobacter pylori Chemotaxis Receptor TlpB (HP0103) Is Required for pH Taxis and for Colonization of the Gastric Mucosa. *Journal of Bacteriology,* 188**,** 2656-2665.

CROXEN, M. A., SISSON, G., MELANO, R. & HOFFMAN, P. S. 2006b. The Helicobacter pylori chemotaxis receptor TlpB (HP0103) is required for pH taxis and for colonization of the gastric mucosa. *J Bacteriol,* 188**,** 2656-65.

CUSUMANO, C. K., PINKNER, J. S., HAN, Z., GREENE, S. E., FORD, B. A., CROWLEY, J. R., HENDERSON, J. P., JANETKA, J. W. & HULTGREN, S. J. 2011. Treatment and prevention of urinary tract infection with orally active FimH inhibitors. *Sci Transl Med,* 3**,** 109ra115.

DAMIAN, L. 2013. Isothermal Titration Calorimetry for Studying Protein–Ligand Interactions. *In:* WILLIAMS, M. A. & DAVITER, T. (eds.) *Protein-Ligand Interactions: Methods and Applications.* Totowa, NJ: Humana Press.

DARANDALE, S. S. & VAVIA, P. R. 2012. Design of a gastroretentive mucoadhesive dosage form of furosemide for controlled release. *Acta Pharmaceutica Sinica B,* 2**,** 509-517.

DAS NEVES, J., BAHIA, M. F., AMIJI, M. M. & SARMENTO, B. 2011. Mucoadhesive nanomedicines: characterization and modulation of mucoadhesion at the nanoscale. *Expert Opinion on Drug Delivery,* 8**,** 1085-1104.

DAUTIN, N. & BERNSTEIN, H. D. 2007. Protein secretion in gram-negative bacteria via the autotransporter pathway. *Annu Rev Microbiol,* 61**,** 89-112.

DAVIS, S. S. 2005. Formulation strategies for absorption windows. *Drug Discovery Today,* 10**,** 249-257.

DAVIS, S. S., HARDY, J. G. & FARA, J. W. 1986. Transit of pharmaceutical dosage forms through the small intestine. *Gut,* 27**,** 886-892.

DE BOLOS, C., GARRIDO, M. & REAL, F. X. 1995. MUC6 apomucin shows a distinct normal tissue distribution that correlates with Lewis antigen expression in the human stomach. *Gastroenterology,* 109**,** 723-34.

DE GROOT, N. S. & VENTURA, S. 2006. Effect of temperature on protein quality in bacterial inclusion bodies. *FEBS Letters,* 580**,** 6471-6476.

DE JONGE, R., POT, R. G., LOFFELD, R. J., VAN VLIET, A. H., KUIPERS, E. J. & KUSTERS, J. G. 2004. The functional status of the Helicobacter pylori sabB adhesin gene as a putative marker for disease outcome. *Helicobacter,* 9**,** 158-64.

DE MARCO, A. 2009. Strategies for successful recombinant expression of disulfide bond-dependent proteins in Escherichia coli. *Microb Cell Fact,* 8**,** 26.

DE SABLET, T., PIAZUELO, M. B., SHAFFER, C. L., SCHNEIDER, B. G., ASIM, M., CHATURVEDI, R., BRAVO, L. E., SICINSCHI, L. A., DELGADO, A. G., MERA, R. M., ISRAEL, D. A., ROMERO-GALLO, J., PEEK, R. M., COVER, T. L., CORREA, P. & WILSON, K. T. 2011. Phylogeographic origin of

Helicobacter pylori is a determinant of gastric cancer risk. *Gut,* 60**,** 1189.

DEMAIN, A. L. & VAISHNAV, P. 2009. Production of recombinant proteins by microbes and higher organisms. *Biotechnology Advances,* 27**,** 297-306.

DESHMUKH, K., RAMANAN, S. R. & KOWSHIK, M. 2019. Novel one step transformation method for Escherichia coli and Staphylococcus aureus using arginine-glucose functionalized hydroxyapatite nanoparticles. *Mater Sci Eng C Mater Biol Appl,* 96**,** 58-65.

DESHPANDE, S., MASURKAR, N. D., GIRISH, V. M., DESAI, M., CHAKRABORTY, G., CHAN, J. M. & DRUM, C. L. 2017. Thermostable exoshells fold and stabilize recombinant proteins. *Nat Commun,* 8**,** 1442.

DEUTSCHER, J. 2008. The mechanisms of carbon catabolite repression in bacteria. *Curr Opin Microbiol,* 11**,** 87-93.

DEUTSCHER, J., FRANCKE, C. & POSTMA, P. W. 2006. How phosphotransferase system-related protein phosphorylation regulates carbohydrate metabolism in bacteria. *Microbiol Mol Biol Rev,* 70**,** 939-1031.

DEVI, R. V. & BASIL-ROSE, M. R. 2018. Lectins as Ligands for Directing Nanostructured Systems. *Curr Drug Deliv,* 15**,** 448-452.

DÍAZ-VILLANUEVA, J. F., DÍAZ-MOLINA, R. & GARCÍA-GONZÁLEZ, V. 2015. Protein Folding and Mechanisms of Proteostasis. *International journal of molecular sciences,* 16**,** 17193-17230.

DILWORTH, M. V., PIEL, M. S., BETTANEY, K. E., MA, P., LUO, J., SHARPLES, D., POYNER, D. R., GROSS, S. R., MONCOQ, K., HENDERSON, P. J. F., MIROUX, B. & BILL, R. M. 2018. Microbial expression systems for membrane proteins. *Methods,* 147**,** 3-39.

DINOS, G., ATHANASSOPOULOS, C., MISSIRI, D., GIANNOPOULOU, P., VLACHOGIANNIS, I., PAPADOPOULOS, G., PAPAIOANNOU, D. & KALPAXIS, D. 2016. Chloramphenicol Derivatives as Antibacterial and Anticancer Agents: Historic Problems and Current Solutions. *Antibiotics,* 5**,** 20.

DOMBKOWSKI, A. A., SULTANA, K. Z. & CRAIG, D. B. 2014. Protein disulfide engineering. *FEBS Letters,* 588**,** 206-212.

DONOVAN, R. S., ROBINSON, C. W. & GLICK, B. R. 1996. Review: optimizing inducer and culture conditions for expression of foreign proteins under the control of the lac promoter. *J Ind Microbiol,* 16**,** 145-54.

DORE, M. P., SEPULVEDA, A. R., EL-ZIMAITY, H., YAMAOKA, Y., OSATO, M. S., MOTOTSUGU, K., NIEDDU, A. M., REALDI, G. & GRAHAM, D. Y. 2001. Isolation of Helicobacter pylori from sheep-implications for transmission to humans. *Am J Gastroenterol,* 96**,** 1396-401.

DU, R., LI, S. & ZHANG, X. 2011. A modified plasmid vector pCMV-3Tag-LIC for rapid, reliable, ligation-independent cloning of polymerase chain reaction products. *Anal Biochem,* 408**,** 357-9.

DUFF, M. R., JR., GRUBBS, J. & HOWELL, E. E. 2011. Isothermal titration calorimetry for measuring macromolecule-ligand affinity. *Journal of visualized experiments : JoVE***,** 2796.

DUNDAS, C. M., DEMONTE, D. & PARK, S. 2013. Streptavidin-biotin technology: improvements and innovations in chemical and biological applications. *Appl Microbiol Biotechnol,* 97**,** 9343-53.

DUNNE, C. 2014. Factors that mediate colonization of the human stomach byHelicobacter pylori. *World Journal of Gastroenterology,* 20**,** 5610.

DVORAK, P., CHRAST, L., NIKEL, P. I., FEDR, R., SOUCEK, K., SEDLACKOVA, M., CHALOUPKOVA, R., DE LORENZO, V., PROKOP, Z. & DAMBORSKY, J. 2015.

Exacerbation of substrate toxicity by IPTG in Escherichia coli BL21(DE3) carrying a synthetic metabolic pathway. *Microb Cell Fact,* 14**,** 201.

EELTINK, S., WOUTERS, S., DORES-SOUSA, J. L. & SVEC, F. 2017. Advances in organic polymer-based monolithic column technology for high-resolution liquid chromatography-mass spectrometry profiling of antibodies, intact proteins, oligonucleotides, and peptides. *Journal of Chromatography A,* 1498**,** 8-21.

EIDA, S., VAN CAUTEREN, M., HOTOKEZAKA, Y., KATAYAMA, I., SASAKI, M., OBARA, M., OKUAKI, T., SUMI, M. & NAKAMURA, T. 2016. Length of intact plasma membrane determines the diffusion properties of cellular water. *Sci Rep,* 6**,** 19051.

ELIA, G. 2008. Biotinylation reagents for the study of cell surface proteins. *Proteomics,* 8**,** 4012-24.

ELIYAHU, S., AHARON, A. & BIANCO-PELED, H. 2018. Acrylated Chitosan Nanoparticles with Enhanced Mucoadhesion. *Polymers (Basel),* 10.

ENGVALL, E. & PERLMANN, P. 1971. Enzyme-linked immunosorbent assay (ELISA) quantitative assay of immunoglobulin G. *Immunochemistry,* 8**,** 871-874.

ENSIGN, L. M., CONE, R. & HANES, J. 2012. Oral drug delivery with polymeric nanoparticles: the gastrointestinal mucus barriers. *Adv Drug Deliv Rev,* 64**,** 557-70.

EOM, G.-E. & KIM, S. 2018. Identification of Nucleophilic Probes for Protease-Mediated Transpeptidation. *Molecules,* 23**,** 2109.

EREÑO-ORBEA, J., SICARD, T., CUI, H., AKULA, I. & JULIEN, J.-P. 2018. Characterization of Glycoproteins with the Immunoglobulin Fold by X-Ray Crystallography and Biophysical Techniques. *Journal of visualized experiments : JoVE***,** 57750.

ERNI, W. & HELD, K. 1987. The hydrodynamically balanced system: a novel principle of controlled drug release. *Eur Neurol,* 27 Suppl 1**,** 21-7.

ESTRADA-MARTÍNEZ, L. E., MORENO-CELIS, U., CERVANTES-JIMÉNEZ, R., FERRIZ-MARTÍNEZ, R. A., BLANCO-LABRA, A. & GARCÍA-GASCA, T. 2017. Plant Lectins as Medical Tools against Digestive System Cancers. *International journal of molecular sciences,* 18**,** 1403.

EZPELETA, I., IRACHE, J. M., STAINMESSE, S., CHABENAT, C., GUEGUEN, J. & ORECCHIONI, A. M. 1996. Preparation of lectin-vicilin nanoparticle conjugates using the carbodiimide coupling technique. *International Journal of Pharmaceutics,* 142**,** 227-233.

FAIRHEAD, M. & HOWARTH, M. 2015. Site-specific biotinylation of purified proteins using BirA. *Methods Mol Biol,* 1266**,** 171-84.

FALK, P. 2001. Why does Helicobacter pylori actually have Lewis antigens? *Trends in Microbiology,* 9**,** 61-62.

FALL, R. R., NERVI, A. M., ALBERTS, A. W. & VAGELOS, P. R. 1971. Acetyl CoA carboxylase: isolation and characterization of native biotin carboxyl carrier protein. *Proc Natl Acad Sci U S A,* 68**,** 1512-5.

FALL, R. R. & VAGELOS, P. R. 1972. Acetyl coenzyme A carboxylase. Molecular forms and subunit composition of biotin carboxyl carrier protein. *J Biol Chem,* 247**,** 8005-15.

FASINU, P., PILLAY, V., NDESENDO, V. M., DU TOIT, L. C. & CHOONARA, Y. E. 2011. Diverse approaches for the enhancement of oral drug bioavailability. *Biopharm Drug Dispos,* 32**,** 185-209.

FEI, Y. Y., SCHMIDT, A., BYLUND, G., JOHANSSON, D. X., HENRIKSSON, S., LEBRILLA, C., SOLNICK, J. V., BOREN, T. & ZHU, X. D. 2011. Use of real-

time, label-free analysis in revealing low-affinity binding to blood group antigens by Helicobacter pylori. *Anal Chem,* 83**,** 6336-41.
FELDMAN, M. 1983. Gastric bicarbonate secretion in humans. Effect of pentagastrin, bethanechol, and 11,16,16-trimethyl prostaglandin E2. *Journal of Clinical Investigation,* 72**,** 295-303.
FELT, O., BURI, P. & GURNY, R. 1998. Chitosan: A unique polysaccharide for drug delivery. *Drug Development and Industrial Pharmacy,* 24**,** 979-993.
FERNÁNDEZ-CASTANÉ, A., CAMINAL, G. & LÓPEZ-SANTÍN, J. 2012. Direct measurements of IPTG enable analysis of the induction behavior of E. coli in high cell density cultures. *Microbial Cell Factories,* 11**,** 58-58.
FERRER-MIRALLES, N., CORCHERO, J. L., KUMAR, P., CEDANO, J. A., GUPTA, K. C., VILLAVERDE, A. & VAZQUEZ, E. 2011. Biological activities of histidine-rich peptides; merging biotechnology and nanomedicine. *Microb Cell Fact,* 10**,** 101.
FOGEN, D., WU, S.-C., NG, K. K.-S. & WONG, S.-L. 2015. Engineering Streptavidin and a Streptavidin-Binding Peptide with Infinite Binding Affinity and Reversible Binding Capability: Purification of a Tagged Recombinant Protein to High Purity via Affinity-Driven Thiol Coupling. *PLOS ONE,* 10**,** e0139137.
FORMOSA-DAGUE, C., CASTELAIN, M., MARTIN-YKEN, H., DUNKER, K., DAGUE, E. & SLETMOEN, M. 2018. The Role of Glycans in Bacterial Adhesion to Mucosal Surfaces: How Can Single-Molecule Techniques Advance Our Understanding? *Microorganisms,* 6**,** 39.
FORSSTROM, B., AXNAS, B. B., STENGELE, K. P., BUHLER, J., ALBERT, T. J., RICHMOND, T. A., HU, F. J., NILSSON, P., HUDSON, E. P., ROCKBERG, J. & UHLEN, M. 2014. Proteome-wide epitope mapping of antibodies using ultra-dense peptide arrays. *Mol Cell Proteomics,* 13**,** 1585-97.
FORSSTRÖM, B., BISŁAWSKA AXNÄS, B., ROCKBERG, J., DANIELSSON, H., BOHLIN, A. & UHLEN, M. 2015. Dissecting Antibodies with Regards to Linear and Conformational Epitopes. *PLoS ONE,* 10**,** e0121673.
FOSTER, N., CLARK, M. A., JEPSON, M. A. & HIRST, B. H. 1998. Ulex europaeus 1 lectin targets microspheres to mouse Peyer's patch M-cells in vivo. *Vaccine,* 16**,** 536-41.
FRAENKEL, D. G. & NEIDHARDT, F. C. 1961. Use of chloramphenicol to study control of RNA synthesis in bacteria. *Biochimica et Biophysica Acta,* 53**,** 96-110.
FRENKEL, L. & BREMER, H. 1986. Increased amplification of plasmids pBR322 and pBR327 by low concentrations of chloramphenicol. *Dna,* 5**,** 539-44.
FUJIMOTO, S., OLANIYI OJO, O., ARNQVIST, A., YIH WU, J., ODENBREIT, S., HAAS, R., GRAHAM, D. Y. & YAMAOKA, Y. 2007. Helicobacter pylori BabA Expression, Gastric Mucosal Injury, and Clinical Outcome. *Clinical Gastroenterology and Hepatology,* 5**,** 49-58.
GABOR, F., BERNKOP-SCHNURCH, A. & HAMILTON, G. 1997. Bioadhesion to the intestine by means of E-coli K99-fimbriae: Gastrointestinal stability and specificity of adherence. *European Journal of Pharmaceutical Sciences,* 5**,** 233-242.
GAMBINOSSI, F., MYLON, S. E. & FERRI, J. K. 2015. Aggregation kinetics and colloidal stability of functionalized nanoparticles. *Advances in Colloid and Interface Science,* 222**,** 332-349.
GAO, Y., HUANG, X., ZHU, Y. & LV, Z. 2018. A brief review of monoclonal antibody technology and its representative applications in immunoassays. *J Immunoassay Immunochem,* 39**,** 351-364.

GARCÍA-DÍAZ, M., BIRCH, D., WAN, F. & NIELSEN, H. M. 2018. The role of mucus as an invisible cloak to transepithelial drug delivery by nanoparticles. *Advanced Drug Delivery Reviews,* 124**,** 107-124.

GARIBYAN, L. & AVASHIA, N. 2013. Polymerase chain reaction. *The Journal of investigative dermatology,* 133**,** 1-4.

GENEVAUX, P., GEORGOPOULOS, C. & KELLEY, W. L. 2007. The Hsp70 chaperone machines of Escherichia coli: a paradigm for the repartition of chaperone functions. *Molecular Microbiology,* 66**,** 840-857.

GEORGE, A., SHAH, P. A. & SHRIVASTAV, P. S. 2019. Natural biodegradable polymers based nano-formulations for drug delivery: A review. *International Journal of Pharmaceutics,* 561**,** 244-264.

GILBREATH, J. J., CODY, W. L., MERRELL, D. S. & HENDRIXSON, D. R. 2011. Change is good: variations in common biological mechanisms in the epsilonproteobacterial genera Campylobacter and Helicobacter. *Microbiology and molecular biology reviews : MMBR,* 75**,** 84-132.

GLICK, B. R. 1995. Metabolic load and heterologous gene expression. *Biotechnol Adv,* 13**,** 247-61.

GOEMANS, C., DENONCIN, K. & COLLET, J.-F. 2014. Folding mechanisms of periplasmic proteins. *Biochimica et Biophysica Acta (BBA) - Molecular Cell Research,* 1843**,** 1517-1528.

GOETTIG, P. 2016. Effects of Glycosylation on the Enzymatic Activity and Mechanisms of Proteases. *International Journal of Molecular Sciences,* 17.

GONZALEZ-MONTALBAN, N., NATALELLO, A., GARCIA-FRUITOS, E., VILLAVERDE, A. & DOGLIA, S. M. 2008. In situ protein folding and activation in bacterial inclusion bodies. *Biotechnology and Bioengineering,* 100**,** 797-802.

GÖRKE, B. & STÜLKE, J. 2008. Carbon catabolite repression in bacteria: many ways to make the most out of nutrients. *Nature Reviews Microbiology,* 6**,** 613-624.

GOYAL, R. K., GUO, Y. & MASHIMO, H. 2019. Advances in the physiology of gastric emptying. *Neurogastroenterology & Motility,* 31**,** e13546.

GRANGE, R. D., THOMPSON, J. P. & LAMBERT, D. G. 2014. Radioimmunoassay, enzyme and non-enzyme-based immunoassays. *BJA: British Journal of Anaesthesia,* 112**,** 213-216.

GRASLUND, S., NORDLUND, P., WEIGELT, J., HALLBERG, B. M., BRAY, J., GILEADI, O., KNAPP, S., OPPERMANN, U., ARROWSMITH, C., HUI, R., MING, J., DHE-PAGANON, S., PARK, H. W., SAVCHENKO, A., YEE, A., EDWARDS, A., VINCENTELLI, R., CAMBILLAU, C., KIM, R., KIM, S. H., RAO, Z., SHI, Y., TERWILLIGER, T. C., KIM, C. Y., HUNG, L. W., WALDO, G. S., PELEG, Y., ALBECK, S., UNGER, T., DYM, O., PRILUSKY, J., SUSSMAN, J. L., STEVENS, R. C., LESLEY, S. A., WILSON, I. A., JOACHIMIAK, A., COLLART, F., DEMENTIEVA, I., DONNELLY, M. I., ESCHENFELDT, W. H., KIM, Y., STOLS, L., WU, R., ZHOU, M., BURLEY, S. K., EMTAGE, J. S., SAUDER, J. M., THOMPSON, D., BAIN, K., LUZ, J., GHEYI, T., ZHANG, F., ATWELL, S., ALMO, S. C., BONANNO, J. B., FISER, A., SWAMINATHAN, S., STUDIER, F. W., CHANCE, M. R., SALI, A., ACTON, T. B., XIAO, R., ZHAO, L., MA, L. C., HUNT, J. F., TONG, L., CUNNINGHAM, K., INOUYE, M., ANDERSON, S., JANJUA, H., SHASTRY, R., HO, C. K., WANG, D., WANG, H., JIANG, M., MONTELIONE, G. T., STUART, D. I., OWENS, R. J., DAENKE, S., SCHUTZ, A., HEINEMANN, U., YOKOYAMA, S., BUSSOW, K. & GUNSALUS, K. C. 2008. Protein production and purification. *Nat Methods,* 5**,** 135-46.

GREENFIELD, N. J. 2006. Using circular dichroism spectra to estimate protein secondary structure. *Nature protocols,* 1**,** 2876-2890.

GRITTI, I., BANFI, G. & ROI, G. S. 2000. Pepsinogens: physiology, pharmacology pathophysiology and exercise. *Pharmacol Res,* 41**,** 265-81.

GRZESZCZUK, M. J., BOCIAN-OSTRZYCKA, K. M., BANAŚ, A. M., ROSZCZENKO-JASINSKA, P., MALINOWSKA, A., STRALOVA, H., HAAS, R., MEYER, T. F. & JAGUSZTYN-KRYNICKA, E. K. 2018. Thioloxidoreductase HP0231 of Helicobacter pylori impacts HopQ-dependent CagA translocation. *International Journal of Medical Microbiology,* 308**,** 977-985.

GUPTA, H., BHANDARI, D. & SHARMA, A. 2009. Recent trends in oral drug delivery: a review. *Recent Pat Drug Deliv Formul,* 3**,** 162-73.

GÜVEN, E., DUUS, K., LYDOLPH, M. C., JØRGENSEN, C. S., LAURSEN, I. & HOUEN, G. 2014. Non-specific binding in solid phase immunoassays for autoantibodies correlates with inflammation markers. *Journal of Immunological Methods,* 403**,** 26-36.

HAGE, N., HOWARD, T., PHILLIPS, C., BRASSINGTON, C., OVERMAN, R., DEBRECZENI, J., GELLERT, P., S. STOLNIK, G., W., S. & FALCONE, F. H. 2015a. Structural basis of Lewisb antigen binding by the Helicobacter pylori adhesin BabA. *Sci. Adv. 1,* , 1.

HAGE, N., RENSHAW, J. G., WINKLER, G. S., GELLERT, P., STOLNIK, S. & FALCONE, F. H. 2015b. Improved expression and purification of the Helicobacter pylori adhesin BabA through the incorporation of a hexa-lysine tag. *Protein Expression and Purification,* 106**,** 25-30.

HALTNER, E., EASSON, J. H. & LEHR, C.-M. 1997. Lectins and bacterial invasion factors for controlling endo- and transcytosis of bioadhesive drug carrier systems. *European Journal of Pharmaceutics and Biopharmaceutics,* 44**,** 3-13.

HANADA, K., UCHIDA, T., TSUKAMOTO, Y., WATADA, M., YAMAGUCHI, N., YAMAMOTO, K., SHIOTA, S., MORIYAMA, M., GRAHAM, D. Y. & YAMAOKA, Y. 2014. Helicobacter pylori infection introduces DNA double-strand breaks in host cells. *Infect Immun,* 82**,** 4182-9.

HANADA, K. & YAMAOKA, Y. 2014. Genetic battle between Helicobacter pylori and humans. The mechanism underlying homologous recombination in bacteria, which can infect human cells. *Microbes Infect,* 16**,** 833-9.

HANLEY, W. B. 1964. Hereditary Aspects of Duodenal Ulceration: Serum-pepsinogen Level in Relation to ABO Blood Groups and Salivary ABH Secretor Status. *British Medical Journal,* 1**,** 936-940.

HARRIS, P. R., SMYTHIES, L. E., SMITH, P. D. & PEREZ-PEREZ, G. I. 2013. Role of childhood infection in the sequelae of H. pylori disease. *Gut Microbes,* 4**,** 426-38.

HARTL, F. U., BRACHER, A. & HAYER-HARTL, M. 2011. Molecular chaperones in protein folding and proteostasis. *Nature,* 475**,** 324-32.

HASSAN, P. A., RANA, S. & VERMA, G. 2015. Making Sense of Brownian Motion: Colloid Characterization by Dynamic Light Scattering. *Langmuir,* 31**,** 3-12.

HAUSER, P. V., PIPPIN, J. W., KAISER, C., KROFFT, R. D., BRINKKOETTER, P. T., HUDKINS, K. L., KERJASCHKI, D., REISER, J., ALPERS, C. E. & SHANKLAND, S. J. 2010. Novel siRNA delivery system to target podocytes in vivo. *PLoS One,* 5**,** e9463.

HEIM, K. P., CROWLEY, P. J., LONG, J. R., KAILASAN, S., MCKENNA, R. & BRADY, L. J. 2014. An intramolecular lock facilitates folding and stabilizes the tertiary structure of Streptococcus mutans adhesin P1. *Proceedings of the National Academy of Sciences,* 111**,** 15746.

HEISSEL, S., FREDERIKSEN, S. J., BUNKENBORG, J. & HOJRUP, P. 2019. Enhanced trypsin on a budget: Stabilization, purification and high-

temperature application of inexpensive commercial trypsin for proteomics applications. *PLoS One,* 14**,** e0218374.
HELPPOLAINEN, SATU H., NURMINEN, KIRSI P., MÄÄTTÄ, JUHA A. E., HALLING, KATRIN K., SLOTTE, J. P., HUHTALA, T., LIIMATAINEN, T., YLÄ-HERTTUALA, S., AIRENNE, KARI J., NÄRVÄNEN, A., JÄNIS, J., VAINIOTALO, P., VALJAKKA, J., KULOMAA, MARKKU S. & NORDLUND, HENRI R. 2007. Rhizavidin from Rhizobium etli: the first natural dimer in the avidin protein family. *Biochemical Journal,* 405**,** 397.
HENDERSON, I. R., NAVARRO-GARCIA, F., DESVAUX, M., FERNANDEZ, R. C. & ALA'ALDEEN, D. 2004. Type V protein secretion pathway: the autotransporter story. *Microbiol Mol Biol Rev,* 68**,** 692-744.
HENNIG, E. E., MERNAUGH, R., EDL, J., CAO, P. & COVER, T. L. 2004. Heterogeneity among Helicobacter pylori Strains in Expression of the Outer Membrane Protein BabA. *Infection and Immunity,* 72**,** 3429-3435.
HEPP, C. & MAIER, B. 2016. Kinetics of DNA uptake during transformation provide evidence for a translocation ratchet mechanism. *Proceedings of the National Academy of Sciences of the United States of America,* 113**,** 12467-12472.
HERSHFIELD, V., BOYER, H. W., YANOFSKY, C., LOVETT, M. A. & HELINSKI, D. R. 1974. Plasmid ColEl as a molecular vehicle for cloning and amplification of DNA. *Proc Natl Acad Sci U S A,* 71**,** 3455-9.
HESSEY, S. J., SPENCER, J., WYATT, J. I., SOBALA, G., RATHBONE, B. J., AXON, A. T. & DIXON, M. F. 1990. Bacterial adhesion and disease activity in Helicobacter associated chronic gastritis. *Gut,* 31**,** 134.
HILPERT, K., HANSEN, G., WESSNER, H., KÜTTNER, G., WELFLE, K., SEIFERT, M. & HÖHNE, W. 2001. Anti-c-myc antibody 9E10: epitope key positions and variability characterized using peptide spot synthesis on cellulose. *Protein Engineering, Design and Selection,* 14**,** 803-806.
HIRABAYASHI, J. & ARAI, R. 2019. Lectin engineering: the possible and the actual. *Interface Focus,* 9**,** 20180068.
HOLLAND, I. B. 2004. Translocation of bacterial proteins--an overview. *Biochim Biophys Acta,* 1694**,** 5-16.
HONG, P., KOZA, S. & BOUVIER, E. S. P. 2012. Size-Exclusion Chromatography for the Analysis of Protein Biotherapeutics and their Aggregates. *Journal of liquid chromatography & related technologies,* 35**,** 2923-2950.
HOSEINI, S. S. & SAUER, M. G. 2015. Molecular cloning using polymerase chain reaction, an educational guide for cellular engineering. *J Biol Eng,* 9**,** 2.
HSU, H.-J., TSAI, K.-C., SUN, Y.-K., CHANG, H.-J., HUANG, Y.-J., YU, H.-M., LIN, C.-H., MAO, S.-S. & YANG, A.-S. 2008. Factor Xa Active Site Substrate Specificity with Substrate Phage Display and Computational Molecular Modeling. *The Journal of Biological Chemistry,* 283**,** 12343-12353.
HUA, S., DE MATOS, M. B. C., METSELAAR, J. M. & STORM, G. 2018. Current Trends and Challenges in the Clinical Translation of Nanoparticulate Nanomedicines: Pathways for Translational Development and Commercialization. *Frontiers in Pharmacology,* 9.
HUA, S., MARKS, E., SCHNEIDER, J. J. & KEELY, S. 2015. Advances in oral nano-delivery systems for colon targeted drug delivery in inflammatory bowel disease: Selective targeting to diseased versus healthy tissue. *Nanomedicine,* 11**,** 1117-32.
HUANG, L., YUAN, H., LIU, M.-F., ZHAO, X.-X., WANG, M.-S., JIA, R.-Y., CHEN, S., SUN, K.-F., YANG, Q., WU, Y., CHEN, X.-Y., CHENG, A.-C. & ZHU, D.-K. 2017. Type B Chloramphenicol Acetyltransferases Are Responsible for

Chloramphenicol Resistance in Riemerella anatipestifer, China. *Frontiers in microbiology,* 8**,** 297-297.

HUANG, Y., WANG, Q.-L., CHENG, D.-D., XU, W.-T. & LU, N.-H. 2016. Adhesion and Invasion of Gastric Mucosa Epithelial Cells by Helicobacter pylori. *Frontiers in cellular and infection microbiology,* 6**,** 159-159.

HUHMANN, S., STEGEMANN, A. K., FOLMERT, K., KLEMCZAK, D., MOSCHNER, J., KUBE, M. & KOKSCH, B. 2017. Position-dependent impact of hexafluoroleucine and trifluoroisoleucine on protease digestion. *Beilstein J Org Chem,* 13**,** 2869-2882.

HULTEN, K., HAN, S. W., ENROTH, H., KLEIN, P. D., OPEKUN, A. R., GILMAN, R. H., EVANS, D. G., ENGSTRAND, L., GRAHAM, D. Y. & EL-ZAATARI, F. A. 1996. Helicobacter pylori in the drinking water in Peru. *Gastroenterology,* 110**,** 1031-5.

HUSSAIN, R. & SILIGARDI, G. 2016. Characterisation of Conformational and Ligand Binding Properties of Membrane Proteins Using Synchrotron Radiation Circular Dichroism (SRCD). *In:* MORAES, I. (ed.) *The Next Generation in Membrane Protein Structure Determination.* Cham: Springer International Publishing.

HUST, M., JOSTOCK, T., MENZEL, C., VOEDISCH, B., MOHR, A., BRENNEIS, M., KIRSCH, M. I., MEIER, D. & DÜBEL, S. 2007. Single chain Fab (scFab) fragment. *BMC biotechnology,* 7**,** 14-14.

ILVER, D., ARNQVIST, A., OGREN, J., FRICK, I. M., KERSULYTE, D., INCECIK, E. T., BERG, D. E., COVACCI, A., ENGSTRAND, L. & BOREN, T. 1998. Helicobacter pylori adhesin binding fucosylated histo-blood group antigens revealed by retagging. *Science,* 279**,** 373-7.

INOUE, M., ITOH, J. & MITSUHASHI, S. 1983. pMS76, a plasmid capable of amplification by treatment with chloramphenicol. *Plasmid,* 9**,** 86-97.

ISLAM, M. M., KHAN, M. A. & KURODA, Y. 2012. Analysis of amino acid contributions to protein solubility using short peptide tags fused to a simplified BPTI variant. *Biochimica et Biophysica Acta (BBA) - Proteins and Proteomics,* 1824**,** 1144-1150.

ISSA, S., MORAN, A. P., USTINOV, S. N., LIN, J. H., LIGTENBERG, A. J. & KARLSSON, N. G. 2010. O-linked oligosaccharides from salivary agglutinin: Helicobacter pylori binding sialyl-Lewis x and Lewis b are terminating moieties on hyperfucosylated oligo-N-acetyllactosamine. *Glycobiology,* 20**,** 1046-57.

ITAYA, M., KAWATA, Y., SATO, M., TOMITA, M. & NAKAHIGASHI, K. 2012. A simple method to provide a shuttling plasmid for delivery to other host ascertained by prolonged stability of extracellular plasmid DNA released from Escherichia coli K12 endA mutant, deficient in major endonuclease. *J Biochem,* 152**,** 501-4.

JABBOUR, S. & ZIRING, B. 2011. Advantages of extended-release metformin in patients with type 2 diabetes mellitus. *Postgrad Med,* 123**,** 15-23.

JAIN, A., BARVE, A., ZHAO, Z., JIN, W. & CHENG, K. 2017. Comparison of Avidin, Neutravidin, and Streptavidin as Nanocarriers for Efficient siRNA Delivery. *Molecular Pharmaceutics,* 14**,** 1517-1527.

JAIN, A. & CHENG, K. 2017. The principles and applications of avidin-based nanoparticles in drug delivery and diagnosis. *Journal of controlled release : official journal of the Controlled Release Society,* 245**,** 27-40.

JAVAHERI, A., KRUSE, T., MOONENS, K., MEJÍAS-LUQUE, R., DEBRAEKELEER, A., ASCHE, C. I., TEGTMEYER, N., KALALI, B., BACH, N. C., SIEBER, S. A., HILL, D. J., KÖNIGER, V., HAUCK, C. R., MOSKALENKO, R., HAAS, R., BUSCH, D.

H., KLAILE, E., SLEVOGT, H., SCHMIDT, A., BACKERT, S., REMAUT, H., SINGER, B. B. & GERHARD, M. 2016. Helicobacter pylori adhesin HopQ engages in a virulence-enhancing interaction with human CEACAMs. *Nature Microbiology,* 2.

JAYAPRAKASH, N. G. & SUROLIA, A. 2017. Role of glycosylation in nucleating protein folding and stability. *Biochemical Journal,* 474**,** 2333-2347.

JENNY, R. J., MANN, K. G. & LUNDBLAD, R. L. 2003. A critical review of the methods for cleavage of fusion proteins with thrombin and factor Xa. *Protein Expr Purif,* 31**,** 1-11.

JERVIS, A. J., WOOD, A. G., CAIN, J. A., CORDWELL, S. J., BUTLER, J. A., LORD, E., FROST, H., LINTON, D., WREN, B. W. & LANGDON, R. 2018. Functional analysis of the Helicobacter pullorum N-linked protein glycosylation system. *Glycobiology,* 28**,** 233-244.

JIN, C., KENNY, D. T., SKOOG, E. C., PADRA, M., ADAMCZYK, B., VITIZEVA, V., THORELL, A., VENKATAKRISHNAN, V., LINDÉN, S. K. & KARLSSON, N. G. 2017. Structural Diversity of Human Gastric Mucin Glycans. *Molecular & cellular proteomics : MCP,* 16**,** 743-758.

JOHANSSON, M. E. 2012. Fast renewal of the distal colonic mucus layers by the surface goblet cells as measured by in vivo labeling of mucin glycoproteins. *PLoS One,* 7**,** e41009.

JOHNSTON, N., DETTMAR, P. W., BISHWOKARMA, B., LIVELY, M. O. & KOUFMAN, J. A. 2007. Activity/Stability of Human Pepsin: Implications for Reflux Attributed Laryngeal Disease. *The Laryngoscope,* 117**,** 1036-1039.

JONG, W. S. P., VIKSTRÖM, D., HOUBEN, D., VAN DEN BERG VAN SAPAROEA, H. B., DE GIER, J.-W. & LUIRINK, J. 2017. Application of an E. coli signal sequence as a versatile inclusion body tag. *Microbial Cell Factories,* 16**,** 50.

JOSENHANS, C., EATON, K. A., THEVENOT, T. & SUERBAUM, S. 2000. Switching of flagellar motility in Helicobacter pylori by reversible length variation of a short homopolymeric sequence repeat in fliP, a gene encoding a basal body protein. *Infect Immun,* 68**,** 4598-603.

JOSENHANS, C., VOSSEBEIN, L., FRIEDRICH, S. & SUERBAUM, S. 2002. The neuA/flmD gene cluster of Helicobacter pylori is involved in flagellar biosynthesis and flagellin glycosylation. *FEMS Microbiol Lett,* 210**,** 165-72.

JUNG, H.-J., KIM, S.-K., MIN, W.-K., LEE, S.-S., PARK, K., PARK, Y.-C. & SEO, J.-H. 2011. Polycationic amino acid tags enhance soluble expression of Candida antarctica lipase B in recombinant Escherichia coli. *Bioprocess and Biosystems Engineering,* 34**,** 833.

KABLE, M. E., HANSEN, L. M., STYER, C. M., DECK, S. L., RAKHIMOVA, O., SHEVTSOVA, A., EATON, K. A., MARTIN, M. E., GIDEONSSON, P., BOREN, T. & SOLNICK, J. V. 2017. Host Determinants of Expression of the Helicobacter pylori BabA Adhesin. *Sci Rep,* 7**,** 46499.

KAHN, R. & RUBIN, R. W. 1975. Quantitation of submicrogram amounts of protein using Coomassie brilliant blue R on sodium dodecyl sulfate-polyacrylamide slab-gels. *Analytical Biochemistry,* 67**,** 347-352.

KALITA, S., DEVI, B., KANDIMALLA, R., SHARMA, K. K., SHARMA, A., KALITA, K., KATAKI, A. C. & KOTOKY, J. 2015. Chloramphenicol encapsulated in poly-epsilon-caprolactone-pluronic composite: nanoparticles for treatment of MRSA-infected burn wounds. *Int J Nanomedicine,* 10**,** 2971-84.

KAMAL, F., ZHANG, L. & REHA-KRANTZ, L. J. 2013. Escherichia coli XL10-gold bacteria produce bacteriophage. *Journal of clinical microbiology,* 51**,** 727-727.

KAMATARI, Y. O., DOBSON, C. M. & KONNO, T. 2003. Structural dissection of alkaline-denatured pepsin. *Protein science : a publication of the Protein Society,* 12**,** 717-724.

KAMPINGA, H. H., ANDREASSON, C., BARDUCCI, A., CHEETHAM, M. E., CYR, D., EMANUELSSON, C., GENEVAUX, P., GESTWICKI, J. E., GOLOUBINOFF, P., HUERTA-CEPAS, J., KIRSTEIN, J., LIBEREK, K., MAYER, M. P., NAGATA, K., NILLEGODA, N. B., PULIDO, P., RAMOS, C., DE LOS RIOS, P., ROSPERT, S., ROSENZWEIG, R., SAHI, C., TAIPALE, M., TOMICZEK, B., USHIODA, R., YOUNG, J. C., ZIMMERMANN, R., ZYLICZ, A., ZYLICZ, M., CRAIG, E. A. & MARSZALEK, J. 2019. Function, evolution, and structure of J-domain proteins. *Cell Stress Chaperones,* 24**,** 7-15.

KARKHAH, A., EBRAHIMPOUR, S., ROSTAMTABAR, M., KOPPOLU, V., DARVISH, S., VASIGALA, V. K. R., VALIDI, M. & NOURI, H. R. 2019. Helicobacter pylori evasion strategies of the host innate and adaptive immune responses to survive and develop gastrointestinal diseases. *Microbiological Research,* 218**,** 49-57.

KAWAKUBO, M., ITO, Y., OKIMURA, Y., KOBAYASHI, M., SAKURA, K., KASAMA, S., FUKUDA, M. N., FUKUDA, M., KATSUYAMA, T. & NAKAYAMA, J. 2004. Natural Antibiotic Function of a Human Gastric Mucin Against Helicobacter pylori Infection. *Science,* 305**,** 1003-1006.

KELLEY, K. D., OLIVE, L. Q., HADZISELIMOVIC, A. & SANDERS, C. R. 2010. Look and See if it is Time to Induce Protein Expression in Eschericia coli Cultures. *Biochemistry,* 49**,** 5405-5407.

KELLY, J., JARRELL, H., MILLAR, L., TESSIER, L., FIORI, L. M., LAU, P. C., ALLAN, B. & SZYMANSKI, C. M. 2006. Biosynthesis of the N-linked glycan in Campylobacter jejuni and addition onto protein through block transfer. *J Bacteriol,* 188**,** 2427-34.

KELLY, S. M., JESS, T. J. & PRICE, N. C. 2005. How to study proteins by circular dichroism. *Biochim Biophys Acta,* 1751**,** 119-39.

KELLY, S. M. & PRICE, N. C. 2000. The use of circular dichroism in the investigation of protein structure and function. *Curr Protein Pept Sci,* 1**,** 349-84.

KENNY, S., DUVAL, C., SAMMUT, S. J., STEELE, I., PRITCHARD, D. M., ATHERTON, J. C., ARGENT, R. H., DIMALINE, R., DOCKRAY, G. J. & VARRO, A. 2008. Increased expression of the urokinase plasminogen activator system by Helicobacter pylori in gastric epithelial cells. *Am J Physiol Gastrointest Liver Physiol,* 295**,** G431-41.

KHANVILKAR, K., DONOVAN, M. D. & FLANAGAN, D. R. 2001. Drug transfer through mucus. *Advanced Drug Delivery Reviews,* 48**,** 173-193.

KHOSLA, R. & DAVIS, S. S. 1987. The effect of polycarbophil on the gastric emptying of pellets. *J Pharm Pharmacol,* 39**,** 47-9.

KIM, J. H., JANG, S. J., YUN, J. W., JUNG, M. H. & WOO, S. H. 2018. Effects of pepsin and pepstatin on reflux tonsil hypertrophy in vitro. *PLOS ONE,* 13**,** e0207090.

KIM, K. I., PARK, S.-C., KANG, S. H., CHEONG, G.-W. & CHUNG, C. H. 1999. Selective degradation of unfolded proteins by the self-compartmentalizing HtrA protease, a periplasmic heat shock protein in Escherichia coli11Edited by W. Baumeister. *Journal of Molecular Biology,* 294**,** 1363-1374.

KIM, M., ASHIDA, H., OGAWA, M., YOSHIKAWA, Y., MIMURO, H. & SASAKAWA, C. 2010. Bacterial interactions with the host epithelium. *Cell Host Microbe,* 8**,** 20-35.

KIM, S.-G., MIN, W.-K., RHO, Y.-T. & SEO, J.-H. 2012. Electrostatic interaction-induced inclusion body formation of glucagon-like peptide-1 fused with ubiquitin and cationic tag. *Protein Expression and Purification,* 84**,** 38-46.

KIM, S. Y., CHOI, D. J. & CHUNG, J.-W. 2015. Antibiotic treatment for Helicobacter pylori: Is the end coming? *World journal of gastrointestinal pharmacology and therapeutics,* 6**,** 183-198.

KIMURA, T. & HIGAKI, K. 2002. Gastrointestinal transit and drug absorption. *Biol Pharm Bull,* 25**,** 149-64.

KIRSCH, M., ZAMAN, M., MEIER, D., DÜBEL, S. & HUST, M. 2005. Parameters affecting the display of antibodies on phage. *Journal of Immunological Methods,* 301**,** 173-185.

KLAUSNER, E. A., LAVY, E., FRIEDMAN, M. & HOFFMAN, A. 2003. Expandable gastroretentive dosage forms. *J Control Release,* 90**,** 143-62.

KLOSE, J., WENDT, N., KUBALD, S., KRAUSE, E., FECHNER, K., BEYERMANN, M., BIENERT, M., RUDOLPH, R. & ROTHEMUND, S. 2004. Hexa-histidin tag position influences disulfide structure but not binding behavior of in vitro folded N-terminal domain of rat corticotropin-releasing factor receptor type 2a. *Protein Science,* 13**,** 2470-2475.

KONRAD, A., METZGER, M., KERN, A. M., BRECHT, M. & MEIXNER, A. J. 2016. Revealing the radiative and non-radiative relaxation rates of the fluorescent dye Atto488 in a λ/2 Fabry–Pérot-resonator by spectral and time resolved measurements. *Nanoscale,* 8**,** 14541-14547.

KOUFMAN, J. A. & JOHNSTON, N. 2012. Potential benefits of pH 8.8 alkaline drinking water as an adjunct in the treatment of reflux disease. *Ann Otol Rhinol Laryngol,* 121**,** 431-4.

KRAUSE, M., UKKONEN, K., HAATAJA, T., RUOTTINEN, M., GLUMOFF, T., NEUBAUER, A., NEUBAUER, P. & VASALA, A. 2010. A novel fed-batch based cultivation method provides high cell-density and improves yield of soluble recombinant proteins in shaken cultures. *Microb Cell Fact,* 9**,** 11.

KUMANO-KURAMOCHI, M., TATEMATSU, K.-I., OHNISHI-KAMEYAMA, M., MAEDA-YAMAMOTO, M., KOBORI, T., SEZUTSU, H. & MACHIDA, S. 2017. Co-expression of BirA with biotin bait achieves in vivo biotinylation of overexpressed stable N-glycosylated sRAGE in transgenic silkworms. *Scientific Reports,* 7**,** 356.

KUMAR, M. & KAUSHIK, D. 2018. An Overview on Various Approaches and Recent Patents on Gastroretentive Drug Delivery Systems. *Recent Pat Drug Deliv Formul,* 12**,** 84-92.

KUO, C.-H., CHEN, P.-K., CHANG, B.-I., SUNG, M.-C., SHI, C.-S., LEE, J.-S., CHANG, C.-F., SHI, G.-Y. & WU, H.-L. 2012. The recombinant lectin-like domain of thrombomodulin inhibits angiogenesis through interaction with Lewis Y antigen. *Blood,* 119**,** 1302-1313.

KURDEKAR, A. D., AVINASH CHUNDURI, L. A., MANOHAR, C. S., HALEYURGIRISETTY, M. K., HEWLETT, I. K. & VENKATARAMANIAH, K. 2018. Streptavidin-conjugated gold nanoclusters as ultrasensitive fluorescent sensors for early diagnosis of HIV infection. *Science advances,* 4**,** eaar6280-eaar6280.

KUSTERS, J. G., VAN VLIET, A. H. & KUIPERS, E. J. 2006. Pathogenesis of Helicobacter pylori infection. *Clin Microbiol Rev,* 19**,** 449-90.

KYRATSOUS, C. A., SILVERSTEIN, S. J., DELONG, C. R. & PANAGIOTIDIS, C. A. 2009. Chaperone-fusion expression plasmid vectors for improved solubility of recombinant proteins in Escherichia coli. *Gene,* 440**,** 9-15.

LAFFLEUR, F., NETSOMBOON, K., BERNKOP-SCHNÜRCH, A., WESTMEIER, D., STAUBER, R. H. & DOCTER, D. 2017. Comprehensive mucoadhesive study of anionic polymers and their derivate. *European Polymer Journal,* 93**,** 314-322.

LAI, S. K., O'HANLON, D. E., HARROLD, S., MAN, S. T., WANG, Y. Y., CONE, R. & HANES, J. 2007. Rapid transport of large polymeric nanoparticles in fresh undiluted human mucus. *Proc Natl Acad Sci U S A,* 104**,** 1482-7.

LAI, S. K., WANG, Y. Y. & HANES, J. 2009. Mucus-penetrating nanoparticles for drug and gene delivery to mucosal tissues. *Adv Drug Deliv Rev,* 61**,** 158-71.

LAITINEN, O. H., HYTÖNEN, V. P., NORDLUND, H. R. & KULOMAA, M. S. 2006. Genetically engineered avidins and streptavidins. *Cellular and Molecular Life Sciences CMLS,* 63**,** 2992-3017.

LAM, S. K. & NG, T. B. 2011. Lectins: production and practical applications. *Applied microbiology and biotechnology,* 89**,** 45-55.

LAMB, A. & CHEN, L.-F. 2013. Role of the Helicobacter pylori-induced inflammatory response in the development of gastric cancer. *Journal of cellular biochemistry,* 114**,** 491-497.

LARENTIS, A. L., NICOLAU, J. F., ESTEVES GDOS, S., VARESCHINI, D. T., DE ALMEIDA, F. V., DOS REIS, M. G., GALLER, R. & MEDEIROS, M. A. 2014. Evaluation of pre-induction temperature, cell growth at induction and IPTG concentration on the expression of a leptospiral protein in E. coli using shaking flasks and microbioreactor. *BMC Res Notes,* 7**,** 671.

LAROUI, H., WILSON, D. S., DALMASSO, G., SALAITA, K., MURTHY, N., SITARAMAN, S. V. & MERLIN, D. 2011. Nanomedicine in GI. *American Journal of Physiology - Gastrointestinal and Liver Physiology,* 300**,** G371-G383.

LE CALVEZ, H., GREEN, J. M. & BATY, D. 1996. Increased efficiency of alkaline phosphatase production levels in Escherichia coli using a degenerate Pe1B signal sequence. *Gene,* 170**,** 51-55.

LEE, J. S., DO, M. S., YUN, S., JEON, Y. J., BAIK, H. S. & CHA, J. Y. 2015. Functional analysis of the aefR mutation and identification of its binding site in Pseudomonas syringae pv. tabaci 11528. *Acta Biochimica et Biophysica Sinica,* 47**,** 938-945.

LEE, J. W., PARK, J. H. & ROBINSON, J. R. 2000. Bioadhesive-based dosage forms: the next generation. *J Pharm Sci,* 89**,** 850-66.

LEHR, C. M. 2000. Lectin-mediated drug delivery: The second generation of bioadhesives. *Journal of Controlled Release,* 65**,** 19-29.

LEHR, C. M., BOUWSTRA, J. A., KOK, W., NOACH, A. B., DE BOER, A. G. & JUNGINGER, H. E. 1992. Bioadhesion by means of specific binding of tomato lectin. *Pharm Res,* 9**,** 547-53.

LEKER, K., LOZANO-POPE, I., BANDYOPADHYAY, K., CHOUDHURY, B. P. & OBONYO, M. 2017. Comparison of lipopolysaccharides composition of two different strains of Helicobacter pylori. *BMC microbiology,* 17**,** 226-226.

LEPPÄNEN, A. & CUMMINGS, R. D. 2010. Chapter Twelve - Fluorescence-Based Solid-Phase Assays to Study Glycan-Binding Protein Interactions with Glycoconjugates. *In:* FUKUDA, M. (ed.) *Methods in Enzymology.* Academic Press.

LESCH, H. P., KAIKKONEN, M. U., PIKKARAINEN, J. T. & YLA-HERTTUALA, S. 2010. Avidin-biotin technology in targeted therapy. *Expert Opin Drug Deliv,* 7**,** 551-64.

LETLEY, D. P., RHEAD, J. L., BISHOP, K. & ATHERTON, J. C. 2006. Paired cysteine residues are required for high levels of the Helicobacter pylori autotransporter VacA. *Microbiology,* 152**,** 1319-25.

LI, G. & YOUNG, K. D. 2014. A cAMP-independent carbohydrate-driven mechanism inhibits tnaA expression and TnaA enzyme activity in Escherichia coli. *Microbiology,* 160**,** 2079-88.

LI, G. W., BURKHARDT, D., GROSS, C. & WEISSMAN, J. S. 2014. Quantifying absolute protein synthesis rates reveals principles underlying allocation of cellular resources. *Cell,* 157**,** 624-35.

LI, H., LIAO, T., DEBOWSKI, A. W., TANG, H., NILSSON, H.-O., STUBBS, K. A., MARSHALL, B. J. & BENGHEZAL, M. 2016a. Lipopolysaccharide Structure and Biosynthesis in Helicobacter pylori. *Helicobacter,* 21**,** 445-461.

LI, H., TANG, H., DEBOWSKI, A. W., STUBBS, K. A., MARSHALL, B. J. & BENGHEZAL, M. 2018. Lipopolysaccharide Structural Differences between Western and Asian Helicobacter pylori Strains. *Toxins (Basel),* 10.

LI, H., YANG, T., LIAO, T., DEBOWSKI, A. W., NILSSON, H. O., FULURIJA, A., HASLAM, S. M., MULLOY, B., DELL, A., STUBBS, K. A., MARSHALL, B. J. & BENGHEZAL, M. 2017. The redefinition of Helicobacter pylori lipopolysaccharide O-antigen and core-oligosaccharide domains. *PLoS Pathog,* 13**,** e1006280.

LI, J., WU, H., HONG, J., XU, X., YANG, H., WU, B., WANG, Y., ZHU, J., LAI, R., JIANG, X., LIN, D., PRESCOTT, M. C. & REES, H. H. 2008. Odorranalectin is a small peptide lectin with potential for drug delivery and targeting. *PLoS One,* 3**,** e2381.

LI, Q., JOGINI, V., WANDERLING, S., CORTES, D. M. & PEROZO, E. 2012. Expression, purification, and reconstitution of the voltage-sensing domain from Ci-VSP. *Biochemistry,* 51**,** 8132-8142.

LI, X., GUAN, F., LI, D., TAN, Z., YANG, G., WU, Y. & HUANG, Z. 2016b. Identification of aberrantly expressed glycans in gastric cancer by integrated lectin microarray and mass spectrometric analyses. *Oncotarget,* 7**,** 87284-87300.

LIN, W.-C., IVERSEN, L., TU, H.-L., RHODES, C., CHRISTENSEN, S. M., IWIG, J. S., HANSEN, S. D., HUANG, W. Y. C. & GROVES, J. T. 2014. H-Ras forms dimers on membrane surfaces via a protein–protein interface. *Proceedings of the National Academy of Sciences,* 111**,** 2996-3001.

LIN, W.-L., CHEN, C.-C., SHI, G.-Y., MA, C.-Y., CHANG, C.-F. & WU, H.-L. 2017. Monocytic thrombomodulin promotes cell adhesion through interacting with its ligand, Lewisy. *Immunology & Cell Biology,* 95**,** 372-379.

LINDEN, S., MAHDAVI, J., HEDENBRO, J., BOREN, T. & CARLSTEDT, I. 2004. Effects of pH on Helicobacter pylori binding to human gastric mucins: identification of binding to non-MUC5AC mucins. *Biochem J,* 384**,** 263-70.

LINDÉN, S., MAHDAVI, J., HEDENBRO, J., BORÉN, T. & CARLSTEDT, I. 2004. Effects of pH on Helicobacter pylori binding to human gastric mucins: identification of binding to non-MUC5AC mucins. *The Biochemical journal,* 384**,** 263-270.

LINDÉN, S., NORDMAN, H., HEDENBRO, J., HURTIG, M., BORÉN, T. & CARLSTEDT, I. 2002. Strain- and blood group–dependent binding of Helicobacter pylori to human gastric MUC5AC glycoforms. *Gastroenterology,* 123**,** 1923-1930.

LINDEN, S. K., SHENG, Y. H., EVERY, A. L., MILES, K. M., SKOOG, E. C., FLORIN, T. H., SUTTON, P. & MCGUCKIN, M. A. 2009. MUC1 limits Helicobacter pylori infection both by steric hindrance and by acting as a releasable decoy. *PLoS Pathog,* 5**,** e1000617.

LINDÉN, S. K., WICKSTRÖM, C., LINDELL, G., GILSHENAN, K. & CARLSTEDT, I. 2008. Four Modes of Adhesion are Used During Helicobacter pylori Binding to Human Mucins in the Oral and Gastric Niches. *Helicobacter,* 13**,** 81-93.

LIPFERT, J., DONIACH, S., DAS, R. & HERSCHLAG, D. 2014. Understanding nucleic acid-ion interactions. *Annual review of biochemistry,* 83**,** 813-841.

LIU, H., SEMINO-MORA, C. & DUBOIS, A. 2012. Mechanism of H. pylori intracellular entry: an in vitro study. *Frontiers in cellular and infection microbiology,* 2**,** 13-13.

LIU, J., JIN, Y., FENG, X., ZOU, S., LV, G., ZHANG, Z. & YANG, Z. 2018a. Solubility-enhanced gMYL6 fused with a hexa-lysine tag promotes the cytotoxicity of human NK cells. *Immunology Letters,* 198**,** 66-73.

LIU, L., YAO, W., RAO, Y., LU, X. & GAO, J. 2017a. pH-Responsive carriers for oral drug delivery: challenges and opportunities of current platforms. *Drug Deliv,* 24**,** 569-581.

LIU, W., SAMANTA, S. K., SMITH, B. D. & ISAACS, L. 2017b. Synthetic mimics of biotin/(strept)avidin. *Chemical Society Reviews,* 46**,** 2391-2403.

LIU, X., LI, T., HART, D. J., GAO, S., WANG, H., GAO, H., XU, S., ZHANG, Y., LIU, Y. & AN, Y. 2018b. A universal mini-vector and an annealing of PCR products (APP)-based cloning strategy for convenient molecular biological manipulations. *Biochemical and Biophysical Research Communications,* 497**,** 978-982.

LOMEDICO, P. T. 1982. Use of recombinant DNA technology to program eukaryotic cells to synthesize rat proinsulin: a rapid expression assay for cloned genes. *Proc Natl Acad Sci U S A,* 79**,** 5798-802.

LOOS, C., SYROVETS, T., MUSYANOVYCH, A., MAILÄNDER, V., LANDFESTER, K., NIENHAUS, G. U. & SIMMET, T. 2014. Functionalized polystyrene nanoparticles as a platform for studying bio–nano interactions. *Beilstein Journal of Nanotechnology,* 5**,** 2403-2412.

LOPES, C. M., BETTENCOURT, C., ROSSI, A., BUTTINI, F. & BARATA, P. 2016. Overview on gastroretentive drug delivery systems for improving drug bioavailability. *Int J Pharm,* 510**,** 144-58.

LU, H., HSU, P. I., GRAHAM, D. Y. & YAMAOKA, Y. 2005. Duodenal ulcer promoting gene of Helicobacter pylori. *Gastroenterology,* 128**,** 833-48.

LUIRINK, J. & SINNING, I. 2004. SRP-mediated protein targeting: structure and function revisited. *Biochim Biophys Acta,* 1694**,** 17-35.

LUND, P., TRAMONTI, A. & DE BIASE, D. 2014. Coping with low pH: molecular strategies in neutralophilic bacteria. *FEMS Microbiology Reviews,* 38**,** 1091-1125.

LUONG, J. H. T., MALE, K. B. & GLENNON, J. D. 2019. Biotin interference in immunoassays based on biotin-strept(avidin) chemistry: An emerging threat. *Biotechnology Advances*.

LYKKEMARK, S., MANDRUP, O. A., FRIIS, N. A. & KRISTENSEN, P. 2014. Degradation of C-terminal tag sequences on domain antibodies purified from E. coli supernatant. *mAbs,* 6**,** 1551-1559.

LYU, ZHI X. & ZHAO, XIN S. 2015. Periplasmic quality control in biogenesis of outer membrane proteins. *Biochemical Society Transactions,* 43**,** 133-138.

MACHIDA, T., NOVOA, A., GILLON, É., ZHENG, S., CLAUDINON, J., EIERHOFF, T., IMBERTY, A., RÖMER, W. & WINSSINGER, N. 2017. Dynamic Cooperative Glycan Assembly Blocks the Binding of Bacterial Lectins to Epithelial Cells. *Angewandte Chemie International Edition,* 56**,** 6762-6766.

MAGALHÃES, A., ISMAIL, M. N. & REIS, C. A. 2010. Sweet receptors mediate the adhesion of the gastric pathogen Helicobacter pylori: glycoproteomic strategies. *Expert Review of Proteomics,* 7**,** 307-310.

MAGALHAES, A. & REIS, C. A. 2010. Helicobacter pylori adhesion to gastric epithelial cells is mediated by glycan receptors. *Braz J Med Biol Res,* 43**,** 611-8.

MAHDAVI, J., SONDEN, B., HURTIG, M., OLFAT, F. O., FORSBERG, L., ROCHE, N., ANGSTROM, J., LARSSON, T., TENEBERG, S., KARLSSON, K. A., ALTRAJA, S., WADSTROM, T., KERSULYTE, D., BERG, D. E., DUBOIS, A., PETERSSON, C., MAGNUSSON, K. E., NORBERG, T., LINDH, F., LUNDSKOG, B. B., ARNQVIST, A., HAMMARSTROM, L. & BOREN, T. 2002. Helicobacter pylori SabA adhesin in persistent infection and chronic inflammation. *Science,* 297**,** 573-8.

MAHONEY, T. F., RICCI, D. P. & SILHAVY, T. J. 2016. Classifying β-Barrel Assembly Substrates by Manipulating Essential Bam Complex Members. *Journal of Bacteriology,* 198**,** 1984-1992.

MAJEWSKA, M., WYSOKIŃSKA, H., KUŹMA, Ł. & SZYMCZYK, P. 2018. Eukaryotic and prokaryotic promoter databases as valuable tools in exploring the regulation of gene transcription: a comprehensive overview. *Gene,* 644**,** 38-48.

MALAKAR, P. & VENKATESH, K. V. 2012. Effect of substrate and IPTG concentrations on the burden to growth of Escherichia coli on glycerol due to the expression of Lac proteins. *Appl Microbiol Biotechnol,* 93**,** 2543-9.

MALEKZAD, H., MIRSHEKARI, H., SAHANDI ZANGABAD, P., MOOSAVI BASRI, S. M., BANIASADI, F., SHARIFI AGHDAM, M., KARIMI, M. & HAMBLIN, M. R. 2018. Plant protein-based hydrophobic fine and ultrafine carrier particles in drug delivery systems. *Crit Rev Biotechnol,* 38**,** 47-67.

MALYALA, P. & SINGH, M. 2010. Micro/nanoparticle adjuvants: preparation and formulation with antigens. *Methods Mol Biol,* 626**,** 91-101.

MANDAL, U. K., CHATTERJEE, B. & SENJOTI, F. G. 2016. Gastro-retentive drug delivery systems and their in vivo success: A recent update. *Asian Journal of Pharmaceutical Sciences,* 11**,** 575-584.

MANDALA, V. S., WILLIAMS, J. K. & HONG, M. 2018. Structure and Dynamics of Membrane Proteins from Solid-State NMR. *Annual Review of Biophysics,* 47**,** 201-222.

MARBACH, A. & BETTENBROCK, K. 2012. lac operon induction in Escherichia coli: Systematic comparison of IPTG and TMG induction and influence of the transacetylase LacA. *Journal of Biotechnology,* 157**,** 82-88.

MARCOS LUCIANO, B. 2019. Lectins and Nanostructured Drug Delivery Systems. *Current Drug Delivery,* 16**,** 268-269.

MARKS, J., KANNAN, K., RONCASE, E. J., KLEPACKI, D., KEFI, A., ORELLE, C., VÁZQUEZ-LASLOP, N. & MANKIN, A. S. 2016. Context-specific inhibition of translation by ribosomal antibiotics targeting the peptidyl transferase center. *Proceedings of the National Academy of Sciences,* 113**,** 12150.

MARSCHALL, L., SAGMEISTER, P. & HERWIG, C. 2017. Tunable recombinant protein expression in E. coli: promoter systems and genetic constraints. *Applied microbiology and biotechnology,* 101**,** 501-512.

MARSHALL, B. J. & WARREN, J. R. 1984. Unidentified curved bacilli in the stomach of patients with gastritis and peptic ulceration. *Lancet,* 1**,** 1311-5.

MARTINEZ, M. N. & AMIDON, G. L. 2002. A mechanistic approach to understanding the factors affecting drug absorption: a review of fundamentals. *J Clin Pharmacol,* 42**,** 620-43.

MASAOKA, Y., TANAKA, Y., KATAOKA, M., SAKUMA, S. & YAMASHITA, S. 2006. Site of drug absorption after oral administration: assessment of membrane permeability and luminal concentration of drugs in each segment of gastrointestinal tract. *Eur J Pharm Sci,* 29**,** 240-50.

MASDOR, N. A., ALTINTAS, Z. & TOTHILL, I. E. 2017. Surface Plasmon Resonance Immunosensor for the Detection of Campylobacter jejuni. *Chemosensors,* 5**,** 16.

MASSON, E. A., PATMORE, J. E., BRASH, P. D., BAXTER, M., CALDWELL, G., GALLEN, I. W., PRICE, P. A., VICE, P. A., WALKER, J. D. & LINDOW, S. W. 2003. Pregnancy outcome in Type 1 diabetes mellitus treated with insulin lispro (Humalog). *Diabet Med,* 20**,** 46-50.

MATSUI, T., HAMAKO, J., OZEKI, Y. & TITANI, K. 2001. Comparative study of blood group-recognizing lectins toward ABO blood group antigens on neoglycoproteins, glycoproteins and complex-type oligosaccharides. *Biochimica et Biophysica Acta (BBA) - General Subjects,* 1525**,** 50-57.

MATSUURA, M. 2013. Structural Modifications of Bacterial Lipopolysaccharide that Facilitate Gram-Negative Bacteria Evasion of Host Innate Immunity. *Frontiers in Immunology,* 4.

MAZALOVSKA, M. & KOUOKAM, J. C. 2018. Lectins as Promising Therapeutics for the Prevention and Treatment of HIV and Other Potential Coinfections. *BioMed Research International,* 2018**,** 12.

MBAE, K. M., UMESHA, S. & MANUKUMAR, H. M. 2018. Therapeutic properties of lectins in herbal supplements. *Phytochemistry Reviews,* 17**,** 627-643.

MCCRACKEN, K. W., CATÁ, E. M., CRAWFORD, C. M., SINAGOGA, K. L., SCHUMACHER, M., ROCKICH, B. E., TSAI, Y.-H., MAYHEW, C. N., SPENCE, J. R., ZAVROS, Y. & WELLS, J. M. 2014. Modelling human development and disease in pluripotent stem-cell-derived gastric organoids. *Nature,* 516**,** 400-404.

MCGOWAN, C. C., NECHEVA, A., THOMPSON, S. A., COVER, T. L. & BLASER, M. J. 1998. Acid-induced expression of an LPS-associated gene in Helicobacter pylori. *Mol Microbiol,* 30**,** 19-31.

MCGUCKIN, M. A., EVERY, A. L., SKENE, C. D., LINDEN, S. K., CHIONH, Y. T., SWIERCZAK, A., MCAULEY, J., HARBOUR, S., KAPARAKIS, M., FERRERO, R. & SUTTON, P. 2007. Muc1 mucin limits both Helicobacter pylori colonization of the murine gastric mucosa and associated gastritis. *Gastroenterology,* 133**,** 1210-8.

MCGUCKIN, M. A., LINDEN, S. K., SUTTON, P. & FLORIN, T. H. 2011. Mucin dynamics and enteric pathogens. *Nat Rev Microbiol,* 9**,** 265-78.

MEGRAUD, F., LEHOURS, P. & VALE, F. F. 2016. The history of Helicobacter pylori: from phylogeography to paleomicrobiology. *Clin Microbiol Infect,* 22**,** 922-927.

MERDANOVIC, M., CLAUSEN, T., KAISER, M., HUBER, R. & EHRMANN, M. 2011. Protein quality control in the bacterial periplasm. *Annu Rev Microbiol,* 65**,** 149-68.

MILES, A. J. & WALLACE, B. A. 2016. Circular dichroism spectroscopy of membrane proteins. *Chem Soc Rev,* 45**,** 4859-72.

MILLER-PODRAZA, H., WEIKKOLAINEN, K., LARSSON, T., LINDE, P., HELIN, J., NATUNEN, J. & KARLSSON, K.-A. 2008. Helicobacter pylori binding to new glycans based on N-acetyllactosamine. *Glycobiology,* 19**,** 399-407.

MILLER, S. I. & SALAMA, N. R. 2018. The gram-negative bacterial periplasm: Size matters. *PLOS Biology,* 16**,** e2004935.

MISHRA, A. & VERMA, M. 2010. Cancer biomarkers: are we ready for the prime time? *Cancers (Basel),* 2**,** 190-208.

MISHRA, M., TIWARI, S., GUNASEELAN, A., LI, D., HAMMOCK, B. D. & GOMES, A. V. 2019. Improving the sensitivity of traditional Western blotting via Streptavidin containing Poly-horseradish peroxidase (PolyHRP). *ELECTROPHORESIS,* 0.

MOHSENI-SHAHRI, F. S., MOEINPOUR, F. & NOSRATI, M. 2018. Spectroscopy and molecular dynamics simulation study on the interaction of sunset yellow food additive with pepsin. *International Journal of Biological Macromolecules,* 115**,** 273-280.

MONTECUCCO, C. & RAPPUOLI, R. 2001. Living dangerously: how Helicobacter pylori survives in the human stomach. *Nature Reviews Molecular Cell Biology,* 2**,** 457-466.

MONTISCI, M. J., GIOVANNUCI, G., DUCHENE, D. & PONCHEL, G. 2001. Covalent coupling of asparagus pea and tomato lectins to poly(lactide) microspheres. *International Journal of Pharmaceutics,* 215**,** 153-161.

MOONENS, K., GIDEONSSON, P., SUBEDI, S., BUGAYTSOVA, J., ROMAO, E., MENDEZ, M., NORDEN, J., FALLAH, M., RAKHIMOVA, L., SHEVTSOVA, A., LAHMANN, M., CASTALDO, G., BRANNSTROM, K., COPPENS, F., LO, A. W., NY, T., SOLNICK, J. V., VANDENBUSSCHE, G., OSCARSON, S., HAMMARSTROM, L., ARNQVIST, A., BERG, D. E., MUYLDERMANS, S., BOREN, T. & REMAUT, H. 2016. Structural Insights into Polymorphic ABO Glycan Binding by Helicobacter pylori. *Cell Host Microbe,* 19**,** 55-66.

MOONENS, K., HAMWAY, Y., NEDDERMANN, M., RESCHKE, M., TEGTMEYER, N., KRUSE, T., KAMMERER, R., MEJIAS-LUQUE, R., SINGER, B. B., BACKERT, S., GERHARD, M. & REMAUT, H. 2018. Helicobacter pylori adhesin HopQ disrupts trans dimerization in human CEACAMs. *Embo j,* 37.

MOORE, M. E., BOREN, T. & SOLNICK, J. V. 2011. Life at the margins: modulation of attachment proteins in Helicobacter pylori. *Gut Microbes,* 2**,** 42-6.

MORAN, A. P., KNIREL, Y. A., SENCHENKOVA, S. N., WIDMALM, G., HYNES, S. O. & JANSSON, P. E. 2002. Phenotypic variation in molecular mimicry between Helicobacter pylori lipopolysaccharides and human gastric epithelial cell surface glycoforms. Acid-induced phase variation in Lewis(x) and Lewis(y) expression by H. Pylori lipopolysaccharides. *J Biol Chem,* 277**,** 5785-95.

MOTOJIMA, F. 2015. How do chaperonins fold protein? *Biophysics,* 11**,** 93-102.

MUDIE, D. M., AMIDON, G. L. & AMIDON, G. E. 2010. Physiological parameters for oral delivery and in vitro testing. *Mol Pharm,* 7**,** 1388-405.

MURRAY, G. L., ATTRIDGE, S. R. & MORONA, R. 2006. Altering the Length of the Lipopolysaccharide O Antigen Has an Impact on the Interaction of Salmonella enterica Serovar Typhimurium with Macrophages and Complement. *Journal of Bacteriology,* 188**,** 2735.

MURRAY, V., HUANG, Y., CHEN, J., WANG, J. & LI, Q. 2012. A novel bacterial expression method with optimized parameters for very high yield production of triple-labeled proteins. *Methods Mol Biol,* 831**,** 1-18.

NAISBETT, B. & WOODLEY, J. 1994. The potential use of tomato lectin for oral drug delivery. 1. Lectin binding to rat small intestine in vitro. *International Journal of Pharmaceutics,* 107**,** 223-230.

NAKAMOTO, H. & BARDWELL, J. C. 2004. Catalysis of disulfide bond formation and isomerization in the Escherichia coli periplasm. *Biochim Biophys Acta,* 1694**,** 111-9.

NAMA, M., GONUGUNTA, C. S. & REDDY VEERAREDDY, P. 2008. Formulation and evaluation of gastroretentive dosage forms of Clarithromycin. *AAPS PharmSciTech,* 9**,** 231-7.

NAMAVAR, F., SPARRIUS, M., VEERMAN, E. C., APPELMELK, B. J. & VANDENBROUCKE-GRAULS, C. M. 1998. Neutrophil-activating protein mediates adhesion of Helicobacter pylori to sulfated carbohydrates on high-molecular-weight salivary mucin. *Infect Immun,* 66**,** 444-7.

NAUTIYAL, K. & KURODA, Y. 2018. A SEP tag enhances the expression, solubility and yield of recombinant TEV protease without altering its activity. *New Biotechnology,* 42**,** 77-84.

NELL, S., KENNEMANN, L., SCHWARZ, S., JOSENHANS, C. & SUERBAUM, S. 2014. Dynamics of Lewis b Binding and Sequence Variation of the babA Adhesin Gene during Chronic Helicobacter pylori Infection in Humans. *mBio,* 5**,** e02281-14.

NGUYEN, T. T., SLY, K. L. & CONBOY, J. C. 2012. Comparison of the Energetics of Avidin, Streptavidin, NeutrAvidin, and Anti-Biotin Antibody Binding to Biotinylated Lipid Bilayer Examined by Second-Harmonic Generation. *Analytical Chemistry,* 84**,** 201-208.

NIU, C., LUO, H., SHI, P., HUANG, H., WANG, Y., YANG, P. & YAO, B. 2016. N-Glycosylation Improves the Pepsin Resistance of Histidine Acid Phosphatase Phytases by Enhancing Their Stability at Acidic pHs and Reducing Pepsin's Accessibility to Its Cleavage Sites. *Applied and Environmental Microbiology,* 82**,** 1004.

NOOR, A., WALSER, G., WESSELING, M., GIRON, P., LAFFRA, A.-M., HADDOUCHI, F., DE GRÈVE, J. & KRONENBERGER, P. 2018. Production of a mono-biotinylated EGFR nanobody in the E. coli periplasm using the pET22b vector. *BMC Research Notes,* 11**,** 751.

NORDMAN, H., BORÉN, T., DAVIES, J. R., ENGSTRAND, L. & CARLSTEDT, I. 1999. pH-dependent binding of Helicobacter pylori to pig gastric mucins. *FEMS Immunology and Medical Microbiology,* 24**,** 175-181.

NYHOLM, D. & LENNERNAS, H. 2008. Irregular gastrointestinal drug absorption in Parkinson's disease. *Expert Opin Drug Metab Toxicol,* 4**,** 193-203.

O'DONOGHUE, E. J., SIRISAENGTAKSIN, N., BROWNING, D. F., BIELSKA, E., HADIS, M., FERNANDEZ-TRILLO, F., ALDERWICK, L., JABBARI, S. & KRACHLER, A. M. 2017. Lipopolysaccharide structure impacts the entry kinetics of bacterial outer membrane vesicles into host cells. *PLoS Pathog,* 13**,** e1006760.

O'NEIL, C. L., STINE, K. J. & DEMCHENKO, A. V. 2018. Immobilization of glycans on solid surfaces for application in glycomics. *Journal of Carbohydrate Chemistry,* 37**,** 225-249.

ODENBREIT, S. 1999. Genetic and functional characterization of the alpAB gene locus essential for the adhesion of Helicobacter pylori to human gastric tissue. *Mol. Microbiol.,* 31**,** 1537-1548.

ODENBREIT, S. 2005. Adherence properties of Helicobacter pylori: impact on pathogenesis and adaptation to the host. *Int J Med Microbiol,* 295**,** 317-24.

OH, S. W. & HAN, S. Y. 2015. Loop Diuretics in Clinical Practice. *Electrolyte & blood pressure : E & BP,* 13**,** 17-21.

OLDENKAMP, H. F., VELA RAMIREZ, J. E. & PEPPAS, N. A. 2018. Re-evaluating the importance of carbohydrates as regenerative biomaterials. *Regenerative Biomaterials,* 6**,** 1-12.

OLEASTRO, M. & MÉNARD, A. 2013. The Role of Helicobacter pylori Outer Membrane Proteins in Adherence and Pathogenesis. *Biology,* 2**,** 1110-1134.

OLMSTED, S. S., PADGETT, J. L., YUDIN, A. I., WHALEY, K. J., MOENCH, T. R. & CONE, R. A. 2001. Diffusion of Macromolecules and Virus-Like Particles in Human Cervical Mucus. *Biophysical Journal,* 81**,** 1930-1937.

OLSEN, J. V., ONG, S.-E. & MANN, M. 2004. Trypsin Cleaves Exclusively C-terminal to Arginine and Lysine Residues. *Molecular & Cellular Proteomics,* 3**,** 608-614.

OPALIŃSKI, Ł., SONG, J., PRIESNITZ, C., WENZ, L.-S., OELJEKLAUS, S., WARSCHEID, B., PFANNER, N. & BECKER, T. 2018. Recruitment of Cytosolic J-Proteins by TOM Receptors Promotes Mitochondrial Protein Biogenesis. *Cell reports,* 25**,** 2036-2043.e5.

ORTIZ-VELEZ, L., ORTIZ-VILLALOBOS, J., SCHULMAN, A., OH, J.-H., VAN PIJKEREN, J.-P. & BRITTON, R. A. 2018. Genome alterations associated with improved transformation efficiency in Lactobacillus reuteri. *Microbial cell factories,* 17**,** 138-138.

PACHATHUNDIKANDI, S. K., TEGTMEYER, N. & BACKERT, S. 2013. Signal transduction of Helicobacter pylori during interaction with host cell protein receptors of epithelial and immune cells. *Gut Microbes,* 4**,** 454-74.

PANG, S. S., NGUYEN, S. T., PERRY, A. J., DAY, C. J., PANJIKAR, S., TIRALONGO, J., WHISSTOCK, J. C. & KWOK, T. 2014. The three-dimensional structure of the extracellular adhesion domain of the sialic acid-binding adhesin SabA from Helicobacter pylori. *J Biol Chem,* 289**,** 6332-40.

PAPANIKOU, E., KARAMANOU, S. & ECONOMOU, A. 2007. Bacterial protein secretion through the translocase nanomachine. *Nat Rev Microbiol,* 5**,** 839-51.

PARASKEVOPOULOU, V., ARTIAGA, V. G., ROWLINSON, R., WINKLER, G. S., GELLERT, P., STOLNIK, S., OVERMAN, R. & FALCONE, F. H. 2019. Introduction of a C-terminal hexa-lysine tag increases thermal stability of the LacDiNac binding adhesin (LabA) exodomain from Helicobacter pylori. *Protein Expression and Purification,* 163**,** 105446.

PARASKEVOPOULOU, V. & FALCONE, F. H. 2018. Polyionic Tags as Enhancers of Protein Solubility in Recombinant Protein Expression. *Microorganisms,* 6**,** 47.

PARDRIDGE, W. M. 2015. Blood-brain barrier drug delivery of IgG fusion proteins with a transferrin receptor monoclonal antibody. *Expert Opin Drug Deliv,* 12**,** 207-22.

PARK, J. W., PARK, A. Y., LEE, S., YU, N. K., LEE, S. H. & KAANG, B. K. 2010. Detection of TrkB receptors distributed in cultured hippocampal neurons through bioconjugation between highly luminescent (quantum dot-neutravidin) and (biotinylated anti-TrkB antibody) on neurons by combined atomic force microscope and confocal laser scanning microscope. *Bioconjug Chem,* 21**,** 597-603.

PATEL, R. C., KERALIYA, R. A., PATEL, M. M. & PATEL, N. M. 2010. Formulation of furosemide solid dispersion with micro crystalline cellulose for achieve rapid dissolution. *Journal of advanced pharmaceutical technology & research,* 1**,** 180-189.

PATRA, J. K., DAS, G., FRACETO, L. F., CAMPOS, E. V. R., RODRIGUEZ-TORRES, M. D. P., ACOSTA-TORRES, L. S., DIAZ-TORRES, L. A., GRILLO, R., SWAMY, M. K., SHARMA, S., HABTEMARIAM, S. & SHIN, H.-S. 2018. Nano based drug delivery systems: recent developments and future prospects. *Journal of Nanobiotechnology,* 16**,** 71.

PAWAR, V. K., KANSAL, S., GARG, G., AWASTHI, R., SINGODIA, D. & KULKARNI, G. T. 2011. Gastroretentive dosage forms: a review with special emphasis on floating drug delivery systems. *Drug Deliv,* 18**,** 97-110.

PEPPAS, N. A., THOMAS, J. B. & MCGINTY, J. 2009. Molecular Aspects of Mucoadhesive Carrier Development for Drug Delivery and Improved Absorption. *Journal of Biomaterials Science-Polymer Edition,* 20**,** 1-20.

PERONA, J. J. & CRAIK, C. S. 1995. Structural basis of substrate specificity in the serine proteases. *Protein Sci,* 4**,** 337-60.

PETERSON, J. H., PLUMMER, A. M., FLEMING, K. G. & BERNSTEIN, H. D. 2017. Selective pressure for rapid membrane integration constrains the sequence of bacterial outer membrane proteins. *Molecular Microbiology,* 106**,** 777-792.

PFLOCK, M., DIETZ, P., SCHAR, J. & BEIER, D. 2004. Genetic evidence for histidine kinase HP165 being an acid sensor of Helicobacter pylori. *FEMS Microbiol Lett,* 234**,** 51-61.

PFLOCK, M., FINSTERER, N., JOSEPH, B., MOLLENKOPF, H., MEYER, T. F. & BEIER, D. 2006. Characterization of the ArsRS regulon of Helicobacter pylori, involved in acid adaptation. *J Bacteriol,* 188**,** 3449-62.

PHILIP, A. K. & PHILIP, B. 2010. Colon targeted drug delivery systems: a review on primary and novel approaches. *Oman medical journal,* 25**,** 79-87.

PICKLES, J., RAFIQ, S., COCHRANE, S. A. & LALLJIE, A. 2014. In vitro pepsin resistance of proteins: Effect of non-reduced SDS-PAGE analysis on fragment observation. *Toxicology Reports,* 1**,** 858-870.

PIPER, D. W. & FENTON, B. H. 1965. pH stability and activity curves of pepsin with special reference to their clinical importance. *Gut,* 6**,** 506-8.

POMPAIAH, M. & BARTFELD, S. 2017. Gastric Organoids: An Emerging Model System to Study Helicobacter pylori Pathogenesis. *In:* TEGTMEYER, N. & BACKERT, S. (eds.) *Molecular Pathogenesis and Signal Transduction by Helicobacter pylori.* Cham: Springer International Publishing.

PONCHEL, G. & IRACHE, J. 1998. Specific and non-specific bioadhesive particulate systems for oral delivery to the gastrointestinal tract. *Adv Drug Deliv Rev,* 34**,** 191-219.

PRAKOBPHOL, A., BOREN, T., MA, W., ZHIXIANG, P. & FISHER, S. J. 2005. Highly glycosylated human salivary molecules present oligosaccharides that mediate adhesion of leukocytes and Helicobacter pylori. *Biochemistry,* 44**,** 2216-24.

PRAKOBPHOL, A., XU, F., HOANG, V. M., LARSSON, T., BERGSTROM, J., JOHANSSON, I., FRANGSMYR, L., HOLMSKOV, U., LEFFLER, H., NILSSON, C., BOREN, T., WRIGHT, J. R., STROMBERG, N. & FISHER, S. J. 2000. Salivary agglutinin, which binds Streptococcus mutans and Helicobacter pylori, is the lung scavenger receptor cysteine-rich protein gp-340. *J Biol Chem,* 275**,** 39860-6.

PRIDE, D. T. & BLASER, M. J. 2002. Concerted evolution between duplicated genetic elements in Helicobacter pylori. *J Mol Biol,* 316**,** 629-42.

PROPROFS https://www.proprofs.com/discuss/q/223655/which-of-the-following-cells-secrete-mucus.

PUSZTAI, A., EWEN, S. W., GRANT, G., BROWN, D. S., STEWART, J. C., PEUMANS, W. J., VAN DAMME, E. J. & BARDOCZ, S. 1993. Antinutritive effects of wheat-germ agglutinin and other N-acetylglucosamine-specific lectins. *Br J Nutr,* 70**,** 313-21.

QIU, X. B., SHAO, Y. M., MIAO, S. & WANG, L. 2006. The diversity of the DnaJ/Hsp40 family, the crucial partners for Hsp70 chaperones. *Cell Mol Life Sci,* 63**,** 2560-70.

QUINTANA-HAYASHI, M. P., PADRA, M., PADRA, J. T., BENKTANDER, J. & LINDÉN, S. K. 2018. Mucus-Pathogen Interactions in the Gastrointestinal Tract of Farmed Animals. *Microorganisms,* 6**,** 55.

RAHIMZADEH, M., SADEGHIZADEH, M., NAJAFI, F., ARAB, S. & MOBASHERI, H. 2016. Impact of heat shock step on bacterial transformation efficiency. *Molecular Biology Research Communications,* 5**,** 257-261.

RAJINIKANTH, P. S., BALASUBRAMANIAM, J. & MISHRA, B. 2007. Development and evaluation of a novel floating in situ gelling system of amoxicillin for eradication of Helicobacter pylori. *International Journal of Pharmaceutics,* 335**,** 114-122.

RANGACHARI, P. K. 2007. Texts in context: Horace Davenport, carbonic anhydrase, and gastric acid secretion. *Adv Physiol Educ,* 31**,** 140-4.

RANJBAR, B. & GILL, P. 2009. Circular dichroism techniques: biomolecular and nanostructural analyses- a review. *Chem Biol Drug Des,* 74**,** 101-20.

RESHETNYAK, V. I. & RESHETNYAK, T. M. 2017. Significance of dormant forms of Helicobacter pylori in ulcerogenesis. *World J Gastroenterol,* 23**,** 4867-4878.

ROCHA, R., PADRA, M., THORELL, A., JIN, C., KARLSSON, N. G., ROXO-ROSA, M., OLEASTRO, M. & LINDÉN, S. K. 2018. BabA-mediated adherence of pediatric ulcerogenic H. pylori strains to gastric mucins at neutral and acidic pH AU - Quintana-Hayashi, Macarena P. *Virulence,* 9**,** 1699-1717.

ROMERO PASTRANA, F., NEEF, J., VAN DIJL, J. M. & BUIST, G. 2017. A Lactococcus lactis expression vector set with multiple affinity tags to facilitate isolation and direct labeling of heterologous secreted proteins. *Applied Microbiology and Biotechnology,* 101**,** 8139-8149.

RONCATO, F., RRUGA, F., PORCÙ, E., CASARIN, E., RONCA, R., MACCARINELLI, F., REALDON, N., BASSO, G., ALON, R., VIOLA, G. & MORPURGO, M. 2018. Improvement and extension of anti-EGFR targeting in breast cancer therapy by integration with the Avidin-Nucleic-Acid-Nano-Assemblies. *Nature Communications,* 9**,** 4070.

ROSANO, C., AROSIO, P. & BOLOGNESI, M. 1999. The X-ray three-dimensional structure of avidin. *Biomolecular Engineering,* 16**,** 5-12.

ROSANO, G. L. & CECCARELLI, E. A. 2014. Recombinant protein expression in Escherichia coli: advances and challenges. *Frontiers in Microbiology,* 5.

ROSSEZ, Y., GOSSET, P., BONECA, I. G., MAGALHÃES, A., ECOBICHON, C., REIS, C. A., CIENIEWSKI-BERNARD, C., JONCQUEL CHEVALIER CURT, M., LÉONARD, R., MAES, E., SPERANDIO, B., SLOMIANNY, C., SANSONETTI, P. J., MICHALSKI, J.-C. & ROBBE-MASSELOT, C. 2014a. The LacdiNAc-Specific Adhesin LabA Mediates Adhesion of Helicobacter pylori to Human Gastric Mucosa. *The Journal of Infectious Diseases,* 210**,** 1286-1295.

ROSSEZ, Y., GOSSET, P., BONECA, I. G., MAGALHAES, A., ECOBICHON, C., REIS, C. A., CIENIEWSKI-BERNARD, C., JONCQUEL CHEVALIER CURT, M., LEONARD, R., MAES, E., SPERANDIO, B., SLOMIANNY, C., SANSONETTI, P. J., MICHALSKI, J. C. & ROBBE-MASSELOT, C. 2014b. The lacdiNAc-specific adhesin LabA mediates adhesion of Helicobacter pylori to human gastric mucosa. *J Infect Dis,* 210**,** 1286-95.

ROSSEZ, Y., MAES, E., LEFEBVRE DARROMAN, T., GOSSET, P., ECOBICHON, C., JONCQUEL CHEVALIER CURT, M., BONECA, I. G., MICHALSKI, J. C. & ROBBE-MASSELOT, C. 2012. Almost all human gastric mucin O-glycans

harbor blood group A, B or H antigens and are potential binding sites for Helicobacter pylori. *Glycobiology,* 22**,** 1193-206.

ROßMANITH, J., WESKAMP, M. & NARBERHAUS, F. 2018. Design of a Temperature-Responsive Transcription Terminator. *ACS Synthetic Biology,* 7**,** 613-621.

ROUGE, N., BURI, P. & DOELKER, E. 1996. Drug absorption sites in the gastrointestinal tract and dosage forms for site-specific delivery. *International Journal of Pharmaceutics,* 136**,** 117-139.

RUIZ-PEREZ, F. & NATARO, J. P. 2014. Bacterial serine proteases secreted by the autotransporter pathway: classification, specificity, and role in virulence. *Cellular and Molecular Life Sciences,* 71**,** 745-770.

RUIZ, N., CHNG, S. S., HINIKER, A., KAHNE, D. & SILHAVY, T. J. 2010. Nonconsecutive disulfide bond formation in an essential integral outer membrane protein. *Proc Natl Acad Sci U S A,* 107**,** 12245-50.

RUSSELL-JONES, G. J. 2001. The potential use of receptor-mediated endocytosis for oral drug delivery. *Adv Drug Deliv Rev,* 46**,** 59-73.

RUSSELL-JONES, G. J., VEITCH, H. & ARTHUR, L. 1999. Lectin-mediated transport of nanoparticles across Caco-2 and OK cells. *Int J Pharm,* 190**,** 165-74.

RUSSELL, T. L., BERARDI, R. R., BARNETT, J. L., DERMENTZOGLOU, L. C., JARVENPAA, K. M., SCHMALTZ, S. P. & DRESSMAN, J. B. 1993. Upper gastrointestinal pH in seventy-nine healthy, elderly, North American men and women. *Pharm Res,* 10**,** 187-96.

SABERI, S., SCHMIDT, A., EYBPOOSH, S., ESMAILI, M., TALEBKHAN, Y., MOHAJERANI, N., OGHALAIE, A., ESHAGH HOSSEINI, M., MOHAGHEGHI, M. A., BUGAYTOVA, J., BOREN, T. & MOHAMMADI, M. 2016. Helicobacter pylori Strains from Duodenal Ulcer Patients Exhibit Mixed babA/B Genotypes with Low Levels of BabA Adhesin and Lewis b Binding. *Dig Dis Sci,* 61**,** 2868-2877.

SALAUN, L., LINZ, B., SUERBAUM, S. & SAUNDERS, N. J. 2004. The diversity within an expanded and redefined repertoire of phase-variable genes in Helicobacter pylori. *Microbiology,* 150**,** 817-30.

SALMANROGHANI, H., MIRVAKILI, M., BAGHBANIAN, M., SALMANROGHANI, R., SANATI, G. & YAZDIAN, P. 2018. Efficacy and Tolerability of Two Quadruple Regimens: Bismuth, Omeprazole, Metronidazole with Amoxicillin or Tetracycline as First-Line Treatment for Eradication of Helicobacter Pylori in Patients with Duodenal Ulcer: A Randomized Clinical Trial. *PLoS One,* 13**,** e0197096.

SAN-MIGUEL, T., PEREZ-BERMUDEZ, P. & GAVIDIA, I. 2013. Production of soluble eukaryotic recombinant proteins in E. coli is favoured in early log-phase cultures induced at low temperature. *Springerplus,* 2**,** 89.

SARVAS, M., HARWOOD, C. R., BRON, S. & VAN DIJL, J. M. 2004. Post-translocational folding of secretory proteins in Gram-positive bacteria. *Biochim Biophys Acta,* 1694**,** 311-27.

SATO, Y., KUBO, T., MORIMOTO, K., YANAGIHARA, K. & SEYAMA, T. 2016. High mannose-binding Pseudomonas fluorescens lectin (PFL) downregulates cell surface integrin/EGFR and induces autophagy in gastric cancer cells. *BMC cancer,* 16**,** 63-63.

SATO, Y., MORIMOTO, K., KUBO, T., YANAGIHARA, K. & SEYAMA, T. 2012. High mannose-binding antiviral lectin PFL from Pseudomonas fluorescens Pf0-1 promotes cell death of gastric cancer cell MKN28 via interaction with α2-integrin. *PloS one,* 7**,** e45922-e45922.

SCHENDEL, F. J., BAUDE, E. J. & FLICKINGER, M. C. 1989. Determination of protein expression and plasmid copy number from cloned genes in Escherichia coli by flow injection analysis using an enzyme indicator vector. *Biotechnol Bioeng,* 34**,** 1023-36.

SCHIAPPARELLI, L. M., MCCLATCHY, D. B., LIU, H.-H., SHARMA, P., YATES, J. R., 3RD & CLINE, H. T. 2014. Direct detection of biotinylated proteins by mass spectrometry. *Journal of proteome research,* 13**,** 3966-3978.

SCHLAERMANN, P., TOELLE, B., BERGER, H., SCHMIDT, S. C., GLANEMANN, M., ORDEMANN, J., BARTFELD, S., MOLLENKOPF, H. J. & MEYER, T. F. 2016. A novel human gastric primary cell culture system for modelling Helicobacter pylori infection in vitro. *Gut,* 65**,** 202.

SCHLUNZEN, F., ZARIVACH, R., HARMS, J., BASHAN, A., TOCILJ, A., ALBRECHT, R., YONATH, A. & FRANCESCHI, F. 2001. Structural basis for the interaction of antibiotics with the peptidyl transferase centre in eubacteria. *Nature,* 413**,** 814-21.

SCHMIEDL, A., BREITLING, F., WINTER, C. H., QUEITSCH, I. & DUBEL, S. 2000. Effects of unpaired cysteines on yield, solubility and activity of different recombinant antibody constructs expressed in E. coli. *J Immunol Methods,* 242**,** 101-14.

SCHNEIDER, H., PELASEYED, T., SVENSSON, F. & JOHANSSON, M. E. V. 2018. Study of mucin turnover in the small intestine by in vivo labeling. *Scientific Reports,* 8**,** 5760.

SCHOONEN, L., VAN ESTERIK, K. S., ZHANG, C., ULIJN, R. V., NOLTE, R. J. M. & HEST, J. C. M. V. 2017. Alternative application of an affinity purification tag: hexahistidines in ester hydrolysis. *Scientific Reports,* 7**,** 14772.

SCHREIBER, S., BUCKER, R., GROLL, C., AZEVEDO-VETHACKE, M., GARTEN, D., SCHEID, P., FRIEDRICH, S., GATERMANN, S., JOSENHANS, C. & SUERBAUM, S. 2005. Rapid loss of motility of Helicobacter pylori in the gastric lumen in vivo. *Infect Immun,* 73**,** 1584-9.

SCHREIBER, S., KONRADT, M., GROLL, C., SCHEID, P., HANAUER, G., WERLING, H. O., JOSENHANS, C. & SUERBAUM, S. 2004. The spatial orientation of Helicobacter pylori in the gastric mucus. *Proc Natl Acad Sci U S A,* 101**,** 5024-9.

SCHUBERT, M. L. & PEURA, D. A. 2008. Control of Gastric Acid Secretion in Health and Disease. *Gastroenterology,* 134**,** 1842-1860.

SCHWARTZ, S. L., WU, J. F. & BERNER, B. 2006. Metformin extended release for the treatment of type 2 diabetes mellitus. *Expert Opin Pharmacother,* 7**,** 803-9.

SCOTT, D., WEEKS, D., MELCHERS, K. & SACHS, G. 1998. The life and death of Helicobacter pylori. *Gut,* 43 Suppl 1**,** S56-60.

SELAS CASTIÑEIRAS, T., WILLIAMS, S. G., HITCHCOCK, A. G. & SMITH, D. C. 2018. E. coli strain engineering for the production of advanced biopharmaceutical products. *FEMS Microbiology Letters,* 365.

SENKOVICH, O. A., YIN, J., EKSHYYAN, V., CONANT, C., TRAYLOR, J., ADEGBOYEGA, P., MCGEE, D. J., RHOADS, R. E., SLEPENKOV, S. & TESTERMAN, T. L. 2011. Helicobacter pylori AlpA and AlpB bind host laminin and influence gastric inflammation in gerbils. *Infect Immun,* 79**,** 3106-16.

SHAH, K. & MAGHSOUDLOU, P. 2016. Enzyme-linked immunosorbent assay (ELISA): the basics. *Br J Hosp Med (Lond),* 77**,** C98-101.

SHAN, W., ZHU, X., LIU, M., LI, L., ZHONG, J., SUN, W., ZHANG, Z. & HUANG, Y. 2015. Overcoming the Diffusion Barrier of Mucus and Absorption Barrier of

Epithelium by Self-Assembled Nanoparticles for Oral Delivery of Insulin. *ACS Nano,* 9**,** 2345-2356.
SHARMA, D., SHARMA, R. K., SHARMA, N., GABRANI, R., SHARMA, S. K., ALI, J. & DANG, S. 2015. Nose-To-Brain Delivery of PLGA-Diazepam Nanoparticles. *AAPS PharmSciTech,* 16**,** 1108-1121.
SHI, J., KANTOFF, P. W., WOOSTER, R. & FAROKHZAD, O. C. 2017. Cancer nanomedicine: progress, challenges and opportunities. *Nat Rev Cancer,* 17**,** 20-37.
SHIRANO, Y. & SHIBATA, D. 1990. Low temperature cultivation of Escherichia coli carrying a rice lipoxygenase L-2 cDNA produces a soluble and active enzyme at a high level. *FEBS Lett,* 271**,** 128-30.
SIIBAK, T., PEIL, L., XIONG, L., MANKIN, A., REMME, J. & TENSON, T. 2008. Erythromycin- and Chloramphenicol-Induced Ribosomal Assembly Defects Are Secondary Effects of Protein Synthesis Inhibition. *Antimicrobial Agents and Chemotherapy,* 53**,** 563-571.
SILBER, K. R., KEILER, K. C. & SAUER, R. T. 1992. Tsp: a tail-specific protease that selectively degrades proteins with nonpolar C termini. *Proc Natl Acad Sci U S A,* 89**,** 295-9.
SINGH, A., UPADHYAY, V., UPADHYAY, A. K., SINGH, S. M. & PANDA, A. K. 2015. Protein recovery from inclusion bodies of Escherichia coli using mild solubilization process. *Microbial Cell Factories,* 14**,** 41.
SINGH, B. & MITRAGOTRI, S. 2019. Harnessing cells to deliver nanoparticle drugs to treat cancer. *Biotechnology Advances*.
SITU, W., LI, X., LIU, J. & CHEN, L. 2015. Preparation and Characterization of Glycoprotein-Resistant Starch Complex As a Coating Material for Oral Bioadhesive Microparticles for Colon-Targeted Polypeptide Delivery. *Journal of Agricultural and Food Chemistry,* 63**,** 4138-4147.
SIURKUS, J. & NEUBAUER, P. 2011. Reducing conditions are the key for efficient production of active ribonuclease inhibitor in Escherichia coli. *Microb Cell Fact,* 10**,** 31.
SKOOG, E. C., PADRA, M., ABERG, A., GIDEONSSON, P., OBI, I., QUINTANA-HAYASHI, M. P., ARNQVIST, A. & LINDEN, S. K. 2017. BabA dependent binding of Helicobacter pylori to human gastric mucins cause aggregation that inhibits proliferation and is regulated via ArsS. *Sci Rep,* 7**,** 40656.
SLIFKIN, M. & DOYLE, R. J. 1990. Lectins and their application to clinical microbiology. *Clinical microbiology reviews,* 3**,** 197-218.
SLOMIANY, B. L. & SLOMIANY, A. 2017. Role of LPS-elicited signaling in triggering gastric mucosal inflammatory responses to H. pylori: modulatory effect of ghrelin. *Inflammopharmacology,* 25**,** 415-429.
SLOUKA, C., KOPP, J., HUTWIMMER, S., STRAHAMMER, M., STROHMER, D., EITENBERGER, E., SCHWAIGHOFER, A. & HERWIG, C. 2018. Custom made inclusion bodies: impact of classical process parameters and physiological parameters on inclusion body quality attributes. *Microbial cell factories,* 17**,** 148-148.
SMART, J. D. 2005. The basics and underlying mechanisms of mucoadhesion. *Adv Drug Deliv Rev,* 57**,** 1556-68.
SOLTES, G. R., MARTIN, N. R., PARK, E., SUTTERLIN, H. A. & SILHAVY, T. J. 2017. Distinctive Roles for Periplasmic Proteases in the Maintenance of Essential Outer Membrane Protein Assembly. *Journal of Bacteriology,* 199**,** e00418-17.

SOLTES, G. R., SCHWALM, J., RICCI, D. P. & SILHAVY, T. J. 2016. The Activity of Escherichia coli Chaperone SurA Is Regulated by Conformational Changes Involving a Parvulin Domain. *Journal of Bacteriology,* 198**,** 921-929.

SON, Y. J., RYU, A. J., LI, L., HAN, N. S. & JEONG, K. J. 2016. Development of a high-copy plasmid for enhanced production of recombinant proteins in Leuconostoc citreum. *Microbial Cell Factories,* 15**,** 12.

SONG, X., HEIMBURG-MOLINARO, J., SMITH, D. F. & CUMMINGS, R. D. 2012. Glycan Microarrays. *In:* ZANDERS, E. D. (ed.) *Chemical Genomics and Proteomics: Reviews and Protocols.* Totowa, NJ: Humana Press.

STERNICKI, L. M., WEGENER, K. L., BRUNING, J. B., BOOKER, G. W. & POLYAK, S. W. 2017. Mechanisms Governing Precise Protein Biotinylation. *Trends Biochem Sci,* 42**,** 383-394.

STETEFELD, J., MCKENNA, S. A. & PATEL, T. R. 2016. Dynamic light scattering: a practical guide and applications in biomedical sciences. *Biophysical Reviews,* 8**,** 409-427.

STRAUSS, J., BURNHAM, N. A. & CAMESANO, T. A. 2009. Atomic force microscopy study of the role of LPS O-antigen on adhesion of E. coli. *J Mol Recognit,* 22**,** 347-55.

STREUBEL, A., SIEPMANN, J. & BODMEIER, R. 2006a. Drug delivery to the upper small intestine window using gastroretentive technologies. *Curr Opin Pharmacol,* 6**,** 501-8.

STREUBEL, A., SIEPMANN, J. & BODMEIER, R. 2006b. Gastroretentive drug delivery systems. *Expert Opin Drug Deliv,* 3**,** 217-33.

STRZELCZYK, P., PLAŻUK, D., ZAKRZEWSKI, J. & BUJACZ, G. 2016. Structural Characterization of the Avidin Interactions with Fluorescent Pyrene-Conjugates: 1-Biotinylpyrene and 1-Desthiobiotinylpyrene. *Molecules,* 21.

SUBEDI, S., MOONENS, K., ROMAO, E., LO, A., VANDENBUSSCHE, G., BUGAYTSOVA, J., MUYLDERMANS, S., BOREN, T. & REMAUT, H. 2014. Expression, purification and X-ray crystallographic analysis of the Helicobacter pylori blood group antigen-binding adhesin BabA. *Acta Crystallogr F Struct Biol Commun,* 70**,** 1631-5.

SUGIKI, T., KOBAYASHI, N. & FUJIWARA, T. 2017. Modern Technologies of Solution Nuclear Magnetic Resonance Spectroscopy for Three-dimensional Structure Determination of Proteins Open Avenues for Life Scientists. *Computational and Structural Biotechnology Journal,* 15**,** 328-339.

SUNG, K., MALONEY, M. T., YANG, J. & WU, C. 2011. A novel method for producing mono-biotinylated, biologically active neurotrophic factors: an essential reagent for single molecule study of axonal transport. *Journal of neuroscience methods,* 200**,** 121-128.

SWANSON, H. I. 2015. Drug Metabolism by the Host and Gut Microbiota: A Partnership or Rivalry? *Drug Metabolism and Disposition,* 43**,** 1499-1504.

SWEENEY, EMILY G. & GUILLEMIN, K. 2016. H. pylori's BabA Embraces Change. *Cell Host & Microbe,* 19**,** 5-7.

SWITZER, R. C., 3RD, MERRIL, C. R. & SHIFRIN, S. 1979. A highly sensitive silver stain for detecting proteins and peptides in polyacrylamide gels. *Anal Biochem,* 98**,** 231-7.

SZCZUKO, M., ZIĘTEK, M., KULPA, D. & SEIDLER, T. 2019. Riboflavin - properties, occurrence and its use in medicine. *Pteridines.*

SZYMANSKI, C. M. & WREN, B. W. 2005. Protein glycosylation in bacterial mucosal pathogens. *Nat Rev Microbiol,* 3**,** 225-37.

TAKAYANAGI-KIYA, S. & JIN, Y. 2016. Altered Function of the DnaJ Family Cochaperone DNJ-17 Modulates Locomotor Circuit Activity in a

Caenorhabditis elegans Seizure Model. *G3: Genes|Genomes|Genetics,* 6**,** 2165-2171.

TANG, B. C., DAWSON, M., LAI, S. K., WANG, Y. Y., SUK, J. S., YANG, M., ZEITLIN, P., BOYLE, M. P., FU, J. & HANES, J. 2009. Biodegradable polymer nanoparticles that rapidly penetrate the human mucus barrier. *Proc Natl Acad Sci U S A,* 106**,** 19268-73.

TANNAES, T., DEKKER, N., BUKHOLM, G., BIJLSMA, J. J. & APPELMELK, B. J. 2001. Phase variation in the Helicobacter pylori phospholipase A gene and its role in acid adaptation. *Infect Immun,* 69**,** 7334-40.

TEICH, A., LIN, H. Y., ANDERSSON, L., MEYER, S. & NEUBAUER, P. 1998. Amplification of ColE1 related plasmids in recombinant cultures of Escherichia coli after IPTG induction. *Journal of Biotechnology,* 64**,** 197-210.

TERESHCHENKOV, A. G., DOBOSZ-BARTOSZEK, M., OSTERMAN, I. A., MARKS, J., SERGEEVA, V. A., KASATSKY, P., KOMAROVA, E. S., STAVRIANIDI, A. N., RODIN, I. A., KONEVEGA, A. L., SERGIEV, P. V., SUMBATYAN, N. V., MANKIN, A. S., BOGDANOV, A. A. & POLIKANOV, Y. S. 2018. Binding and Action of Amino Acid Analogs of Chloramphenicol upon the Bacterial Ribosome. *Journal of Molecular Biology,* 430**,** 842-852.

THAKUR, A., PAL, L., AHMAD, A. & KHAN, M. I. 2007. Complex carbohydrate specificity of lectin from fruiting body of Ganoderma lucidum. A surface plasmon resonance study. *IUBMB Life,* 59**,** 758-764.

THIE, H., BINIUS, S., SCHIRRMANN, T., HUST, M. & DÜBEL, S. 2009. Multimerization domains for antibody phage display and antibody production. *New Biotechnology,* 26**,** 314-321.

THOMAS, K., AALBERS, M., BANNON, G. A., BARTELS, M., DEARMAN, R. J., ESDAILE, D. J., FU, T. J., GLATT, C. M., HADFIELD, N., HATZOS, C., HEFLE, S. L., HEYLINGS, J. R., GOODMAN, R. E., HENRY, B., HEROUET, C., HOLSAPPLE, M., LADICS, G. S., LANDRY, T. D., MACINTOSH, S. C., RICE, E. A., PRIVALLE, L. S., STEINER, H. Y., TESHIMA, R., VAN REE, R., WOOLHISER, M. & ZAWODNY, J. 2004. A multi-laboratory evaluation of a common in vitro pepsin digestion assay protocol used in assessing the safety of novel proteins. *Regulatory Toxicology and Pharmacology,* 39**,** 87-98.

TIRAFERRI, A. & BORKOVEC, M. 2015. Probing effects of polymer adsorption in colloidal particle suspensions by light scattering as relevant for the aquatic environment: An overview. *Science of The Total Environment,* 535**,** 131-140.

TIRAT, A., FREULER, F., STETTLER, T., MAYR, L. M. & LEDER, L. 2006. Evaluation of two novel tag-based labelling technologies for site-specific modification of proteins. *International Journal of Biological Macromolecules,* 39**,** 66-76.

TOLLER, I. M., NEELSEN, K. J., STEGER, M., HARTUNG, M. L., HOTTIGER, M. O., STUCKI, M., KALALI, B., GERHARD, M., SARTORI, A. A., LOPES, M. & MULLER, A. 2011. Carcinogenic bacterial pathogen Helicobacter pylori triggers DNA double-strand breaks and a DNA damage response in its host cells. *Proc Natl Acad Sci U S A,* 108**,** 14944-9.

TOMIZAWA, J. I., SAKAKIBARA, Y. & KAKEFUDA, T. 1975. Replication of colicin E1 plasmid DNA added to cell extracts. *Proc Natl Acad Sci U S A,* 72**,** 1050-4.

TOPCU, Z. 2000. An optimized recipe for cloning of the polymerase chain reaction-amplified DNA inserts into plasmid vectors. *Acta Biochim Pol,* 47**,** 841-6.

TRIPATHI, J., THAPA, P., MAHARJAN, R. & JEONG, S. H. 2019. Current State and Future Perspectives on Gastroretentive Drug Delivery Systems. *Pharmaceutics,* 11.

TWING, K. I., KIRCHMAN, D. L. & CAMPBELL, B. J. 2011. Temporal study of Helicobacter pylori presence in coastal freshwater, estuary and marine waters. *Water Res,* 45**,** 1897-905.

TYNDALL, J. D., NALL, T. & FAIRLIE, D. P. 2005. Proteases universally recognize beta strands in their active sites. *Chem Rev,* 105**,** 973-99.

ULLAH, R., SHAH, M. A., TUFAIL, S., ISMAT, F., IMRAN, M., IQBAL, M., MIRZA, O. & RHAMAN, M. 2016. Activity of the Human Rhinovirus 3C Protease Studied in Various Buffers, Additives and Detergents Solutions for Recombinant Protein Production. *PLOS ONE,* 11**,** e0153436.

VALE, F. F. & VITOR, J. M. 2010. Transmission pathway of Helicobacter pylori: does food play a role in rural and urban areas? *Int J Food Microbiol,* 138**,** 1-12.

VAN DEN ENT, F. & LOWE, J. 2006. RF cloning: a restriction-free method for inserting target genes into plasmids. *J Biochem Biophys Methods,* 67**,** 67-74.

VAN DER WEL, C., BOSSERT, N., MANK, Q. J., WINTER, M. G. T., HEINRICH, D. & KRAFT, D. J. 2017. Surfactant-free Colloidal Particles with Specific Binding Affinity. *Langmuir : the ACS journal of surfaces and colloids,* 33**,** 9803-9810.

VAN ULSEN, P., RAHMAN, S. U., JONG, W. S. P., DALEKE-SCHERMERHORN, M. H. & LUIRINK, J. 2014. Type V secretion: From biogenesis to biotechnology. *Biochimica et Biophysica Acta (BBA) - Molecular Cell Research,* 1843**,** 1592-1611.

VAN WEEMEN, B. K. & SCHUURS, A. H. W. M. 1971. Immunoassay using antigen—enzyme conjugates. *FEBS Letters,* 15**,** 232-236.

VASU, K. & NAGARAJA, V. 2013. Diverse functions of restriction-modification systems in addition to cellular defense. *Microbiology and molecular biology reviews : MMBR,* 77**,** 53-72.

VERMA, V., KAUR, C., GROVER, P., GUPTA, A. & CHAUDHARY, V. K. 2018. Biotin-tagged proteins: Reagents for efficient ELISA-based serodiagnosis and phage display-based affinity selection. *PLOS ONE,* 13**,** e0191315.

VERMETTE, P., GENGENBACH, T., DIVISEKERA, U., KAMBOURIS, P. A., GRIESSER, H. J. & MEAGHER, L. 2003. Immobilization and surface characterization of NeutrAvidin biotin-binding protein on different hydrogel interlayers. *Journal of Colloid and Interface Science,* 259**,** 13-26.

VISWANATHAN, P., MURALIDARAN, Y. & RAGAVAN, G. 2017. Chapter 7 - Challenges in oral drug delivery: a nano-based strategy to overcome. *In:* ANDRONESCU, E. & GRUMEZESCU, A. M. (eds.) *Nanostructures for Oral Medicine.* Elsevier.

WACKER, M., LINTON, D., HITCHEN, P. G., NITA-LAZAR, M., HASLAM, S. M., NORTH, S. J., PANICO, M., MORRIS, H. R., DELL, A., WREN, B. W. & AEBI, M. 2002. N-linked glycosylation in Campylobacter jejuni and its functional transfer into E. coli. *Science,* 298**,** 1790-3.

WALLACE, B. A. & JANES, ROBERT W. 2010. Synchrotron radiation circular dichroism (SRCD) spectroscopy: an enhanced method for examining protein conformations and protein interactions. *Biochemical Society Transactions,* 38**,** 861-873.

WALSH, P., BURSAC, D., LAW, Y. C., CYR, D. & LITHGOW, T. 2004. The J-protein family: modulating protein assembly, disassembly and translocation. *EMBO Rep,* 5**,** 567-71.

WALZ, A., ODENBREIT, S., STUHLER, K., WATTENBERG, A., MEYER, H. E., MAHDAVI, J., BOREN, T. & RUHL, S. 2009. Identification of glycoprotein

receptors within the human salivary proteome for the lectin-like BabA and SabA adhesins of Helicobacter pylori by fluorescence-based 2-D bacterial overlay. *Proteomics,* 9**,** 1582-92.

WANG, W., SORIANO, B. & CHEN, Q. 2017. Glycan profiling of proteins using lectin binding by Surface Plasmon Resonance. *Analytical Biochemistry,* 538**,** 53-63.

WANG, W. W.-S., DAS, D. & SURESH, M. R. 2005. Biotin carboxyl carrier protein Co-purifies as a contaminant in core-streptavidin preparations. *Molecular Biotechnology,* 31**,** 29-40.

WANG, X., ZHOU, B., HU, W., ZHAO, Q. & LIN, Z. 2015. Formation of active inclusion bodies induced by hydrophobic self-assembling peptide GFIL8. *Microbial cell factories,* 14**,** 88-88.

WANG, Z., XIANG, L., SHAO, J., WEGRZYN, A. & WEGRZYN, G. 2006. Effects of the presence of ColE1 plasmid DNA in Escherichia coli on the host cell metabolism. *Microb Cell Fact,* 5**,** 34.

WANG, Z., XIANG, L., SHAO, J. & WĘGRZYN, G. 2007. Adenosine monophosphate-induced amplification of ColE1 plasmid DNA in Escherichia coli. *Plasmid,* 57**,** 265-274.

WARITANI, T., CHANG, J., MCKINNEY, B. & TERATO, K. 2017. An ELISA protocol to improve the accuracy and reliability of serological antibody assays. *MethodsX,* 4**,** 153-165.

WATERMAN, K. C. 2007. A critical review of gastric retentive controlled drug delivery. *Pharm Dev Technol,* 12**,** 1-10.

WATKINSON, G., HOPKINS, A. & AKBAR, F. A. 1988. The therapeutic efficacy of misoprostol in peptic ulcer disease. *Postgrad Med J,* 64 Suppl 1**,** 60-77.

WEGRZYN, G. 1999. Replication of plasmids during bacterial response to amino acid starvation. *Plasmid,* 41**,** 1-16.

WEN, H., JUNG, H. & LI, X. 2015. Drug Delivery Approaches in Addressing Clinical Pharmacology-Related Issues: Opportunities and Challenges. *The AAPS Journal,* 17**,** 1327-1340.

WEN, Z., YAN, Z., HE, R., PANG, Z., GUO, L., QIAN, Y., JIANG, X. & FANG, L. 2011a. Brain targeting and toxicity study of odorranalectin-conjugated nanoparticles following intranasal administration. *Drug Deliv,* 18**,** 555-61.

WEN, Z., YAN, Z., HU, K., PANG, Z., CHENG, X., GUO, L., ZHANG, Q., JIANG, X., FANG, L. & LAI, R. 2011b. Odorranalectin-conjugated nanoparticles: preparation, brain delivery and pharmacodynamic study on Parkinson's disease following intranasal administration. *J Control Release,* 151**,** 131-8.

WESSLER, S., SCHNEIDER, G. & BACKERT, S. 2017. Bacterial serine protease HtrA as a promising new target for antimicrobial therapy? *Cell Communication and Signaling,* 15**,** 4.

WESTWOOD, J. A., MURRAY, W. K., TRIVETT, M., HAYNES, N. M., SOLOMON, B., MILESHKIN, L., BALL, D., MICHAEL, M., BURMAN, A., MAYURA-GURU, P., TRAPANI, J. A., PEINERT, S., HÖNEMANN, D., MILES PRINCE, H., SCOTT, A. M., SMYTH, M. J., DARCY, P. K. & KERSHAW, M. H. 2009. The Lewis-Y Carbohydrate Antigen is Expressed by Many Human Tumors and Can Serve as a Target for Genetically Redirected T cells Despite the Presence of Soluble Antigen in Serum. *Journal of Immunotherapy,* 32**,** 292-301.

WHITMORE, L. & WALLACE, B. A. 2008. Protein secondary structure analyses from circular dichroism spectroscopy: Methods and reference databases. *Biopolymers,* 89**,** 392-400.

WIJEKOON, C. J. K., UKUWELA, A. A., WEDD, A. G. & XIAO, Z. 2016. Evaluation of employing poly-lysine tags versus poly-histidine tags for purification and

characterization of recombinant copper-binding proteins. *Journal of Inorganic Biochemistry,* 162**,** 286-294.
WILCHEK, M. & BAYER, E. A. 1988. The avidin-biotin complex in bioanalytical applications. *Analytical Biochemistry,* 171**,** 1-32.
WILCHEK, M. & BAYER, E. A. 1999. Foreword and introduction to the book (strept)avidin-biotin system. *Biomol Eng,* 16**,** 1-4.
WIRTH, M., GERHARDT, K., WARM, C. & GABOR, F. 2002a. Lectin-mediated drug delivery: influence of mucin on cytoadhesion of plant lectins in vitro. *Journal of Controlled Release,* 79**,** 183-191.
WIRTH, M., GERHARDT, K., WURM, C. & GABOR, F. 2002b. Lectin-mediated drug delivery: influence of mucin on cytoadhesion of plant lectins in vitro. *Journal of Controlled Release,* 79**,** 183-191.
WOO, H. D., FERNANDEZ-JIMENEZ, N., GHANTOUS, A., DEGLI ESPOSTI, D., CUENIN, C., CAHAIS, V., CHOI, I. J., KIM, Y. I., KIM, J. & HERCEG, Z. 2018. Genome-wide profiling of normal gastric mucosa identifies Helicobacter pylori- and cancer-associated DNA methylome changes. *Int J Cancer,* 143**,** 597-609.
WOODLEY, J. 2001. Bioadhesion: new possibilities for drug administration? *Clin Pharmacokinet,* 40**,** 77-84.
WOODLEY, J. F. 2000. Lectins for gastrointestinal targeting - 15 years on. *Journal of Drug Targeting,* 7**,** 325-333.
WU, G., YAN, Q., JONES, J. A., TANG, Y. J., FONG, S. S. & KOFFAS, M. A. G. 2016. Metabolic Burden: Cornerstones in Synthetic Biology and Metabolic Engineering Applications. *Trends in Biotechnology,* 34**,** 652-664.
WU, H., LI, J., ZHANG, Q., YAN, X., GUO, L., GAO, X., QIU, M., JIANG, X., LAI, R. & CHEN, H. 2012. A novel small Odorranalectin-bearing cubosomes: preparation, brain delivery and pharmacodynamic study on amyloid-beta(2)(5)(-)(3)(5)-treated rats following intranasal administration. *Eur J Pharm Biopharm,* 80**,** 368-78.
WURM, D. J., VEITER, L., ULONSKA, S., EGGENREICH, B., HERWIG, C. & SPADIUT, O. 2016. The E. coli pET expression system revisited-mechanistic correlation between glucose and lactose uptake. *Applied microbiology and biotechnology,* 100**,** 8721-8729.
XU, C. & NG, D. T. W. 2015. Glycosylation-directed quality control of protein folding. *Nature Reviews Molecular Cell Biology,* 16**,** 742.
XU, S., CUI, F., HUANG, D., ZHANG, D., ZHU, A., SUN, X., CAO, Y., DING, S., WANG, Y., GAO, E. & ZHANG, F. 2018. PD-L1 monoclonal antibody-conjugated nanoparticles enhance drug delivery level and chemotherapy efficacy in gastric cancer cells. *International journal of nanomedicine,* 14**,** 17-32.
YAMAOKA, Y. 2008. Roles of Helicobacter pylori BabA in gastroduodenal pathogenesis. *World Journal of Gastroenterology,* 14**,** 4265.
YAMAOKA, Y. 2010. Mechanisms of disease: Helicobacter pylori virulence factors. *Nat Rev Gastroenterol Hepatol,* 7**,** 629-41.
YAMAOKA, Y., KWON, D. H. & GRAHAM, D. Y. 2000. A M(r) 34,000 proinflammatory outer membrane protein (oipA) of Helicobacter pylori. *Proc Natl Acad Sci U S A,* 97**,** 7533-8.
YANG, I., NELL, S. & SUERBAUM, S. 2013. Survival in hostile territory: the microbiota of the stomach. *FEMS Microbiol Rev,* 37**,** 736-61.
YTTERBERG, A. J., ZUBAREV, R. A. & BAUMGARTEN, T. 2019. Posttranslational Targeting of a Recombinant Protein Promotes Its Efficient Secretion into the

Escherichia coli Periplasm. *Applied and Environmental Microbiology,* 85**,** e00671-19.

YUE, Y., WANG, Z., ZHANG, Y., WANG, Z., LV, Q. & LIU, J. 2019. Binding of triclosan and triclocarban to pepsin: DFT, spectroscopic and dynamic simulation studies. *Chemosphere,* 214**,** 278-287.

ZENG, H.-J., QI, T., YANG, R., YOU, J. & QU, L.-B. 2014a. Spectroscopy and Molecular Docking Study on the Interaction Behavior Between Nobiletin and Pepsin. *Journal of Fluorescence,* 24**,** 1031-1040.

ZENG, H. J., QI, T., YANG, R., YOU, J. & QU, L. B. 2014b. Spectroscopy and molecular docking study on the interaction behavior between nobiletin and pepsin. *J Fluoresc,* 24**,** 1031-40.

ZHANG, Y., CHAN, J. W., MORETTI, A. & UHRICH, K. E. 2015. Designing polymers with sugar-based advantages for bioactive delivery applications. *Journal of Controlled Release,* 219**,** 355-368.

ZHANG, Z., YOMO, D. & GRADINARU, C. 2017. Choosing the right fluorophore for single-molecule fluorescence studies in a lipid environment. *Biochimica et Biophysica Acta (BBA) - Biomembranes,* 1859**,** 1242-1253.

ZHAO, S., LV, Y., ZHANG, J. B., WANG, B., LV, G. J. & MA, X. J. 2014. Gastroretentive drug delivery systems for the treatment of Helicobacter pylori. *World J Gastroenterol,* 20**,** 9321-9.

ZHENG, P. Y., HUA, J., NG, H. C., YEOH, K. G. & BOW, H. 2003. Expression of Lewis(b) blood group antigen in Helicobacter pylori does not interfere with bacterial adhesion property. *World J Gastroenterol,* 9**,** 122-4.

ZHENG, P. Y., HUA, J., YEOH, K. G. & HO, B. 2000. Association of peptic ulcer with increased expression of Lewis antigens but not cagA, iceA, andvacA in Helicobacter pylori isolates in an Asian population. *Gut,* 47**,** 18.

ZHOU, K., AERTSEN, A. & MICHIELS, C. W. 2014. The role of variable DNA tandem repeats in bacterial adaptation. *FEMS Microbiology Reviews,* 38**,** 119-141.

ZHU, S., GONG, C., REN, L., LI, X., SONG, D. & ZHENG, G. 2013. A simple and effective strategy for solving the problem of inclusion bodies in recombinant protein technology: His-tag deletions enhance soluble expression. *Applied Microbiology and Biotechnology,* 97**,** 837-845.

ZORDAN, R. E., BELIVEAU, B. J., TROW, J. A., CRAIG, N. L. & CORMACK, B. P. 2015. Avoiding the ends: internal epitope tagging of proteins using transposon Tn7. *Genetics,* 200**,** 47-58.